

SUPPLEMENTO
AL VOLUME XIII, SERIE X,
DEL
NUOVO CIMENTO

1959

3° Trimestre

SUPPLEMENTO
AL VOLUME XIII, SERIE X
DEL
NUOVO CIMENTO

A CURA DELLA SOCIETÀ ITALIANA DI FISICA

1959

3° Trimestre

PRINTED IN ITALY

NICOLA ZANICHELLI EDITORE
BOLOGNA

SUPPLEMENTO
AL VOLUME XIII, SERIE X, DEL
NUOVO CIMENTO
A CURA DELLA SOCIETÀ ITALIANA DI FISICA

1959

3° Trimestre

N. 1

RENDICONTI
DEL
VI CORSO CHE NELLA VILLA MONASTERO A VARENNA
DAL 23 GIUGNO AL 5 LUGLIO 1958
FU TENUTO A CURA
DELLA SCUOLA INTERNAZIONALE DI FISICA
DELLA SOCIETÀ ITALIANA DI FISICA
SULLA
FISICA DEL PLASMA
E RELATIVE APPLICAZIONI ASTROFISICHE

INDICE

Introduzione.

G. POLVANI - Parole inaugurali	pag. 3
G. RIGHINI - Prolusione al Corso	» 7

Lezioni e seminari.

V. FERRARO - General theory of plasma	» 9
B. LEHNERT - Plasma physics on cesmical and laboratory scale	» 59
P. C. THONEMANN - High temperature plasmas	» 111

A. GILARDINI - Microwaves in ionized gas	pag. 132
E. SCHATZMAN - Le plasma stellaire	» 166
L. BIERMANN - Stellar atmospheres in plasma	» 189
H. C. VAN DE HULST - The interstellar plasma	» 205
R. GALLET - Propagation and production of electromagnetic waves in a plasma	» 234
J. G. LINHART - Plasma confinement by external magnetic fields . . .	» 257
C. DE JAGER - Optical and radiophenomena associated with a solar activity centre	» 284
C. DE JAGER - Dynamical features of the chromosphere	» 291
R. GIOVANELLI - Solar disturbances producing type II radio bursts . .	» 299
R. GIOVANELLI - Flare surges, puffs and type III bursts	» 302
K. O. KIEPENHEUER - The observability of hydromagnetic phenomena on the sun	» 305
H. WILHELMSSON - The scattering of electromagnetic waves by an electron beam	» 311
T. GOLD - Magnetic field in the solar system	» 318
L. DAVIS jr. - The origin of cosmic rays	» 324
R. LÜST - Some theoretical aspects of magneto-hydrodynamics and thermonuclear fusion	» 329

*La Direzione del Corso rivolge un particolare ringraziamento al
prof. GIOVANNI GODOLI, ai dott. MARIO RIGUTTI e GIANCARLO
NOCI dell'Osservatorio Astrofisico di Arcetri per l'aiuto dato prima
nell'organizzazione del Corso, poi nello svolgimento di esso e infine
nella compilazione di questo fascicolo, per il quale particolari rin-
graziamenti vanno anche al dott. ANTONIO SCOTTI dell'Istituto di
Scienze Fisiche dell'Università di Milano.*

INTRODUZIONE

Parole inaugurali

DI

GIOVANNI POLVANI

Presidente della Società Italiana di Fisica

La Scuola Internazionale di Fisica della Società Italiana di Fisica si presenta a Villa Monastero a Varenna, quest'anno, sesto dalla sua fondazione, con quattro Corsi successivi che rispettivamente riguardano il primo la Fisica del plasma e le relative applicazioni ai problemi d'Astrofisica, il secondo la Teoria della informazione sotto i suoi vari aspetti fisici, matematici e applicativi, il terzo i Problemi matematici della Teoria quantistica delle particelle e dei campi, e il quarto infine la Fisica dei mesoni.

In totale sono quest'anno ben sessanta giorni di scuola su quattro grossi temi della nostra disciplina.

L'aumento del numero dei Corsi e l'aver esaurito qualsiasi disponibilità dei posti pur di contentare il numero massimo dei postulanti, hanno portato che lo sforzo organizzativo e finanziario che la nostra Società sostiene quest'anno è veramente notevolissimo. Esso però corrisponde sia alla esigenza di affinare la preparazione dei giovani migliori nelle questioni che più urgono attualmente in Fisica, sia anche alle numerose sollecitazioni pervenute dall'Italia e dall'estero.

In realtà questi nostri corsi di Fisica a Varenna sono divenuti un impegno morale della nostra Società non solo di fronte al nostro paese, ma anche di fronte a tutti coloro che nel mondo si danno agli studi di Fisica.

E mi è oltremodo gradito dichiarare che non sarebbe stato possibile, nè sarebbe possibile sostenere questo sforzo senza l'aiuto di vari Enti che qui desidero nominare per esprimere loro la gratitudine della Società Italiana di Fisica e di coloro che partecipano quest'anno alla attività della Scuola Internazionale di Fisica di Varenna.

Ricorderò anzitutto il Ministero della Pubblica Istruzione e per esso il Ministro prof. A. MORO e il Direttore Generale per l'Istruzione superiore dottor

MARIO DI DOMIZIO; il Consiglio Nazionale delle Ricerche e per esso il suo Presidente prof. F. GIORDANI e il Presidente del Comitato Nazionale per la Fisica prof. E. PERUCCA; il Comitato Nazionale per le Ricerche Nucleari e per esso il Presidente prof. sen. B. FOCACCIA e il Segretario generale prof. F. IPPOLITO; la Prefettura di Como e il suo prefetto dott. G. BIANCHI DI LAVAGNA; il Comune di Varenna e il Sindaco sig. A. TANTARDINI; l'Università di Milano e il suo Rettore prof. G. DE FRANCESCO; l'Università di Napoli e il suo Rettore prof. E. PONTIERI; la Radio Italiana e il suo Presidente prof. A. CARRELLI; la Moto Guzzi di Mandello sul Lario, il suo Presidente dott. E. PARODI e il Consigliere delegato dott. G. BONELLI; la Società Badoni di Lecco e il suo Presidente ing. G. BADONI; la Società Caleotto di Lecco e il suo Presidente comm. E. BONAITI; la Società Serpentino Italiana di Lecco e il suo Presidente on. sen. P. AMIGONI; la Società Fabbrica Italiana Lampadine Elettriche di Lecco e il suo Presidente comm. L. BUTTI; la Società Metalgraf di Lecco e il suo Presidente cav. E. BIFFI; la Società Orobia e il Direttore della Sezione di Lecco ing. V. ZOCCOLINI; la Condor di Milano e il suo Consigliere delegato dott. M. MORTARA; ed inoltre, ciò che è molto significativo, la Fondazione Ford di New York, il suo Segretario J. M. McDANIEL jr. e il prof. J. A. WHEELER che tanto si è interessato alla nostra Scuola e al suo sviluppo; l'Institute of Technology di Cambridge del Massachusetts; la Plasmadyne Corporation di Santa Ana (Cal.) e il suo Vicepresidente dott. A. C. DUCATI; l'Ente Villa Monastero, così saggiamente retto dall'avv. G. BOSISIO di Como e infine, anche se nominati per ultimi, non davvero ultimi nella collaborazione, la Casa Zanichelli e il suo Direttore generale dott. E. DELLA MONICA che tanto fanno per le pubblicazioni degli atti di questi Corsi varennini.

* * *

Restringendomi ora a considerare il Corso che oggi si inaugura e che, primo di quest'anno e sesto dall'inizio dei Corsi avvenuto nel 1953, tratta — come ho detto — della Fisica del plasma, un ringraziamento di vero cuore va anzitutto al prof. G. RIGHINI, Direttore dell'Osservatorio Astrofisico di Arcetri a Firenze, organizzatore appassionato e valente del Corso e Direttore del Corso stesso; e oltre che a lui va ai vari professori che hanno accolto il nostro invito e sono venuti qui a Varenna a far partecipi i loro ascoltatori del proprio sapere.

Essi sono: L. BIERMANN di Göttingen, V. FERRARO di London, R. GALLET di Boulder, Colo., A. GILARDINI di Roma, R. G. GIOVANELLI di Sydney, T. GOLD di Cambridge, Mass., H. C. VAN DE HULST di Leiden, C. DE JAGER di Utrecht, K. O. KIEPENHEUER di Freiburg im Breisgau, B. LEHNERT di Stockholm, J. G. LINHART di Genève, SCHATZMAN di Paris e P. C. THONEMANN di Harwell.

Gli allievi ammessi al Corso sono ben cinquantauno; ai quali anche quest'anno, debbono aggiungersi gli uditori. Permettete che, seguendo un'usanza,

stabilita fin dal primo Corso, io li nomini tutti, in modo da presentarli reciprocamente tra loro e ai maestri.

Ecco gli allievi: U. ASCOLI BARTOLI di Roma, P. AVIVI di Jerusalem, R. BALESCU di Bruxelles, G. BARSANTI di Pisa, G. C. BONAZZOLA di Torino, C. M. BRAAMS di Utrecht, B. BRUNELLI di Roma, E. CANOBBIO di Milano, D. CATTANI di Bologna, R. CROCI di Milano, L. DAVIS jr. di Göttingen, V. DE SABBATA di Bologna, T. EL-KHALAFawi di Aachen, E. G. FORBES di Firenze, M. GALLI di Bologna, A. GIBSON di Harwell, G. GODOLI di Firenze, G. GOLDSTEIN di Paris, M. GUTMANN di Paris, M. HACK di Merate, R. E. HARRISON di Harwell, J. HEIDMANN di Neuilly, H. KEVER di Aachen, R. KIPPENHAHN di Göttingen, C. T. JACOBSEN di Trondheim, Z. JANKOVIČ di Zagreb, D. LA ROY di Amsterdam, W. LINDT di Berne, E. LÜSCHER di Lausanne, R. LÜST di Göttingen, F. MAGISTRELLI di Roma, D. W. MAHAFFEY di Belfast, G. MEISTER di Bonn, L. MUSUMECI di Livorno, G. NOCI di Firenze, D. OEPTS di Amstelveen, D. D. REAGAN di Oxford, M. RIGUTTI di Firenze, P. ROTHWELL di London, K. SCHINDLER di Aachen, F. R. SCHWARZL di Delft, S. SEGRE di Roma, A. H. SILLESEN di Copenhagen, P. SONA di Milano, P. STURROCK di Genève, N. TALINI di Livorno, J. C. TERLOUW di Utrecht, H. TREFALL di Bergen, E. WEIBEL di Redondo Beach, Cal., B. WIEDER di Boulder, Colo., H. WILHELMSSON di Copenhagen.

Ed ecco gli uditori: M. BINEAU di Paris, C. CIANCIA di Genova, T. CONSOLI di Paris, A. C. DUCATI di Santa Ana, Cal., P. GRATREAU di Genève, L. HOGBERG di Uppsala, P. J. KELLOGG di Minneapolis, Minn., A. KRANJC di Bologna, F. LERDA di Torino, C. MAISONNIER di Genève, C. MERCIER di Saclay, L. PENNELEGION di Southampton, J. P. SOMON di Saclay, G. VIANO di Torino.

In totale tra allievi e uditori sono più di sessanta le persone che costituiscono (per così dire) la scolaresca del Corso; molto maggiore è stato però il numero di coloro che avevano fatto la domanda di frequentarlo. Purtroppo le limitazioni imposte dalle possibilità materiali della Scuola han reso anche quest'anno penoso il contrasto in cui la Direzione si è trovata tra il dover dir di no pur desidesiderando dir di sì. Noi confidiamo di essere compresi ed approvati.

* * *

Chi abbia seguito gli elenchi dei nomi che ho letto avrà notato che ben diciassette sono i vari paesi qui rappresentati. La disciplina comune trattata, le lezioni a comune seguite, le discussioni che insorgeranno tra i vari partecipanti al Corso, la collaborazione tra i giovani che dovranno raccogliere le lezioni, il mangiare insieme, il fare insieme il bagno, la vita comune... tutto favorirà l'annodarsi o il rinsaldarsi di amicizie. E a Corso finito una tenue, ma tenace rete di conoscenze, d'interessi, di simpatie si troverà spontanea-

mente ad essersi formata sotto il comune titolo della Scuola Internazionale di Fisica di Varenna, e costituirà per la sua parte, anche se minima, una specie di viatico attraverso a quelle barriere che gli uomini hanno tristamente inventato per separarsi tra loro anche in uno stesso paese, e combattersi e che la Scienza tende, per vie non diverse sostanzialmente di quelle dell'amore e della stima, a superare.

Sicchè coloro che a questa Scuola partecipano ricorderanno, io credo, ancor più che le lezioni ricevute per imparare a leggere il libro eterno della Natura — libro che qui a Varenna porta scritte alcune delle sue pagine più belle: i monti sorgenti dalle acque del Lago verso l'azzurro del cielo nella cornice impareggiabile delle sue rive — ricorderanno, credo, il viver calmo della Villa Monastero, tra quelle acque e quei monti, nell'istintiva aspirazione di migliorare se stessi aumentando il proprio sapere.

Con l'augurio che questo scopo umano e scientifico a un tempo sia raggiunto, ho l'onore di dichiarare aperto il I Corso 1958 — VI dall'inizio della Scuola Internazionale di Fisica della nostra Società — dedicato alla Fisica del plasma e alle applicazioni di essa ai problemi di Astrofisica.

Prolusione al Corso.

DI

G. RIGHINI

Direttore del Corso

È un grande onore per me dirigere il primo corso del 1958 che si tiene in questa Villa nota ormai in tutto il mondo sia per la sua incomparabile bellezza, sia per la Scuola che essa ospita.

Di questo onore io sono grato al nostro Presidente, prof. POLVANI, che, con fine intuito, volle riunire, in un solo corso, due branche promettenti della scienza: la Fisica del plasma e l'Astrofisica.

Se è vero che la Fisica del plasma è venuta alla ribalta in questi ultimi anni in seguito alle ricerche svolte da alcuni gruppi di studiosi, fra i quali è preminente il gruppo inglese di Harwell, è altrettanto vero che per lunghi anni i ricercatori che si occuparono di scariche nei gas rarefatti, dello studio dell'arco elettrico e di analoghi fenomeni, debbono considerarsi i precursori e i pionieri di questo nuovo ramo della Fisica.

L'Astrofisica, scienza più giovane, entra di prepotenza in questo quadro soltanto più tardi e soprattutto ad opera degli osservatori solari. Si parlava allora dei gas incandescenti che formavano le protuberanze solari, della cromosfera assimilata da ANGELO SECCHI ad una « prateria ardente », mentre i pennacchi coronali osservati durante le eclissi totali facevano sospettare l'esistenza di un campo magnetico solare.

Si deve a ELLERY GEORGE HALE se queste vaghe ipotesi sul comportamento del plasma solare sono state messe sul giusto binario. L'invenzione dello spettroeliografo (1889), che permetteva di fotografare lo strato superiore della cromosfera in proiezione sul disco solare, e la scoperta del campo magnetico delle macchie (1908), dovevano incidere fortemente sulla corretta formulazione delle idee riguardanti la natura e le condizioni fisiche dei gas solari. Si può dire anzi a ragion veduta che questi fatti sono alla base della Magnetoidrodinamica delle atmosfere stellari.

L'Astrofisica offre quindi al ricercatore che studia il plasma un campo vastissimo di fenomeni che sono relativi al plasma stesso e avvengono sotto condizioni fisiche non riproducibili in laboratorio. Basse densità, quantità enormi di materia, elevatissime temperature, campi magnetici estesi su migliaia o milioni di chilometri quadrati...: ecco le condizioni che prevalentemente regnano nell'ambiente astrofisico; qui è anche il dominio delle onde magneto-idrodinamiche la cui predizione e teoria si deve ad HANNES ALFVÉN.

D'altronde le ricerche di laboratorio offrono all'Astrofisica le basi per l'interpretazione di fenomeni fino a ieri misteriosi. Le spicule cromosferiche, i moti delle protuberanze, la natura stessa delle macchie sono oggi spiegabili grazie alle conoscenze sui plasmi che sono state acquisite in laboratorio. Persino il fenomeno dei « brillamenti » o « flares » che per decenni ha affaticato inutilmente i teorici dell'Astrofisica, si spiega bene col nuovo meccanismo della contrazione magnetica del plasma, meglio noto col nome di « pinch-effect ».

Ma numerosi e vasti sono ancora gli aspetti poco chiari del comportamento del plasma e vastissime sono le applicazioni potenziali delle tecniche sviluppate; così pure molti fenomeni astrofisici attendono ancora dai progressi di questi studi una completa ed esauriente interpretazione.

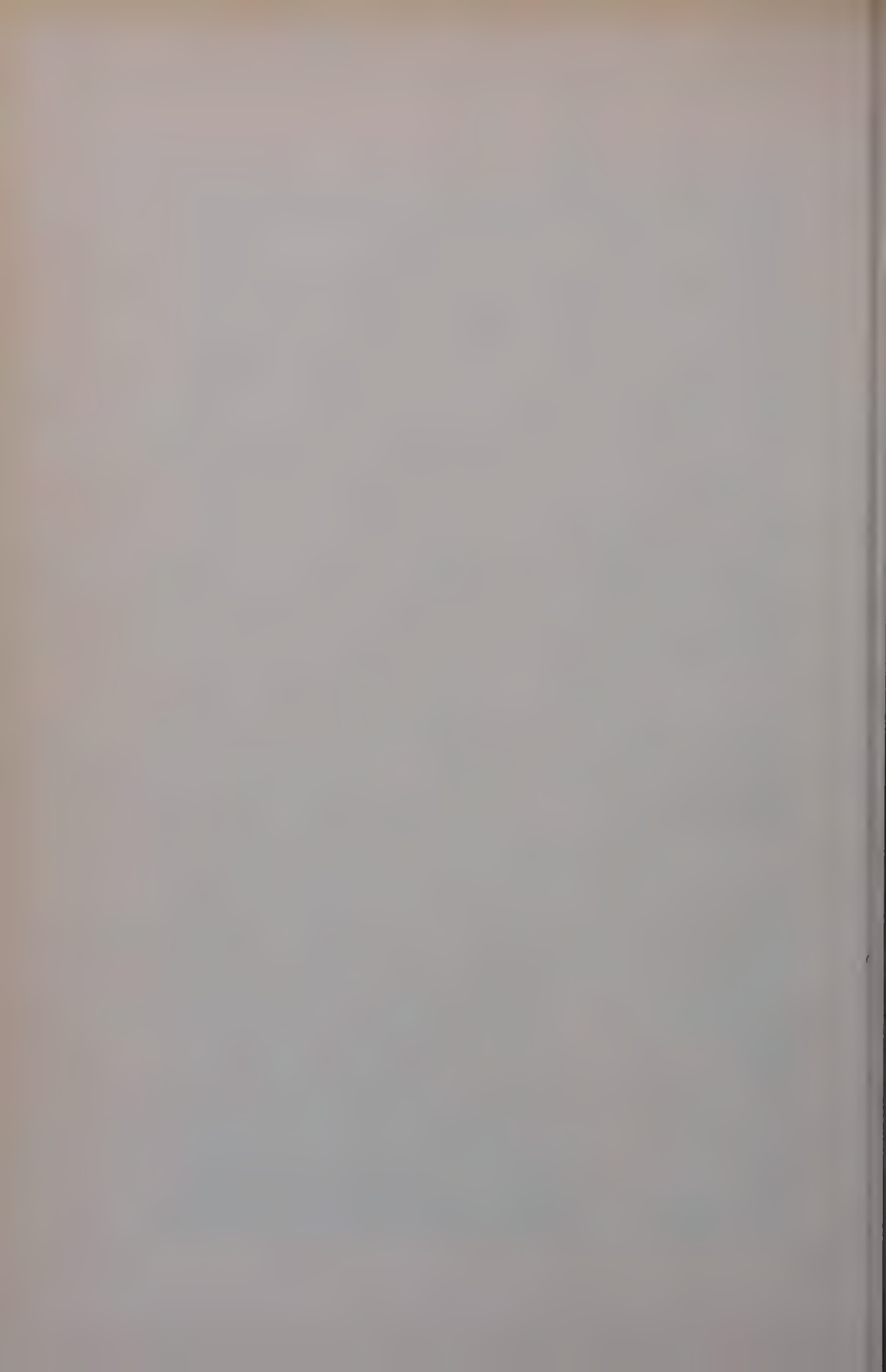
Ora sembra il momento di fare il punto sulla situazione raggiunta, di discutere i risultati, di progettare nuove esperienze, di creare una schiera di collaboratori e di giovani studiosi che, ricchi del patrimonio e dell'esperienza di altri, possano proseguire nel cammino intrapreso.

Principalmente con questo scopo la Società Italiana di Fisica ha organizzato questo Corso di Fisica del Plasma con applicazioni astrofisiche che oggi si inaugura ed al quale partecipano specialisti e studiosi di ambo le scienze in misura pressochè uguale. L'interesse da esso suscitato nel mondo scientifico è documentato dal numero sovrabbondante di domande che la Direzione del Corso ha dovuto selezionare e ridurre per ragioni essenzialmente pratiche.

Nel chiudere questo breve discorso desidero formulare l'augurio che l'incontro fra i cultori della Fisica del plasma e gli astrofisici sia ricco di risultati e che questa collaborazione porti ad un maggiore progresso sia nel campo scientifico che in quello non meno importante delle applicazioni pratiche del plasma.



1.	R. Kiepenheuer	14.	C. M. Braams	27.	J. Heidmann	40.	L. Hogberg	53.	P. J. Kellogg	66.	L. Musunneck
2.	D. Reagan	15.	G. Barsanti	28.	P. Gratreau	41.	C. Maissner	54.	P. Arvi	67.	A. Rughini
3.	F. Lerda	16.	R. E. Harrison	29.	D. La Roy	42.	T. El-Khalafawi	55.	L. Davis Jr.	68.	E. G. Forbes
4.	P. Sona	17.	B. Brunelli	30.	V. Ferraro	43.	G. Noci	56.	R. C. Giovanelli	69.	A. H. Sillesen
5.	M. Galli	18.	C. Mercier	31.	F. R. Schwarzl	44.	P. Sturrock	57.	E. Welbel	70.	T. Gold
6.	T. Consofi	19.	C. Bonazzola	32.	S. Segre	45.	P. Rothwell	58.	P. C. Thonemann	71.	C. De Jager
7.	V. De Sabbata	20.	B. Wieder	33.	U. Ascoli Bartoli	46.	B. Lehnert	59.	G. Meister	72.	C. Goldstein
8.	A. Kranjc	21.	R. Gallet	34.	G. Godoli	47.	W. Lindt	60.	H. Trefall	73.	D. Oepts
9.	A. C. Ducati	22.	C. Terlouw	35.	M. Hack	48.	A. Gibson	61.	E. Lischer	74.	D. Catiani
10.	M. Bineau	23.	N. Talini	36.	Z. Jankovic	49.	C. Cipriani	62.	E. Canobbio		
11.	E. Schatzman	24.	G. Righini	37.	H. Wilhelmsson	50.	D. W. Mahaffey	63.	G. Rughini		
12.	A. Giaridini	25.	C. T. Jacobsen	38.	M. Gutmann	51.	L. Pennelegion	64.	C. Clancia		



General Theory of Plasma.

V. FERRARO

Queen Mary College - London

1. - Introduction.

The purpose of these lectures is to give an elementary discussion of the dynamics of ionized gases following the macroscopic method of the kinetic theory of gases. For a more complete account reference must be made principally to the treatise on gases by CHAPMAN and COWLING [1]; for this reason we shall, in these lectures, adopt the notation of this book.

Certain assumptions are made on the classical theory of gases; the salient ones are, firstly, the assumption of molecular chaos, in which it is supposed that particles having velocity resolutes lying within a certain range are, at any instant, distributed at random, independently of the position and velocities of the other particles. Secondly, it is assumed sufficient to consider only binary encounters between the particles. In an ionized gas, the Coulomb electrostatic interaction between ions and electrons, which are long range forces, makes this assumption suspect and indeed certain integrals in the theory of gases diverge to infinity for the inverse square law of force. However, COHEN, SPITZER and RUTLY [2] have shown that under certain conditions the effect of multiple encounters between ions and electrons is the same *as if* the collisions were binary ones, provided the collision cross-section is suitably defined.

The fundamental equation in the theory is the Boltzmann equation for the velocity distribution function f ; its solution is a matter of some difficulty. Methods of successive approximation have been devised for the two extreme cases, namely, the case when a characteristic length L comparable with the dimensions of the gas is large compared with the mean free path, l , and secondly when L is small compared with l . The first can be referred to as the case of high density and can be solved by the methods of CHAPMAN and ENSKOG [1]. The second was first treated by JAFFÉ [3] who obtained successive approximations to the solution of Boltzmann's equation by expanding f in inverse powers of the free path l .

In these lectures only the case of high density will be considered; to simplify the discussion we shall use the procedure of adopting a «time of relaxation» as is done in the theory of metals; support for this is lent by the investigations of BAYET, DELCROIX and DENISSE for a Lorentzian gas [4].

2. – Definitions.

2.1. *Velocity space.* – The position vector of a point P in space relative to an origin O will be denoted by \mathbf{r} (x, y, z) and an element of volume centred about P will be denoted by $d\mathbf{r}$. Thus $d\mathbf{r}$ has ranges $\pm \frac{1}{2}dx$, $\pm \frac{1}{2}dy$, $\pm \frac{1}{2}dz$, in cartesian co-ordinates.

The linear velocity of a particle will be denoted by \mathbf{c} and its speed by $c = |\mathbf{c}|$. The vector \mathbf{c} may likewise be regarded as the position vector in a *velocity space* and this point may be called the velocity point of the particle.

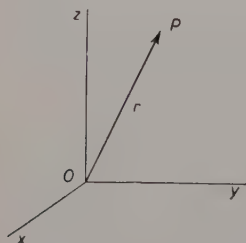


Fig. 1. – Position vector \mathbf{r} of a particle in ordinary space.

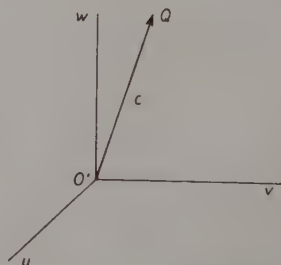


Fig. 2. – Velocity vector \mathbf{c} of a particle in velocity space.

An element of volume in the velocity space centred about \mathbf{c} will be denoted by $d\mathbf{c}$; it has ranges $\pm \frac{1}{2}du$, $\pm \frac{1}{2}dv$, $\pm \frac{1}{2}dw$ in cartesian co-ordinates.

The resolutes (x, y, z) of the position vector \mathbf{r} and the resolutes (u, v, w) of the velocity \mathbf{c} may be regarded as the co-ordinates of a point in a six dimensional phase space.

2.2. *Density and peculiar velocity.* – In a continuous medium the density at any point \mathbf{r} is defined to be the limit as $\delta\mathbf{r} \rightarrow 0$ of the ratio $\delta m / \delta\mathbf{r}$, where δm is the mass contained in the element of volume $\delta\mathbf{r}$. This definition cannot be applied to a gas of discrete particles since this would make the density fluctuate rapidly from point to point. We therefore proceed as follows; supposing that the particles are all alike, we define a physically small volume element $d\mathbf{r}$ as one which is large enough to contain a great number of particles, yet small enough compared with the scale of variation of physical quan-

tities in the gas. Then, the mass of the gas contained in the element $d\mathbf{r}$ averaged over an interval of time dt , small compared with the scale of time variations of the physical quantities, will be proportional to the volume of the element and independent of its shape. We may therefore denote it by $\varrho d\mathbf{r}$; then ϱ is the mass density.

Similarly the *number* of particles in $d\mathbf{r}$ averaged over dt is proportional to $d\mathbf{r}$ and may be written $n d\mathbf{r}$. Then n is called the number density. If m is the mass of a molecule then

$$(1) \quad \varrho = nm.$$

The *mean molecular velocity* at (\mathbf{r}, t) in the gas will be denoted by \mathbf{c}_0 and is defined by

$$(2) \quad (n d\mathbf{r})\mathbf{c}_0 = \sum \mathbf{c},$$

where the summation extends over all molecules in the element $d\mathbf{r}$ and $\sum \mathbf{c}$ is the average value over the time interval dt . Other mean values may be defined similarly. We may also specify the velocity \mathbf{c} of a particle by its velocity \mathbf{C} relative to axes moving with the mean velocity \mathbf{c}_0 . The velocity \mathbf{C} is then called the *peculiar velocity* of the particle. Its magnitude $C = |\mathbf{C}|$ is called the *peculiar speed*. The mean peculiar velocity of all molecules in the element $d\mathbf{r}$ is zero, by definition. The components of \mathbf{C} are denoted by U, V, W .

2'3. Velocity distribution function. — The probable number of particles which, at time t , are situated in the volume element $d\mathbf{r}$ centred at \mathbf{r} and have velocities in the range $\mathbf{c}, d\mathbf{c}$, is defined to be

$$(3) \quad f(\mathbf{c}, \mathbf{r}, t) d\mathbf{c} d\mathbf{r}.$$

This implies that any result which explicitly depends on f is an average characteristic of the gas. The function f is called the *velocity distribution function*; the number of velocity points in a volume element $d\mathbf{r}$ is clearly unaffected by a change of origin in the velocity space. If we change the origin to \mathbf{c}_0 , then, since the number of particles (3) is the same, it is also given by

$$(4) \quad f(\mathbf{C} + \mathbf{c}_0, \mathbf{r}, t) d\mathbf{C} d\mathbf{r},$$

which is often abbreviated to

$$(5) \quad f(\mathbf{C}, \mathbf{r}, t) d\mathbf{C} d\mathbf{r}.$$

The total number of particles in the element $d\mathbf{r}$ is obtained by integrating (3)

or (5) throughout the velocity space and this number is by hypothesis, $n d\mathbf{r}$. Thus

$$(6) \quad n = \int f(\mathbf{c}, \mathbf{r}, t) d\mathbf{c} \quad \text{or} \quad \int f(\mathbf{C}, \mathbf{r}, t) d\mathbf{C}.$$

3. - Mean values of functions of molecular velocities.

Let $\varphi(\mathbf{c}, \mathbf{r}, t)$ be a function of \mathbf{c} as well as of position and time. Then the time average of $\sum \varphi$ for the $n d\mathbf{r}$ particles in the element $d\mathbf{r}$ is by definition

$$(7) \quad (n d\mathbf{r}) \bar{\varphi} = \sum \varphi,$$

where $\bar{\varphi}$ is the mean value of φ . Since the contribution to $\sum \varphi$ from the molecules with velocity range $d\mathbf{c}$ about \mathbf{c} is $f\varphi d\mathbf{c} d\mathbf{r}$ we have by integration over the whole velocity space that

$$(8) \quad \sum \varphi = d\mathbf{r} \int f\varphi d\mathbf{c}.$$

Hence,

$$\bar{\varphi} = \frac{\int \varphi f d\mathbf{c}}{n} = \frac{\int \varphi f d\mathbf{c}}{\int f d\mathbf{c}}.$$

In particular, by definition, $\bar{\mathbf{c}} = \mathbf{c}_0$ whence

$$(9) \quad \mathbf{c}_0 = \frac{1}{n} \int \mathbf{c} f d\mathbf{c}.$$

4. - Boltzmann's equation.

The equation satisfied by the function f , from which all macroscopic or average properties of the gas are derived, was first derived by Boltzmann. It supposes that only binary encounters are important. Suppose that each particle is acted on by a force $m\mathbf{F}$ independent of \mathbf{c} . Then in a time dt in which a particle suffers no collision the position vector of its center of mass will change from \mathbf{r} to $\mathbf{r} + \mathbf{c}dt$, and its velocity from \mathbf{c} to $\mathbf{c} + \mathbf{F}dt$. Clearly, if the particles did not collide the same particles that occupied the volume of phase space $d\mathbf{r} d\mathbf{c}$ at time t would occupy the volume of phase space at time $t + dt$ centred at $\mathbf{r} + \mathbf{c}dt$, $\mathbf{c} + \mathbf{F}dt$. But the number in this set is

$$f(\mathbf{c} + \mathbf{F}dt, \mathbf{r} + \mathbf{c}dt, t + dt) d\mathbf{c} d\mathbf{r}.$$

The difference

$$[f(\mathbf{c} + \mathbf{F}dt, \mathbf{r} + \mathbf{c}dt, t + dt) - f(\mathbf{c}, \mathbf{r}, t)]d\mathbf{c}d\mathbf{r},$$

must therefore represent the difference in the gain of particles by the final set and the loss of particles to the original set in time dt . This must be proportional to $d\mathbf{c}d\mathbf{r}dt$ and is generally written $(\partial_e f / \partial t)_{\text{coll}} d\mathbf{c}d\mathbf{r}dt$. Thus, taking the limiting form of this equation as $dt \rightarrow 0$, we have Boltzmann's equation for f , *viz.*

$$(10) \quad \frac{\partial f}{\partial t} + (\mathbf{c} \cdot \nabla)f + (\mathbf{F} \cdot \nabla_c)f = \left(\frac{\partial f}{\partial t} \right)_{\text{coll}},$$

where ∇_c stands for the operator $(\partial/\partial u, \partial/\partial v, \partial/\partial w)$, *i.e.* the gradient vector operator in the velocity space. Thus $\partial_e f / \partial t$ is equal to the rate of change, by encounters, in the number of the class \mathbf{c} , $d\mathbf{c}$, per unit volume of real space in a *fixed* element of volume $d\mathbf{r}$ at \mathbf{r} , t .

In this derivation we have assumed that the volume element $d\mathbf{c}$ at time $t+dt$ is unaltered; this will only be the case, in general, if \mathbf{F} is independent of \mathbf{c} . Fortunately for an ionized gas in which a magnetic field \mathbf{B} is present, it can be shown that the Lorentz force $\mathbf{c} \times \mathbf{B}$ acting on a charge will leave the velocity range $d\mathbf{c}$ invariant in magnitude. Consequently, Boltzmann's equation for a gas consisting of ions of mass m and carrying a charge e is

$$(11) \quad \frac{\partial f}{\partial t} + (\mathbf{c} \cdot \nabla)f + \frac{e}{m}(\mathbf{E} + \mathbf{c} \times \mathbf{B}) \cdot \nabla_c f = \left(\frac{\partial f}{\partial t} \right)_{\text{coll}},$$

where \mathbf{E} is the electric field (expressed in e.m.u. units).

5. - Steady state.

Maxwell showed that a steady state solution of (10) in which $\partial f / \partial t = 0$ exists. In the absence of a body force the velocity distribution function is

$$(12) \quad f = A \exp [-hC^2],$$

where A and h are constants which can be found in terms of the temperature of the gas and the number density.

By definition, the kinetic temperature T of a gas is given by the equation

$$(13) \quad \frac{3}{2}kT = \frac{1}{2}m\overline{C^2},$$

where m is the mass of the particle and k an absolute constant, called Boltzmann's constant. Its value is $1.372 \cdot 10^{-16}$ erg $^{\circ}\text{K}$. It can also be shown that T is proportional to temperature on the thermodynamic scale. Using spherical polar co-ordinates in the velocity space (C, ϑ, φ) we have that $dC = C^2 dC \sin \vartheta d\vartheta d\varphi$, $0 \leq C \leq \infty$. Hence, using (6) we have

$$(14) \quad n = \int f(C) dC = \int_0^{\infty} A \exp[-hC^2] C^2 dC \int_0^{\pi} \sin \vartheta d\vartheta \int_0^{2\pi} d\varphi = A \left(\frac{\pi}{h}\right)^{\frac{3}{2}},$$

giving A . Also by (13)

$$\frac{3}{2} kT = \frac{1}{2} \frac{m}{r} \int f C^2 dC = \frac{mA}{2n} \int_0^{\infty} C^4 \exp[-hC^2] dC \int_0^{\pi} \sin \vartheta d\vartheta \int_0^{2\pi} d\varphi = \frac{3m}{4h}.$$

by (14).

Thus, finally

$$(15) \quad f(C) = n \left(\frac{m}{2\pi kT} \right)^{\frac{3}{2}} \exp \left[-\frac{mC^2}{2kT} \right].$$

If a conservative field of force is present, derived from a potential $\psi(\mathbf{r})$, it can be shown that

$$(16) \quad f(C, \mathbf{r}) = A \exp \left[-\frac{mC^2}{2kT} \right] \cdot \exp \left[-\frac{\psi}{kT} \right] = n \exp \left[-\frac{\psi}{kT} \right].$$

COWLING [1, p. 322-23] has shown that this result is unaffected by the presence of magnetic fields in ionized gases.

6. - Relaxation towards the steady state.

The solution of Boltzmann's equation for non-uniform gases can be found by successive approximation. The method is to write

$$f = f_0(1 + \varepsilon_1)$$

for the next approximation, where f_0 is the Maxwell velocity distribution function and ε_1 is small compared with unity. This corrects the distribution function by terms proportional to the derivatives of the temperature (heat conduction), velocity (viscosity) and density (diffusion). A non-uniform gas at rest will approach a Maxwellian distribution in a time τ comparable with the «collision interval». That is, the time which a molecule takes to describe a free path with the mean molecular speed $C = (8kT/m\pi)^{\frac{1}{2}}$.

In certain cases it can be shown that $\partial_e f / \partial t$ is of the form

$$(17) \quad -\frac{f(\mathbf{c}, \mathbf{r}, t) - f_0}{\tau(\mathbf{c}, \mathbf{r})},$$

where τ is the «time of relaxation» defined above. This means in effect that, if f_0 is the distribution function at time $t = 0$ and f the Maxwellian distribution function, then, the departure from the Maxwellian state $f - f_0 \rightarrow 0$ varies with time as $\exp[-t/\tau]$: *i.e.*

$$f = f_0 (1 - \exp[-t/\tau]).$$

7. - The equation of continuity and motion for a simple gas.

Let $\varphi(\mathbf{c})$ the any molecular property which is independent of \mathbf{r} and t . Multiply Boltzmann's equation by $\varphi d\mathbf{c}$ and integrate throughout the velocity space. Assuming that all the integrals are convergent we get the moment equation

$$(18) \quad \int \varphi \left(\frac{\partial f}{\partial t} + (\mathbf{c} \cdot \nabla) f + (\mathbf{F} \cdot \nabla_c) f \right) d\mathbf{c} = \int \varphi \frac{\partial f}{\partial t} d\mathbf{c};$$

but since φ is independent of \mathbf{r} and t we have, by (8),

$$\int \varphi \frac{\partial f}{\partial t} d\mathbf{c} = \frac{\partial}{\partial t} \int \varphi f d\mathbf{c} = \frac{\partial n \overline{\varphi}}{\partial t},$$

$$\int \varphi u \frac{\partial f}{\partial x} d\mathbf{c} = \frac{\partial}{\partial x} \int \varphi u f d\mathbf{c} = \frac{\partial n \overline{\varphi u}}{\partial x}, \quad \text{(for the first component of the second term in (18))}$$

$$\int \varphi \frac{\partial f}{\partial u} d\mathbf{c} = \int [\varphi f]_{u=-\infty}^{u=+\infty} dv dw - \int f \frac{\partial \varphi}{\partial u} d\mathbf{c} = -n \frac{\partial \overline{\varphi}}{\partial u}, \quad (f \text{ vanishes at } \pm \infty)$$

whence (18) becomes

$$(19) \quad \frac{\partial n \overline{\varphi}}{\partial t} + \nabla \cdot (n \overline{\varphi \mathbf{c}}) - n \mathbf{F} \cdot \overline{\nabla_c \varphi} = \int \varphi \frac{\partial_e f}{\partial t} d\mathbf{c}.$$

Also $\int \varphi (\partial_e f / \partial t) d\mathbf{c}$ represents the rate of change of the mean value of φ due to collisions.

If we set $\varphi = 1$, $\overline{\varphi \mathbf{c}} = \mathbf{c}_0$, $\nabla_c \varphi = 0$; also $\int \varphi (\partial_e f / \partial t) d\mathbf{c} = 0$ since the number density in an element of volume cannot be changed by collisions. Hence (19)

becomes

$$(20) \quad \frac{\partial n}{\partial t} + \nabla \cdot (n \mathbf{c}_0) = 0,$$

which is the equation of continuity.

If we set $\varphi = m\mathbf{c}$, then $\overline{\varphi} = m\mathbf{c}_0$, also $\overline{\varphi\mathbf{c}} = \overline{m\mathbf{c}\mathbf{c}} = m(\overline{\mathbf{c}_0 + \mathbf{C}})(\overline{\mathbf{c}_0 + \mathbf{C}}) = m\mathbf{c}_0\mathbf{c}_1 + m\overline{\mathbf{C}\mathbf{C}}$. We define $nm\overline{\mathbf{C}\mathbf{C}}$ to be the pressure tensor in the gas at time t relative to a set of axes moving with the mean velocity \mathbf{c}_0 ; we may write $n\overline{\varphi\mathbf{c}} = nm\mathbf{c}_0\mathbf{c}_0 + \mathbf{p}$ and

$$\nabla \cdot (n\overline{\varphi\mathbf{c}}) = \nabla \cdot nm\mathbf{c}_0\mathbf{c}_0 + \nabla \cdot \mathbf{p} = nm\mathbf{c}_0 \cdot \nabla \mathbf{c}_0 + \mathbf{c}_0 \nabla \cdot (nm\mathbf{c}_0) + \nabla \cdot \mathbf{p}.$$

Hence, (19) gives

$$\frac{\partial}{\partial t} (nm\mathbf{c}_0) + nm\mathbf{c}_0 \cdot \nabla \mathbf{c}_0 + \mathbf{c}_0 \nabla \cdot (nm\mathbf{c}_0) + \nabla \cdot \mathbf{p} - nm\mathbf{F} = \int \varphi \frac{\partial \mathbf{c}}{\partial t} d\mathbf{c},$$

since $\mathbf{F} = \mathbf{F} \cdot \overline{\nabla_{\mathbf{c}} \varphi}$. Also using (20) this reduces to

$$(21) \quad nm \frac{\partial \mathbf{c}_0}{\partial t} + nm\mathbf{c}_0 \cdot \nabla \mathbf{c}_0 = nm\mathbf{F} - \nabla \cdot \mathbf{p},$$

remembering that the momentum of an element is conserved during collision. The pressure tensor \mathbf{p} is then

$$(22) \quad \mathbf{p} = \varrho \begin{bmatrix} \overline{U^2}, & \overline{UV}, & \overline{UW} \\ \overline{VU}, & \overline{V^2}, & \overline{VW} \\ \overline{WU}, & \overline{WV}, & \overline{W^2} \end{bmatrix}.$$

where ϱ is the density.

If the velocity is isotropic, then $\overline{VW} = 0$, etc., and $\overline{U^2} = \overline{V^2} = \overline{W^2} = \frac{1}{3}(\overline{U^2} + \overline{V^2} + \overline{W^2}) = \frac{1}{3}\overline{C^2}$ and

$$(23) \quad \mathbf{p} = \begin{bmatrix} \frac{1}{3}\varrho\overline{C^2} & 0 & 0 \\ 0 & \frac{1}{3}\varrho\overline{C^2} & 0 \\ 0 & 0 & \frac{1}{3}\varrho\overline{C^2} \end{bmatrix},$$

which represents a hydrostatic pressure. Since by definition $\frac{1}{2}m\overline{C^2} = \frac{3}{2}kT$, this gives the gas equation

$$(24) \quad p = knT.$$

3. - The equations for a plasma.

We may consider a plasma to be a mixture of two different gases, namely the positive ion gas, (referred to by the suffix 1), and the electron gas (referred to by the suffix 2). Thus, n_1 and n_2 denote the densities of the ions and electrons at r, t , respectively and m_1, m_2 denote their respective molecular masses and we write

$$(25) \quad \rho_1 = n_1 m_1, \quad \rho_2 = n_2 m_2$$

for the densities of the gases. Likewise, c_1, c_2 denote the velocities of a typical ion or electron and \bar{c}_1, \bar{c}_2 their mean values. Let

$$(26) \quad n_0 = n_1 + n_2, \quad \rho_0 = \rho_1 + \rho_2.$$

Then n_0 is the number density of the plasma and ρ_0 its mass density.

The mean mass velocity of the plasma c_0 is defined by equation

$$(27) \quad \rho_0 c_0 = \rho_1 \bar{c}_1 + \rho_2 \bar{c}_2$$

and the *peculiar velocities* of the ions and electrons, C_1 and C_2 are defined by the equations

$$(28) \quad C_1 = c_1 - c_0, \quad C_2 = c_2 - c_0.$$

It follows from (27) that

$$(29) \quad \rho_1 \bar{C}_1 + \rho_2 \bar{C}_2 = 0.$$

The partial and total pressures are defined as for a simple gas in a frame of reference moving with the mean velocity c_0 . Thus

$$(30) \quad p_1 = \rho_1 \overline{C_1 C_1}, \quad p_2 = \rho_2 \overline{C_2 C_2}, \quad p_0 = p_1 + p_2$$

give the partial pressure tensors for the ion gas and electron gas respectively, and the total pressure tensor is p_0 . The hydrostatic partial pressures are defined by

$$(31) \quad p_1 = \frac{1}{3} \rho_1 \overline{C_1^2}, \quad p_2 = \frac{1}{3} \rho_2 \overline{C_2^2},$$

and the corresponding mean kinetic temperatures by T_1, T_2, T_0 where, in accordance with (24),

$$(32) \quad p_1 = k n_1 T_1, \quad p_2 = k n_2 T_2, \quad p_0 = k n_0 T_0$$

whence

$$(33) \quad n_0 T_0 = n_1 T_1 + n_2 T_2.$$

The velocity distribution function for the ion and electron gases are denoted by

$$(34) \quad f_1(\mathbf{c}_1, \mathbf{r}, t); \quad f_2(\mathbf{c}_2, \mathbf{r}, t)$$

or briefly, f_1, f_2 if the suffixes 1, 2 are understood to be operative on variables also. Boltzmann's equations for the two functions f_1 and f_2 are:

$$(35) \quad \frac{\partial f_i}{\partial t} + (\mathbf{c}_i \cdot \nabla) f_i + (\mathbf{F}_i \cdot \nabla_{\mathbf{c}_i}) f_i = \frac{\partial_e f_i}{\partial t}, \quad (i = 1, 2),$$

and $m_1 \mathbf{F}_1, m_2 \mathbf{F}_2$ are the forces acting on an ion and electron respectively. Thus, if these are due to an electric field \mathbf{E} and a magnetic field \mathbf{B} ,

$$(36) \quad \mathbf{F}_1 = \frac{e_1}{m_1} (\mathbf{E} + \mathbf{c}_1 \times \mathbf{B}), \quad \mathbf{F}_2 = \frac{e_2}{m_2} (\mathbf{E} + \mathbf{c}_2 \times \mathbf{B}),$$

where e_1 and e_2 are the charges carried by an ion and electron respectively.

We next derive the equations for changes of molecular properties: let $\varphi_i(\mathbf{c}_i)$ be any such molecular property for the two gases, which as before, we shall suppose to be independent of \mathbf{r} and t .

Then as in Sect. 7, we derive the equations

$$(37) \quad \frac{\partial n_i \bar{\varphi}_i}{\partial t} + \nabla \cdot (n_i \bar{\varphi}_i \mathbf{c}_i) - n_i \mathbf{F}_i \cdot \nabla_{\mathbf{c}_i} \bar{\varphi}_i = \int \varphi_i \frac{\partial_e f}{\partial t} d\mathbf{c}_i, \quad (i = 1, 2).$$

The right hand side represents the rate of change of the mean value of φ_i , due to collision. As before, this vanishes if $\varphi_i = 1$ (since the rate at which the number density of either gas is being changed by collision is zero), and (37) gives

$$(38) \quad \frac{\partial n_i}{\partial t} + \nabla \cdot (n_i \mathbf{c}_0) + \nabla \cdot (n_i \bar{\mathbf{c}}_i) = \frac{\partial n_i}{\partial t} + \nabla \cdot (n_i \bar{\mathbf{c}}_i) = 0, \quad (i = 1, 2)$$

where $\bar{\mathbf{c}}_i$ is defined by

$$(39) \quad n_i \bar{\mathbf{c}}_i = \int \mathbf{c}_i f_i d\mathbf{c}_i.$$

This is the equation of continuity for the separate ionic and electronic constituents of the plasma.

Again multiplying the two equations (38) corresponding to the ions and electrons by m_1 and m_2 respectively, and adding, we find:

$$(40) \quad \frac{\partial \varrho_0}{\partial t} + \nabla \cdot (\varrho_0 \mathbf{c}_0) = 0,$$

which is the equation of continuity of mass of the plasma as a whole.

Now set $\varphi_i = m_i \mathbf{c}_i$, $i = 1, 2$; then

$$(41) \quad \overline{\varphi_i} = m_i \overline{\mathbf{c}_i} = m_i \mathbf{c}_0 + m_i \overline{\mathbf{C}_i},$$

$$(42) \quad \overline{\varphi_i \mathbf{C}_i} = m_i \overline{\mathbf{c}_i \mathbf{C}_i} = m_i \mathbf{c}_0 \mathbf{c}_0 + m_i \mathbf{c}_0 \overline{\mathbf{C}_i} + m_i \overline{\mathbf{C}_i} \mathbf{c}_0 + m_i \overline{\mathbf{C}_i \mathbf{C}_i}$$

and proceeding as before we find from (37), (writing $\varrho_i = n_i m_i$, $\mathbf{p}_i = n_i m_i \overline{\mathbf{C}_i \mathbf{C}_i}$),

$$(43, 44) \quad \frac{\partial \varrho_i \mathbf{c}_0}{\partial t} + \frac{\partial \varrho_i \overline{\mathbf{C}_i}}{\partial t} + \nabla \cdot \mathbf{p}_i - \varrho_i \mathbf{F}_i + \nabla \cdot (\varrho_i \mathbf{c}_0 \mathbf{c}_0) \\ + \nabla \cdot (\varrho_i \mathbf{c}_0 \overline{\mathbf{C}_i}) + \nabla \cdot (\varrho_i \overline{\mathbf{C}_i} \mathbf{c}_0) = \int m_i \mathbf{c}_i \frac{\partial f_i}{\partial t} d\mathbf{c}_i. \quad (i = 1, 2).$$

Using the identity $\nabla \cdot (\mathbf{u}\mathbf{v}) = (\mathbf{u} \cdot \nabla)\mathbf{v} + (\nabla \cdot \mathbf{u})\mathbf{v}$ to expand the last three terms on the left hand side of (44) and eliminating $\nabla \cdot (\varrho_i \mathbf{c}_0)$ between this equation and that obtained from (38) after multiplication by $m_i \mathbf{c}_0$, we find finally

$$(45) \quad \varrho_i \frac{d\mathbf{c}_0}{dt} + (\nabla \cdot \mathbf{p}_i - \varrho_i \mathbf{F}_i) + \frac{d\varrho_i \overline{\mathbf{C}_i}}{dt} + \varrho_i (\overline{\mathbf{C}_i} \cdot \nabla) \mathbf{c}_0 + \varphi_i \overline{\mathbf{C}_i} (\nabla \cdot \mathbf{c}_0) = \int m_i \mathbf{c}_i \frac{\partial f_i}{\partial t} d\mathbf{c}_i,$$

where

$$(46) \quad \frac{d}{dt} = \frac{\partial}{\partial t} + \mathbf{c}_0 \cdot \nabla.$$

Add the equations (45) for the ions and electrons; then noting that the sum

$$\int m_i \mathbf{c}_i \frac{\partial f_i}{\partial t} d\mathbf{c}_i + \int m_2 \mathbf{c}_2 \frac{\partial f_2}{\partial t} d\mathbf{c}_2,$$

vanishes, since the total momentum of the ions and electrons is unaltered by collisions, we find, using (29), that

$$(47) \quad \varrho_0 \frac{d\mathbf{c}_0}{dt} = -\nabla \cdot \mathbf{p}_0 + \varrho_1 \mathbf{F}_1 + \varrho_2 \mathbf{F}_2,$$

which is the equation of mass motion. Equation (45) refers effectively to an element of either gas following the mass motion of the gas. An equation can be obtained by referring the motion to the local mean velocity of an element of either gas. Denoting by d_i/dt the mobile operator following the mean motion of the i -th constituent of the gas, so that

$$(48) \quad \frac{d_i}{dt} = \frac{\partial}{\partial t} + \bar{\mathbf{c}}_i \cdot \nabla,$$

we find after some rearrangement of the terms the following equation

$$(49) \quad \varrho_i \frac{d_i \bar{\mathbf{C}}_i}{dt} + \nabla \cdot \mathbf{P}_i - \varrho_i \mathbf{F}_i - \nabla \cdot (\varrho_i \bar{\mathbf{C}}_i \bar{\mathbf{c}}_i) = \int m_i \mathbf{c}_i \frac{\partial f_i}{\partial t} d\mathbf{c}_i.$$

It is therefore appropriate to introduce the *relative pressure tensor* \mathbf{P}_i defined by

$$(50) \quad \mathbf{P}_i = \varrho_i \bar{\mathbf{C}}_i \bar{\mathbf{C}}_i - \varrho_i \bar{\mathbf{C}}_i \bar{\mathbf{c}}_i$$

so that (49) becomes

$$(51) \quad \varrho_i \frac{d_i \bar{\mathbf{C}}_i}{dt} + \nabla \cdot \mathbf{P}_i - \varrho_i \mathbf{F}_i = \int m_i \mathbf{c}_i \frac{\partial f_i}{\partial t} d\mathbf{c}_i.$$

This corresponds to equation (2.4), pag. 18, given by L. SPITZER in his book on ionized gases. It should however be noted that Spitzer's definition of the pressure tensor does not coincide with that given in (49), *i.e.* with the Chapman-Cowling definition.

Since for a simple gas $\bar{\mathbf{C}}_i = 0$, it follows that in this case (51) reduces to (21) as should be the case. Whether one uses equations referred to the mean mass velocity or to the mass velocity of a particle depends to a large extent on the problem one is considering. When one is concerned with the motion of the gas as a whole it is best to use a pressure evaluated relative to the mass velocity. When one is concerned with the motion of a single constituent Spitzer's definition has something to recommend it.

The pressure tensor (50) will in general have 6 components since $P_{ij} = P_{ji}$; if the distribution of random velocities is isotropic, the non-diagonal elements vanish. There are then two possibilities: firstly the three elements are all equal. In this case the pressure tensor reduces to a scalar, the hydrostatic pressure P , and $\nabla \cdot \mathbf{P}$ reduces to ∇P . Secondly, P_{xx} , P_{yy} , P_{zz} are all different so that the «pressure» is different in different directions. Such a situation can arise in the absence of collisions, when the compression of the gas in one direction increases the root mean square velocity in that direction without affecting it in the other two. The case when the «non-diagonal elements» differ from zero, gives rise to the phenomenon of viscosity.

9. - Approximate calculation of the collision terms.

An exact evaluation of the collision terms on the right hand side of (51) can only be obtained by considering detailed collisions. An approximate evaluation, however, can be affected by using the time of relaxation as defined in Sect. 6. Let τ_i be the «relaxation time» appropriate to the i -th gas constituent so that we may write approximately

$$(52) \quad \frac{\partial_i f_i}{\partial t} = \frac{f_i^{(0)} - f_i}{\tau_i},$$

where $f_i^{(0)}$ denotes the Maxwellian distribution function for this gas. Write also

$$(53) \quad \mathbf{c}_i = \mathbf{c}_0 + \mathbf{C}_i;$$

then the right hand side of (51) becomes

$$(54) \quad \int m_i \mathbf{c}_0 \frac{\partial_i f_i}{\partial t} d\mathbf{c}_i + \int m_i \mathbf{C}_i \frac{\partial_i f_i}{\partial t} d\mathbf{c}_i.$$

But since \mathbf{c}_0 can be treated as constant in the first integral, and since $\int (\partial_i f_i / \partial t) d\mathbf{c}_i = 0$, it follows that (54) reduces to

$$(55) \quad \int m_i \mathbf{C}_i \frac{\partial_i f_i}{\partial t} d\mathbf{c}_i.$$

Substituting (52) in (55) and since $d\mathbf{c}_1 = d\mathbf{C}_i$, this reduces to

$$(56) \quad \int m_i \mathbf{C}_i (f_i^{(0)} / \tau_i) d\mathbf{C}_i - \int m_i \mathbf{C}_i (f_i / \tau_i) d\mathbf{c}_i.$$

But $\int \tau_i^{-1} \mathbf{C}_i f_i^{(0)} d\mathbf{C}_i$, vanishes identically; hence (56) reduces to

$$(57) \quad -n_i m_i \tau_i^{-1} \bar{\mathbf{C}}_i.$$

Adding the integrals corresponding to the ions and electrons we have

$$(58) \quad n_1 m_1 \tau_1^{-1} \bar{\mathbf{C}}_1 + n_2 m_2 \tau_2^{-1} \bar{\mathbf{C}}_2 = 0.$$

However, the times of relaxation for the ion and electron gases must be the

same, whence, denoting this common relaxation time by τ

$$(59) \quad \tau^{-1}(n_1 m_1 \bar{C}_1 + n_2 m_2 \bar{C}_2) = 0,$$

which is equation (29). Let the integral on the right hand side of (51) be denoted by I_i ; then $I_1 + I_2 = 0$, by (59). Also

$$\bar{C}_1 = -I_1 \tau / n_1 m_1, \quad \bar{C}_2 = -I_2 \tau / n_2 m_2$$

and thus

$$(60) \quad \bar{C}_1 - \bar{C}_2 = \bar{c}_1 - \bar{c}_2 = -(I, \tau) \left(\frac{1}{\varrho_1} + \frac{1}{\varrho_2} \right) = -\frac{\varrho_0 \tau}{\varrho_1 \varrho_2} I_1.$$

Thus we may express I_1 in the form

$$(61) \quad I_1 = -\frac{\varrho_1 \varrho_2}{\varrho_0} (\bar{c}_1 - \bar{c}_2) / \tau,$$

and (51) can finally be written

$$(62) \quad \varrho_i \frac{d_i \bar{c}_i}{dt} + \nabla \cdot P_i - \varrho_i F_i = -\frac{\varrho_1 \varrho_2}{\varrho_0 \tau} (\bar{c}_1 - \bar{c}_2).$$

This is the equation of motion of an ion or electron in the plasma and is fundamental in the theory.

10. - The existence of a time of relaxation.

We shall now attempt to justify the assumption of a relaxation time; the discussion, however, is not rigorous. The collision terms for a plasma $\partial_e f_i / \partial t$ can be expressed as the sum of two terms, namely d_{ii} and d_{ij} ($i, j = 1, 2$), which represent respectively the effect of collision between particles of the same kind and those of opposite charges. It will suffice to confine our attention to the latter case. Suppose then that a particle A_i of the class i collides with one of class j and that the radius of the « sphere S of action » is R . The value of R will be determined in Sect. 12. Let the velocities of the particle A_i before and after impact be c_i, c'_i . The number of particles of class i colliding with an element dS of surface of the sphere S subtending a solid angle $d\omega$ at the centre during time dt is equal to the number of particles of class i in a cylinder whose slant height is $c_i dt$ and whose base is the element dS .

The volume of this element is

$$R^2 d\omega dt c_i \cdot n,$$

where \mathbf{n} is a unit vector along the normal of the sphere at the point of « contact ». The number of collisions per unit time undergone by the particles of class i whose velocities lie in the range \mathbf{c}_i , $d\mathbf{c}_i$ is

$$R^2 d\omega \mathbf{c}_i \cdot \mathbf{n} f_i(\mathbf{c}_i) d\mathbf{c}_i.$$

Likewise the number of collisions whose velocities *after* collisions lie in the range \mathbf{c}_i , $d\mathbf{c}_i$ is

$$R^2 d\omega \mathbf{c}_i \cdot \mathbf{n} f_i(\mathbf{c}_i') d\mathbf{c}_i.$$

If the number of particles of class j per unit volume is n_j , we have therefore that the number of particles of class i gained by the element $d\mathbf{r} d\mathbf{c}_i$ of phase space by collisions in time dt is

$$(63) \quad \frac{\partial_e f_i}{\partial t} d\mathbf{c}_i = n_j R^2 \int [f_i(\mathbf{c}_i') - f_i(\mathbf{c}_i)] \mathbf{c}_i \cdot \mathbf{n} d\omega.$$

Since Boltzmann's equation is linear in the velocity, it suggests that we should seek a solution of the form

$$(64) \quad f_i(\mathbf{c}_i) = f_i^{(0)}(\mathbf{c}_i) + \mathbf{c}_i \cdot \boldsymbol{\chi}_i(\mathbf{c}_i),$$

where $f_i^{(0)}$ is the Maxwellian distribution function and $\boldsymbol{\chi}_i$ a vector function to be found. Also, since the normal results of velocity of a particle of class i is reversed on impact we have

$$(65) \quad \mathbf{c}_i = \mathbf{c}_i' + 2(\mathbf{c}_i \cdot \mathbf{n}) \mathbf{n}.$$

Substituting (64) and (65) in (61) we find that

$$(66) \quad \left(\frac{\partial_e f}{\partial t} \right)_{\text{coll}} = n_j R \int (\mathbf{c}_i \cdot \mathbf{n}) (\mathbf{c}_i' - \mathbf{c}_i) \cdot \boldsymbol{\chi}_i(\mathbf{c}_i) d\omega = -2n_j R^2 \int (\mathbf{c}_i \cdot \mathbf{n})^2 \mathbf{n} \cdot \boldsymbol{\chi}_i d\omega.$$

Let θ be the angle made by \mathbf{c}_i with $-\mathbf{n}$ and α the angle made by $\boldsymbol{\chi}_i$ with \mathbf{n} ; then (66) may be written

$$(67) \quad \left(\frac{\partial_e f}{\partial t} \right)_{\text{coll}} = -2n_j R^2 c_i^2 \chi_i \int \cos \alpha \cos^2 \theta d\omega,$$

where $\chi_i = |\boldsymbol{\chi}_i|$.

Draw OP in the direction of \mathbf{c}_i from an origin O to cut the unit sphere of centre O in P . Let OQ be drawn in the direction of \mathbf{n} and OX in the direction

of χ . Then if φ be the angle XOP , we have

$$\cos \alpha = \cos \theta \cos \varphi + \sin \theta \sin \varphi \cos \psi.$$

Integrating with OP as polar axis and noting that $0 \leq \theta \leq \pi/2$, $0 \leq \psi \leq 2\pi$, we find

$$\cos \alpha \cos^2 \theta d\omega = \frac{1}{2}\pi \cos \varphi = \frac{1}{2}\pi(\mathbf{c}_i \cdot \boldsymbol{\chi})/c_i \chi.$$

Substituting in (67) we find finally,

$$\frac{\partial_e f}{\partial t} = -\pi n_j R^2 c_i (f_i - f_i^{(0)}),$$

which is of the form $(f_i^{(0)} - f_i)/\tau$ if we set $\tau = (\pi n_j R^2 c_i)^{-1}$.

11. - Electrical neutrality. The Debye distance.

A plasma will in general rapidly attain a state of almost complete neutrality. This is because the potential energy per particle resulting from any space charge would be enormously greater than its thermal energy. We can obtain the order of magnitude of the distance over which departures from neutrality can occur as follows. Maxwell's distribution functions for the positive ions and electrons are

$$(68) \quad n_1 \propto \exp[-eV/kT], \quad n_2 \propto \exp[eV/kT],$$

where T is the temperature of the plasma and V the electrostatic potential. Poisson's equation is

$$(69) \quad \nabla^2 V = -4\pi(n_1 - n_2)e.$$

Except where n_1 and n_2 differ greatly from unity, we can write to the first order

$$(70) \quad n_1 = \frac{1}{2}n_0 + \nu, \quad n_2 = \frac{1}{2}n_0 - \nu,$$

so that n_0 is the number density of a plasma, as is evident by expanding the exponential to the first power of eV/kT . Thus

$$(71) \quad n_1 - n_2 = 2\nu = -\frac{n_0 e V}{kT},$$

and (69) becomes

$$(72) \quad \nabla^2 V = \frac{4\pi n_0 e^2}{kT} V,$$

or putting

$$(73) \quad b^2 = \frac{kT}{4\pi n_0 e^2},$$

we have

$$(74) \quad \nabla^2 V = \frac{V}{b^2}.$$

Here b has the dimensions of a length and is called the Debye shielding distance. The reason is that the spherically symmetrical solution of (74) gives the potential of the field of a unit charge in the plasma, namely

$$(75) \quad \frac{1}{r} \exp \left[-\frac{r}{b} \right],$$

where r is the distance from the charge. At distances of few multiples of b the electric field of the point charge is shielded by the surrounding charges. LANGMUIR has, indeed, defined a plasma as an ionized gas whose dimensions are large compared with b . At the temperature of 1000° we find

$$(76) \quad b = 21/\sqrt{n_0} \text{ cm.}$$

So that for $n = 10^{16}$, we have $b = 2.1 \cdot 10^{-7}$ cm and so it is small. The quantity b is also roughly the thickness of the sheets which develop in plasma in contact with a solid surface; for in equilibrium a potential gradient arises near the walls reflecting most of the charges back into the plasma. And to do this the potential difference must be such that $eV \sim kT$. It follows at once that the thickness of the sheet is of the order of the Debye distance.

The rate of approach to the steady state given by eq. (74), may be obtained by using the equation of diffusion appropriate to a plasma at a uniform temperature and pressure, but non uniform in the number densities. Let these be $\frac{1}{2}n_0 \pm \nu$ as before; then the equation of diffusion is

$$(77) \quad \frac{\partial \nu}{\partial t} = D \nabla^2 \nu - \frac{\nu}{\tau_0},$$

where

$$(78) \quad \tau_0 = kT/4\pi n_0 e^2 D$$

and D is the coefficient of diffusion for the mixture of ions and electrons; D varies only very slightly with n over a large range of densities and tempe-

ratures, but varies as $T^{\frac{1}{2}}$. For a temperature of 1000° , its value is of the order of $4 \cdot 10^{17}$ and the corresponding value of τ_0 is of the order of 10^{-13} s. Thus the steady state is approached very rapidly, though the value of τ_0 is smaller than one would have expected.

12. - Collision interval and mean free path in a plasma.

Some idea of the order of magnitude of the mean free path in a plasma is of interest in connection with certain problems that will arise later. There are two methods of defining the mean free path in an ionized gas like a plasma. The first is to compare the formula for the coefficient of diffusion D derived, by elementary theory in terms of the mean free path, with the exact formula for D derived by the exact methods of the kinetic theory of gases. The second and more exact method which will be followed here, consists in determining the time taken for the path of a particle to be deflected through an angle δ say, which is usually taken to be 90° . Such a deflection may be produced by a single encounter with another particle or by a succession of feeble binary encounters in which the deflection of the path of a particle is less than δ , but

which produces a resultant deflection equal to δ . In the case of a plasma such feeble encounters are more effective in deflecting the particles than a single encounter because of the long range electrostatic forces between the charged particles. This was first pointed out by JEANS and the theory was refined by CHANDRASEKHAR.

The plasma will be supposed to be at uniform temperature and pressure and, as we have seen, electrically neutral. Let the charge on the positive ions be Ze , where e is the electronic charge. Then since the plasma is neutral, we must have

$$(79) \quad n_2 = Zn_1,$$

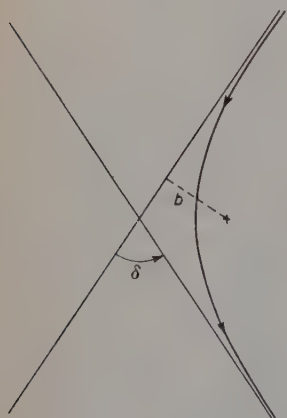


Fig. 3. - Hyperbolic orbit of an electron around a positive charge; b is the distance of the relative path at infinity from the positive charge, (impact parameter); δ is the angle through which the direction of motion of the electron is turned by the encounter.

the notations being the same as before.

In the first instance we neglect the encounters between the electrons and consider only those between ions and electrons. Let g denote the relative velocity of an electron and a ion in the relative hyperbolic orbit, b the perpendicular distance between the charge and the asymptotes, and δ the deflection of the relative path after the encounter.

Then we have

$$(80) \quad b = \frac{Ze^2}{g^2} \operatorname{ctg} \left(\frac{1}{2} \delta \right) \left(\frac{1}{m_1} + \frac{1}{m_2} \right).$$

We must now adopt some mean value for g^2 . If we neglect the ratio m_2/m_1 compared with unity, then g will be approximately the velocity of the electron before encounter. It is sufficient for the present purpose to take g^2 to be the mean square of the individual velocities so that

$$(81) \quad g^2 = 3kT/m_2,$$

whence (80) becomes

$$(82) \quad b = \left(\frac{Ze^2}{3kT} \right) \operatorname{ctg} \left(\frac{\delta}{2} \right).$$

Hence the probability that during an encounter between an electron and a positive ion the path of the electron is turned through an angle $\geq \delta$ after the encounter is such that the electron must be aimed at an ion within a perpendicular distance b . Since, on the whole, the motion of the ions can be ignored during encounters, the number of such encounters per electron per unit time is

$$(83) \quad \pi n_1 b^2 \bar{c}_2,$$

where \bar{c}_2 is the mean velocity of the electrons. The *collision interval* τ' is thus

$$(84) \quad \tau' = 1/\pi n_1 b^2 \bar{c}_2.$$

This expression must now be corrected for the effect of distant encounters; since we may neglect the velocity of the ion during an encounter, the relative velocity g will not differ greatly from the velocity of the electron. Now, the total change of velocity along the line of nearest approach is $2Ze^2/bgm_2$. The component of this velocity, c_n say, perpendicular to the direction of the relative velocity g is

$$(85) \quad 2Ze^2 \cos \left(\frac{1}{2} \delta \right) / bgm_2.$$

Since all direction of the plane containing g and the line of closest approach are all equally probable, the expectation of c_n after a series of encounters is

$$(86) \quad c_n^2 = \sum \left(\frac{2Ze^2}{bgm_2} \right)^2 \cos^2 \left(\frac{\delta}{2} \right).$$

Eliminating δ between this equation and (77) we find

$$(87) \quad c_n^2 = 4 \sum \left(\frac{Ze^2}{gm_2} \right)^2 \frac{1}{b^2 + \mu^2},$$

where

$$(88) \quad \mu = Ze^2/3kT.$$

It suffices to replace g^2 by its mean value given by (81) in the eq. (87) since the effect of encounters for which g is small are negligible. In an interval τ the number of encounters for which b lies between b and $b+db$ is

$$(89) \quad 2\pi n_1 \bar{c}_2 b db \tau$$

and hence from (87), the expectation of c_n^2 after time τ is

$$(90) \quad c_n^2 = \int_{b_1}^{b_2} 8\pi n_1 \bar{c}_1 \left(\frac{Ze^2}{gm_2} \right)^2 \tau \frac{b db}{b^2 + \mu^2} = 4\pi n_1 \bar{c}_2 \left(\frac{Ze^2}{gm_2} \right)^2 \tau \log \frac{b_2^2 + \mu^2}{b_1^2 + \mu^2}.$$

We may take $b_1 = 0$; as regards the upper limit we might set, after CHAPMAN, b_2 equal to the mean distance between the particles in the gas, *viz.* $n^{-\frac{1}{3}}$. But it has been shown that at distances greater than this, encounters are still correctly given by the formula for binary encounters. In fact, SPITZER has shown that a better approximation is to set b_2 equal to the Debye distance (*), *viz.*

$$(91) \quad b_2 = (kT/4\pi n e^2)^{\frac{1}{2}}.$$

We now define a collision between an electron and a ion when the direction of motion of the electron is turned through a right angle. For this to happen c_n must be comparable with c_2^2 or say g^2 . The free path of the electron l_2 is given by $\bar{c}_2 \tau$ and supposing that $\tau < \tau'$, we deduce from (90) that

$$(92) \quad l_2 = \frac{1}{4\pi n_1} \left(\frac{3kT}{Ze^2} \right)^2 \frac{1}{\log(1+a^2)},$$

where

$$(93) \quad a = \frac{b_2}{\mu} = \left(\frac{kT}{4\pi n_1 e^2} \right)^{\frac{1}{2}} \frac{3kT}{Ze^2} = \frac{3}{2Ze^3} \left(\frac{k^3 T^3}{\pi n} \right)^{\frac{1}{2}}.$$

(*) Dr. GALLET has pointed out that, in fact, the two different methods of approximation lead to practically the same result as far as orders of magnitude are concerned.

Likewise the collision interval τ_2 for the electrons may be defined as the time necessary for deflections less than a right angle to produce a resultant deflection of a right angle is

$$(94) \quad \tau_2 = \frac{1}{8n_1e^4} \left(\frac{3m_2}{2Z\pi} \right)^{\frac{1}{2}} \left(\frac{3kT}{Z} \right)^{\frac{3}{2}} \frac{1}{\log(1+a^2)}.$$

In deriving this expression we have not taken into account the encounters between electrons themselves. But in considering phenomena such as the electrical and thermal conductivities, depending on the diffusion between ions and electrons, encounters between α like particles are rightly neglected. Thus (92) and (94) give the values of the mean free path and collision interval for diffusion processes

These expressions, however, have been derived on the supposition that the relative orbits of the electrons around a positive nucleus are hyperbolic. This will be the case only if the mean kinetic energy of an electron $3kT/2$ exceeds its potential energy $2e^2/b_2$ at the distance b_2 from the ions defined by (91). Otherwise the electronic bound is an elliptic orbit. From (91) we see that this implies that $a \gg 1$. Hence, in the above formula we may replace the logarithmic term by $2 \log a$. Furthermore this condition makes $\tau < \tau'$, a condition already assumed earlier. In fact $\tau/\tau' = \frac{1}{4} \log(1+a^2)$ and since $a \gg 1$, we have $\tau/\tau' \sim (8 \log a)^{-1}$.

In dealing with a phenomenon such as viscosity, collisions between the particles are important, and the above expressions for l_2 and τ are thus too large. If it is found sufficient to consider collisions between the electrons the effect of which is to shorten the free path and collision intervals in the rates $1/(1+2^{\frac{1}{2}}/Z)$. Thus the correction is only necessary in the case of a proton plasma.

(Note: In Sect. 10 R_i was left undefined; its value for the electrons is given by $(\pi n_2 c_2 \tau_2)^{-\frac{1}{2}}$, where τ_2 is given by (94)).

13. - Numerical values.

Since $a \gg 1$, (92) and (94) may be written very nearly as

$$(95) \quad l_2 = \frac{1}{8\pi n_1 \log a} \left(\frac{3kT}{Ze^2} \right)^2,$$

$$(96) \quad \tau = \frac{1}{16n_1e^4 \log a} \left(\frac{3m_2}{2Z\pi} \right)^{\frac{1}{2}} \left(\frac{3kT}{Z} \right)^{\frac{3}{2}}.$$

SPITZER [5, p. 73] has given a table of values of $\log a$ for a proton-electron plasma for various values of the densities and temperatures. With permission

of the Publishers, Interscience Publ., New York, we reproduce part of that here; n denoting the electron density.

$\begin{smallmatrix} n \\ T \end{smallmatrix}$	1	10^3	10^6	10^9	10^{12}	10^{15}	10^{18}
10^2	16.3	12.8	9.43	5.97			
10^3	19.7	16.3	12.8	9.43	5.97		
10^4	23.2	19.7	16.3	12.8	9.43	5.99	
10^5	26.7	23.2	19.7	16.3	12.8	9.43	5.97
10^6	29.7	26.3	22.8	19.3	15.9	12.4	8.96
10^7	32.0	28.5	25.1	21.6	18.1	14.7	11.2
10^8	34.3	30.9	27.4	24.0	20.5	17.0	13.6

Inserting numerical values for the various constants ($e = 4.8 \cdot 10^{-10}$ e.s.u., $k = 1.37 \cdot 10^{-16}$ c.g.s.) we find from (95) that

$$(90a) \quad l_2 = \frac{1.26 \cdot 10^5 T}{n_1 Z^2 \log a} \quad \text{cm},$$

and

$$(91a) \quad \tau_2 = .214 \cdot \frac{T}{Z^2 n_1 \log a} \quad \text{s}.$$

For *protons* the corresponding time is $(1823)^{\frac{1}{2}} \tau_2$ or

$$(96b) \quad \tau_p = 9.15 \cdot T^{\frac{1}{2}} / (n_1 \log a) \quad \text{s},$$

which agrees with the values given by SPITZER.

The value of τ_p given by (96b) determines the value of the adiabatic constant γ to be used to determine the temperature T in an adiabatic compression ($T \propto n^{\gamma-1}$). If the time of compression is slow compared with τ_p , then $\gamma = \frac{5}{3}$. For compressions more rapid than τ_p , γ is equal to 2 or 3 according as the compression is two dimensional or one-dimensional.

14. - Electric currents in a plasma.

The *charge density* in the gas is defined by

$$(97) \quad \nu = (Zn_1 - n_2)e,$$

where e is the electronic charge in e.s.u. The *current density* vector is defined by

$$(98) \quad \mathbf{i} = n_1 Z_1 e \bar{\mathbf{c}}_1 - n_2 e \bar{\mathbf{c}}_2$$

or using (28) and considering mean values

$$(99) \quad \mathbf{i} = n_1 Z_1 e (\mathbf{c}_0 + \bar{\mathbf{C}}_1) - n_2 e (\mathbf{c}_0 + \bar{\mathbf{C}}_2) = \nu \mathbf{c}_0 + \mathbf{j},$$

where

$$(100) \quad \mathbf{j} = n_1 Z_1 e \bar{\mathbf{C}}_1 - n_2 e \bar{\mathbf{C}}_2.$$

Also

$$(101) \quad n_1 m_1 \bar{\mathbf{C}}_1 + n_2 m_2 \bar{\mathbf{C}}_2 = 0,$$

hence

$$(102) \quad \mathbf{j} = n_1 \left(Z_1 + \frac{m_1}{m_2} \right) e \bar{\mathbf{C}}_1 = -n_2 \left(\frac{Z_1 m_2}{m_1} + 1 \right) e \bar{\mathbf{C}}_2 = \frac{\varrho_1 \varrho_2}{\varrho_0} \left(\frac{Z}{m_1} + \frac{1}{m_2} \right) (\bar{\mathbf{C}}_1 - \bar{\mathbf{C}}_2) e.$$

Reference to eq. (62) shows that $\bar{\mathbf{c}}_1 - \bar{\mathbf{c}}_2 = \bar{\mathbf{C}}_1 - \bar{\mathbf{C}}_2$ and hence a current density may be produced by external forces (such as an electric field), a pressure gradient or by the inertia of the charges. We can evaluate the differential velocity $\bar{\mathbf{C}}_1 - \bar{\mathbf{C}}_2$ by considering the Boltzmann equation for each gas. An alternative procedure due to SCHLÜTER is to consider (62) and we shall consider this first. We shall assume that the pressure tensor reduces to hydrostatic pressure P_i , say, so that (62) becomes

$$(103) \quad \varrho_i \frac{d\bar{\mathbf{c}}_i}{dt} + \nabla P_i - \varrho_i \mathbf{F}_i = -\frac{\varrho_1 \varrho_2}{\varrho_0 \tau} (\mathbf{C}_1 - \mathbf{C}_2).$$

Let \mathbf{E} and \mathbf{B} denote the electric and magnetic field strength in e.m.u., ν the density as before and \mathbf{g} the gravitational acceleration on a particle.

Then

$$(104) \quad m_i \mathbf{F}_i = Z_i e (\mathbf{E} + \bar{\mathbf{c}}_i \times \mathbf{B}) + m_i \mathbf{g}$$

and since

$$\bar{\mathbf{c}}_i = \mathbf{c}_0 + \bar{\mathbf{C}}_i$$

this becomes

$$(105) \quad m_i \mathbf{F}_i = Z_i e (\mathbf{E} + \mathbf{c}_0 \times \mathbf{B}) + Z_i e \bar{\mathbf{C}}_i \times \mathbf{B} + m_i \mathbf{g}.$$

Comparing the equation

$$(106) \quad \varrho_1 \frac{d\bar{\mathbf{c}}_1}{dt} + \nabla P_1 - \varrho_1 \mathbf{F}_1 = -\frac{\varrho_1 \varrho_2}{\varrho_0 \tau} (\bar{\mathbf{C}}_1 - \bar{\mathbf{C}}_2),$$

for ions and the corresponding one for the electrons

$$(107) \quad \varrho_2 \frac{d\bar{\mathbf{c}}_2}{dt} + \nabla P_2 - \varrho_2 \mathbf{F}_2 = \frac{\varrho_1 \varrho_2}{\varrho_0 \tau} (\bar{\mathbf{C}}_1 - \bar{\mathbf{C}}_2),$$

we see that the left hand sides of the two equations are equal in magnitude; because the inertia of the electrons is so small we may neglect the first term on the left hand sides of (101) which then becomes approximately

$$(108) \quad \frac{\varrho_1 \varrho_2}{\varrho_0 \tau'} (\bar{C}_1 - \bar{C}_2) = \nabla P_2 - \varrho_2 \mathbf{F}_2;$$

gravitational terms may also be excluded from the equation for the same reason.

This equation can also be obtained by considering the solution of the Boltzmann equation and the approximation given in a previous section. Neglecting also the ratio m_2/m_1 compared with unity we find from (97) that approximately

$$(109) \quad \mathbf{j} \tau^{-1} = \frac{e}{m_2} (\nabla P_2 - \varrho_2 \mathbf{F}_2).$$

Also let

$$(110) \quad \mathbf{E}' = \mathbf{E} + \mathbf{c}_0 \times \mathbf{B},$$

be the electric field relative to axes moving with the mean-velocity \mathbf{c}_0 and using (103) to express \bar{C}_2 in terms of \mathbf{j} (neglecting the ratio m_2/m_1), we find approximately

$$(111) \quad \mathbf{j} \tau^{-1} + \mathbf{j} \times e \mathbf{B} / m_2 = \frac{n_2 e^2}{m_2} \mathbf{E}' + \frac{e}{m_2} \nabla P_2.$$

In the absence of a magnetic field, gravitational forces and pressure gradients, (111) reduces to Ohm's law

$$(112) \quad \mathbf{j} = \frac{n_2 e^2 \tau}{m_2} \mathbf{E}.$$

Thus the coefficient of \mathbf{E} is the electrical conductivity σ , where

$$(113) \quad \sigma = \frac{n_2 e^2 \tau}{m_2},$$

and e is measured in e.m.u. Introducing also the cyclotron angular velocity of the electrons $\omega_2 = e |\mathbf{B}| / m_2$, (105) may be rewritten in the form

$$(114) \quad \mathbf{j} + \omega_2 \tau \mathbf{j} \times \mathbf{B} / B = \sigma \left(\mathbf{E}' + \frac{1}{n_2 e} \nabla P_2 \right).$$

This is the approximate equation satisfied by the current in the plasma; the relative electron pressure gradient is equivalent to an extra electric field $\mathbf{E}'' = (1/n_2 e) \nabla P_2$ which may be considered additional to the existing field \mathbf{E}' due to the presence of external field sources.

Finally we consider the equation of mass motion; by (105) we have

$$\begin{aligned} m_1 \mathbf{F}_1 &= Z_1 e (\mathbf{E} + \mathbf{c}_0 \times \mathbf{B}) + Z_1 e \overline{\mathbf{C}}_0 \times \mathbf{B} + m_1 \mathbf{g}, \\ m_2 \mathbf{F}_2 &= -e (\mathbf{E} + \mathbf{c}_0 \times \mathbf{B}) - e \overline{\mathbf{C}}_2 \times \mathbf{B} + m_2 \mathbf{g}. \end{aligned}$$

Using (97), (98) and (110), we find from (47) that

$$(114a) \quad \varrho_0 \frac{d\mathbf{c}_0}{dt} = -\nabla \cdot p_0 + \nu \mathbf{E}' + \mathbf{j} \times \mathbf{B} + \varrho_0 \mathbf{g},$$

if the plasma is neutral, $\nu = 0$ and (108a) reduces to

$$(114b) \quad \varrho_0 \frac{d\mathbf{c}_0}{dt} = \mathbf{j} \times \mathbf{B} + \varrho_0 \mathbf{g} - \nabla \cdot p_0,$$

which is the equation of mass motion.

15. - Electrical and thermal conductivities in a plasma at rest.

To simplify the discussion we shall first of all suppose that there is no magnetic field present. Then in accordance with (105) and neglecting the ratio m_2/m_1 we have

$$(114c) \quad \mathbf{j} = -n_2 e \overline{\mathbf{C}}_2.$$

To evaluate this vector we must consider the solution of the Boltzmann equation. An approximate method of investigation is to assume a time of relaxation and replace the right hand side of (35) by

$$(115) \quad \frac{f_2^{(0)} - f_2}{\tau(C_2)},$$

in which $f_2^{(0)} - f_2$ is small compared with $f_2^{(0)}$. Substituting in (35) and retaining only first order terms on the left hand side we obtain:

$$(116) \quad f_2 = f_2^{(0)} - \tau (\mathbf{C}_2 \cdot \nabla) f_2^{(0)} - \tau (\mathbf{F}_2 \cdot \nabla_{\mathbf{c}_2}) f_2^{(0)},$$

where

$$(117) \quad f_2^{(0)} = n_2 \left(\frac{m_2}{2\pi kT} \right)^{\frac{3}{2}} \exp [-m_2 C_2^2 / 2kT].$$

Also, in the absence of a magnetic field,

$$(118) \quad \mathbf{F}_2 = -\frac{e}{m_2} \mathbf{E},$$

where \mathbf{E} is the electric field, so that (116) may be written

$$(119) \quad f_2 = f_2^{(0)} \left[1 - \tau (\mathbf{C}_2 \cdot \nabla) \log f_2^{(0)} + \frac{e\tau}{m_2} (\mathbf{E} \cdot \nabla \mathbf{C}_2) \log f_2^{(0)} \right];$$

now,

$$(120) \quad \log f_2^{(0)} = \text{const} + \log (n_2 T^{-\frac{1}{2}}) - m_2 C_2^2 / 2kT$$

and in a plasma, as we have seen, $\gamma = \frac{5}{3}$ in general, so that since $T \propto n_2^{\gamma-1}$, we have that $n_2 T^{-\frac{1}{2}}$ is constant. Thus

$$(121) \quad \nabla \log f_2^{(0)} = \frac{m_2 C_2^2}{2kT^2} \nabla T, \quad \nabla_{\mathbf{C}_2} \log f_2^{(0)} = -m_2 \mathbf{C}_2 / kT,$$

so that

$$(122) \quad f_2 = f_2^{(0)} \left[1 - \tau (\mathbf{C}_2 \cdot \nabla T) \frac{m_2 C_2^2}{2kT^2} - \frac{e\tau}{kT} (\mathbf{C}_2 \cdot \mathbf{E}) \right].$$

Hence

$$(123) \quad \mathbf{j} = e \int \mathbf{C}_2 f_2 d\mathbf{C}_2 = -e \int f_2^{(0)} \mathbf{C}_2 d\mathbf{C}_2 + e \int \tau f_2^{(0)} \mathbf{C}_2 \left[(\mathbf{C}_2 \cdot \nabla T) \frac{m_2 C_2^2}{2kT^2} + \frac{e}{kT} (\mathbf{C}_2 \cdot \mathbf{E}) \right] d\mathbf{C}_2,$$

or, since the first term vanishes identically,

$$(124) \quad \mathbf{j} = e \int \tau f_2^{(0)} (\mathbf{C}_2 \cdot \mathbf{B}) \mathbf{C}_2 d\mathbf{C}_2,$$

where

$$(125) \quad \mathbf{B} = \frac{m_2 C_2^2}{2kT^2} \nabla T + \frac{e\mathbf{E}}{kT}.$$

Now it is easily shown that

$$(126) \quad \int F(C_2) (\mathbf{A} \cdot \mathbf{C}_2) \mathbf{C}_2 d\mathbf{C}_2 = \frac{1}{3} \mathbf{A} \int F(C_2) C_2^2 d\mathbf{C}_2,$$

whence

$$(127) \quad \mathbf{j} = \frac{1}{3} \frac{em_2}{2kT^2} \nabla T J_2 + \frac{e^2 \mathbf{E}}{3kT} J_1,$$

where

$$(128) \quad J_1 = \int \tau C_2^4 f_2^{(0)} d\mathbf{C}_2, \quad J_2 = \int \tau C_2^4 f_2^{(0)} d\mathbf{C}_2,$$

In a first approximation we shall regard τ as independent of C_2 but depending on T and n . Then we find

$$(129) \quad J_1 = \frac{3kTn_2\tau}{m_2}, \quad J_2 = \frac{15}{4}n_2\left(\frac{2kT}{m_2}\right)^2\tau,$$

where τ is given by (96). Hence

$$(130) \quad \mathbf{j} = \frac{5n_2\tau ek}{2m_2}\nabla T + \frac{n_2e^2\tau}{m_2}\mathbf{E}.$$

Comparing with (112) we see that the coefficient of \mathbf{E} is the electrical conductivity as previously defined; hence we may write

$$(131) \quad \mathbf{j} = \sigma\mathbf{E} + \frac{5}{2}(k/e)\sigma\nabla T.$$

Thus the presence of a temperature gradient will give rise to an electric current associated with thermoelectric effects. The temperature gradient also gives rise to a flow of heat which we investigate next.

The heat density of a simple gas due to kinetic energy is defined to be $\frac{1}{2}nm\bar{C}^2$. In general therefore, the rate of heat flow is defined by the flux vector

$$(132) \quad \mathbf{q} = \frac{1}{2}nm\bar{C}^2\mathbf{C} = \int \frac{1}{2}mC^2Cf(\mathbf{C})d\mathbf{C}.$$

In the absence of a magnetic field the heat conduction will be mainly due to the electrons, so that we may treat the electron constituent in the plasma as a simple gas as before. Thus

$$(133) \quad \mathbf{q} = \frac{1}{2}m_2\int C_2^2C_{2f_2}(C_2)dC_2.$$

Using (122) we can write

$$(134) \quad \mathbf{q} = \frac{1}{2}m_2\int C_2^2C_2f_2^{(0)}dC_2 - \frac{1}{2}m_2\int \tau C_2^2C_2\frac{m_2C_2^2}{2kT^2}(C_2\cdot\nabla T)f_2^{(0)}dC_2 - \\ - \frac{1}{2}m_2\int \frac{e\tau}{kT}(C_2\cdot\mathbf{E})C_2^2C_2f_2^{(0)}dC_2.$$

In this expression the first term vanishes and using (126) we have

$$(135) \quad \mathbf{q} = -\frac{1}{12}\frac{m_2^2}{kT^2}\nabla T\int \tau C_2^6f_2^{(0)}dC_2 - \frac{1}{6}\frac{em_2}{kT}\mathbf{E}\int \tau C_2^4f_2^{(0)}dC_2,$$

whence we may write

$$(136) \quad \mathbf{q} = -\frac{1}{12} \frac{m_2^2}{kT^2} \nabla T J_3 - \frac{1}{6} \frac{em_2}{kT} \mathbf{E} J_2,$$

where J_2 is defined in (129) and

$$(137) \quad J_3 = \int \tau C_2^6 f_2^{(0)} dC_2.$$

If τ is assumed to be independent of C_2 , then

$$(138) \quad J_3 = \frac{105}{8} n_2 \tau \left(\frac{2kT}{m_2} \right)^3,$$

whence

$$(139) \quad \mathbf{q} = -\frac{35}{8} n_2 \tau k \left(\frac{2kT}{m_2} \right) \nabla T - \frac{5}{4} n_2 \tau e \left(\frac{2kT}{m_2} \right) \mathbf{E}.$$

Thus an electric field produces heat flow additional to that produced by the temperature gradient ∇T . In a steady state no current can flow in the direction of the temperature gradient due to this cause, since a secondary electric field is set up to balance the flow set up by the temperature gradient. Thus, in measuring the thermal conductivity we have a state in which $\mathbf{j} = 0$ in (131). Thus $\mathbf{E} = -\frac{5}{2}(k/e)\nabla T$ and substituting in (139) we find

$$(140) \quad \mathbf{q} = -\lambda \nabla T,$$

where

$$(141) \quad \lambda = \frac{5}{2} \frac{n_2 \tau k^2 T}{m_2}.$$

We note that $\lambda/\sigma = \frac{5}{2}(k/e)^2 T$.

16. - Modification due to the presence of the magnetic field.

In the presence of a magnetic field \mathbf{B} the force on an electron is

$$(142) \quad \mathbf{F}_2 = \frac{e}{m_2} (\mathbf{E} + \mathbf{C}_2 \times \mathbf{B}).$$

However, since $\mathbf{C}_2 \cdot (\mathbf{C}_2 \times \mathbf{B}) = 0$, we cannot proceed as in Sect. 15 but must consider the expression

$$(143) \quad f_1 = f_2^{(0)}(1 + \varphi)$$

and substitute in Boltzmann's equation. This becomes, since $\mathbf{C}_2 \cdot (\mathbf{C}_2 \times \mathbf{B}) = 0$,

$$(144) \quad (\mathbf{C}_2 \nabla) f_2^{(0)} + (\mathbf{F}_2 \cdot \nabla_{\mathbf{C}_2}) f_2^{(0)} + \frac{e}{m_2} f_2^{(0)} (\mathbf{C}_2 \times \mathbf{B}) \cdot \nabla_{\mathbf{C}_2} \varphi = -f_2^{(0)} \varphi / \tau,$$

where now $\mathbf{F}_2 = e\mathbf{E}/m_2$.

Now assume that

$$(145) \quad \varphi = \mathbf{d} \cdot \mathbf{C}_2 + \mathbf{d}' \cdot (\mathbf{C}_2 \times \mathbf{B}),$$

where \mathbf{d} and \mathbf{d}' are vectors perpendicular to \mathbf{B} and depending on C_2 only. Substituting in (144) we find

$$(146) \quad \mathbf{C}_2 \cdot \left[\nabla f_2^{(0)} + \frac{\mathbf{F}_2}{C_2} \frac{\partial f_2^{(0)}}{\partial C_2} \right] = -\frac{f_2^{(0)}}{\tau} [\mathbf{d} \cdot \mathbf{C}_2 + \mathbf{d}' \cdot (\mathbf{C}_2 \times \mathbf{B})] - \frac{e}{m_2} f_2^{(0)} [\mathbf{d} \cdot (\mathbf{C}_2 \times \mathbf{B}) - B^2 \mathbf{C}_2 \cdot \mathbf{d}'].$$

Equating the coefficients of \mathbf{C}_2 and $(\mathbf{C}_2 \times \mathbf{B})$ on both sides of the equation we find:

$$(147) \quad \nabla f_2^{(0)} + \frac{\mathbf{F}_2}{C_2} \frac{\partial f_2^{(0)}}{\partial C_2} = -f_2^{(0)} \left[\mathbf{d} \tau^{-1} - \frac{eB^2}{m_2} \mathbf{d}' \right],$$

$$(148) \quad 0 = -f_2^{(0)} \left[\mathbf{d}' \tau^{-1} + \frac{e}{m_2} \mathbf{d} \right].$$

Let $\omega = eB/m_2$, then solving this pair of equations for \mathbf{d} and \mathbf{d}' and substituting in (145) we find

$$(149) \quad f_2 = f_2^{(0)} - \frac{1}{1 + \omega^2 \tau^2} \left(\nabla f_2^{(0)} + \frac{\mathbf{F}_2}{C_2} \frac{\partial f_2^{(0)}}{\partial C_2} \right) \cdot \left(\mathbf{C}_2 - \frac{\omega \tau}{B} \mathbf{C}_2 \times \mathbf{B} \right),$$

$$(150) \quad = f_2^{(0)} \left\{ 1 - \frac{\tau}{1 + \omega^2 \tau^2} \mathbf{C}_2 \cdot \left[\mathbf{A} - \frac{\omega \tau}{B} \mathbf{B} \times \mathbf{A} \right] \right\},$$

where

$$(151) \quad \mathbf{A} = \nabla \log f_2^{(0)} + \frac{1}{C_2} \mathbf{F}_2 \frac{\partial \log f_2^{(0)}}{\partial C_2} = \frac{m_2 C_2^2}{2kT^2} \nabla T - \frac{m_2}{kT} \mathbf{F}_2 = \frac{m_2 C_2^2}{2kT^2} \nabla T - \frac{m_2}{kT} \mathbf{E}.$$

Comparing with (122) we see that the presence of the magnetic field can be accounted for by replacing the vectors ∇T and \mathbf{E} by

$$(152) \quad \frac{1}{1 + \omega^2 \tau^2} \left[\nabla T - \frac{\omega \tau}{B} \mathbf{B} \times \nabla T \right], \quad \frac{1}{1 + \omega^2 \tau^2} \left[\mathbf{E} - \frac{\omega \tau}{B} \mathbf{B} \times \mathbf{E} \right],$$

respectively.

Thus a magnetic field reduces conduction in the direction of the electric field (or temperature gradient) in the ratios $1:(1+\omega^2\tau^2)$ and in addition causes a transverse flow $\omega\tau$ times as large. These results are however approximate as no account has been taken of electron-electron interaction.

17. - Correction to the integrals J_1 , J_2 , J_3 .

In evaluating these integrals we have assumed that τ was independent of C_2 ; this is, in fact, not the case. A reference to Sect. 12 shows that

$$(153) \quad \tau = \mu C_2^3,$$

where

$$(154) \quad \mu = \frac{m_2^2}{16n_2e^4Z} \sqrt{\frac{3}{2\pi}} \frac{1}{\log_e a}.$$

Thus

$$(155) \quad J_1 = \mu \int C_2^5 f_2^{(0)} dC_2, \quad J_2 = \mu \int C_2^7 f_2^{(0)} dC_2, \quad J_3 = \mu \int C_2^9 f_2^{(0)} dC_2.$$

Evaluating these integrals and proceeding as in Sect. 15 we find the effective coefficient of thermal conductivity to be

$$(156) \quad \lambda = \frac{4\sqrt{3}}{\pi e^4 Z} \frac{k(kT)^{\frac{3}{2}}}{m_2^{\frac{1}{2}} \log_e a},$$

and the electrical conductivity

$$(157) \quad \sigma = \frac{e^2 J_1}{3kT} = \frac{\sqrt{3}}{\pi e^2 Z} \frac{(kT)^{\frac{3}{2}}}{m_2^{\frac{1}{2}} \log_e a}.$$

Inserting numerical values for the various constants we find

$$(158) \quad \lambda = 1.03 \cdot 10^{-12} \frac{T^{\frac{3}{2}}}{Z \log_e a} \quad \text{cal/(s deg cm)},$$

and

$$(159) \quad \sigma = 1.43 \cdot 10^{-13} \frac{T^{\frac{3}{2}}}{Z \log_e a} \quad \text{e.m.u.}$$

18. - The various conductivities. Dissipation of energy.

The results obtained in Sect. 16 may be derived more simply by considering equation (114)

$$(160) \quad \mathbf{j} + \omega_2 \tau \mathbf{j} \times \mathbf{B} / B = \sigma(\mathbf{E}' + \mathbf{E}'') \equiv \sigma \mathbf{E}_t,$$

say.

If \mathbf{E}_t is parallel to \mathbf{B} we have

$$\mathbf{j} \times \mathbf{B} + \frac{\omega_2 \tau}{B} [-(\mathbf{j} \cdot \mathbf{B})\mathbf{B} + B^2 \mathbf{j}] = 0,$$

whence (160) becomes

$$(161) \quad \mathbf{j} + \frac{\omega_2^2 \tau^2}{B^2} [B^2 \mathbf{j} - (\mathbf{B} \cdot \mathbf{j})\mathbf{B}] = \mathbf{j} = \sigma \mathbf{E}_t.$$

Hence conduction along lines of force is unaffected by the magnetic field. Consider next the case when \mathbf{E}_t is perpendicular to \mathbf{B} so that $\mathbf{E}_t \cdot \mathbf{B} = 0$. Then, from (160),

$$\mathbf{j} = \sigma \mathbf{E}_t - \frac{\omega_2 \tau}{B} \left[\sigma \mathbf{E}_t - \frac{\omega_2 \tau}{B} \mathbf{j} \times \mathbf{B} \right] \times \mathbf{B} = \sigma \mathbf{E}_t - \sigma \frac{\omega_2 \tau}{B} \mathbf{E}_t \times \mathbf{B} - \omega_2^2 \tau^2 \mathbf{j}.$$

Since $\mathbf{B} \cdot \mathbf{j} = \mathbf{B} \cdot \sigma \mathbf{E}_t$, by (160), this vanishes since $\mathbf{B} \cdot \mathbf{E}_t = 0$. Hence

$$(162) \quad \mathbf{j} = \sigma_{\parallel} \mathbf{E}_t + \sigma_{\perp} \mathbf{B} \times \mathbf{E}_t / B,$$

where

$$(163) \quad \sigma_{\parallel} = \sigma \frac{1}{1 + \omega_2^2 \tau^2}, \quad \sigma_{\perp} = \sigma \frac{\omega_2 \tau}{1 + \omega_2^2 \tau^2}.$$

Comparing with (131) and (152) we see that we recover the result of sect. 16. The conductivities σ_{\parallel} and σ_{\perp} are called respectively the « direct » and « transverse » conductivities, whilst in (162) the last term represents the Hall current. The effect of the magnetic field depends roughly on the magnitude of the product $\omega_2 \tau$, i.e., on the ratio of the cyclotron frequency to the collision frequency $1/\tau$. Thus, if the electrons are able to spiral freely between collisions, then $\omega_2 \tau \gg 1$, and $\sigma_{\parallel}/\sigma \sim 1/\omega_2^2 \tau^2$, so that the direct conductivity is greatly reduced. On the other hand, $\sigma_{\perp}/\sigma \sim (\omega_2 \tau)^{-1}$ and, though smaller than

the normal conductivity, is much larger than the direct conductivity. In this case the magnetic field greatly impedes the flux of electrons across the field. However, if the Hall current is perpendicular to the walls of the vessel containing the plasma, an electric field can often be set up which prevents any further flow of the current. Let the field be $\lambda \mathbf{B} \times \mathbf{E}_t$, where λ is a constant such that it prevents the flow of the Hall current. The total electric field is now $\mathbf{E} + \lambda \mathbf{B} \times \mathbf{E}_t$ and substituting in (162) and simplifying we find

$$(164) \quad \mathbf{j} = (\sigma_{\parallel} - \lambda \sigma_{\perp} B) \mathbf{E}_t + \sigma_{\parallel} \left[\lambda + \frac{\sigma_{\perp}}{\sigma_{\parallel} B} \mathbf{B} \times \mathbf{E}_t \right].$$

Thus if $\lambda = -\sigma_{\perp}/(\sigma_{\parallel} B)$, this reduces to

$$(165) \quad \mathbf{j} = \left(\sigma_{\parallel} + \frac{\sigma_{\perp}^2}{\sigma_{\parallel}} \right) \mathbf{E}_t = \sigma \mathbf{E}_t,$$

from (163).

Again, multiplying (160) scalarly by \mathbf{j} we have

$$(166) \quad j^2 = \sigma \mathbf{j} \cdot \mathbf{E}_t.$$

But $\mathbf{j} \cdot \mathbf{E}_t$ is the rate at which work is done on the electric current per unit volume, and j^2/σ must therefore represent the heating of the gas by the current, the same as in the absence of the magnetic field.

Alternatively, we may interpret the dissipation of the electric current as due to the work done against the collision drag in maintaining the relative velocity of the ions and electrons. Thus the rate of dissipation of energy is

$$\frac{\varrho_1 \varrho_2}{\varrho_0 \tau} (\bar{\mathbf{C}}_1 - \bar{\mathbf{C}}_2)^2,$$

or, by (103), approximately, $m_2 j^2 / (n_2 e^2 \tau)$, that is j^2/σ as before.

19. - Equation of diffusion.

19.1. *Plasma at rest and no magnetic field.* - In a plasma at rest, equations (45) and (57) can be combined in the form

$$(167) \quad \frac{\partial \varrho_1 \bar{\mathbf{C}}_1}{\partial t} - \varrho_1 \frac{Ze\mathbf{E}}{m_1} - \varrho_1 \mathbf{g} - \nabla p_1 = - n_1 m_1 \tau^{-1} \bar{\mathbf{C}}_1,$$

where \mathbf{E} is the electric field and \mathbf{g} the acceleration due to gravitational forces. Likewise

$$(168) \quad \frac{\partial \varrho_2 \bar{\mathbf{C}}_2}{\partial t} + \varrho_2 \frac{e\mathbf{E}}{m_2} - \varrho_2 \mathbf{g} - \nabla p_2 = -n_2 m_2 \tau^{-1} \bar{\mathbf{C}}_2 = -\varrho_2 \tau^{-1} \bar{\mathbf{C}}_2,$$

also

$$(169) \quad \varrho_1 \bar{\mathbf{C}}_1 + \varrho_2 \bar{\mathbf{C}}_2 = 0,$$

whence, by addition we get

$$(170) \quad e\mathbf{E} \left(\frac{\varrho_2}{m_2} - \frac{Z\varrho_1}{m_1} \right) - \varrho_0 \mathbf{g} - \nabla p = 0,$$

or

$$(171) \quad e\mathbf{E}(n_2 - Zn_1) - \varrho_0 \mathbf{g} - \nabla p = 0.$$

If the plasma is strictly neutral ($n_2 = Zn_1$) this reduces to the usual equation of hydrostatic equilibrium. Since the inertia of the electrons may be neglected compared with that of the ions we have, very nearly

$$(172) \quad \frac{\partial \varrho_2 \bar{\mathbf{C}}_2}{\partial t} + \varrho_2 \bar{\mathbf{C}}_2 \tau^{-1} = -n_2 e\mathbf{E},$$

and

$$(173) \quad n_2 \bar{\mathbf{C}}_2 e = -\mathbf{J}$$

by (103). Hence we have, by (172),

$$(174) \quad \frac{\partial \mathbf{j}}{\partial t} + \frac{\mathbf{j}}{\tau} = \frac{n_2^2 e^2}{m_2} \mathbf{E} = \frac{\sigma}{\tau} \mathbf{E}.$$

Considering the simplest case of all, suppose that at time $t=0$ an electric field is set up in the plasma. Neglecting all induced electric and magnetic fields produced by the changing current, the solution of (174) is

$$(175) \quad \mathbf{j} = \sigma \mathbf{E} (1 - \exp[-t/\tau]),$$

so that \mathbf{j} approaches its steady value very nearly within a few collision intervals.

19.2. - If a magnetic field is present, (174) must be replaced by

$$(176) \quad \frac{\partial \mathbf{j}}{\partial t} + \frac{\mathbf{j}}{\tau} + \omega_2 \mathbf{j} \times \mathbf{B}/B = \frac{\sigma}{\tau} \mathbf{E},$$

the solution of which is

$$(177) \quad \mathbf{j} = (\sigma_{\parallel} \mathbf{E} + \sigma_{\perp} \mathbf{B} \times \mathbf{E}/B)(1 - \exp[-t/\tau]).$$

20. - Vorticity theorems.

It will suffice to consider the equation for the ions: from (106) we then have

$$(178) \quad \frac{d_1 \bar{\mathbf{c}}_1}{dt} + \frac{1}{\varrho_1} \nabla P_1 - \frac{Z_1 e}{m_1} (\mathbf{E} + \bar{\mathbf{c}}_1 \times \mathbf{B}) + \mathbf{g} = -\frac{\varrho_2}{\varrho_0 \tau} (\bar{\mathbf{c}}_1 - \bar{\mathbf{c}}_2).$$

Let us suppose that the frictional term on the right hand side of (166) is negligible; than introducing the scalar and vector potentials φ , \mathbf{A} for the electric and magnetic fields we may write (178) in the form

$$(179) \quad \frac{\partial \mathbf{Q}_1}{\partial t} + \nabla \left(\frac{1}{2} m_1 \bar{\mathbf{c}}_1^2 + 2e\varphi \right) + m_1 \mathbf{g} - \bar{\mathbf{c}}_1 \times (\nabla \times \mathbf{Q}_1) + \frac{m_1}{\varrho_1} \nabla P_1 = 0,$$

where we have written

$$(180) \quad \mathbf{Q}_1 = m_1 \bar{\mathbf{c}}_1 + Ze\mathbf{A},$$

taking the curl of this equation, we obtain

$$(181) \quad \frac{\partial \boldsymbol{\Omega}_1}{\partial t} - \nabla \times (\bar{\mathbf{c}}_1 \times \boldsymbol{\Omega}_1) = -\nabla \left(\frac{m_1}{\varrho_1} \right) \times \nabla P_1,$$

where

$$(182) \quad \boldsymbol{\Omega}_1 = \nabla \times \mathbf{Q}_1 = \nabla \times m_1 \bar{\mathbf{c}}_1 + Ze\mathbf{B}.$$

(i) If ϱ_1 and P_1 are connected by a functional relation as is usually the case, the right hand side of (181) vanishes and the equations reduces to

$$(183) \quad \frac{\partial \boldsymbol{\Omega}_1}{\partial t} = \nabla \times (\bar{\mathbf{c}}_1 \times \boldsymbol{\Omega}_1).$$

It follows that the flux of the vector $\boldsymbol{\Omega}_1$, through a closed curve moving with the local velocity of the ions, is then constant, *i.e.* the «lines of force» of the field $\boldsymbol{\Omega}_1$ move with the ionic fluid. But if P_1 and ϱ_1 are not related by functional relations, then the right hand side of (181) represents the creation or annihilation of these «lines of force». Likewise for the electrons we find

$$(184) \quad \frac{\partial \boldsymbol{\Omega}_2}{\partial t} - \nabla \times (\mathbf{c}_2 \times \boldsymbol{\Omega}_2) = -\nabla \left(\frac{1}{\varrho_2} \right) \times \nabla P_2,$$

where

$$(185) \quad \Omega_2 = \nabla \times m_2 \bar{\mathbf{c}}_2 - e \mathbf{B}.$$

(ii) Supposing that the partial pressures due to the ions and electrons are functions of the respective densities, the equations reduce to (183) and the like equation for the electrons. It follows that if the flux of the lines of force of the vectors Ω_1 and Ω_2 through closed curves moving with the respective fluids is initially zero, the flux will always vanish. In this case it follows that

$$(186) \quad \Omega_1 = 0, \quad \Omega_2 = 0.$$

This equation implies that

$$(187) \quad \nabla \times \bar{\mathbf{c}}_1 = \frac{Ze}{m_1} \mathbf{B}, \quad \nabla \times \bar{\mathbf{c}}_2 = -\frac{e}{m_2} \mathbf{B},$$

and since

$$(188) \quad e(\bar{\mathbf{c}}_1 - \bar{\mathbf{c}}_2) = \frac{\rho_0}{\rho_1 \rho_2} \frac{\mathbf{j}}{(Z/m_1) + (1/m_2)},$$

we derive from (187) that

$$(189) \quad \nabla \times \left(\frac{\rho_0}{\rho_1 \rho_2} \mathbf{j} \right) = - \left(\frac{Z}{m_1} + \frac{1}{m_2} \right)^2 e^2 \mathbf{B}.$$

This equation holds, for example, in cases in which a magnetic field external to the plasma is suddenly set up. Since $m_2 \ll m_1$ we have $\rho_0/\rho_1 \rho_2 \sim 1/n_2 m_2$ so that (189) is approximately equal to

$$(190) \quad \nabla \times (\mathbf{j}/n_2) = \frac{e^2}{m_2} \mathbf{B}.$$

Neglecting displacement currents we have also

$$(191) \quad \nabla \times \mathbf{B} = 4\pi \mathbf{j},$$

eliminating \mathbf{B} we have

$$(192) \quad \nabla \times (\nabla \times \mathbf{j}/n_2) = - (4\pi e^2/m_2) \mathbf{j}.$$

The solution of this equation indicates that the current falls off expo-

nentially from its maximum at surface, the characteristics length being of the order of

$$(193) \quad \left(\frac{m_2}{4\pi n_2 e^2} \right)^{\frac{1}{2}}.$$

If this distance is small compared with the dimensions of the plasma, the currents are confined to the surface layers of the plasma. Such a situation arises for instance, during the pinching of a gas discharge.

(iii) Equation (183) and the corresponding equation of the electrons may be expressed in the form

$$(194a) \quad \frac{\partial \mathbf{B}}{\partial t} - \nabla \times (\mathbf{c}_0 \times \mathbf{B}) = -\frac{m_1}{Ze} \nabla \times \left[\frac{\partial \bar{\mathbf{c}}_1}{\partial t} - \bar{\mathbf{c}}_1 \times (\nabla \times \bar{\mathbf{c}}_1) \right] + \nabla \times (\bar{\mathbf{C}}_1 \times \mathbf{B}),$$

$$(194b) \quad = \frac{m_2}{e} \nabla \times \left[\frac{\partial \bar{\mathbf{c}}_2}{\partial t} - \bar{\mathbf{c}}_2 \times (\nabla \times \bar{\mathbf{c}}_2) \right] + \nabla \times (\bar{\mathbf{C}}_2 \times \mathbf{B}).$$

From this it is clear that the magnetic lines of force do not move with the mean mass-velocity \mathbf{c}_0 . However in a strictly neutral plasma we have

$$(195) \quad n_2 = Zn_1.$$

Also, by (169)

$$(196) \quad n_1 m_1 \bar{\mathbf{C}}_1 + n_2 m_2 \bar{\mathbf{C}}_2 = 0,$$

whence

$$(197) \quad m_1 \bar{\mathbf{C}}_1 + Z m_2 \bar{\mathbf{C}}_2 = 0.$$

It follows therefore that the peculiar velocity of the electron is much higher than that of the positive ions. Thus the last term on the right hand side of (194b) exceeds that on the right hand side of (194a), whereas the opposite is true of the first terms on the right hand side of these equations. Thus, very nearly the first term on the right hand side of (194a) is comparable with the second term on the right hand side of (194b) and is therefore larger than the first on the right hand side of this equation. Thus very nearly,

$$(198) \quad \frac{\partial \mathbf{B}}{\partial t} - \nabla \times (\mathbf{c}_0 \times \mathbf{B}) - \nabla (\bar{\mathbf{C}}_2 \times \mathbf{B}) = 0,$$

or

$$(199) \quad \frac{\partial \mathbf{B}}{\partial t} - \nabla \times (\bar{\mathbf{c}}_2 \times \mathbf{B}) = 0.$$

The lines of force of the magnetic field may thus be said to move the electron gas. Also we have approximately,

$$(200) \quad -\frac{m_1}{Ze} \nabla \times \left[\frac{\partial \bar{\mathbf{c}}_1}{\partial t} - \bar{\mathbf{c}}_1 \times (\nabla \times \bar{\mathbf{c}}_1) \right] = \nabla \times (\bar{\mathbf{C}}_2 \times \mathbf{B}),$$

or using (197)

$$(201) \quad \nabla \times \left[\frac{\partial \bar{\mathbf{c}}_1}{\partial t} - \bar{\mathbf{c}}_1 \times (\nabla \times \bar{\mathbf{c}}_1) \right] = \left[\frac{e}{m_2} \nabla \times (\bar{\mathbf{C}}_1 \times \mathbf{B}) \right].$$

From (103), neglecting the mass of the electrons compared with that of the ions, we can write this in the form

$$(202) \quad \frac{\partial \boldsymbol{\omega}_1}{\partial t} - \nabla \times (\bar{\mathbf{c}}_1 \times \boldsymbol{\omega}_1) = \nabla \times \left(\frac{1}{\rho_1} \mathbf{j} \times \mathbf{B} \right),$$

where

$$(203) \quad \boldsymbol{\omega}_1 = \nabla \times \bar{\mathbf{c}}_1$$

is the vorticity of the ionic flow. In general therefore, the vortex lines do not move with the ions unless the right hand side of (202) vanishes as, for instance, for a force free field.

21. - Waves in a plasma.

Oscillations in a plasma may be exceedingly complex and for the most part we shall consider only harmonic oscillations.

There appear to be three fundamental types of waves into which all plasma waves may be analysed:

- 1) electrostatic waves,
- 2) electromagnetic waves,
- 3) hydromagnetic waves,

each of them can only be excited under controlled laboratory conditions.

The three types of waves correspond to special cases: (1) if \mathbf{E} and \mathbf{j} are parallel to the direction of propagation of the waves we have electrostatic waves; (2) if \mathbf{E} is perpendicular to the direction of propagation, we have electromagnetic waves. But these can only be propagated if the electron density exceeds a certain critical value. Finally, (3) in the presence of an external magnetic field

and for frequencies small compared with the cyclotron frequency of the positive ions we have the case of magneto-hydrodynamic waves.

22. — Electrostatic waves.

Two main types of oscillations are possible according as the positive ions can be considered to remain stationary or not. In analysing the electron oscillations these may be so rapid that we can no longer neglect the inertia of the electrons and we must use equation (103).

Assuming a solution proportional to $\exp[i\omega t]$, the equation becomes

$$(204) \quad (i\omega\tau + 1)\mathbf{j} = \sigma(\mathbf{E} + \mathbf{E}'').$$

Now

$$(205) \quad \mathbf{E}'' = (1/n_2 e) \nabla p_e$$

and

$$(206) \quad \nabla p_2 = \gamma kT \nabla n_2 = -(\gamma kT_2/e) \nabla v,$$

where $4\pi v$ is the volume charge density.

Whence operating with $\nabla \cdot$ on (204) one obtains

$$(207) \quad (i\omega\tau + 1)\nabla \cdot \mathbf{j} = \sigma \left(4\pi v - \gamma \frac{kT_2}{n_2 e^2} \nabla^2 v \right),$$

or

$$(208) \quad -i\omega(i\omega\tau + 1)v = \sigma \left(4\pi v - \gamma \frac{kT_2}{n_2 e^2} \nabla^2 v \right),$$

or

$$(209) \quad v(\omega^2 p - \omega^2 + i\omega/\tau) - \gamma \frac{kT_2}{m_2} \nabla^2 v = 0,$$

where $\omega_p^2 = 4\pi n e^2/m_2$ is the square of the « plasma frequency ». Assuming a solution of the form $\exp[ikx]$, we have $\nabla^2 = -k^2$, and hence

$$(210) \quad \omega^2 - i\omega/\tau - \omega_p^2 - \gamma \frac{kT_2}{m_2} k^2 = 0.$$

If we neglect the effect of collisions and write

$$(211) \quad \omega_0^2 = \omega_p^2 + \gamma \frac{kT_2}{m_2} k^2,$$

the phase velocity

$$V = \omega_0/k = (\omega_p^2/k^2 + \gamma kT_e/m_e)^{\frac{1}{2}}$$

and in the limit of very low temperature, only one frequency can be excited, namely, the plasma frequency, independently of the wave length. This result was first given by LANGMUIR and TONKS [11]. The effect of collision is to attenuate the waves; if ω/τ is small we have very nearly

$$(212) \quad k = \left(\frac{m_2}{\gamma k T_2} \right)^{\frac{1}{2}} (\omega^2 - \omega_p^2)^{\frac{1}{2}} \left(1 - \frac{i\omega}{2\pi(\omega^2 - \omega_p^2)} \right),$$

so that the attenuation factor is

$$\exp \left(- \frac{m_2 \omega x}{2\gamma k T_2 (\omega^2 - \omega_p^2)^{\frac{1}{2}} \tau} \right),$$

and the wave is attenuated in a distance

$$2(\gamma k T_2 / m_2)^{\frac{1}{2}} (\omega^2 - \omega_p^2)^{\frac{1}{2}} / \omega = 2 \left(\gamma \frac{k T_2}{m_2} \right)^{\frac{1}{2}} (1 - \omega_p^2 / \omega^2)^{\frac{1}{2}} \tau.$$

Since $(\gamma k T_2 / m_2)^{\frac{1}{2}}$ is comparable with the mean square of the peculiar velocity, the attenuation distance is comparable with a free path. Since the oscillations are essentially one-dimensional the value of γ can be set equal to 3 corresponding to one degree of freedom.

Observations of electron oscillation were first obtained by PENNING [12] in 1926; more recent work by LOONEY and BROWN [13] shows that the frequency of these oscillations is very nearly equal to the plasma frequency:

$$(213) \quad f_p = \omega_p / 2\pi = 8.97 \cdot 10^3 n_2^{\frac{1}{2}}.$$

It is not at all clear as to the manner in which the electron oscillations are excited; LOONEY and BROWN have suggested that they may originate in the sheath between the plasma and the walls. They also state that the other waves are not electromagnetic in origin but are longitudinal pressure waves set up in the plasma electrons. This agrees with the above theory.

We next consider the positive ion oscillations; these are much slower than the electron oscillations so that the electron density has very nearly its equilibrium value at all times. To simplify the discussion we shall assume that the ion temperature is zero.

It will be convenient to consider departures of the densities of the electrons and positive ions from the equilibrium values; since the gas is initially neutral these are related by the equation

$$(214) \quad n_{20} = Z n_{10}.$$

Let v_1 and v_2 denote the variation of the ion and electron densities; let also ξ denote the mean displacement of a positive ion from its equilibrium position. Then v_1 may be expressed in terms of ξ by means of the equation of continuity of the ions

$$(215) \quad \partial n_1 / \partial t = - \nabla \cdot (n_1 \bar{c}_1).$$

Since $\bar{c}_1 = \partial \xi / \partial t$, and $n_1 = n_{10} + v_1$, retaining first order terms only, this equation can be integrated to give

$$(216) \quad v_1 = - n_{10} \nabla \cdot \xi.$$

Also, the electron density attains its Maxwellian distribution at each instant, whence

$$(217) \quad v_2 = n_{20} (\exp [eV/kT] - 1),$$

where V is the electrostatic potential and T the electron temperature. To the first order in eV/kT this gives

$$(218) \quad v_2 = n_{20} eV/kT = Zn_{10} eV/kT.$$

The electrostatic potential satisfies Poisson's equation

$$(219) \quad \nabla^2 V = - 4\pi e (v_1 - v_2)$$

and since the ion temperature is zero, the equation of motion of the positive ion is

$$(220) \quad m_1 \ddot{\xi} = - Ze \nabla V.$$

Combining (216) and (218) and writing n for n_{10} we have

$$(221) \quad \nabla^2 V = - 4\pi ne (- \nabla \cdot \xi - ZeV/kT).$$

Also by (220) $\nabla \times \xi = 0$, whence $\nabla \nabla \cdot \xi = \nabla^2 \xi$; hence operating with ∇ on (220) we find

$$(222) \quad \nabla^2 \xi = \omega_p^2 \left(- \nabla^2 \xi + \frac{m_1}{kT} \ddot{\xi} \right),$$

where

$$(223) \quad \omega_1^2 = 4\pi ne^2/m_1,$$

thus ω_1 is the plasma frequency for the positive ions.

Considering waves for which $\xi \propto \exp [i(\omega t - x/\lambda)]$ so that $2\pi\lambda$ is the wave length, we find

$$(224) \quad \omega^2 = \omega_1^2 / (1 + m_1 \omega_1^2 \lambda^2 / kT),$$

so that the velocity U of the wave is given by

$$(225) \quad U^2 = (kT/m_1)(1/[1 + (\lambda^2/b^2)]),$$

where b is the Debye shielding distance, given by

$$(226) \quad b = (kT/4\pi Z n_1 e^2)^{\frac{1}{2}}.$$

Let ω_2 be the electron plasma frequency given by

$$(227) \quad \omega_2 = (4\pi n e^2 / m_2)^{\frac{1}{2}}$$

then (224) may also be written

$$(228) \quad \omega^2 = \omega_2^2 \left(\frac{m_2}{m_1} \right) (1 + \lambda^2/b^2)^{-1}.$$

There are thus two distinct cases according as $b \gg \lambda$ or $b \ll \lambda$. In the former case, the frequency $\omega/2\pi$ of the oscillation is nearly equal to $\omega_2(m_2/m_1)^{\frac{1}{2}}$ *i.e.* a slower oscillation than that corresponding to electron oscillation. If $b \ll \lambda$, then $U \sim (kT/m_1)^{\frac{1}{2}}$ which is the velocity of acoustic waves. In this case the positive ion oscillations lose their similarity to electron plasma oscillations and change to sound waves. This mechanism depends on the shielding of the field of the electrons by the positive ions (since $\lambda \gg b$). When the wave length of the waves is less than the Debye shielding distance b , shielding by the electrons is no longer possible and plasma oscillations result. Such oscillations have been observed by HERNQVIST [14].

23. - Electromagnetic and hydromagnetic waves.

We now suppose that a uniform magnetic field B_0 permeates the plasma and consider waves in which the mean particle velocity is transverse to this field and dependent only on the coordinate parallel to the field. Let this be the z -coordinate of a rectangular system of coordinates $O(xyz)$. Under these conditions the equations of continuity of the ions and electrons become

$$(229) \quad \frac{dn_i}{dt} + n_i \nabla \cdot \bar{c}_i = 0, \quad (i=1, 2),$$

and since $\partial/\partial x$, $\partial/\partial y$ are zero operators, and the mean velocity of the particles has no resolutes parallel to the field this reduces to $dn_i/dt = 0$. Hence both n_1 and n_2 are constant and if the plasma is initially neutral it will always be so. If Ze is the charge on a positive ion, where e is the electronic charge, than

$$(230) \quad n_2 = Zn_1.$$

Neglecting collisions, the equation of motion for the electrons is

$$(231) \quad m_2 \frac{d\bar{\mathbf{c}}_2}{dt} = -\frac{1}{n_2} \nabla \cdot p_2 - e(\mathbf{E} + \bar{\mathbf{c}}_2 \times \mathbf{B}),$$

where \mathbf{E} and \mathbf{B} are the electric and magnetic fields associated with the wave. They satisfy the equations

$$(232a) \quad \nabla \times \mathbf{E} = -\frac{\partial \mathbf{B}}{\partial t},$$

$$(232b) \quad \nabla \times \mathbf{B} = 4\pi \mathbf{j} + \frac{1}{c^2} \frac{\partial \mathbf{E}}{\partial t}.$$

where \mathbf{j} , the current density, is given by

$$(233) \quad \mathbf{j} = ne(\bar{\mathbf{c}}_1 - Z\bar{\mathbf{c}}_2)$$

if we write n for n_1 . Let \mathbf{b} be the perturbing magnetic field associated with the wave so that

$$(234) \quad \mathbf{B} = \mathbf{B}_0 + \mathbf{b};$$

than (232) may be rewritten

$$(235) \quad \nabla \times \mathbf{E} = -\frac{\partial \mathbf{b}}{\partial t}, \quad \nabla \times \mathbf{b} = 4\pi \mathbf{j} + \frac{1}{c^2} \frac{\partial \mathbf{E}}{\partial t}.$$

Operating with $\nabla \times$ on (231) to eliminate the pressure, and using (232) we than have

$$(236) \quad m_1 \nabla \times \frac{\partial \bar{\mathbf{c}}_1}{\partial t} = e \frac{\partial \mathbf{b}}{\partial t} - e \nabla \times (\mathbf{c}_1 \times \mathbf{B}).$$

Writing

$$(237) \quad \bar{\mathbf{c}}_1 = (U, V, 0), \quad \bar{\mathbf{c}}_2 = (u, v, 0), \quad \mathbf{B} = (b_x, b_y, B_0)$$

and taking resolutes of (236) we find

$$(238) \quad \frac{\partial}{\partial t} \left(-\frac{\partial v}{\partial z} - \frac{eb_x}{m_2} \right) = -\frac{eB_0}{m_2} \frac{\partial u}{\partial z},$$

$$(239) \quad \frac{\partial}{\partial t} \left(\frac{\partial u}{\partial z} - \frac{eb_y}{m_2} \right) = -\frac{eB_0}{m_2} \frac{\partial v}{\partial z}.$$

The two similar equations for the positive ions can be derived from this by changing the suffix from 2 to 1 and replacing $-e$ by Ze . Writing

$$(240) \quad w = u + iv, \quad W = U + iV, \quad b = b_x + ib_y,$$

these may be confined into the single equations

$$(241) \quad \frac{\partial}{\partial z} \left(i \frac{\partial w}{\partial t} + \omega_2 w \right) = \frac{e}{m_2} \frac{\partial b}{\partial t},$$

$$(242) \quad \frac{\partial}{\partial z} \left(i \frac{\partial W}{\partial t} - \omega_1 W \right) = -\frac{Ze}{m_1} \frac{\partial b}{\partial t},$$

where

$$(243) \quad \omega_2 = eB_0/m_2, \quad \omega_1 = ZeB_0/m_1$$

are the electronic and ionic cyclotron frequencies respectively. The electric field has resolutes $(E_x, E_y, 0)$ and writing $E = E_x + iE_y$, equation (232a) can be written

$$(244) \quad \frac{\partial E}{\partial z} = i \frac{\partial b}{\partial t},$$

whence Maxwell's equation (232b) can be written

$$(245) \quad i \frac{\partial b}{\partial z} = 4\pi ne(W - Zw) + \frac{1}{c^2} \frac{\partial E}{\partial t}.$$

Eliminating E between these equations we find

$$(246) \quad \frac{\partial^2 b}{\partial z^2} = -4\pi nei \left(\frac{\partial W}{\partial z} - Z \frac{\partial w}{\partial z} \right) + \frac{1}{c^2} \frac{\partial^2 b}{\partial t^2}.$$

Using (241) and (242) to eliminate $\partial W/\partial z$ and $\partial w/\partial z$ we find finally that

$$(247) \quad \left[\frac{\partial^2}{\partial t^2} + i(\omega_1 - \omega_2) \frac{\partial}{\partial t} + \omega_1 \omega_2 \right] \left(\frac{\partial^2 b}{\partial z^2} - \frac{\partial^2 b}{c^2 \partial t^2} \right) = \frac{4\pi Zne^2}{M} \frac{\partial^2 b}{\partial t^2},$$

where $M = m_1 m_2 / (m_1 + m_2)$. Assuming a solution of the form $\exp[i(kz + \omega t)]$, the frequency equation is

$$(248) \quad (\omega - \omega_2)(\omega + \omega_1)(\omega^2 - c^2 k^2) = \omega_p^2 \omega^2,$$

where

$$(249) \quad \omega_p^2 = \frac{4\pi Z n e^2}{M},$$

and ω_p is thus very nearly equal to the electronic plasma frequency. The dispersion relation becomes

$$(250) \quad U^2 = \frac{c^2}{1 - \frac{\omega_p^2}{\omega^2} \frac{1}{(1 - (\omega_2/\omega))(1 + \omega_1/\omega)}}$$

The waves are clearly circularly polarized.

Electromagnetic waves. — If we set B_0 equal 0, we have the case of plane electromagnetic waves propagating in a plasma; since $\omega_1 = 0 = \omega_2$, the frequency equation reduces to

$$(251) \quad U^2 = \frac{c^2}{1 - \omega_p^2/\omega^2}.$$

When $\omega < \omega_p$, U becomes imaginary and the wave cannot be propagated. In this case the wave penetrates some distance into the plasma, but the amplitude decreases exponentially by the factor $1/e$ in a distance of the order

$$(252) \quad d = \frac{c}{\omega_p} \left(1 - \frac{\omega^2}{\omega_p^2}\right)^{-\frac{1}{2}},$$

and if $\omega \ll \omega_p$, then d is very nearly $(1/2\pi) \times$ wave length in vacuo.

When a magnetic field is present, we must use the dispersion formula (250). Ignoring the motion of the ions, we set $\omega_1 = 0$ in (250) so that it becomes

$$(253) \quad \frac{U^2}{c^2} = \frac{1}{1 - \frac{\omega_p^2}{\omega^2} \frac{1}{1 \pm \omega_2/\omega}},$$

the positive or negative sign being chosen according to the right handed or left handed polarization of the waves. Set,

$$(254) \quad x = \frac{\omega}{\omega_p}, \quad z = \frac{U^2}{c^2}, \quad \alpha = \frac{\omega_2}{\omega_p} = \frac{1}{\beta} - \beta,$$

then this relation may be written

$$(255) \quad z = 1 + \frac{1}{(x \mp \beta)(x \pm 1/\beta)},$$

and if $\beta^2 < 1$ we have the following situation. Large values of x correspond to large frequencies so that $U \rightarrow c$ as $\omega \rightarrow \infty$, the case of pure electromagnetic waves. For other frequencies the variation of U will be shown in the diagram.

Hydromagnetic waves. — These are characterized by the fact that the frequency is small compared with the ion frequency. In this case the dispersion relation reduces to

$$(256) \quad U^2 = \frac{c^2}{1 + \omega_p^2/\omega_1\omega_2} = \frac{c^2}{1 + 4\pi n(m_1 + m_2)c^2/B_0^2}.$$

Since $n(m_1 + m_2)$ is the density of the plasma ρ_0 , we may write

$$(257) \quad U^2 = \frac{c}{K^{\frac{1}{2}}} \equiv \left(\frac{c^2}{1 + 4\pi\rho_0 c^2/B_0^2} \right)^{\frac{1}{2}}.$$

And if $K \gg 1$, this reduces approximately to $B_0(4\pi\rho_0)^{-\frac{1}{2}}$. This type of

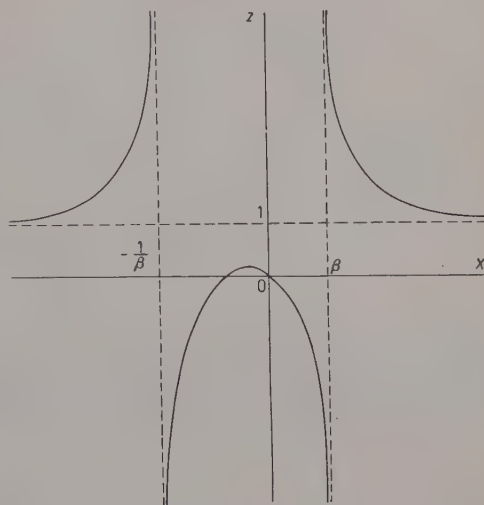


Fig. 4a. — Graph of the function z as function of x [see equation (255)]. The physical part of the curve corresponds to the upper half of the plane ($z \geq 0$). The *ordinary ray* corresponds to positive values of x and the *extraordinary ray* corresponds to negative values of x . Thus the extraordinary ray curve is obtained by reflecting the diagram for $z \geq 0$ in the z -axis (*). This is shown in Fig. 4b.

wave was first discovered by ALFVÉN and may be regarded as a normal electromagnetic wave in a gas of high dielectric constant. It will be noted that the wave is circularly polarized.

We next consider longitudinal hydromagnetic waves; we shall suppose that the mean mass velocity is parallel to the direction of propagation of the wave and that the magnetic field is perpendicular to this. Furthermore, as for acoustic waves we shall restrict the discussion to small displacements. Neglecting the inertia of the electrons, equation (231)

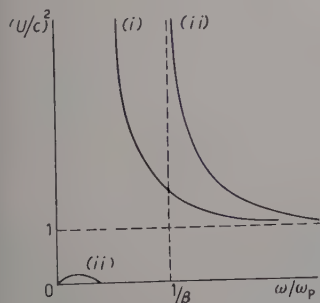


Fig. 4b. — Dispersion curves: (i) for the ordinary ray; (ii) for the extraordinary ray.

(*) I owe this inference to Dr. WEIBEL (see this issue, pag. 58).

becomes:

$$(258) \quad 0 = -\nabla p_2 - n_2 e (\mathbf{E} + \bar{\mathbf{c}}_2 \times \mathbf{B}_0),$$

and that for the positive ions

$$(259) \quad \varrho_1 \frac{\partial \bar{\mathbf{c}}_1}{\partial t} = -\nabla p_1 + Z n_1 e (\mathbf{E} + \bar{\mathbf{c}}_1 \times \mathbf{B}_0).$$

Adding these equations we get

$$(260) \quad \varrho_1 \frac{\partial \mathbf{c}_1}{\partial t} = -\nabla p + \nu \mathbf{E} + \mathbf{j} \times \mathbf{B}_0,$$

where ν is the charge density and \mathbf{j} the current density. However, since both ν and \mathbf{E} are small quantities of the first order, their product is negligible, being of the second order. Thus to the first order, (262) becomes

$$(261) \quad \varrho_1 \frac{\partial \bar{\mathbf{c}}_1}{\partial t} = -\nabla p + \mathbf{j} \times \mathbf{B}_0.$$

Since we may ignore the peculiar velocity of the ions and electrons, operating with $\nabla \times$ on (258) we have

$$(262) \quad -n_2 e \nabla \times \mathbf{E} - n_2 e \nabla \times (\bar{\mathbf{c}}_0 \times \mathbf{B}_0) = 0$$

or to the first order,

$$(263) \quad \frac{\partial \mathbf{b}}{\partial t} = \nabla \times (\mathbf{c}_0 \times \mathbf{B}_0),$$

since $\nabla \times \mathbf{E} = -\partial \mathbf{b} / \partial t$; \mathbf{c}_0 is the mean mass velocity. Using Maxwell's equation

$$(264) \quad \nabla \times \mathbf{b} = 4\pi \mathbf{j} + \frac{1}{c^2} \frac{\partial \mathbf{E}}{\partial t},$$

(261) may be written

$$(265) \quad \varrho_0 \frac{\partial \mathbf{c}_0}{\partial t} = -\nabla p + \frac{1}{4\pi} \left[\nabla \times \mathbf{b} - \frac{1}{c^2} \frac{\partial \mathbf{E}}{\partial t} \right] \times \mathbf{B}_0.$$

We must now express the pressure in terms of \mathbf{c}_0 . The equation of continuity of the ions and electron gives, to the first order,

$$(266) \quad \frac{\partial \varrho_1}{\partial t} = -\varrho_1 \nabla \cdot \mathbf{c}_0, \quad \frac{\partial \varrho_2}{\partial t} = -\varrho_2 \nabla \cdot \mathbf{c}_0.$$

Whence

$$p = p_1 + p_2 = \gamma k T (1 + Z) \varrho_0 / m_1, \quad \text{since} \quad n_2 = Z n_1$$

and hence

$$(267) \quad \frac{\partial p}{\partial t} = - \frac{(1 + Z) \gamma k T \varrho_0}{m_1} \nabla \cdot \mathbf{c}_0.$$

Thus, differentiating (265) with respect to the time we get (ignoring the mass of the electrons)

$$(268) \quad \varrho_0 \frac{\partial^2 \mathbf{c}_0}{\partial t^2} = \frac{1 + Z}{m_1} \gamma k T \varrho_0 \nabla \nabla \cdot \mathbf{c}_0 + \frac{1}{4\pi} \left[\nabla \times \frac{\partial \mathbf{b}}{\partial t} - \frac{1}{c^2} \frac{\partial^2 \mathbf{E}}{\partial t^2} \right] \times \mathbf{B}_0.$$

Suppose that the direction of the wave is parallel to the x -axis, so that \mathbf{c}_0 is parallel to the x -axis, and \mathbf{B}_0 parallel to the z -axis. From (263) it follows that \mathbf{b} is also parallel to Oz and \mathbf{E} parallel to Oy and such that their intensities b , E satisfy the equations

$$(269) \quad \frac{\partial b}{\partial t} = -B_0 \frac{\partial c_0}{\partial x}, \quad \frac{\partial E}{\partial x} = -\frac{\partial b}{\partial t}.$$

Hence (268) becomes

$$(270) \quad \varrho_0 \frac{\partial^2 c_0}{\partial t^2} = \frac{(1 + Z) \gamma k T \varrho_0}{m_1} \frac{\partial^2 c_0}{\partial x^2} + \frac{B_0^2}{4\pi} \frac{\partial^2 c_0}{\partial x^2} - \frac{B_0}{4\pi c^2} \frac{\partial^2 E}{\partial t^2}.$$

But from (269) we find easily that

$$(271) \quad \frac{\partial^2 E}{\partial t^2} = B_0 \frac{\partial^2 c_0}{\partial t^2},$$

whence

$$(272) \quad K \frac{\partial^2 c_0}{\partial t^2} = \left[\frac{(1 + Z) \gamma k T}{m_1} (K - 1) + c^2 \right] \frac{\partial^2 c_0}{\partial x^2},$$

or

$$(273) \quad \frac{\partial^2 c_0}{\partial t^2} = \left[\frac{(1 + Z) \gamma k T}{m_1} \left(1 - \frac{1}{K} \right) + \frac{c^2}{K} \right] \frac{\partial^2 c_0}{\partial x^2},$$

where as before

$$(274) \quad K = 1 + \frac{4\pi \varrho_0 c^2}{B_0^2}.$$

If this is much larger than unity, then the phase velocity U is given by

$$(275) \quad U^2 = \frac{(1+Z)\gamma kT}{m_1} + \frac{B_0^2}{4\pi\varrho_0} = (1+Z)a^2 + V_a^2,$$

where a is the sonic speed and V_a the Alfvén velocity.

If the magnetic pressure $B^2/8\pi$ is small compared with the gas pressure p , the longitudinal wave is essentially an acoustic wave. If $B^2/8\pi \gg p$, the velocity of the hydromagnetic waves is the same as that of an Alfvén wave.

When the amplitude of this new type of waves is sufficiently great, a hydromagnetic shock may develop.

Finally, the results only hold so long as the frequency of the wave is less than the positive ion cyclotron frequency.

REFERENCES

- [1] S. CHAPMAN and T. G. COWLING: *The Mathematical Theory of Non-Uniform Gases* (Cambridge, 1939).
- [2] R. S. COHEN, L. SPITZER and P. McR. RUTLY: *Phys. Rev.*, **80**, 230 (1950).
- [3] H. JAFFE: *Ann. Phys.*, **6**, 195 (1930).
- [4] M. BAYET, J. L. DELCROIX and J. L. DENISSE: *Compt. Rend. Acad. Sci. (Paris)*, **238**, 2146 (1954).
- [5] L. SPITZER: *Physics of Fully Ionized Gases* (New York, 1956).
- [6] S. CHAPMAN and V. C. A. FERRARO: *M. N. Roy. Astr. Soc.*, **89**, 456 (1929).
- [7] V. C. A. FERRARO: *M. N. Roy. Astr. Soc.*, **93**, 416 (1933).
- [8] J. H. JEANS: *Problems of Cosmology and Stellar Dynamics* (Cambridge, 1919), p. 224.
- [9] S. CHANDRASEKHAR: *Principles of Stellar Dynamics* (Chicago, 1942).
- [10] V. C. A. FERRARO: *Proc. Lond. Math. Soc.*, II, **49**, 77 (1945).
- [11] L. TONKS and I. LANGMUIR: *Phys. Rev.*, **33**, 195 (1929).
- [12] F. M. PENNING: *Physica*, **6**, 241 (1926).
- [13] D. H. LOONEY and S. C. BROWN: *Phys. Rev.*, **93**, 965 (1954).
- [14] K. G. HERNQVIST: *Journ. App. Phys.*, **26**, 1029 (1955).

INTERVENTI E DISCUSSIONI

— E. WEIBEL:

When one writes the Boltzmann-equation one usually thinks of a collision term on the right hand side and on binary collision.

— V. FERRARO:

Yes.

— E. WEIBEL:

In the gas that you considered this morning consisting of ions, say, collisions are rarely binary. The important collisions are the ones which involve many particles.

— V. FERRARO:

That is true, but I think you probably know Dr. SPITZER wrote a paper four years ago in which he showed that the effect of the multiple collisions leads effectively to the same consequences as the binary ones. In other words you can consider binary collisions provided you have introduced the right collision intervals.

— E. WEIBEL:

Yes, so everything of importance is contained in this relaxation time.

V. FERRARO:

Yes, that is one of the reasons why, I prefer to work with this collision interval rather than to consider the collision integral.

— E. WEIBEL:

The collision term of binary collisions is then really fictitious?

— V. FERRARO:

Well, not altogether. I think you can show that it is so in effect, but this can be effectively equivalent to the multiple collisions. It does not affect the method.

— E. WEIBEL:

I have one other question. By your equations the pressure $p = nkT$. I just wondered why the Coulomb repulsion did not show up.

— V. FERRARO:

Well, it would show up if one were to consider the right Virial term.

— L. GOLDSTEIN:

I wish to make one remark regarding the theory which we have had the opportunity to more or less check experimentally concerning the electron-ion collision frequency and the relaxation time separately. It seems to us that the theory is verified to a very good approximation, probably to about 30%, so that the Debye distance does play the proper role for the shielding.

— V. FERRARO:

That is the distance to take.

— L. GOLDSTEIN:

Yes, and we have also had the opportunity to check the relaxation time τ_e by determining the deviation from the Maxwellian distribution of the electrons. So I think that the theory is in a rather good shape.

— B. LEHNERT:

Just a formal question. When you use the Coulomb potential you have to cut off at the Debye distance so that the formulas should not diverge. Would it be possible to use the potential for which instead you originally include the Debye distance and the scattering formula converges when $b_2 \dots ?$

— V. FERRARO:

I think it will come to the same thing. Except that it will make these formulas a little more difficult. But it will certainly remove the difficulty of the divergent integral.

— Dr. E. WEIBEL (made the following remarks with respect to the curves on page 53).

In fact the curves for the ordinary and the extraordinary waves represent one analytical function; the part for which x is positive corresponds to the extraordinary wave, negative x to the ordinary one (opposite polarization). So we have the following picture: The ranges of x for which z becomes negative are the attenuation bands: — $(1/\beta) < x < A$ for the ordinary wave, $0 < x < \beta$ for the extraordinary wave. To see the behaviour of the following picture: f is the frequency of the transmitted wave, f_c is the cyclotron-frequency of the electrons, f_p is the plasma frequency.

The region (1) represents the attenuation band for the extraordinary wave, (2) for the ordinary wave.

One sees that these bands become narrower with increasing magnetic field.

— Dr. R. GALLET:

Remarks that when there is a magnetic field present, the properties of the shock are totally different.

Plasma Physics on Cosmical and Laboratory Scale.

B. LEHNERT

Royal Institute of Technology - Stockholm

To the 50-th birthday of HANNES ALFVÉN

1. - Introduction.

Astrophysical research in its most favourable situation consists of a combination of observational, theoretical and experimental work. Then, the main features of an observed phenomenon would form the basis of a theory which could be tested in a model experiment where all the parameters of the cosmical phenomenon are «scaled down» in a proper way. In the experiment a variation of the parameters can easily be performed, which possibility does not exist for the corresponding cosmical phenomenon. In addition, even when a complete theory cannot be worked out, the cosmical phenomenon could be studied directly in the laboratory, provided that the correct scaling has been performed. Finally, there also exist phenomena which may be of astrophysical importance and which have been detected in the laboratory before having been predicted by theory or suggested by observational results. One such example is given by Bostick's plasmoids (BOSTICK [15]).

Unfortunately, the idealized situation of a complete similarity between a cosmical phenomenon and its experimental model is far from being realizable in the laboratory. The best to be expected is a strongly distorted reproduction of the more important properties. This is mainly due to the fact that the scaling refers to a very large step in linear dimensions and that the electric conductivity of the best conductors available at terrestrial conditions is far too small for a proper similarity to be established. Even so, the experiments serve the important purpose of testing theoretical results which can be extended over a long chain of situations. If there is agreement between theory and experiment at one end one may hope—at least in some cases—that there should be agreement between theory and observation at the other, even if there is no direct connection between observation and experiment.

In the present discussion and attempt shall be made to examine the prevailing conditions in a plasma in a magnetic field in cosmical physics as well as in the laboratory. Since laboratory experiments are not always made by using the collected resources of a power station the discussion will be extended to include a partially ionized gas. The physics of such a gas has earlier been treated by SCHLÜTER [63] and COWLING [20, 21] and has been applied to the ionosphere by LUCAS and SCHLÜTER [47], LUCAS [46] and GERSHMAN and GINZBURG [29], to dissipation in cool interstellar clouds by COWLING [21] and to the heating of the solar chromosphere with magnetohydrodynamic waves by PIDDINGTON [58]. At the end of this paper two examples will be given as experimental illustrations; torsional oscillations in a magnetohydrodynamic « waveguide » representing the non-stationary state and the diffusion of a plasma in a cylindrical column representing the stationary state.

2. - The macroscopic equations of an ionized gas.

2.1. *The partially ionized gas.* - According to the long range of the Coulomb forces the interactions between charged constituents of an ionized gas predominate over the interactions involving neutral particles, even at moderate ionization degrees. Thus, in a great number of astrophysical problems as well as in high current discharges in the laboratory the gas may be treated as « fully ionized ». When this simplification is inapplicable, however, the ionized gas must be considered as a system of three mutually interacting fluids composed of ions, electrons and neutral particles (SCHLÜTER [63, 64], LUCAS and SCHLÜTER [47], COWLING [20, 21]).

The basic macroscopic equations of a partially and singly ionized, non-relativistic ideal gas consisting of n_i ions, n_e electrons and n_n neutral particles per unit volume will now be introduced. For the deduction on the basis of Boltzmann's equation reference can be made to SPITZER [67]. Conservation of mass and charge is given by

$$(1) \quad \frac{\partial n_i}{\partial t} + \operatorname{div} (n_i \mathbf{v}_i) = 0, \quad \frac{\partial n_e}{\partial t} + \operatorname{div} (n_e \mathbf{v}_e) = 0,$$

and

$$(2) \quad \frac{\partial n_n}{\partial t} + \operatorname{div} (n_n \mathbf{v}_n) = 0,$$

where \mathbf{v}_i , \mathbf{v}_e and \mathbf{v}_n are macroscopic mean velocities and indices (i), (e) and (n) refer to ions, electrons and neutral particles in the formulae throughout this

paper. Conservation of momentum is expressed by

$$(3) \quad n_i m_i \left[\frac{\partial \mathbf{v}_i}{\partial t} + (\mathbf{v}_i \cdot \nabla) \mathbf{v}_i \right] = e n_i (\mathbf{E} + \mathbf{v}_i \times \mathbf{B}) - \nabla p_i + 2 n_i m_i \mathbf{v}_i \times \boldsymbol{\Omega} + \\ + n_i m_i [\mathbf{g} + \boldsymbol{\Omega} \times (\mathbf{r} \times \boldsymbol{\Omega})] - n_e m_e \nu_{ei} (\mathbf{v}_i - \mathbf{v}_e) + n_i m_i \nu_{in} (\mathbf{v}_n - \mathbf{v}_i),$$

$$(4) \quad n_e m_e \left[\frac{\partial \mathbf{v}_e}{\partial t} + (\mathbf{v}_e \cdot \nabla) \mathbf{v}_e \right] = - e n_e (\mathbf{E} + \mathbf{v}_e \times \mathbf{B}) - \nabla p_e + 2 n_e m_e \mathbf{v}_e \times \boldsymbol{\Omega} + \\ + n_e m_e [\mathbf{g} + \boldsymbol{\Omega} \times (\mathbf{r} \times \boldsymbol{\Omega})] + n_e m_e \nu_{ei} (\mathbf{v}_i - \mathbf{v}_e) + n_e m_e \nu_{en} (\mathbf{v}_n - \mathbf{v}_e),$$

and

$$(5) \quad n_n m_n \left[\frac{\partial \mathbf{v}_n}{\partial t} + (\mathbf{v}_n \cdot \nabla) \mathbf{v}_n \right] = - \nabla p_n + 2 n_n m_n \mathbf{v}_n \times \boldsymbol{\Omega} + \\ + n_n m_n [\mathbf{g} + \boldsymbol{\Omega} \times (\mathbf{r} \times \boldsymbol{\Omega})] - n_i m_i \nu_{in} (\mathbf{v}_n - \mathbf{v}_i) - n_e m_e \nu_{en} (\mathbf{v}_n - \mathbf{v}_e),$$

where m_i , m_e , m_n are the particle masses, \mathbf{E} the electric field, \mathbf{B} the magnetic field, p_i , p_e , p_n denote the partial pressures, $\boldsymbol{\Omega}$ is supposed to be a constant angular velocity of the entire gas mixture, \mathbf{g} the acceleration due to gravity, \mathbf{r} the radius vector from an origin at the axis of rotation, and ν_{ei} , ν_{en} , ν_{in} the collision frequencies for encounters between non-identical particles. It should be observed that an electron loses approximately all its systematically directed momentum in one collision with an ion or a neutral molecule, whereas an ion loses about half of its momentum in a collision with a neutral molecule (COWLING [4]). The factor one half should be considered as included in the symbol ν_{in} .

The stress tensor has been approximated by a scalar pressure in eqs. (3), (4) and (5) which implies that shearing forces due to viscosity have been neglected. The physical significance of this approximation can be estimated in the following elementary way. Suppose that a particle of mass m_s ($s=i, e, n$) after the end of a free flight starting at a point \mathbf{r} has a mean, systematically directed momentum $m_s \mathbf{v}_s(\mathbf{r})$ given by the mean velocity $\mathbf{v}_s(\mathbf{r})$ of the s -th gas at the point \mathbf{r} . After a mean free path l it collides again at a point $\mathbf{r} + \mathbf{l}$ with a particle of mass m_r and velocity $\mathbf{v}_r(\mathbf{r} + \mathbf{l})$. By the collision the loss of momentum measured in a co-ordinate system following the mean motion of the s -th gas at the point \mathbf{r} becomes

$$(6) \quad f \cdot m_s [\mathbf{v}_s(\mathbf{r}) - \mathbf{v}_r(\mathbf{r} + \mathbf{l})] \approx f m_s [\mathbf{v}_s(\mathbf{r}) - \mathbf{v}_r(\mathbf{r}) - (\mathbf{l} \cdot \nabla) \mathbf{v}_r(\mathbf{r})],$$

where f is about $\frac{1}{2}$ and 1 for $s=r$ and $s=e$, $r=i, n$ respectively. The variation in \mathbf{v}_r along the distance l due to second order space derivatives has been assumed to be negligible in formula (6). In the succeeding discussions we shall assume that the mean free path l is much smaller than the characteristic dimension over which the mean velocities $\mathbf{v}_r(\mathbf{r})$ change appreciably, i.e., $|(\mathbf{l} \cdot \nabla) \mathbf{v}_r| / |\mathbf{v}_r| \ll 1$. Then, the frictional forces are mainly given by inter-

actions between the gas components moving at different mass velocities and coupled across a single mean free path. Thus, the viscous forces can be neglected since they represent a frictional coupling between neighbouring layers of identical particles; this coupling has to operate across the characteristic distance $|\mathbf{v}_r|/|\partial\mathbf{v}_r/\partial x_\alpha|$ in order to be of the same importance as the friction between different gas components. One exception may occur for viscous forces in the neutral gas when the ionization degree is very low and collisions between neutral particles are much more frequent than between neutral and charged particles. This special case will not be considered here.

A temperature T_i , T_e , T_n is assumed to have established itself for each of the gas components so that we may write

$$(7) \quad p_s = n_s k T_s \quad (s = i, e, n).$$

We shall not deal with the energy theorem in its general form here and shall only use the relations

$$(8) \quad dp_s = C_s^2 m_s dn_s, \quad C_s = (\gamma_s k T_s / m_s)^{1/2} \quad (s = i, e, n),$$

where C_i , C_e , C_n are sound velocities and γ_i , γ_e , γ_n ratios of the specific heats. Eq. (8) is valid for small amplitudes as well as for motions in a non-dissipative medium (cf. LEHNERT [42]).

Finally, we add Maxwell's equations

$$(9) \quad \text{curl } \mathbf{B} / \mu_0 = \mathbf{i} + \epsilon_0 \frac{\partial \mathbf{E}}{\partial t},$$

$$(10) \quad \text{div } \mathbf{E} = e(n_i - n_e) / \epsilon_0,$$

and

$$(11) \quad \text{curl } \mathbf{E} = - \frac{\partial \mathbf{B}}{\partial t},$$

to the set of basic equations, where μ_0 and ϵ_0 are the permeability and dielectric constant in vacuum. Rationalized MKSA units are used in this tract.

2'1.1. Deviations from electric neutrality. — Deviations from electric neutrality are now estimated by dividing eq. (3) by n_i and taking the divergence of the obtained equation

$$(12) \quad e \text{ div } \mathbf{E} = e^2(n_i - n_e) / \epsilon_0 = m_i \text{ div } \left[\frac{\partial \mathbf{v}_i}{\partial t} + (\mathbf{v}_i \cdot \nabla) \mathbf{v}_i \right] - e \text{ div } [\mathbf{v}_i \times (\mathbf{B}_0 + \mathbf{b})] + \\ + \text{div} \left[\frac{1}{n_i} \nabla (n_i k T_i) \right] - 2m_i \text{ div } [\mathbf{v}_i \times \boldsymbol{\Omega}] - m_i \text{ div } [\mathbf{g} + \boldsymbol{\Omega} \times (\mathbf{r} \times \boldsymbol{\Omega})] + \\ + \text{div} \left[\frac{n_e}{n_i} m_e \nu_{ei} (\mathbf{v}_i - \mathbf{v}_e) \right] - \text{div} [m_i \nu_{in} (\mathbf{v}_n - \mathbf{v}_i)],$$

where use has been made of eqs. (7) and (10) and the magnetic field $\mathbf{B} = \mathbf{B}_0 + \mathbf{b}$ has been divided into one part \mathbf{B}_0 generated by external currents and another part \mathbf{b} given by currents inside the region to be considered. An equation similar to eq. (12) is obtained by division of eq. (4) by n_e . To obtain dimensionless relations the transformations

$$(13) \quad \mathbf{Q} = \mathbf{Q}_e \cdot \mathbf{Q}', \quad x_\alpha = L_e \cdot x'_\alpha, \quad t = t_e \cdot t',$$

are now introduced, where \mathbf{Q} stands for any of the field quantities, x_α and t are space and time co-ordinates. Primed quantities are dimensionless, whereas quantities with subscript (e) are constants with the dimensions of \mathbf{Q} , x_α and t . Further, introduce the Debye distances

$$(14) \quad h_i = \sqrt{\frac{\varepsilon_0 k T_{ic}}{e^2 n_{ic}}}, \quad h_e = \sqrt{\frac{\varepsilon_0 k T_{ec}}{e^2 n_{ec}}},$$

the plasma frequencies

$$(15) \quad \omega_{pi} = \sqrt{\frac{e^2 n_{ic}}{\varepsilon_0 m_i}} = \frac{1}{\sqrt{2}} w_i / h_i, \quad \omega_{pe} = \sqrt{\frac{e^2 n_{ec}}{\varepsilon_0 m_e}} = \frac{1}{\sqrt{2}} w_e / h_e,$$

and the gyro frequencies

$$(16) \quad \left\{ \begin{array}{ll} \omega_{i0} = e B_{0c} / m_i = w_i / a_{i0}, & \omega_{e0} = e B_{0c} / m_e = w_e / a_{e0}, \\ \omega_i = e b_c / m_i = w_i / a_i, & \omega_e = e b_c / m_e = w_e / a_e, \end{array} \right.$$

where w_i and w_e are $(3/2)^{\frac{1}{2}}$ times the thermal velocities of the ions and electrons and a_{i0} , a_{e0} , a_i and a_e are the radii of gyration in corresponding magnetic fields. The physical significance of the parameters (14) and (15) can be understood qualitatively if all charges n_s of one sign are imagined to be removed a distance x_1 in one direction inside a limited region. An electric field $en_s x_1 / \varepsilon_0$ is generated and the work performed when the charges are removed up to $x_1 = h$ becomes $e^2 n_s^2 h^2 / 2 \varepsilon_0$. If this work is taken from the thermal energy which is imagined to be entirely converted into electrostatic energy we obtain

$$(17) \quad e^2 n_s^2 h^2 / 2 \varepsilon_0 = \frac{3}{2} n_s k T_s,$$

which gives a value h of the order of h_s (see also SPITZER [67]). From eq. (15) we also see that the times $1/\omega_{pi}$ and $1/\omega_{pe}$ are the times required for a particle with thermal velocity to travel the distances h_i and h_e . The dimensionless

equation (12) is now multiplied by $\varepsilon_0/e^2 n_{ic}$ and the following result is obtained:

$$\begin{aligned}
 (18) \quad \frac{n_i - n_e}{n_{ic}} = & \frac{v_{ic}/L_c}{\omega_{pi}^2 t_c} \operatorname{div}' \frac{\partial \mathbf{v}_i'}{\partial t'} + \frac{v_{ic}^2}{\omega_{pi}^2 L_c^2} \operatorname{div}' [(\mathbf{v}_i' \cdot \nabla) \mathbf{v}_i'] + \\
 & + \sqrt{2} \frac{h_i}{a_{i0}} \frac{v_{ic}}{\omega_{xi} L_c} \operatorname{div}' (\mathbf{v}_i' \times \mathbf{B}_0') + \sqrt{2} \frac{h_i}{a_i} \cdot \frac{v_{ic}}{\omega_{pi} L_c} \operatorname{div}' (\mathbf{v}_i' \times \mathbf{b}') + \\
 & + \left(\frac{h_i}{L_c} \right)^2 \operatorname{div}' \left(\frac{1}{n_i'} \nabla' (n_i' k T_i') \right) - 2 \frac{v_{ic}}{\omega_{pi} L_c} \cdot \frac{\Omega}{\omega_{pi}} \operatorname{div}' (\mathbf{v}_i' \times \Omega) - \\
 & - \frac{g_c}{\omega_{pi}^2 L_c} \operatorname{div}' \mathbf{g}' - \left(\frac{\Omega}{\omega_{xi}} \right)^2 \frac{r_c}{L_c} \operatorname{div}' [\Omega' \times (\mathbf{r}' \times \Omega)] + \\
 & + \frac{m_e}{m_i} \cdot \frac{n_{ec}}{n_{ic}} \cdot \frac{v_{eic}}{\omega_{pi}} \cdot \frac{v_{ic}}{\omega_{pi} L_c} \cdot \operatorname{div}' \left(\frac{n_e'}{n_i'} v_{ei}' v_i' \right) - \\
 & - \frac{m_e}{m_i} \cdot \frac{n_{ec}}{n_{ic}} \cdot \frac{v_{eic}}{\omega_{pi}} \cdot \frac{v_{ec}}{\omega_{pi} L_c} \cdot \operatorname{div}' \left(\frac{n_e'}{n_i'} v_{ei}' v_e' \right) - \\
 & - \frac{v_{inc}}{\omega_{pi}} \cdot \frac{v_{nc}}{\omega_{pi} L_c} \cdot \operatorname{div}' (v_{in}' v_n') + \frac{v_{inc}}{\omega_{pi}} \cdot \frac{v_{ic}}{\omega_{pi} L_c} \cdot \operatorname{div}' (v_{in}' v_i').
 \end{aligned}$$

A similar equation may be deduced for the electron gas where

$$v_{eic} v_{ic} \operatorname{div}' (v_{ei}' v_i') / (\omega_{pe}^2 L_c) \quad \text{and} \quad v_{eic} v_{ec} \operatorname{div}' (v_{ei}' v_e') / (\omega_{pe}^2 L_c)$$

replace the ninth and tenth terms of the right hand member. Further, this member should be multiplied by n_{ec}/n_i , the index (e) replace (i) in the remaining terms and the two last terms change sign.

Besides being regarded simply as a transformation to dimensionless variables, eq. (18) can also be used to estimate the order of magnitude of the relative deviation $(n_i - n_e)/n_{ic}$ from electric neutrality. If all the field quantities vary appreciably only within the length L_c and time t_c and if this variation is of the order given by the quantities with subscript (c) all the primed, dimensionless expressions will be of the order unity. Then, the coefficients of the dimensionless expressions indicate the order of magnitude of corresponding terms.

Eq. (18) shows that the deviations from electric neutrality are small when the Debye distances h_i and h_e are much less than the characteristic dimension L_c and the plasma periods $1/\omega_{pi}$ and $1/\omega_{pe}$ small compared with the characteristic time t_c and the times L_c/v_{ic} , L_c/v_{ec} , L_c/v_{nc} for matter to pass the distance L_c . Both in cosmical and terrestrial applications the acceleration due to gravity g_c is much less than $\omega_{pi}^2 L_c$ and $\omega_{pe}^2 L_c$ and the angular velocity Ω much less than the plasma frequencies. Some examples given in Table I may serve as an illustration.

TABLE I. — *Estimations of the deviations from electric neutrality.*

	Sunspots at solar surface	Tidal motion in the ionospheric E-region	Low current experiments with helium	High current experiments with deuterium
n_{ic} (m^{-3})	10^{20}	10^{11}	$3 \cdot 10^{14}$	10^{20}
n_{nc} (m^{-3})	$3 \cdot 10^{23}$	$2 \cdot 10^{18}$	$3 \cdot 10^{22}$	—
T_i ($^{\circ}K$)	10^4	250	800	10^6
T_e ($^{\circ}K$)	10^4	250	$5 \cdot 10^4$	10^6
T_n ($^{\circ}K$)	10^4	250	300	—
L_c (m)	$2 \cdot 10^7$	$2 \cdot 10^4$	0.1	0.1
t_c (s)	$6 \cdot 10^5$	$8.7 \cdot 10^4$	10^{-4}	$4 \cdot 10^{-3}$
v_{ic} (m/s)	$3 \cdot 10^3$	1	10^3	500
v_{ec} (m/s)	$3 \cdot 10^3$	1	10^3	500
v_{nc} (m/s)	$3 \cdot 10^3$	1	0	—
B_{0c} (Vs/m ²)	$10^{-4} \dots 10^{-3}$	$6 \cdot 10^{-5}$	0.1	0.2
b_c (Vs/m ²)	0.2	10^{-7}	10^{-4}	0.2
g_c (m/s ²)	274	9.81	9.81	9.81
Ω (s ⁻¹)	$3 \cdot 10^{-6}$	$1.15 \cdot 10^{-5}$	$< 10^3$	$< 10^3$
r_c (m)	$6 \cdot 10^8$	$5 \cdot 10^6$	0.1	0.1
v_{eic} (s ⁻¹)	$2 \cdot 10^9$	500	500	$2 \cdot 10^6$
v_{inc} (s ⁻¹)	10^9	10^3	$3 \cdot 10^7$	—
v_{enc} (s ⁻¹)	$2 \cdot 10^{10}$	$3 \cdot 10^4$	$3 \cdot 10^9$	—
ω_{pi} (s ⁻¹)	10^{10}	$8 \cdot 10^4$	$2 \cdot 10^7$	10^{10}
ω_{pe} (s ⁻¹)	$5 \cdot 10^{11}$	$2 \cdot 10^7$	10^9	$5 \cdot 10^{11}$
h_i (m)	$8 \cdot 10^{-7}$	$3 \cdot 10^{-3}$	10^{-4}	$5 \cdot 10^{-5}$
h_e (m)	$8 \cdot 10^{-7}$	$3 \cdot 10^{-3}$	$9 \cdot 10^{-4}$	$5 \cdot 10^{-5}$
$ n_i - n_e /n_{ic}$	10^{-17}	10^{-12}	10^{-3}	10^{-8}

The assumption of electric quasi-neutrality is very well satisfied in all cosmical applications where phenomena of cosmical dimensions L_c are concerned. In the laboratory deviations from electric neutrality are negligible in a high current discharge such as in Zeta (THONEMANN *et al.* [68]), but not necessarily in low current discharges such as in the subnormal positive column at current densities below some 10^{-4} ampere.

There are, of course, also important phenomena both in cosmical physics and in the laboratory characterized by a small scale in space and short scale in time. Plasma oscillations or other rapid displacements of charges, sometimes within distances comparable to h_i and h_e correspond to marked deviations from electric neutrality, as is also indicated by eq. (18). Another example is given by the thin plasma sheath near a probe or a wall in a discharge experiment, the sheath thickness being of the order of h_e . It should also be observed that the quasi-neutral situation, whenever it is indicated by eq. (18), makes the approximation $n_i \approx n_e$ possible in eqs. (3) and (4) but that this

does not necessarily imply that one should put $\text{div } \mathbf{E} = 0$. Even the slightest charge separation in a quasi-neutral plasma may give rise to strong electric fields. One such example is given by the field arising from ambipolar diffusion, which will be discussed at the end of this paper.

The Debye distance also indicates the distance outside of which the electric field of a charge mainly will be screened from the surrounding plasma. A redistribution of charge is made by the thermal velocity and, according to eq. (5), the time required for this redistribution within the distances h_e and h_i is about $1/\omega_{pi}$ and $1/\omega_{pe}$. Evidently, this rearrangement of charges can be delayed by a magnetic field and by collisions, provided that these take place inside the Debye distances, *i.e.*, when the radii of gyration a_i and a_e become comparable to h_i and h_e and when the collision frequencies ν_{ei} , ν_{in} and ν_{en} become comparable to ω_{pi} and ω_{pe} . This explains the existence of the terms containing $\mathbf{v}_i \times \mathbf{B}$ and $\mathbf{v}_e \times \mathbf{B}$ and the collision terms in eq. (18). It is also clear that a difference in friction forces acting on the ion and electron fluids by collisions with the neutral gas could produce charge separation. The terms arising from the Coriolis force can be understood in a similar way from the analogy between the influence of a magnetic field \mathbf{B} and the angular velocity $\boldsymbol{\Omega}$. Finally, there should also exist a possibility of charge separation caused by the gravitation and centrifugal potential as indicated in eq. (18). This effect can be seen in an isothermal, fully ionized, static atmosphere for which eqs. (3) and (4) reduce to

$$(19) \quad \begin{cases} 0 = -en_i \mathbf{E} - kT \nabla n_i + n_i m_i [\mathbf{g} + \boldsymbol{\Omega} \times (\mathbf{r} \times \boldsymbol{\Omega})], \\ 0 = -en_e \mathbf{E} - kT \nabla n_e + n_e m_e [\mathbf{g} + \boldsymbol{\Omega} \times (\mathbf{r} \times \boldsymbol{\Omega})]. \end{cases}$$

Because of their smaller mass electrons have a tendency to escape more easily than ions and an electric field caused by charge separation is needed to establish an equilibrium (cf. SPITZER 67, p. 23]). Charge separation by the gravitation field is, of course, also taking place when $\text{div } \mathbf{g} = 0$ as indicated by eq. (19). The terms containing divergences of the gravitation and centrifugal forces in eq. (18) are only terms of higher order. Consequently, the values of g_c to be put into eq. (18) are less than the surface gravities in the nearly homogeneous gravitation fields in the examples of Table I.

2.1.2. Reformulation of the basic equations. — Electric quasi-neutrality is now assumed throughout this paper by putting $n_i \approx n_e = n$. Introduce

$$(20) \quad \varrho = n_i m_i + n_e m_e = nm, \quad \varrho_n = n_n m_n,$$

$$(21) \quad \mathbf{v} = (n_i m_i \mathbf{v}_i + n_e m_e \mathbf{v}_e) / \varrho,$$

$$(22) \quad \mathbf{i} = e(n_i \mathbf{v}_i - n_e \mathbf{v}_e),$$

$$(23) \quad \mathbf{v}_i = \mathbf{v} + \frac{m_e}{enm} \mathbf{i},$$

$$(24) \quad \mathbf{v}_e = \mathbf{v} - \frac{m_i}{enm} \mathbf{i},$$

and

$$(25) \quad p = p_i + p_e,$$

where ϱ and ϱ_n are the densities of the plasma and the neutral gas, \mathbf{v} the mean velocity of the plasma and p the plasma pressure. Substitution of these expressions into eqs. (3) and (4) gives

$$(26) \quad nm_i \frac{\partial}{\partial t} \left(\mathbf{v} + \frac{m_e}{e} \mathbf{i} / \varrho \right) + nm_i \left[\left(\mathbf{v} + \frac{m_e}{e} \mathbf{i} / \varrho \right) \cdot \nabla \right] \cdot \left(\mathbf{v} + \frac{m_e}{e} \mathbf{i} / \varrho \right) = \\ = en(\mathbf{E} + \mathbf{v} \times \mathbf{B}) + \frac{m_e}{m} \mathbf{i} \times \mathbf{B} - \nabla p_i + 2nm_i \mathbf{v} \times \boldsymbol{\Omega} + 2 \frac{m_i m_e}{em} \mathbf{i} \times \boldsymbol{\Omega} + \\ + nm_i [\mathbf{g} + \boldsymbol{\Omega} \times (\mathbf{r} \times \boldsymbol{\Omega})] - \frac{m_e v_{ei}}{e} \mathbf{i} + nm_i v_{in} (\mathbf{v}_n - \mathbf{v}) - \frac{m_i m_e}{em} v_{in} \mathbf{i},$$

and

$$(27) \quad nm_e \frac{\partial}{\partial t} \left(\mathbf{v} - \frac{m_i}{e} \mathbf{i} / \varrho \right) + nm_e \left[\left(\mathbf{v} - \frac{m_i}{e} \mathbf{i} / \varrho \right) \cdot \nabla \right] \cdot \left(\mathbf{v} - \frac{m_i}{e} \mathbf{i} / \varrho \right) = \\ = -en(\mathbf{E} + \mathbf{v} \times \mathbf{B}) + \frac{m_i}{m} \mathbf{i} \times \mathbf{B} - \nabla p_e + 2nm_e \mathbf{v} \times \boldsymbol{\Omega} - 2 \frac{m_i m_e}{em} \mathbf{i} \times \boldsymbol{\Omega} + \\ + nm_e [\mathbf{g} + \boldsymbol{\Omega} \times (\mathbf{r} \times \boldsymbol{\Omega})] + \frac{m_e v_{ei}}{e} \mathbf{i} + nm_e v_{en} (\mathbf{v}_n - \mathbf{v}) + \frac{m_i m_e}{em} v_{en} \mathbf{i}.$$

The sum of these equations becomes

$$(28) \quad \varrho \frac{d\mathbf{v}}{dt} + \frac{m_i m_e}{e^2} (\mathbf{i} \cdot \nabla) (\mathbf{i} / \varrho) = \mathbf{i} \times \mathbf{B} - \nabla p + 2\varrho \mathbf{v} \times \boldsymbol{\Omega} + \\ + \varrho [\mathbf{g} + \boldsymbol{\Omega} \times (\mathbf{r} \times \boldsymbol{\Omega})] - \varrho \alpha (\mathbf{v} - \mathbf{v}_n) + \beta \mathbf{i},$$

where the derivative $d/dt \equiv \partial/\partial t + (\mathbf{v} \cdot \nabla)$ following the center of mass of the plasma has been introduced together with the notations

$$(29) \quad \alpha = (m_i v_{in} + m_e v_{en})/m, \quad \beta = m_i m_e (v_{en} - v_{in})/em.$$

Eq. (28) can be regarded as the conservation of momentum of the mean motion of the plasma considered as one entity. The corresponding equation for a fully ionized gas has earlier been derived by SCHLÜTER [65] and for small amplitudes in a partially ionized gas by LUCAS and SCHLÜTER [47].

If eq. (26) is multiplied by $m_e/e\rho$ and eq. (27) by $m_i/e\rho$ the difference of the resulting equations becomes

$$(30) \quad \frac{m_i m_e}{e^2} \frac{d}{dt} (\mathbf{i}/\rho) + \frac{m_i m_e}{e^2 \rho} (\mathbf{i} \cdot \nabla) \mathbf{v} - \frac{m_i m_e (m_i - m_e)}{e^3 \rho} (\mathbf{i} \cdot \nabla) (\mathbf{i}/\rho) = \\ = \mathbf{E} + \mathbf{v} \times \mathbf{B} - \frac{m_i - m_e}{e \rho} \mathbf{i} \times \mathbf{B} + \frac{1}{e \rho} (m_i \nabla p_e - m_e \nabla p_i) + \\ + 2 \frac{m_i m_e}{e^2 \rho} \mathbf{i} \times \boldsymbol{\Omega} + \beta (\mathbf{v} - \mathbf{v}_n) - \gamma \mathbf{i}/\rho,$$

where

$$(31) \quad \gamma = m m_e \left[\nu_{ei} + \left(\frac{m_i}{m} \right)^2 \nu_{en} + \frac{m_i m_e}{m^2} \nu_{in} \right] / e^2.$$

Eq. (30) is a generalization of Ohm's law and can be considered to express the conservation of momentum of the relative motion between the ion and electron gases. It has earlier been derived by SCHLÜTER [65] for a fully ionized gas and by GERSHMAN and GINZBURG [29] for small amplitudes in a partially ionized gas.

Finally, conservation of momentum of the neutral gas motion given by eq. (5) has the form

$$(32) \quad \rho_n \left[\frac{\partial \mathbf{v}_n}{\partial t} + (\mathbf{v}_n \cdot \nabla) \mathbf{v}_n \right] = -\nabla p_n + 2 \rho_n \mathbf{v}_n \times \boldsymbol{\Omega} + \\ + \rho_n [\mathbf{g} + \boldsymbol{\Omega} \times (\mathbf{r} \times \boldsymbol{\Omega})] + \rho \alpha (\mathbf{v} - \mathbf{v}_n) - \beta \mathbf{i}.$$

The sum of eqs. (28) and (32) becomes

$$(33) \quad \rho \frac{d\mathbf{v}}{dt} + \rho_n \left[\frac{\partial \mathbf{v}_n}{\partial t} + (\mathbf{v}_n \cdot \nabla) \mathbf{v}_n \right] + \frac{m_i m_e}{e^2} (\mathbf{i} \cdot \nabla) (\mathbf{i}/\rho) = \mathbf{i} \times \mathbf{B} - \nabla(p + p_n) + \\ + 2(\rho \mathbf{v} + \rho_n \mathbf{v}_n) \times \boldsymbol{\Omega} + (\rho + \rho_n) [\mathbf{g} + \boldsymbol{\Omega} \times (\mathbf{r} \times \boldsymbol{\Omega})].$$

When the coupling between plasma and neutral gas is strong so that $\mathbf{v} \approx \mathbf{v}_n$ eq. (33) is suitable for the description of the balance between the total forces acting on the gas mixture considered as an entirety. However, in the limit of negligible coupling, i.e., when the two last terms in eqs. (28) and (32) disappear the relation (33) merely becomes the sum of two independent equations and it is then preferable to discuss eqs. (28) and (32) separately.

2.1.3. Estimations of the conditions in a quasi-neutral gas. — Eq. (28) is now transformed to a dimensionless form. The current density \mathbf{i} is substituted from eq. (9) into eq. (28) which, after having been multiplied

by $\mu_0 L_c / b_c^2$ becomes

$$(34) \quad \frac{v_c L_c}{V^2 t_c} \cdot \frac{\partial \mathbf{v}'}{\partial t'} + \frac{v_c^2}{V^2} \cdot (\mathbf{v}' \cdot \nabla') \mathbf{v}' + \frac{m_i c^2}{m \omega_{pe}^2 L_c^2} \left\{ \left[\left(\text{curl}' \mathbf{b}' - \frac{E_c L_c}{c^2 t_c b_c} \cdot \frac{\partial \mathbf{E}'}{\partial t'} \right) \cdot \nabla' \right] \cdot \left(\frac{1}{\varrho'} \text{curl}' \mathbf{b}' - \frac{E_c L_c}{c^2 t_c b_c \varrho'} \cdot \frac{\partial \mathbf{E}'}{\partial t'} \right) \right\} = \left(\text{curl}' \mathbf{b}' - \frac{E_c L_c}{c^2 t_c b_c} \cdot \frac{\partial \mathbf{E}'}{\partial t'} \right) \times \left(\frac{B_{0c}}{b_c} \mathbf{B}' + \mathbf{b}' \right) - \frac{p_c}{b_c^2 / \mu_0} \nabla' p' + 2 \frac{v_c \Omega L_c}{V^2} \varrho' \mathbf{v}' \times \boldsymbol{\Omega}' + \frac{g_c L_c}{V^2} \varrho' \mathbf{g}' + \frac{\Omega^2 L_c r_c}{V^2} \varrho' \boldsymbol{\Omega}' \times (\mathbf{r}' \times \boldsymbol{\Omega}') - \frac{\alpha_c L_c v_c}{V^2} \varrho' \alpha' \mathbf{v}' + \frac{\alpha_c L_c v_{nc}}{V^2} \varrho' \alpha' \mathbf{v}'_n + \frac{m_i}{m} \cdot \frac{v_{enc} - v_{inc}}{\omega_e} \left(\text{curl}' \mathbf{b}' - \frac{E_c L_c}{c^2 t_c b_c} \cdot \frac{\partial \mathbf{E}'}{\partial t'} \right),$$

where $V = b_c / (\mu_0 \varrho_c)^{\frac{1}{2}}$ is the Alfvén velocity corresponding to the density ϱ_c and the magnetic self-field b_c and $c = 1 / (\mu_0 \varepsilon_0)^{\frac{1}{2}}$ is the velocity of light. Similarly, eq. (33) transforms to

$$(35) \quad \frac{v_c L_c}{V^2 t_c} \frac{\partial \mathbf{v}'}{\partial t'} + \frac{v_c^2}{V^2} \cdot (\mathbf{v}' \cdot \nabla') \mathbf{v}' + \frac{v_{nc} L_c}{V_n^2 t_c} \cdot \frac{\partial \mathbf{v}'_n}{\partial t'} + \frac{v_{nc}^2}{V_n^2} (\mathbf{v}'_n \cdot \nabla') \mathbf{v}'_n + \frac{m_i}{m} \frac{c^2}{\omega_{pe}^2 L_c^2} \cdot \left\{ \left[\left(\text{curl}' \mathbf{b}' - \frac{E_c L_c}{c^2 t_c b_c} \cdot \frac{\partial \mathbf{E}'}{\partial t'} \right) \cdot \nabla' \right] \cdot \left(\frac{1}{\varrho'} \text{curl}' \mathbf{b}' - \frac{E_c L_c}{c^2 t_c b_c \varrho'} \cdot \frac{\partial \mathbf{E}'}{\partial t'} \right) \right\} = \left(\text{curl}' \mathbf{b}' - \frac{E_c L_c}{c^2 t_c b_c} \cdot \frac{\partial \mathbf{E}'}{\partial t'} \right) \times \left(\frac{B_{0c}}{b_c} \mathbf{B}' + \mathbf{b}' \right) - \frac{p_c}{b_c^2 / \mu_0} \nabla' p' - \frac{p_{nc}}{b_c^2 / \mu_0} \nabla' p + 2 \frac{v_c \Omega L_c}{V^2} \varrho' \mathbf{v}' \times \boldsymbol{\Omega}' + 2 \frac{v_{nc} \Omega L_c}{V_n^2} \varrho'_n \mathbf{v}'_n \times \boldsymbol{\Omega}' + \frac{g_c L_c}{V^2} \varrho' \mathbf{g}' + \frac{g'_n L_c}{V_n^2} \varrho'_n \mathbf{g}' + \frac{\Omega^2 L_c r_c}{V^2} \varrho' \boldsymbol{\Omega}' \times (\mathbf{r}' \times \boldsymbol{\Omega}') + \frac{\Omega^2 L_c r'_n}{V_n^2} \varrho'_n \boldsymbol{\Omega}' \times (\mathbf{r}' \times \boldsymbol{\Omega}'),$$

where $V_n = b_c / (\mu_0 \varrho_n)^{\frac{1}{2}}$. Further, we multiply eq. (30) by $e L_c / m_i V^2$ and obtain the transformed equation

$$(36) \quad \frac{1}{\omega_e t_c} \cdot \frac{\partial}{\partial t'} \left(\frac{1}{\varrho'} \text{curl}' \mathbf{b}' - \frac{E_c L_c}{c^2 t_c b_c \varrho'} \cdot \frac{\partial \mathbf{E}'}{\partial t'} \right) + \frac{v_c}{\omega_e L_c} (\mathbf{v}' \cdot \nabla') \left(\frac{1}{\varrho'} \text{curl}' \mathbf{b}' - \frac{E_c L_c}{c^2 t_c b_c \varrho'} \cdot \frac{\partial \mathbf{E}'}{\partial t'} \right) + \frac{v_c}{\omega_e L_c} \cdot \frac{1}{\varrho'} \left[\left(\text{curl}' \mathbf{b}' - \frac{E_c L_c}{c^2 t_c b_c} \cdot \frac{\partial \mathbf{E}'}{\partial t'} \right) \cdot \nabla' \right] \mathbf{v}' - \left(1 - \frac{m_e}{m_i} \right) \frac{m_i}{m} \cdot \frac{c^2}{\omega_{pe}^2 L_c^2} \frac{1}{\varrho'} \left[\left(\text{curl}' \mathbf{b}' - \frac{E_c L_c}{c^2 t_c b_c} \cdot \frac{\partial \mathbf{E}'}{\partial t'} \right) \cdot \nabla' \right] \cdot \left(\frac{1}{\varrho'} \text{curl}' \mathbf{b}' - \frac{E_c L_c}{c^2 t_c b_c \varrho'} \cdot \frac{\partial \mathbf{E}'}{\partial t'} \right) = \frac{\omega_i L_c}{V^2} \cdot \frac{E_c}{b_c} \mathbf{E}' + \frac{\omega_i L_c v_c}{V^2} \left[\mathbf{v}' \times \left(\frac{B_{0c}}{b_c} \mathbf{B}' + \mathbf{b}' \right) \right] - \left(1 - \frac{m_e}{m_i} \right) \left(\text{curl}' \mathbf{b}' - \frac{E_c L_c}{c^2 t_c b_c} \cdot \frac{\partial \mathbf{E}'}{\partial t'} \right) \times \left(\frac{B_{0c}}{b_c} \mathbf{B}' + \mathbf{b}' \right) + \frac{p_{ec}}{b_c^2 / \mu_0} \nabla' p'_e -$$

$$\begin{aligned}
& -\frac{p_{ic}}{b_c^2/\mu_0} \nabla' p_i + 2 \frac{\Omega}{\omega_e} \left(\text{curl}' \mathbf{b}' - \frac{E_c L_c}{c^2 t_c b_c} \cdot \frac{\partial \mathbf{E}'}{\partial t'} \right) \times \boldsymbol{\Omega}' + \\
& + \frac{m_e}{m} \cdot \frac{(v_{enc} - v_{inc}) L_c v_c}{V^2} \mathbf{v}' - \frac{m_e}{m} \cdot \frac{(v_{enc} - v_{inc}) L_c v_{nc}}{V^2} \mathbf{v}'_n - \\
& - \frac{m}{m_i} \left[v_{eic} + \left(\frac{m_i}{m} \right)^2 v_{enc} + \frac{m_i m_e}{m^2} v_{inc} \right] \frac{1}{\omega_e} \left(\text{curl}' \mathbf{b}' - \frac{E_c L_c}{c^2 t_c b_c} \cdot \frac{\partial \mathbf{E}'}{\partial t'} \right) / \varrho'.
\end{aligned}$$

Finally, eq. (11) becomes

$$(37) \quad \frac{E_c t_c}{b_c L_c} \text{curl}' \mathbf{E}' + \frac{\partial \mathbf{b}'}{\partial t'} = 0.$$

In a manner analogous to that used in the preceding Sect. 2'1.1. orders of magnitude of the different forces acting on the gas mixture are now estimated from the values of the coefficients containing quantities with subscript (*c*). Assuming L_c to be the characteristic dimension within which the field variables change noticeably eq. (37) indicates that the characteristic field E_c is of the order $b_c L_c / t_c$ and from this the coefficient of the dimensionless displacement current $\partial \mathbf{E}' / \partial t'$ in eqs. (34), (35) and (36) will be of the order of $L_c^2 / t_c^2 c^2$. We shall restrict our discussion to situations where the phase velocity L_c / t_c of the phenomena to be considered at least does not exceed the velocity of light considerably. This implies that we are going to discuss cases where the dimensionless current density term, $\text{curl}' \mathbf{b}' - (L_c^2 / t_c^2 c^2) \partial \mathbf{E}' / \partial t'$, does not exceed unity very much.

The way in which eqs. (34) and (35) have been written makes possible a rough comparison between the electrodynamic force $\mathbf{i} \times \mathbf{B}$ and other forces acting on the gas mixture. For phenomena with a small magnetic self-field b_c compared with the field B_{0c} generated by external currents the relative magnitude of the electrodynamic force is of the order B_{0c} / b_c . On the other hand the relative magnitude of the same force should be put equal to about unity when phenomena with strong self-fields ($b_c \geq B_{0c}$) are concerned. It should be observed that the propagation of magnetohydrodynamic waves in an external field is controlled by the term $B_{0c} \mathbf{B}'_0 / b_c$ in eqs. (34) and (35) whereas the self-field \mathbf{b} mainly takes part in the internal pressure balance of the wave. In eq. (36) the Hall term, $(m_i - m_e) \mathbf{i} \times \mathbf{B} / e \varrho$, is compared with other terms in an analogous manner. The examples given in Table I will now be used to illustrate the following effects.

a) «Creeping diffusion» in the plasma. When the difference between the non-linear acceleration terms in eqs. (3) and (4) is assumed to be negligible, *i.e.* when

$$(38) \quad (\mathbf{v}_i \cdot \nabla) \mathbf{v}_i \approx (\mathbf{v}_e \cdot \nabla) \mathbf{v}_e \approx (\mathbf{v} \cdot \nabla) \mathbf{v}$$

the plasma is said to be in a state of «creeping diffusion» according to SCHLÜTER [63, 64]. This is equivalent to neglecting the terms in eqs. (28) and (30) containing $(\mathbf{i} \cdot \nabla)$ and $(\mathbf{v} \cdot \nabla)(\mathbf{i}/\rho)$. According to eqs. (34), (35) and (36) this is a fair approximation provided that

$$(39a) \quad \frac{b_c}{B_{0c}} (c^2/\omega_{pe}^2 L_c^2) \ll 1, \quad \frac{b_c}{B_{0c}} (v_c/\omega_e L_c) \ll 1,$$

for phenomena with weak self-fields and

$$(39b) \quad c^2/\omega_{pe}^2 L_c^2 \ll 1, \quad v_c/\omega_e L_c \ll 1$$

for phenomena with strong self-fields. These conditions are usually very well satisfied in cosmical phenomena of large scale, as is illustrated in the two first examples of Table II, but it is not necessary that they should always be satisfied to a high degree of approximation in experiments, as seen from the two last examples in the same table. «Creeping diffusion» between plasma and neutral gas, however, shall not be assumed as a general rule here since weak coupling between charged and uncharged particles may occur in some important cases.

b) Inertia forces acting on the currents. The first term in the left hand member of eq. (36) can be regarded as an equivalent electric field acting on the moving charges and produced by their inertia and is present also when non-linear terms can be neglected. It is negligible in situations with weak self-fields when

$$(40a) \quad 1/\omega_{e0} t_c \ll 1$$

and for strong self-fields when

$$(40b) \quad 1/\omega_e t_c \ll 1.$$

This situation seems to be frequent in cosmical physics as well as in the laboratory.

c) Coriolis force. When the relative magnitude of the Coriolis force is estimated the cases of weak and strong coupling between plasma and neutral gas should be distinguished from each other. When both the coupling and the self-field are weak (or the influence of the external field is estimated separately) the Coriolis force is negligible compared with the electrodynamic force in eq. (28) when

$$(41a) \quad v_c \Omega L_c / V V_0 \ll 1,$$

TABLE II. — *Estimations of the relative importance of different effects in an ionized gas.*
Values taken from Table I.

Different effects		Sunspots at solar surface	Tidal motion in the ionospheric E-region	Low current experiments with helium	High current experiments with deuterium
« Creeping diffusion » in the plasma	$(b_c/B_{0c})(c^2/\omega_{pe}^2 L_c^2)$	—	10^{-9}	10^{-2}	—
	$(b_c/B_{0c})(v_c/\omega_e L_c)$	—	$5 \cdot 10^{-11}$	$5 \cdot 10^{-7}$	—
	$c^2/\omega_{pe}^2 L_c^2$	10^{-19}	—	—	$4 \cdot 10^{-3}$
	$v_c/\omega_e L_c$	$4 \cdot 10^{-15}$	—	—	10^{-7}
Inertia forces acting on the currents	$1/\omega_{e0} t_c$	—	10^{-11}	$5 \cdot 10^{-7}$	—
	$1/\omega_e t_c$	$5 \cdot 10^{-17}$	—	—	10^{-8}
Coriolis force	$v_c \Omega L_c / V V_0$	—	—	$< 5 \cdot 10^{-8}$	—
	$v_c \Omega L_c / V^2$	—	—	—	$< 5 \cdot 10^{-7}$
	$v_c \Omega L_c [(1/V V_0) + (1/V_n V_{n0})]$	1 ... 10	10^{-2}	—	—
	$v_c \Omega L_c [(1/V)^2 + (1/V_n)^2]$	10^{-2}	2	—	—
	Ω/ω_{e0}	$2 \cdot 10^{-14} \dots 2 \cdot 10^{-13}$	10^{-12}	$< 5 \cdot 10^{-14}$	—
	Ω/ω_e	10^{-16}	$6 \cdot 10^{-10}$	—	$< 3 \cdot 10^{-8}$
Gravitation force	$g_c L_c / V V_0$	—	—	$3 \cdot 10^{-13}$	—
	$g_c L_c / V^2$	—	—	$3 \cdot 10^{-10}$	10^{-11}
	$g_c L_c [(1/V V_0) + (1/V_n V_{n0})]$	$10^4 \dots 10^5$	$3 \cdot 10^3$	—	—
	$g_c L_c [(1/V)^2 + (1/V_n)^2]$	10^2	$2 \cdot 10^6$	—	—
Centrifugal force	$\Omega^2 L_c r_c / V V_0$	—	—	$< 3 \cdot 10^{-9}$	—
	$\Omega^2 L_c r_c / V^2$	—	—	$< 3 \cdot 10^{-6}$	$< 10^{-7}$
	$\Omega^2 L_c r_c [(1/V V_0) + (1/V_n V_{n0})]$	0.4 ... 4	0.17	—	—
	$\Omega^2 L_c r_c [(1/V)^2 + (1/V_n)^2]$	$2 \cdot 10^{-3}$	100	—	—
Hall term	$\omega_{e0} / \left[v_{eic} + \left(\frac{m_i}{m} \right)^2 v_{enc} + \frac{m_i m_e}{m^2} v_{inc} \right]$	—	0.5	20	—
	$\omega_e / \left[v_{eic} + \left(\frac{m_i}{m} \right)^2 v_{enc} + \frac{m_i m_e}{m^2} v_{inc} \right]$	1	—	—	$2 \cdot 10^6$

where $V_0 = B_0/(\mu_0 \varrho_c)^{\frac{1}{2}}$. When the coupling is still weak but the self-field strong the condition becomes

$$(41b) \quad v_c \Omega L_c / V^2 \ll 1.$$

On the other hand, the conditions in the case of strong coupling are

$$(42a) \quad v_c \Omega L_c [(1/V V_0) + (1/V_n V_{n0})] \ll 1$$

and

$$(42b) \quad v_c \Omega L_c [(1/V)^2 + (1/V_n)^2] \ll 1,$$

respectively, where $V_{n0} = B_0/(\mu_0 \varrho_{nc})^{\frac{1}{2}}$ and the comparison is carried out between the forces in eq. (35).

Finally, the influence of the Coriolis force on the motion of the moving charges in Ohm's law (36) can be neglected if

$$(43) \quad \Omega/\omega_{e0} \ll 1 \quad \text{and} \quad \Omega/\omega_e \ll 1$$

in cases of weak and strong self-fields, respectively.

This latter situation is likely to be true both in cosmical physics and in experiments as is also illustrated by the examples in Table II. However, in some cosmical applications, such as the propagation of magnetohydrodynamic waves in the sun (LEHNERT [40, 41]) and tidal motions in the ionosphere (LUCAS [46]), the Coriolis force plays a role in the balance expressed by eqs. (28) and (33). When the influence of the Coriolis force on the propagation of magnetohydrodynamic waves in an external field is treated conditions should be examined with eqs. (41a) and (42a). To realize situations in the laboratory with detectable magnetic fields and important contributions from the Coriolis force at the same time seems to be very difficult with ionized gases. With liquid metals, however, this situation is obtainable.

d) Gravitation and centrifugal forces. Conditions for the gravitation force to be negligible when the coupling between plasma and neutral gas is weak are

$$(44a) \quad g_c L_c / V V_0 \ll 1$$

and

$$(44b) \quad g_c L_c / V^2 \ll 1$$

with weak and strong self-fields, respectively. Strong coupling results in the

conditions

$$(45a) \quad g_c L_c [(1/V V_0) + (1/V_n V_{n0})] \ll 1$$

and

$$(45b) \quad g_c L_c [(1/V)^2 + (1/V_n)^2] \ll 1.$$

Equivalent conditions are obtained for the centrifugal force;

$$(46) \quad \Omega^2 L_c r_c / V V_0 \ll 1,$$

$$(46b) \quad \Omega^2 L_c r_c / V^2 \ll 1,$$

$$(47a) \quad \Omega^2 L_c r_c / [(1/V V_0) + (1/V_n V_{n0})] \ll 1,$$

and

$$(47b) \quad \Omega^2 L_c r_c / [(1/V)^2 + (1/V_n)^2] \ll 1.$$

The examples of Table II indicate that these forces often have to be taken into account in cosmical physics but can be neglected completely in gas discharge experiments, (*) when the plasma does not rotate with higher angular speeds than about 10^3 s^{-1} .

e) The Hall term. The term containing $\mathbf{i} \times \mathbf{B}$ in Ohm's law (30) gives rise to an electric field which is perpendicular to both \mathbf{i} and \mathbf{B} . As seen from eq. (36) it can be neglected besides the dissipation term $\gamma \mathbf{i} / \rho$ when

$$(48a) \quad \omega_{e0} / \left[v_{etic} + \left(\frac{m_i}{m} \right)^2 v_{en} + \frac{m_i m_e}{m^2} v_{inc} \right] \ll 1,$$

and the self-field is weak. When the self-field is strong the corresponding condition becomes

$$(48b) \quad \omega_e / \left[v_{etic} + \left(\frac{m_i}{m} \right)^2 v_{en} + \frac{m_i m_e}{m^2} v_{inc} \right] \ll 1.$$

This implies that the mean free path of an electron should be much smaller than the radius of gyration. In the four examples of Table II the Hall term is of importance, but there could easily be found examples both in cosmical physics and in experiments where the opposite is true.

The possible existence of force-free magnetic fields (LUNDQUIST [49, 50] and LÜST and SCHLÜTER [51]) should not be forgotten in connection with the

(*) Note added in proof: An exception is given by the homopolar experiments (Project Sherwood, Ed. by A. S. BISHOP, Cambridge, Mass. 1958) where rotation is produced by crossed electric and magnetic fields.

estimations made in this section. Even if b_c^2/μ_0 is large compared with other characteristic mean values such as p_c and p_{nc} the electrodynamic force may be of the same order of magnitude as the pressure gradients when \mathbf{i} and \mathbf{B} are almost parallel. For such fields estimations carried out by means of eqs. (34), (35) and (36) give too high values of the electrodynamic force $\mathbf{i} \times \mathbf{B}$.

For a more detailed analysis of the remaining terms in eqs. (34), (35) and (36) we shall turn to a simplified analysis in the succeeding sections.

2.2. Plane disturbance for small amplitudes. The discussion will now be limited to phenomena which can be studied in gas discharge experiments with reasonable efforts. Thus, we are going to neglect the Coriolis, gravitation and centrifugal forces as well as the inertia acting on the currents. Further, sufficiently high charge densities and small amplitudes of the velocities \mathbf{v} , \mathbf{v}_n and the induced fields \mathbf{b} and \mathbf{E} will be assumed to justify the assumption of «creeping diffusion» and to neglect all non-linear terms. Eqs. (1), (2), (28), (30) and (32) reduce to

$$(49) \quad \operatorname{div} \mathbf{v} = -\frac{1}{\varrho_0} \frac{\partial \varrho}{\partial t}, \quad \operatorname{div} \mathbf{v}_n = -\frac{1}{\varrho_{n0}} \frac{\partial \varrho_n}{\partial t},$$

$$(50) \quad \varrho_0 \frac{\partial \mathbf{v}}{\partial t} = \mathbf{i} \times \mathbf{B}_0 - C^2 \nabla \varrho - \varrho_0 \alpha (\mathbf{v} - \mathbf{v}_n) + \beta \mathbf{i},$$

$$(51) \quad \gamma \mathbf{i} / \varrho_0 = \mathbf{E} + \mathbf{v} \times \mathbf{B}_0 - \frac{m_i - m_e}{e \varrho_0} \mathbf{i} \times \mathbf{B}_0 + \frac{m_i m_e}{em \varrho_0} (C_e^2 - C_i^2) \nabla \varrho + \beta (\mathbf{v} - \mathbf{v}_n),$$

and

$$(52) \quad \varrho_{n0} \frac{\partial \mathbf{v}_n}{\partial t} = -C_n^2 \nabla \varrho_n + \varrho_0 \alpha (\mathbf{v} - \mathbf{v}_n) - \beta \mathbf{i},$$

where ϱ and ϱ_n now indicate the deviations of the densities from their static equilibrium values, $\varrho_0 = mn_0$ and $\varrho_{n0} = m_n n_{n0}$, and ϱ_{n0} should be used in the expressions for α , β and γ .

The physical significance of the terms containing α and β in eqs. (50) and (51) is obvious. Suppose that $\mathbf{v} = \mathbf{v}_n$ at a certain instant. The sum of the frictional forces acting on the ion and electron gases together then becomes $\beta \mathbf{i}$ which gives a net force when $v_{in} \neq v_{en}$ and the drags on ions and electrons differ. Now, suppose instead that $\mathbf{i} = 0$ so that $\mathbf{v}_i = \mathbf{v}_e = \mathbf{v} \neq \mathbf{v}_n$. Then, the sum of the frictional forces on ions and electrons becomes $-\varrho_0 \alpha (\mathbf{v} - \mathbf{v}_n)$. If \mathbf{i} has to vanish for all times t an electric field \mathbf{E} must be present which equalizes the accelerations $en\mathbf{E}/m_i + nv_{in}(\mathbf{v}_n - \mathbf{v})$ and $-en\mathbf{E}/m_e + nv_{en}(\mathbf{v}_n - \mathbf{v})$. This gives $\mathbf{E} = -\beta (\mathbf{v} - \mathbf{v}_n)$.

2.2.1. The coupling between plasma and neutral gas. - A plane disturbance where all field quantities vary as $\exp[j\omega t + j\kappa z]$ is the simplest

case to be studied. From eq. (49) is obtained

$$(53) \quad \varrho = -\varrho_0 \kappa v_z / \omega, \quad \varrho_n = -\varrho_{n0} \kappa v_{nz} / \omega.$$

The second of these relations is substituted into eq. (52)

$$(54) \quad \mathbf{v} = \frac{\mathbf{v}}{1 + j(1 - \delta_{sz} C_n^2 / U^2) F} - \frac{\beta}{\alpha \varrho_0} \frac{\mathbf{i}}{1 + j(1 - \delta_{sz} C_n^2 / U^2) F},$$

where

$$(55) \quad F = \omega \varrho_{n0} / \varrho_0 \alpha.$$

$U = \omega / \kappa$ is the phase velocity, $s = x, y, z$ and $\delta_{sz} = 0$ for $s \neq z$ and 1 for $s = z$. The velocity of the neutral gas is eliminated from eqs. (50) and (51) by means of eq. (54) and for the balance of forces acting on a fluid element

$$(56) \quad j\omega\varrho_0 \left[1 + \frac{\varrho_{n0}/\varrho_0}{1 + j(1 - \delta_{sz} C_n^2 / U^2) F} \right] \mathbf{v} = \mathbf{i} \times \mathbf{B}_0 + \\ + j\delta_{sz} \frac{\omega}{U^2} \left[\varrho_0 C^2 + \frac{\varrho_{n0} C_n^2}{1 + j(1 - \delta_{sz} C_n^2 / U^2) F} \right] \mathbf{v} + \frac{\beta}{1 + j(1 - \delta_{sz} C_n^2 / U^2) F} \mathbf{i}.$$

If the pressure terms containing C and C_n and the term with β are neglected in eq. (56) and if $m_e \nu_{en}$ is dropped in the expression (29) for α this result agrees with an earlier one derived by PIDDINGTON [51]. With the same substitutions Ohm's law becomes

$$(57) \quad \left[\gamma - \frac{\beta^2 / \alpha}{1 + j(1 - \delta_{sz} C_n^2 / U^2) F} \right] \mathbf{i} / \varrho_0 = \mathbf{E} + \mathbf{v} \times \mathbf{B}_0 - \frac{m_i - m_e}{e \varrho_0} \mathbf{i} \times \mathbf{B}_0 - \\ - \mathbf{i} \delta_{sz} \frac{m_i m_e}{em} \omega \frac{C_s^2 - C_i^2}{U^2} \mathbf{v} + \frac{\beta}{1 + j(1 - \delta_{sz} C_n^2 / U^2) F} \mathbf{v}.$$

These results have been obtained without making any assumptions about the displacement current.

The physical significance of eqs. (54), (55), (56) and (57) can be understood in the following way. The coefficient α defined by eq. (29) can be regarded as the « collision frequency » between the plasma and the neutral gas. Within a period $1/\omega$ of the phenomenon in question α/ω such « collisions » will take place. Since the relative number of ions compared with neutral particles is ϱ_0/ϱ_{n0} the neutral gas will be accelerated to the full velocity of the plasma well within the period $1/\omega$ provided that $(\alpha/\omega)(\varrho_0/\varrho_{n0}) = 1/F \gg 1$. Consequently, the parameter F is connected with the coupling between plasma and neutral

gas. To discuss the results more in detail attention will be paid to the following limiting cases.

a) Strong coupling. The factor containing C_n^2/U^2 in front of the parameter F is first discussed. For motions where $C_n^2/U^2 \ll 1$ the «rigidity» of the neutral gas is small. If, at the same time, $F \ll 1$ the plasma will be strongly coupled to the neutral gas which will move nearly with the plasma mean velocity, apart from a small motion caused by the difference in the friction with the ion and electron gases as shown by eqs. (54) and (29). This is also expressed by eq. (56) which shows that the whole gas mixture will move as one entity consisting of the total mass $\varrho_0 + \varrho_{n0}$ and with a mechanical rigidity given by pressure fluctuations due to the total sound velocity $(\varrho_0 C^2 + \varrho_{n0} C_n^2)^{1/2} / (\varrho_0 + \varrho_{n0})^{1/2}$.

On the other hand, if $C_n^2/U^2 \gg 1$ this will have a decoupling tendency since the neutral gas will be «rigid» and will oppose motions introduced by the plasma. The net result will still be a strong coupling also for compression waves ($m = z$) provided that the momentum exchange expressed by F is strong enough to make $(C_n^2/U^2)F \ll 1$.

b) Weak coupling. When the momentum exchange between plasma and neutral gas is small $F \gg 1$ and the coupling is necessarily weak as shown by eq. (56) which indicates that the plasma moves without influence from the mass and pressure of the neutral gas. As shown by eq. (54) this also implies that the neutral gas is unable to take part in transverse motions ($m \neq z$) as well as in compressive motions ($m = z$) with phase velocities different from C_n . It may, of course, move with its own velocity of sound C_n according to eq. (52) but is effectively decoupled from the plasma motion and acts only as a frictional brake on the latter.

Consequently, the general conditions for strong and weak coupling are $(1 - \delta_{sz} C_n^2/U^2)F \ll 1$ and $\gg 1$, respectively.

In Table III the coupling has been estimated for a number of situations in cosmical physics where partially ionized gases have to be taken into account (PIDDINGTON [58], PICKELNER [55], COWLING [21]). Data have been taken partly from the works by MINNAERT [53] and ALLEN [2]. The order of the phase velocity U of a phenomenon has been defined as L_c/t_c or as $B_0/(\mu_0 \varrho_0)^{1/2}$ and $B_0/[\mu_0(\varrho_0 + \varrho_{n0})]^{1/2}$ when magnetohydrodynamic waves are concerned. In cases where C_n does not exceed U considerably, as in the examples of the present table, the coupling is given by F and defined as strong, intermediate or weak when $F \ll 1$, $F \approx 1$, and $F \gg 1$, respectively. The characteristic velocity

$$(58) \quad U_1 = \varrho_0 \alpha L_c / \varrho_{n0}$$

corresponds to $F = 1$. When $U \ll U_1$ phenomena of the dimension L_c have a strong coupling between plasma and neutral gas, when $U \gg U_1$

TABLE III. — *The coupling between plasma and neutral gas.*

	Photo- spheric granu- lation	Magnetohydro- dynamic waves in the middle chromosphere	Giant pulsations in the F_1 -region		Magneto- hydrodynamic waves in cool interstellar clouds
			Outside auroral zones	Inside auroral zones	
n_0 (m ⁻³)	$3 \cdot 10^{19}$	$5 \cdot 10^{15}$	$2 \cdot 10^{11}$	$5 \cdot 10^{13}?$	$10^5?$
n_{n0} (m ⁻³)	$3 \cdot 10^{22}$	10^{18}	$3 \cdot 10^{15}$	$3 \cdot 10^{15}$	10^8
$T_i \approx T_e \approx T_n$ (°K)	4700	5000	600	600	100
α/n_{n0} (m ³ /s)	10^{-15}	10^{-15}	10^{-15}	10^{-15}	$2 \cdot 10^{-16}$
L_c (m)	10^6	10^6	10^5	10^5	10^{17}
t_c (s)	240	—	100	100	—
B_{0c} (Vs/m ²)	$10^{-4} \dots 10^{-3}$	$5 \cdot 10^{-4} \dots 5 \cdot 10^{-2}$	$6 \cdot 10^{-5}$	$6 \cdot 10^{-5}$	10^{-9}
C_n (m/s)	$6.2 \cdot 10^3$	$6.4 \cdot 10^3$	400	400	10^3
U (strong coup- ling; m/s)	$4 \cdot 10^3$	$10^4 \dots 10^6$	10^3	10^3	$2 \cdot 10^3$
U (weak coup- ling; m/s)		$2 \cdot 10^5 \dots 2 \cdot 10^7$			$7 \cdot 10^4?$
U_1 (m/s)		$5 \cdot 10^6$			10^7
coupling	strong	intermediate	weak	inter- mediate?	strong?

the coupling becomes weak. The situation of an almost completely ionized gas with weak coupling is not impossible. This only implies that the very few neutral gas particles present collide too seldom with the plasma to be accelerated to the velocity of the latter within the characteristic time. This is possible at low gas densities. The ratio α/q_{n0} in the expression (55) for F is a relatively slowly varying function of the temperatures. In experiments it is therefore easy to realize both the situations of strong and weak coupling by adjusting the frequency or the plasma density properly. The latter adjustment can be done, *e.g.* by variation of the discharge current.

The following notations are now introduced,

(59)
$$\varrho_* = \varrho_0 \{ 1 - \delta_{sz} C^2/U^2 + (\varrho_{n0}/\varrho_0) (1 - \delta_{sz}/C_n^2 U^2) / [1 + j(1 - \delta_{sz} C_n^2/U^2) F] \}$$

(60)
$$\beta_* = \beta / [1 + 1/j(1 - \delta_{sz} C_n^2 U^2) F],$$

(61)
$$\lambda_* = \{ \gamma - (\beta^2/\alpha) / [1 + j(1 - \delta_{sz} C_n^2/U^2) F] \} / \mu_0 \varrho_0$$

and

(62)
$$\vartheta_* = \delta_{sz} \omega m_i m_e (C_e^2 - C_i^2) / e m U^2,$$

which have to be considered as operators acting on the vector components. Eqs. (56) and (57) become

$$(63) \quad j\omega\varrho_*\mathbf{v} = \mathbf{i} \times \mathbf{B}_0 + \beta_*\mathbf{i}$$

and

$$(64) \quad \mu_0\lambda_*\mathbf{i} = \mathbf{E} + \mathbf{v} \times \mathbf{B}_0 - \frac{m_i - m_e}{e\varrho_0}\mathbf{i} \times \mathbf{B}_0 + (\beta_* - j\vartheta_*)\mathbf{v}.$$

λ_* can be regarded as a generalized «electromagnetic viscosity» having the values

$$(65) \quad \lambda_*(0) \equiv \lambda_*(F \ll 1) = [m_e\nu_{ei} + m_i\nu_{in}m_e\nu_{en}/(m_i\nu_{in} + m_e\nu_{en})]/\mu_0e^2n$$

and

$$(66) \quad \lambda_*(\infty) \equiv \lambda_*(F \gg 1) = m_e[\nu_{ei} + (m_i/m)^2\nu_{en} + (m_im_e/m^2)\nu_{in}]/\mu_0e^2n$$

in the limits of strong and weak coupling, respectively. The conductivity $1/\mu_0\lambda_*(0)$ given by eq. (65) has earlier been discussed by SCHLÜTER [54] in a study of the situation $(\mathbf{v}_n \cdot \nabla)\mathbf{v}_n \approx (\mathbf{v} \cdot \nabla)\mathbf{v}$, *i.e.*, when the plasma and the neutral gas are coupled strongly and \mathbf{v}_n differs little from \mathbf{v} . The results are physically plausible. In the low frequency limit and for large values of at least one of the collision frequencies ν_{in} and ν_{en} the coupling becomes strong. If then, *e.g.*, the electron gas is assumed to have no frictional couplings at all ($\nu_{ei} = \nu_{en} = 0$) the electron current will not be braked and the conductivity $1/\mu_0\lambda_*$ should be infinite as indicated by eq. (65), but not by eq. (66) which is inapplicable. On the other hand, in the high frequency limit and for moderate values of the collision frequencies ν_{in} and ν_{en} the coupling becomes weak. Assuming again, that the electron gas has no frictional couplings the electrons will, contrary to the low frequency situation, still be coupled electromagnetically with the ions. Thus, the system will be damped by the friction between ions and the neutral gas as indicated by eq. (66), but not by eq. (65) which is inapplicable in the high frequency limit.

2.2.2. *The dispersion relation.* — Introduce the notations $\boldsymbol{\kappa} = (0, 0, \kappa)$ $V_* = B_0/(\mu_0\varrho_*)^{\frac{1}{2}}$, $eB_0/(m_i - m_e) = \omega_0$ and write eqs. (9) and (11) in the forms

$$(67) \quad \mathbf{i} = j\boldsymbol{\kappa} \times \mathbf{b}/\mu_0 - j\omega\mathbf{E}/\mu_0c^2$$

and

$$(68) \quad \mathbf{b} = \mathbf{E} \times \boldsymbol{\kappa}/\omega.$$

\mathbf{v} is now substituted from eq. (63) into eq. (64) and \mathbf{i} and \mathbf{b} are written in terms of \mathbf{E} by means of eqs. (67) and (68). After some straightforward deduc-

tions the result becomes

$$\begin{aligned}
 (69) \quad & \left[1 + j \frac{\omega \lambda_*}{c^2} - \frac{V_*^2}{c^2} \frac{\beta_* (\beta_* - j \vartheta_*)}{B_0^2} \right] \mathbf{E} + \\
 & + \left[\frac{V_*^2}{U^2} \frac{\beta_* (\beta_* - j \vartheta_*)}{B_0^2} - j \frac{\omega \lambda_*}{U^2} \right] \cdot \hat{\mathbf{x}} \times (\mathbf{E} \times \hat{\mathbf{x}}) + \\
 & + \left[\frac{V_*^2}{c^2} \frac{\beta_* - j \vartheta_*}{B_0} - j \frac{\omega}{\omega_0} \frac{V_0^2}{c^2} \right] \cdot \left\{ \left[-\mathbf{E} + \frac{c^2}{U^2} \hat{\mathbf{x}} \times (\mathbf{E} \times \hat{\mathbf{x}}) \right] \times \mathbf{B}_0 \right\} + \\
 & + \left\{ \frac{V_*^2}{c^2} \left[-\mathbf{E} \times \hat{\mathbf{B}}_0 + \frac{c^2}{U^2} [\hat{\mathbf{x}} \times (\mathbf{E} \times \hat{\mathbf{x}})] \times \mathbf{B}_0 \right] \right\} \times \hat{\mathbf{B}}_0 + \\
 & + \left\{ \frac{V_*^2}{c^2} \frac{\beta_*}{B_0} \left[-\mathbf{E} + \frac{c^2}{U^2} \hat{\mathbf{x}} \times (\mathbf{E} \times \hat{\mathbf{x}}) \right] \right\} \times \hat{\mathbf{B}}_0 = 0,
 \end{aligned}$$

where $\hat{\mathbf{x}}$ and $\hat{\mathbf{B}}_0$ are unit vectors along \mathbf{x} and \mathbf{B}_0 . Eq. (69) gives the dispersion relation for a plane disturbance.

Only a few special cases will be studied in detail here.

a) No neutral gas ($\varrho_{n0} = 0$), no dissipation ($\nu_{ei} = 0$) vanishing sound velocities ($C_i = C_e = 0$), $\hat{\mathbf{B}}_0$ along the z -axis and low frequencies ($\omega \ll \omega_0$).

From the first and fourth terms of eq. (69) the phase velocity U reduces to the well-known result

$$(70) \quad U^2 = c^2 V_0^2 / (c^2 + V_0^2)$$

first derived by ÅSTRÖM [3].

b) The displacement current is neglected ($c^2 \gg U^2$, V_*^2 and V_0^2), low frequencies ($\omega \ll \omega_0$ and $\vartheta_*/B_0 = \delta_{sz}(m_i/m)(C_e^2 - C_i^2)(1/U^2)(\omega/\omega_0) \ll 1$) and \mathbf{B}_0 along the y -axis.

From eqs. (69) and (59) two sets of solutions are obtained. The first has an electric field E_y along the magnetic field. It is of no special interest here, whereas the second set with the fields E_x and E_z corresponds to

$$\begin{aligned}
 (71) \quad U^2 = & \frac{V_0^2}{1 - C^2/U^2 + (\varrho_{n0}/\varrho_0) \frac{1 - C_n^2/U^2}{1 + j(1 - C_n^2/U^2)F}} + j \frac{\omega}{\mu_0 \varrho_0} \left(\gamma - \frac{\beta^2/\alpha}{1 + jF} \right) - \\
 & - \frac{(\beta/B_0)^2 V_0^2}{(1 + 1/jF)^2 \left(1 + \frac{\varrho_{n0}/\varrho_0}{1 + jF} \right)}.
 \end{aligned}$$

We now introduce the notation $U = P + jQ$, where P and Q are real.

When the coupling is strong and the dissipation relatively small eq. (71) gives

$$(72) \quad P^2 = \frac{\varrho_0 V_n^2 + \varrho_0 C^2 + \varrho_{n0} C_n^2}{\varrho_0 + \varrho_{n0}}; \quad Q = \frac{1}{2} \frac{\varrho_0}{\varrho_0 + \varrho_{n0}} \frac{\omega V_0^2}{P^3} \lambda_{\text{eff}}(0),$$

where the « effective electromagnetic viscosity » is

$$(73) \quad \lambda_{\text{eff}}(0) = \lambda_*(0) + \left(\frac{\varrho_{n0}}{\varrho_0} \right)^2 P^2 (P^2 - C_n^2) / \alpha V_0^2,$$

the first term being given by eq. (65). From the values of P and Q the damping distance $z_0 = (P^2 + Q^2) / \omega Q$ can be calculated.

If instead the coupling is weak, $\alpha / \omega \ll 1$ and $\beta / B_0 \ll 1$ eq. (71) tends to

$$(74) \quad P^2 = V_0^2 + C^2; \quad Q = \frac{\omega V_0^2}{2P^3} \lambda_*(\infty).$$

In more complicated situations the phase velocities and damping distances should be calculated directly from eq. (71). The phase velocity given in eq. (74) agrees with that earlier obtained by DE HOFFMANN and TELLER [32], HERLOFSON [31], and VAN DE HULST [33].

c The displacement current is neglected, $\beta / B_0 \ll 1$, vanishing sound velocities, $\hat{\mathbf{B}} = (\sin \psi, 0, \cos \psi)$ where ψ is the angle between \mathbf{B}_0 and the z -axis:

The dispersion relation is obtained from the first, second and fourth terms of eq. (69) and becomes

$$(75) \quad U^2 = (\varrho_0 / \varrho_*) V_0^2 \left\{ 1 - \frac{1}{2} \sin^2 \psi \pm \left[\frac{1}{4} \sin^4 \psi + \left(\frac{\omega}{\omega_0} \frac{\varrho_*}{\varrho_0} \right)^2 \cos^2 \psi \right]^{\frac{1}{2}} \right\} + j \omega \lambda_*.$$

A similar situation has been studied by PIDDINGTON [57, 58], who neglects the influence of the neutral gas on Ohm's law (51) and drops the term $\beta \mathbf{i}$ in the equation of motion (50). This corresponds to $\lambda_* = m_e v_{ei} / \mu_0 e^2 n$ and with this value of λ_* eq. (75) becomes identical with PIDDINGTON's result.

d) The displacement current is neglected, vanishing sound velocities, low frequencies ($\omega \ll \omega_0$), \mathbf{B}_0 along the z -axis.

The dispersion relation is obtained from

$$(76) \quad (E_x, E_y, E_z) + (V_*^2 \beta_*^2 / U^2 B_0^2 - j \omega \lambda_* / U^2 - V_*^2 / U^2) (E_x, E_y, 0) + \\ + 2(V_*^2 / U^2) (\beta_* / B_0) (E_y, -E_x, 0) = 0.$$

It should be observed that E_x and E_y are linked together by the last term in eq. (76) which contains β . This is physically plausible since eq. (76) gives rise to a transverse, plane-polarised Alfvén wave in the non-dissipative situation. If this wave has its velocity v in the y -direction, current will flow in the x -direction. Consequently, if collisions are introduced as a perturbation eqs. (50) and (51) show that the current produces a net drag in the x -direction and the velocity an electric field and an additional current in the y -direction when $\beta \neq 0$. Eq. (76) gives the dispersion relation

$$(77) \quad U^2 = \frac{V_0^2}{1 + (\varrho_{n0}/\varrho_0)/(1 + jF)} \left[1 \pm j \frac{\beta/B_0}{1 + 1/jF} \right]^2 + j\omega[\gamma - \beta^2/\alpha(1 + jF)]/\mu_0\varrho_0.$$

For strong coupling and small losses we have

$$(78) \quad P^2 = V_0^2\varrho_0/(\varrho_0 + \varrho_{n0}), \quad Q = \frac{\omega}{2P} \lambda_{\text{eff}}(0),$$

where

$$(79) \quad \lambda_{\text{eff}}(0) = \lambda_*(0) + \left(\frac{\varrho_{n0}}{\varrho_0 + \varrho_{n0}} \right)^2 V_0^2/\alpha.$$

This result is identical with that obtained in a different way by COWLING ([20] p. 121) who assumes that the constituents of the gas move with small relative velocities, *i.e.*, the coupling is assumed to be strong.

For weak coupling, $\alpha/\omega \ll 1$ and $\beta/B_0 \ll 1$, the corresponding result becomes

$$(80) \quad P^2 = V_0^2, \quad Q = \frac{\omega}{2P} \lambda_*(\infty).$$

The phase velocities in eqs. (78) and (80) correspond to transverse Alfvén waves with and without the neutral gas taking part in the oscillations, respectively (see also ALFVÉN [1]).

2.2.3. - The electrical conductivity in a magnetic field. Extensive discussions have been devoted to the electric conductivity in an ionized gas in a magnetic field. A great number of investigators have preferred to generalize Ohm's law to a form

$$(81) \quad \mathbf{i} = \sigma_0(\mathbf{E}' \cdot \hat{\mathbf{B}}) \times \hat{\mathbf{B}} + \sigma_1 \hat{\mathbf{B}} \times (\mathbf{E}' \times \hat{\mathbf{B}}) + \sigma_2 (\hat{\mathbf{B}} \times \mathbf{E}')$$

expressing the relation between the current density \mathbf{i} and a total effective electric field \mathbf{E}' in terms of the parallel, cross and Hall conductivities σ_0 , σ_1 and σ_2 . Such an approach could easily have been used here, *e.g.*, by solving

explicitely for i in eq. (51). One important question which immediately arises is how the conductivity coefficients in eq. (81) are connected with the rate of dissipation i^2/σ_3 , *i.e.*, how an « effective » conductivity σ_3 should be defined in terms of σ_0 , σ_1 and σ_2 . Another question intimately related with the former concerns the form of the effective field E' to be put into eq. (81). A binary fully ionized gas was treated by COWLING [19] who found that $\sigma_3 = \sigma_1 + \sigma_2^2/\sigma_1$ was the value to be used and showed that σ_3 became equal to the parallel conductivity σ_0 . This result is also obtained from the effective conductivities determining the dissipation lengths in eqs. (72), (74), (78) and (80) in the previous examples. By using the basic equations for the ion, electron and neutral gas fluids and by skilful manipulation with equivalent electric fields SCHLÜTER [62, 63] in certain cases came to the conclusion that the conductivity σ_0 was determining the rate of dissipation. He criticized the interpretation of eq. (81) as expressing a reduction of the electric conductivity across a magnetic field. This introduces unnecessary complications which can be avoided by using the basic equations for the gas fluids without application of an explicit expression for the current density such as eq. (81).

In a partially ionized gas σ_3 will differ from σ_0 as pointed out by BAKER and MARTYN [6]. The increased dissipation caused by friction between plasma and neutral gas was shown by PIDDINGTON [56, 58] to be of importance for the damping of magnetohydrodynamic waves in the solar chromosphere and by COWLING [20] for the decay of magnetic fields in cool interstellar clouds. Thus, for a partially ionized gas dissipation is actually increased by a magnetic field (cf. also SCHLÜTER and BIERMANN [65]).

Both PIDDINGTON and COWLING assume that the gas constituents move with small relative velocities. In the examples given by the two first columns of Table IV the coupling is seen to be strong ($I' \ll 1$) and such an assumption becomes justified. For plane disturbances we then arrive at the expression (79) for the electromagnetic viscosity when pressure effects are neglected. This expression is used by COWLING and also by PIDDINGTON in a reduced form where the ion-electron collisions have been neglected ($v_{ei} = 0$). The sound velocities are about $C = C_n = 6400$ m/s for the chromosphere and $C = C_n = 910$ m/s for cool interstellar clouds. For compressive motions eqs. (72) and (73) should be used instead of eqs. (78) and (79) and $P = 7 \cdot 10^3$ m/s, $\lambda_{\text{eff}} = 2 \cdot 10^8$ m²/s and $P = 2 \cdot 10^3$ m/s, $\lambda_{\text{eff}} = 4 \cdot 10^{11}$ m²/s are the values to replace those given for incompressible motions in the two first columns of Table IV. A comparison between the values of $\lambda_*(0)$ and λ_{eff} given here supports the conclusions earlier drawn by PIDDINGTON and COWLING about the increased dissipation in the chromosphere and in cool interstellar clouds. The values adopted for the chromosphere in Table IV are of the same order of magnitude as those used by PIDDINGTON. Recently, BIERMANN and LÜST [9] have reconsidered this situation, especially for somewhat lower frequencies where

the damping becomes less important, as is also seen from eqs. (72), (73), (78) and (79).

TABLE IV. — Phase velocities and damping distances of transverse magnetohydrodynamic oscillations. Values taken from Tables I and III.

		Magnetohydrodynamic waves in the middle chromosphere (from granulation)	Magnetohydrodynamic waves in cool interstellar clouds	Giant pulsations in the F_1 -region	
				Outside auroral zones	Inside auroral zones
L_c	(m)	10^6	10^{17}	10^5	10^5
ω	(s ⁻¹)	0.1	$2 \cdot 10^{-13}$	$6 \cdot 10^{-2}$	$6 \cdot 10^{-2}$
B_0	(Vs/m ²)	$5 \cdot 10^{-4}$	10^{-9}	$6 \cdot 10^{-5}$	$6 \cdot 10^{-5}$
v_{ei}	(s ⁻¹)	$3 \cdot 10^5$	$2 \cdot 10^{-3}$	200	$5 \cdot 10^4?$
v_{in}	(s ⁻¹)	10^3	$2 \cdot 10^{-8}$	2	2
v_{en}	(s ⁻¹)	$6 \cdot 10^4$	$4 \cdot 10^{-5}$	$1.3 \cdot 10^3$	$1.3 \cdot 10^3$
β	(Vs/m ²)	$3 \cdot 10^{-7}$	$2 \cdot 10^{-17}$	$7 \cdot 10^{-9}$	$7 \cdot 10^{-9}$
F		0.02	0.01?	300	1?
V_0	(m/s)	10^5	$7 \cdot 10^4?$	$7 \cdot 10^5$	$4 \cdot 10^4?$
$\lambda_*(0)$	(m ² /s)	$2 \cdot 10^3$	$5 \cdot 10^5$	—	$3 \cdot 10^4?$
$\lambda_*(\infty)$	(m ² /s)	—	—	$2 \cdot 10^5$	—
P	(m/s)	10^4	$2 \cdot 10^3?$	10^4	$5 \cdot 10^3?$
$2\pi P/\omega L_c$		0.6	0.6	14	5?
λ_{eff}	(m ² /s)	$2 \cdot 10^7$	$2 \cdot 10^{17}$	10^{11}	$5 \cdot 10^8?$
z_0	(m)	10^7	$2 \cdot 10^{18}$	$8 \cdot 10^3$	$2 \cdot 10^5?$
z_0/L_c		10	20	0.08	2?

The last two examples given in Table IV refer to giant pulsation in the ionosphere. It has been suggested that these pulsations could be caused by magnetohydrodynamic oscillations which may exist inside the auroral zones where the ionization degree is increased by the auroral discharge, but not outside of the same zones under normal ionospheric conditions (LEHNERT [42, 43]). PICKELNER [55] has pointed out that the coupling between plasma and neutral gas may be too weak to cause the gas mixture to oscillate as an entity. From Tables III and IV this criticism is seen to be justified, at least when motions outside the auroral zones are concerned. However, inside the zones a hundred-fold increase in charge density could make possible oscillations which are excluded, neither by too small relative damping distances z_0/L_c , nor by too long relative wave lengths, $2\pi P/\omega L_c$, for a phenomenon of «ionospheric» dimensions.

A discussion of the damping of plane waves under experimental conditions

will not be performed here. Instead, the question about dissipation in laboratory phenomena will be treated in some specific cases in the next section.

Finally, to sum up the results of this section, the dispersion relations obtained from eq. (69) are applicable to any phenomenon which can be treated in terms of plane partial solutions. The results obtained give the dissipation and the effective electrical conductivities, and it has been shown that earlier derived results by COWLING, SCHLÜTER, PIDDINGTON and others are included as special cases. The results obtained by these authors apply either to fully ionized gases or to partially ionized gases where the plasma is strongly coupled with the neutral gas. However, they are not applicable when the coupling is intermediate or weak, and some of the earlier derived formulae for the conductivity have to be modified by pressure effects also in the case of strong coupling, as shown, *e.g.*, by eq. (73).

3. - Experimental investigations of the plasma.

3.1. *Summary of the methods of measurement.* - To give a complete description of all possible methods of exploring a plasma experimentally would not be within the frame of this paper. For a more complete treatment of this subject reference can be made to textbooks on gaseous discharges as such as *Handbuch der Physik* (FLÜGGE [28]) and that by VON ENGEL and STEENBECK [25]. In particular, when discharges with a magnetic field are concerned the literature is not too extensive; contributions by GUTHRIE and WAKERLING [30], LANDSHOFF [39], BICKERTON and VON ENGEL [7, 8] and THONEMANN *et al.* [68] may be mentioned. Only brief comments will be given here to some important problems.

3.1.1. *Measurements of «external» parameters.* - One of the main difficulties in making measurements of the properties of a plasma is to avoid the measuring device from interfering with the quantities to be measured. Therefore, the simplest way to study a plasma is to measure its «external» parameters such as the total current, the total potential drop and the observed shape of the discharge. A number of examples may be mentioned.

In a discharge which takes place along a magnetic field, as well as in absence of a magnetic field, the mean charge density can be determined from the total current and the potential drop in the plasma column when the mobility is known and the magnetic self-field can be neglected.

In the diffusion experiment described later in this paper the balance between charge production by ionization and charge losses by diffusion to the walls can be studied from the potential drop along a plasma column.

Changes in the state of motion of a plasma column are often reflected in

changes in the total current, the potential drop and the visual diameter of the column. Examples are given by oscillations of a pinched discharge and by plasma oscillations or «electromagnetic» turbulence. The latter phenomena can be detected by studying the noise in the potential drop across a resistor which carries the total discharge current.

In high current discharges the variations of magnetic field strengths can be estimated from the cross-section of the discharge when the magnetic field is assumed to be «frozen» to the gas. Balance between electrodynamic and pressure forces leads to an estimation of the temperature when the total current is known. When highly ionized gases with «frozen» fields are studied one should not exclude the possible existence of phenomena which may take place inside the gas without producing any detectable changes in the surroundings.

3.1.2. Probe measurements. — The measuring technique developed for electric probes in a plasma in absence of a magnetic field is well established and may be used to determine the plasma potential, the charge density and the ion and electron temperatures by measuring the current to the probe as a function of its voltage. The probe theory has been developed under the assumption that the mean free path is much larger than the probe dimensions and the thickness of the probe sheath, which is of the order of the Debye distance h_e for an isolated probe. It has been shown by BOHM [12] that the probe sheath will be stable when there is a weak electric field penetrating through the plasma edge and causing ions to reach the probe with a mean energy corresponding to half the electron temperature T_e , and not to the ion temperature T_i which may be much less than T_i in low current experiments.

However, when a strong magnetic field is introduced the situation becomes complicated as soon as the radius of curvature of the electron motion in the magnetic field becomes comparable to the probe dimensions and the Debye distance. How the probe behaves under such conditions has been investigated in some details by BICKERTON and VON ENGEL [7, 8]. In any case an isolated probe should be charged negatively if $T_e > T_i$, even if the electron mobility is smaller than that of ions when the magnetic field is present. This is seen if the probe is assumed originally to be unchanged and placed in a plasma. At the first moment particles will hit the probe surface with their full thermal velocity regardless of the magnetic field being present or not. This will give an electron current to the probe which is greater than the corresponding ion current. A simplified theory has been developed by BOHM, BURHOP and MASSEY [13] which is applicable when the Larmor radius of the positive ions is large compared with the probe dimensions. Then, the ion current can still be used to determine the charge density by the theory developed in absence of a magnetic field.

Magnetic field changes in the interior of an ionized gas which cannot be

detected by external indicators, can be studied by means of probe coils. When the conductivity of the gas is high and the magnetic field practically « frozen » to matter care is necessary in the interpretation of the measurements in order not to conflict with the theorem by BONDY and GOLD [14].

3.1.3. Spectroscopic measurements. — Broadening of the spectral lines in a gaseous discharge may be caused by the Stark, Doppler and Zeeman effects. A broadening of the Balmer lines can occur in the electric fields from the charged particles and can be used as a measure of the charge density (KOLB [38], DICKERMAN [23]). In the high current experiments with deuterium performed by THONEMANN *et al.* [68] this effect, as well as the Zeeman effect, was shown to be negligible compared with the Doppler broadening. The latter was studied by means of the spark lines of some small quantities of oxygen and nitrogen which were introduced into the discharge and served as an indicator of the kinetic ion temperature.

There is also a possibility of determining the temperature from the neutron yield in a deuterium gas in thermal equilibrium.

2.1.4. Microwave measurements. — Determination of the ion density of an ionized gas by means of the reflection properties of microwaves has been known in ionospheric research since long ago. When this technique is applied to a plasma with a strong magnetic field the influence of the latter on the critical frequencies should be taken into account.

The Doppler shift of a microwave reflected by a shock front could also be used to determine the shock velocity (KOLB [38]).

Finally, DRUMMOND [24] has recently suggested to use the temperature dependent transmission properties of microwaves in an ionized gas as a « microwave thermometer » for millions of degrees.

3.2. *Torsional magnetohydrodynamic motion in a cylindrical plasma column.* — The investigation in Sect. 2.2 of the dissipation and the phase velocities of magnetohydrodynamic oscillations will now be completed with an example on laboratory scale. We shall prefer to study a specific example with given boundaries rather than to discuss plane waves. The reason for this is that the wave length of a magnetohydrodynamic wave in a plasma usually exceeds laboratory dimensions considerably and becomes much larger than the cross-section of the discharge tube to be used. As will be shown later this implies that the damping is determined mainly by the dimension of the cross-section, and not by the wave length. A convenient arrangement for an experiment on magnetohydrodynamic waves consists of a long discharge tube surrounded by a magnetic coil which produces a field along the tube axis. An experiment of this kind has already been suggested by POST [60] and

NEWCOMB [54] who discuss a « hydromagnetic wave guide » where the magnetic field lines are being « shaken » at one end by a short high frequency coil surrounding the tube. At the other end disturbances are received by an identical coil and the damping and phase velocity are determined. NEWCOMB gives solutions for the different modes in the case of an infinitely conducting tube wall. The way in which the waves are generated gives rise to a mixture of longitudinal and transverse wave motions.

A somewhat similar experiment will be discussed here with torsional oscillations which consist of purely transverse and incompressible modes. The tube wall is assumed to be non-conducting and the waves generated by a pair of concentric electrodes and received by another identical pair. In a highly conducting plasma it might be necessary to place indicators in the interior of the gas since there might exist motions which do not give rise to external field changes.

The basic equations (50), (51), (52), (9) and (11) for small disturbances are now applied with a homogeneous magnetic field \mathbf{B}_0 along the z -axis of a cylindrical co-ordinate system. The displacement current is neglected and ρ and ρ_n assumed to be constant. Modes which oscillate as $\exp[j\omega t]$ are investigated and \mathbf{v}_n can be substituted into eqs. (50) and (51). The procedure is analogous to that carried out in Sect. 2'2.1 and gives the results (56), (57), (59), (60) and (61) with $C = C_n = 0$. After substituting \mathbf{v} from eq. (56), \mathbf{E} from eq. (11) and \mathbf{i} from eq. (9) into eq. (57) the result becomes

$$(82) \quad \mathbf{b} + (V_*^2/\omega^2) \operatorname{curl} \{ [\operatorname{curl} \mathbf{b}] \times \hat{\mathbf{B}}_0 \} \times \hat{\mathbf{B}}_0 - j(\lambda_*/\omega - \beta_*^2 V_*^2/B_0^2 \omega^2) \operatorname{curl}^2 \mathbf{b} + \\ + (2\beta_* V_*^2/B_0 \omega^2 - jV_*^2/\omega \omega_0) \operatorname{curl} [(\operatorname{curl} \mathbf{b}) \times \hat{\mathbf{B}}_0] = 0.$$

The term containing ω_0 will now be dropped and this is a reasonable approximation in an experiment where the gyro frequency ω_i of ions exceeds the frequency ω considerably. The last term containing β_* still links the field components b_r and b_z with b_φ which contradicts the original assumption of purely torsional waves. This is understandable since a torsional wave has a field b_φ which is produced by currents i_r and i_z and these currents generate compressions in the rz -planes as seen from eq. (49). Consequently, to be able to discuss purely torsional oscillations β_*/B_0 has to be assumed much less than unity. This will also be seen to be a good approximation in the examples given in Table V.

With these approximations eq. (82) reduces to the form earlier studied by LUNDQUIST [48] in experiments with liquid mercury:

$$(83) \quad \frac{\partial^2 b_\varphi}{\partial r^2} + \frac{1}{r} \frac{\partial b_\varphi}{\partial r} + (\kappa_{1s}^2 - 1/r^2) b_\varphi = 0,$$

TABLE V. - *Estimations of the deviation from virtually undamped torsional oscillations. Values taken from Tables I, III and IV.*

	Giant pulsations in F_1 -region, inside auroral zones	Experiment under conditions given by BOSTICK and LEVINE		High current experiments with deuterium
		$n/n_n = \infty$	$n/n_n = 10^{-4}$	
n (m^{-3})	$5 \cdot 10^{13} ?$	$8 \cdot 10^{20}$	$8 \cdot 10^{-4}$	10^{20}
n_n (m^{-3})	$3 \cdot 10^{15}$	0	$8 \cdot 10^{20}$	0
$T_i = T_e = T_n$ ($^{\circ}\text{K}$)	600	$10^5 ?$	$10^5 ?$	10^5
ν_{ei} (s^{-1})	$5 \cdot 10^4 ?$	$4 \cdot 10^8$	$4 \cdot 10^4$	$2 \cdot 10^3$
ν_{in} (s^{-1})	2	0	$8 \cdot 10^5$	0
ν_{en} (s^{-1})	$1.3 \cdot 10^3$	0	$6 \cdot 10^7$	0
L (m)	10^5	1	1	1
κ (m^{-1})	—	6.28	6.28	6.28
R (m)	—	$1.9 \cdot 10^{-2}$	$1.9 \cdot 10^{-2}$	0.1
κ_{11} (m^{-1})	0	200	200	38.3
ω (s^{-1})	$6 \cdot 10^{-2}$	$6 \cdot 10^4$	$6 \cdot 10^4$	$1.6 \cdot 10^3$
ω_0 (s^{-1})	200	$1.2 \cdot 10^6$	$1.2 \cdot 10^6$	10^7
B_0 (Vs/m^2)	$6 \cdot 10^{-5}$	0.05	0.05	0.2
β (Vs/m^2)	$7 \cdot 10^{-3}$	0	$3.4 \cdot 10^{-4}$	0
F	1?	0	750	0
V_0 (m/s)	$4 \cdot 10^4 ?$	$2 \cdot 10^4$	$2 \cdot 10^6$	$3 \cdot 10^5$
G	$(1+j)?$	$(1.14 + 10.7j) \cdot 10^{-2}$	$(-91 + 6.9j) \cdot 10^{-5}$	$0.85 + 0.36j$
$2\kappa V_*/\lambda_*(\kappa_{11}^2 + \kappa^2)$	—	0.45 (aperiodic)	—	8100 (periodic)

where propagation of the form $\exp[j\omega t + j\kappa z]$ has been assumed and

$$(84) \quad \kappa_{1s}^2 = (\omega^2 - \kappa^2 V_*^2 - j\omega \lambda_* \kappa^2) / j\omega \lambda_*.$$

The solution of eq. (83) which is finite at $r=0$ becomes

$$(85) \quad b_\varphi = b_0 J_1(\kappa_{1s} r) \exp[j\omega t + j\kappa z]$$

and the radial current density component is

$$(86) \quad i_r = -j(\kappa b_0 / \mu_0) J_1(\kappa_{1s} r).$$

The boundary condition at the wall $r=R$ is that i_r vanishes and this determines κ_{1s}

$$(87) \quad \kappa_{1s} R = K_{1s} \quad (s=1, 2, \dots),$$

where K_{1s} is the s -th zero of the Bessel function J_1 . Thus, the dispersion

relation for the s -th mode becomes from eq. (84)

$$(88) \quad U^2 = \frac{V_*^2 + j\omega\lambda_*}{1 - j\kappa_{1s}^2\lambda_*/\omega},$$

which can also be written in the form

$$(89) \quad \omega = \frac{1}{2}j\lambda_*(\kappa_{1s}^2 + \kappa^2) \pm [\kappa^2V_*^2 - \frac{1}{4}\lambda_*^2(\kappa_{1s}^2 + \kappa^2)]^{\frac{1}{2}}.$$

The damping distance and phase velocity can be determined from eq. (88), where the plane wave solution is obtained by putting $\kappa_{1s} = 0$. Eq. (88) also includes forced oscillations in weak magnetic fields occurring when the skin effect dominates. Such oscillations may have large damping lengths in some cases, but this does not imply that they correspond to slowly damped wave motion. They are instead to be compared with a temperature « wave » which is generated by a periodically varying temperature at a given boundary and penetrates from the boundary into the medium inside. In order to decide whether magnetohydrodynamic waves may exist or not the wave number should instead be considered to be given as an initial condition. The development in time of a mode for a certain (real) κ is then given by ω which is solved from eq. (88). The real part of ω gives the eigenfrequency of the possible oscillations and the imaginary part the inverted damping time. If the real part vanishes no eigenoscillations occur, *i.e.*, no waves can be propagated. To ask this question ω has to be solved explicitly from eq. (88) which contains $F = F(\omega)$. This will be a somewhat lengthy procedure in case of intermediate coupling. However, for a fully ionized gas or when the coupling is very strong or very weak so that the damping introduced by F can be neglected besides that coming from $\lambda_*(0)$ or $\lambda_*(\infty)$ the quantities V_* and λ_* become real and ω is given by eq. (89). The condition for a wave of the wave length $L = 2\pi/\kappa$ to exist then becomes (cf. LEHNERT [46])

$$(90) \quad 2\kappa V_*/\lambda_*(\kappa_{1s}^2 + \kappa^2) > 1.$$

In order to estimate the deviations from a virtually undamped magnetohydrodynamic wave in the general case eq. (88) may be written in the form

$$(91) \quad U^2 = \frac{\varrho_{n0}/\varrho_0 + 1 + F^2}{(\varrho_{n0}/\varrho_0 + 1)^2 + F^2} \cdot V_0^2 \cdot G,$$

where

$$(92) \quad G = \left[1 + j \frac{(\varrho_{n0}/\varrho_0)F}{\varrho_{n0}/\varrho_0 + 1 + F^2} \right] \cdot \frac{1 + j\omega\lambda_*/V_*^2}{1 - j\kappa_{1s}^2\lambda_*/\omega}.$$

The deviation of G from $1 + j \cdot 0$ can be taken as a measure of the deviation from the virtually undamped situation.

Conditions somewhat similar to those existing in an earlier investigation with a toroidal tube carried out by BOSTIC and LEVINE [17] and given by the

second and third columns of Table V may serve as an illustration to the least damped mode $s=1$. The situations with full and 10^{-2} percent ionization are given here at an assumed temperature of 10^5 °K. It is seen that G differs fundamentally from unity even in the fully ionized situation. This also agrees with the result at the bottom of the second column which, according to eq. (80) shows that no transverse magnetohydrodynamic waves can exist at the conditions given when the temperature is below 10^5 °K. An important reason for this is the smallness of the tube cross-section which makes the resistance large for the induced currents and diminishes the electrodynamic restoring force. Thus, the situation is not improved by making the dimensions along the direction of propagation large, *i.e.*, by making the wave length large and κ small, as soon as the cross-section still remains small and κ_{1s} large.

In the fourth column of Table V, however, the cross-section has been increased as well as the temperature to values about those present in the Zeta machine. Now, G becomes comparable to unity and the parameter given in eq. (90) exceeds unity very much, which shows that virtually undamped Alfvén waves with 1 m wave length exist in this case. Some modification of the obtained result may be caused by the viscosity damping which is of the same order as the Joule heat damping when the mean free path becomes comparable to the linear dimension R . In any case, it may be concluded that magnetohydrodynamic waves, at least of the transverse type, can only be produced in the laboratory in a gas of high ionization degree, at tube cross-sections of at least 0.1 m, with fields of at least some thousand gauss and at temperatures exceeding 10^5 °K. The low ionization potential of caesium should perhaps not be forgotten in this connexion. A caesium discharge becomes fully ionized even at moderate power inputs and the possibility of making wave experiments in such a discharge without being forced to mobilize too large resources should be investigated.

Finally, the first column of Table V shows that rather slowly damped oscillations of the period of giant pulsations might occur inside the auroral zones, provided that the charge density is about hundred times larger than its value outside the same zones.

3.3. Diffusion in the positive column in a magnetic field. — The motion of a charged particle in a magnetic field may be described as a sum of a gyration around the field lines, a drift motion across the same lines and a motion parallel with the field (ALFVÉN [2]). In an ionized gas this picture has to be modified by particle interactions, such as collisions and phenomena caused by space charges. The macroscopic correspondance to a situation where the transverse drift due to particle interactions and inertia forces can be neglected and where the motions are slow relative to the gyro frequencies of ions and electrons is a gas nearly «frozen» to the magnetic field lines. This strong

coupling between ionized matter and magnetic fields is of great importance, not only in astrophysics but also for the confinement of the plasma in a future fusion reactor.

However, it has been emphasized by BOHM, BURHOP, MASSEY and WILLIAMS [13] that random fluctuations of charge density and plasma oscillations may produce electric fields which in their turn give drift motions across the magnetic field lines. This «drain» diffusion provides an additional mechanism for ionized matter to «slip» across a magnetic field and may, in the case that it predominates over collision diffusion, introduce considerable difficulties into the physics of a plasma in a magnetic field. BOHM and collaborators made experiments with an arc plasma in a magnetic field and came to the conclusion that the diffusion was not consistent with collision phenomena but could be explained by «drain». This interpretation was criticized by SIMON [66] who pointed out that the transverse diffusion of the plasma is not necessarily ambipolar. Thus, in the arc experiment space-charge neutralization can be maintained by the conducting end walls which produce an electron short-circuit across the magnetic field. With this new interpretation SIMON was able to show that the arc experiments did not conflict with the binary collision theory.

The purpose of the investigation to be described here is to study diffusion across a magnetic field in a configuration which is free from short-circuiting effects such as those pointed out by SIMON. It provides the possibility to decide if collision or «drain» diffusion is operative. For this purpose a long cylindrical plasma column with a homogeneous magnetic field along the axis has been chosen. On the basis of the collision diffusion theory TONKS [69], ROKHLIN [61], CUMMINGS and TONKS [22], FATAILEV [27], BICKERTON [7] and BICKERTON and VON ENGEL [8] have pointed out that a longitudinal magnetic field will reduce the losses of particles to the walls. Consequently, when the magnetic field is present a lower electron temperature and a smaller potential drop along the plasma column should be required to sustain a certain ion density. An experiment performed by BICKERTON and VON ENGEL was in good agreement with these expectations. The experiment to be described here forms an extension of the former into a range of higher pressures and stronger magnetic fields.

3.3.1. Theory of the positive column in a longitudinal magnetic field. — A cylindrically symmetric, stationary column of ionized gas is assumed to be situated in a constant, homogeneous, longitudinal magnetic field B_0 . The following conditions are assumed to be valid.

a) The mean free path of ions and electrons is small compared with the tube radius.

b) The gas is electrically quasi-neutral: $n_i = n_e = n$.

c) The production rate of charged particles is Zn , where Z is a function of the electron temperature and the neutral gas density. Two stage ionization and volume recombination are neglected. An ion may sometimes capture an electron from a neutral gas particle and this may modify the diffusion coefficient to some extent. However, this effect will be neglected in the simplified theory given here since only appreciable changes in the diffusion coefficient will be detectable in the present experiment.

d) The ionization degree is low and the frictional coupling between charged particles and the neutral gas produces a small pressure gradient and negligible mass motion in the latter. v_{ei} is neglected (cf. Tables I and V).

e) Electron attachment is neglected. This is true for a rare gas as helium which is used in the present experiment (see LOEB [45]).

f) The ion and electron gases are assumed to have Maxwellian velocity distributions with constant temperatures T_i and T_e . The effect of striations is assumed to be negligible when mean values are taken of the potential drop along a considerable part of the positive column.

g) The column is extended very far in its axial direction such as to make end effects and deviations from cylindrical symmetry negligible.

h) The velocities v_i and v_e are assumed to be small and non-linear terms can be neglected.

From eq. (11) in the cylindrically symmetric case is obtained

$$(93) \quad E_r = -\frac{\partial \Phi}{\partial r}, \quad E_\varphi = 0, \quad E_z = \text{const} \equiv E,$$

since E_φ is finite at the axis $r=0$. From the φ -components of eqs. (3) and (4)

$$(94) \quad v_{i\varphi} = -(\omega_i/\nu_{in})v_{ir}, \quad v_{e\varphi} = -(\omega_e/\nu_{en})v_{er},$$

where the index (0) has been dropped in the notation of the gyrofrequencies. The motions $v_{i\varphi}$ and $v_{e\varphi}$ arise partly from the radial density gradients, partly from drift motion in the crossed fields E_r and B_0 . In the axial direction

$$(95) \quad v_{iz} = (e/m_i\nu_{in})E, \quad v_{ez} = (e/m_e\nu_{en})E.$$

The radial components of eqs. (3) and (4) combine with eq. (94) to

$$(96) \quad nv_i = -\beta_i n \frac{\partial \Phi}{\partial r} - D_i \frac{dn}{dr},$$

$$(97) \quad nv_e = \beta_e n \frac{\partial \Phi}{\partial r} - D_e \frac{dn}{dr},$$

where the diffusion coefficients

$$(98) \quad D_i = \frac{kT_i}{m_i v_{in}(1 + \omega_i^2/v_{in}^2)} = kT_i \beta_i / e,$$

and

$$(99) \quad D_e = \frac{kT_e}{m_e v_{en}(1 + \omega_e^2/v_{en}^2)} = kT_e \beta_e / e,$$

have been introduced. The symmetry condition for the radial component of eq. (9) requires $v_{ir} = v_{er}$. After elimination of Φ from eqs. (96) and (97) the conservation laws (1) are applied with Zn substituted for $-\partial n/\partial t$ and

$$(100) \quad \frac{d^2 n}{dr^2} + \frac{1}{r} \frac{dn}{dr} + \frac{Z}{D_a} n = 0,$$

where

$$(101) \quad D_a = (D_i \beta_e + D_e \beta_i) / (\beta_i + \beta_e)$$

is the ambipolar diffusion coefficient. The solution which is finite at $r=0$ becomes

$$(102) \quad n(r) = n_0 J_0(\alpha r), \quad \alpha = (Z/D_a)^{1/2}.$$

The deviations from electric neutrality are obtained by combination of eqs. (10), (96), (97) and (102);

$$(103) \quad n'/n_0 \equiv (n_i - n_e)/n_0 = \alpha^2 \frac{\beta_e h_e^2 - \beta_i h_i^2}{\beta_i + \beta_e} (1 + J_1^2/J_0^2).$$

The result shows that the quasi-neutral approximation is valid throughout the major part of the column as soon as the Debye distances h_i and h_e are much smaller than the tube radius R . At low charge densities this approximation is not valid and the ions and electrons will then diffuse separately as determined by the coefficients (98) and (99) and not by the ambipolar coefficient (101).

The density n_0 at the axis is calculated from eqs. (95), (22) and (102):

$$(104) \quad n_0 = \frac{\alpha I}{2\pi e^2 R' E (1/m_i v_{in} + 1/m_e v_{en}) \cdot J_1(\alpha R')},$$

where I is the total current and $r = R'$ is the edge of the wall sheath. Situations where $(R - R')/R \ll 1$ are studied here.

The discussion is now restricted to a non-conducting wall. Per unit length and time there are created

$$(105) \quad N = 2\pi n_0 Z R' J_1(\alpha R') / \alpha$$

particles inside $r = R'$. If the ions are supposed to leave the plasma edge at $r = R'$ with a mean velocity towards the wall corresponding to an equivalent « temperature » T'_i the wall will absorb

$$(106) \quad N = \frac{1}{2} \pi R' \cdot n(R') (3kT'_i/m_i)^{\frac{1}{2}}$$

particles per unit length and time. Balance between created and lost charges is given by the equality of expressions (105) and (106):

$$(107) \quad n(R')/n_0 = 4(ZD_a m_i / 3kT'_i)^{\frac{1}{2}} J_1(\alpha R').$$

We introduce the mean free paths

$$(108) \quad \lambda_{in} = (3kT_i/m_i)^{\frac{1}{2}}/v_{in}, \quad \lambda_{en} = (3kT_e/m_e)^{\frac{1}{2}}/v_{en}.$$

since $n(r) \geq 0$ eqs. (101), (102), (107) and (108) give the condition

$$(109) \quad n(R')/n_0 = J_0(\alpha R') \leq \bar{\lambda}/R' \approx \bar{\lambda}/R,$$

where

$$(110) \quad \bar{\lambda} = 1.66 \frac{\lambda_{in} \lambda_{en} [m_i(T_i + T_e)^2/T'_i]^{\frac{1}{2}}}{\lambda_{in}(1 + \omega_e^2/v_{en}^2)(m_e T_e)^{\frac{1}{2}} + \lambda_{en}(1 + \omega_i^2/v_{in}^2)(m_i T_i)^{\frac{1}{2}}},$$

can be regarded as a mean value of the mean free paths and is equivalent to a mean value earlier used by VON ENGEL and STEENBECK [25].

In order to estimate $\bar{\lambda}$ the magnitude of T'_i has to be determined. For the non-magnetic case BICKERTON [7] and BICKERTON and VON ENGEL [8] assume that $T'_i = T_i$. On the other hand, BOHM [12] has pointed out that a stable sheath cannot exist unless the ions leave the plasma edge with a velocity corresponding to $T'_i \approx T_e/2$. This is caused by an acceleration in a weak electric field which penetrates from the wall region through the plasma edge.

When a magnetic field is present, and in cases of interest in this connection, the Larmor radius of ions is larger than the Debye distances and the thickness of the wall sheath. This implies that the collection of ions by the wall across the sheath is largely unaffected by the magnetic field (BOHM [12], BOHM, BURHOP and MASSEY [13], BICKERTON [7] and BICKERTON and VON ENGEL [8]). According to BOHM and collaborators T'_i should still be of the order of $T_e/2$ when a magnetic field is present and $T_e > T_i$.

In the next part of this section the condition $\bar{\lambda}/R \ll 1$ is assumed to be valid. It is seen that a strong reduction of $\bar{\lambda}/R$ takes place according to eq. (110) when the magnetic field is increased (cf. BICKERTON [7]).

3'3.2. Determination of the electron temperature.

a) The plasma balance equation. When $\bar{\lambda}/R \ll 1$ the balance between charge production and wall losses is given by

$$(111) \quad ZR^2/D_a = K_1^2,$$

where $K_1 = 2.4048$ is the first zero of J_0 . Combination of equations (107) and (109) gives a corresponding balance equation which leads to a « modified Schottky theory » applicable also to situations when $\bar{\lambda}/R \ll 1$ (cf. BICKERTON [7] and BICKERTON and VON ENGEL [8]). Assuming Maxwellian distribution VON ENGEL and STEENBECK [25] have deduced the number Z of ion pairs produced per unit time and per electron:

$$(112) \quad Z = \frac{2}{\sqrt{\pi}} \cdot \frac{m_e}{e} ap(273/T_n) \cdot (2kT_e/m_e)^{3/2} \cdot (1 + eV_j/2kT_e) \exp[-eV_j/kT_e],$$

where p now stands for the neutral gas pressure in newtons/m² (1 mm Hg = = 132.8 N/m²) V_j is the ionization potential and a is a constant with a numerical value 0.754 times that given by VON ENGEL and STEENBECK when eq. (112) is expressed in MKSA-units. For helium $a = 0.0347$ amp s⁵/kg² m² and $V_j = 24.54$ V. The notations

$$(113) \quad x = eV_j/kT_e, \quad x_i = eV_j/kT_i,$$

$$(114) \quad \lambda_{en} = A_e/p, \quad \lambda_{in} = A_i/p,$$

$$(115) \quad A_e = A_{e0}(T_n/273), \quad A_i = A_{i0}(T_n/273),$$

are introduced, where A_{e0} is a function of the electron and ion temperatures given by VON ENGEL and STEENBECK [25] and MAIER-LEIBNITZ [52]. Eq. (111) now becomes

$$(116) \quad H(x) = A(Rp)^2 \cdot [K(x, x_i) + y^2 M(x, x_i)],$$

where

$$(117) \quad H(x) = \sqrt{x} e^x / (1 + 2/x),$$

$$(118) \quad A = 2(6/\pi)^{1/2} a(273/T_n) V_j (m_i/m_e)^{1/2} \cdot K_1^{-2},$$

$$(119) \quad K(x, x_i) = \frac{x_i^{1/2}}{A_i(1 + x_i/x)} \cdot \left[1 + \frac{A_i}{A_e} \cdot \left(\frac{m_e x_i}{m_i x} \right)^{1/2} \right],$$

$$(120) \quad y = \omega_i/p,$$

$$(121) \quad M(x, x_i) = \frac{m_i x_i^{1/2} A_i}{3e V_j (1 + x_i/x)} \cdot \left[1 + \frac{A_e}{A_i} \left(\frac{m_i x}{m_e x_i} \right)^{1/2} \right].$$

With helium $A = 31.7$ s²/kg when $T_n = 300$ °K.

b) The relation between the ion and electron temperatures. — VON ENGEL and STEENBECK [25] obtain the energies

$$(122) \quad \left(\frac{dW}{dt}\right)_i = \frac{4\kappa_i}{\lambda_{in}\sqrt{\pi}} \left(\frac{2kT_i}{m_i}\right)^{\frac{1}{2}} k(T_i - T_n),$$

and

$$(123) \quad \left(\frac{dW}{dt}\right)_e = \frac{2m_e\kappa_e}{\lambda_{en}\sqrt{\pi}} \left(\frac{2kT_e}{m_e}\right)^{\frac{1}{2}},$$

which are transferred to the neutral gas by collisions with ions and electrons, respectively. In eqs. (122) and (123) κ_i and κ_e are the mean fractions of the total energy of a particle being lost in a collision. The energy is supplied by the electric field \mathbf{E} which is parallel with the magnetic field \mathbf{B}_0 . The energy supply is given by

$$(124) \quad \left(\frac{dW}{dt}\right)_i = ev_{iz}E \quad \text{and} \quad \left(\frac{dW}{dt}\right)_e = -ev_{ez}E,$$

both in presence and in absence of the magnetic field and from eqs. (95), (122), (123) and (124)

$$T_e^2 = (\lambda_e^2\kappa_i/\lambda_i^2\kappa_e) T_i(T_i - T_n),$$

or

$$(125) \quad (x_i/x)^2 = [A_{e0}(x)/A_{i0}(x_i)]^2 \cdot [\kappa_i/\kappa_e(x)] \cdot (1 - x_i/x_n),$$

where

$$x_n = eV_i/kT_n.$$

The ion temperature is not very much greater than that of the neutral gas and ions may be assumed to lose their energy by elastic collisions, *i.e.*, $\kappa_i \approx 0.5$. For electrons, however, inelastic collisions will be taken into account and κ_e becomes a function of T_e as shown in the next paragraph. The electron temperature is determined by the root x of eqs. (116)–(121) and (125). In the integration of the expressions leading to eqs. (122) and (123) κ_i and κ_e have been approximated by constant mean values.

3.3.3. The longitudinal electric field in a helium discharge. —

The total fractional loss of energy of an electron in a collision with a neutral gas particle is

$$(126) \quad \kappa_e = \kappa_{el} + \kappa_{ion} + \kappa_{exc} + \kappa_{wall},$$

where $\kappa_{el} = 2m_e/m_n$ is the energy loss from elastic collisions,

$$(127) \quad \kappa_{ion} = (eV_i Z)/(\frac{3}{2}kT_e \cdot v_{en}) = \frac{2}{3}xZ/v_{en}$$

is the ionization loss, where the rate Z is given by eq. (112) and

$$(128) \quad \kappa_{\text{exc}} = \sum_s (eV_s Z_s) / \left(\frac{3}{2} kT_e \cdot \nu_{en} \right) = \sum_s \frac{2}{3} x \frac{V_s}{V_j} Z_s / \nu_{en},$$

is the total excitation loss, where V_s and Z_s are the excitation potential and excitation rate of the s -th level. Since the electrons diffuse in radial direction there is a wall loss as well. The plasma balance not only requires the ionization work to be done at the rate Z ; the electron which is produced must also be «heated» to the temperature T_e . Since Z electrons of this temperature are lost to the walls per unit time and electron the fractional wall loss becomes

$$(129) \quad \kappa_{\text{wall}} = (\frac{3}{2} kT_e Z) / (\frac{3}{2} kT_e \cdot \nu_{en}) = Z / \nu_{en} = \frac{3}{2} \kappa_{\text{ion}} / x.$$

In order to calculate the excitation loss in helium the experimentally determined excitation cross-section (MAIER-LEIBNITZ [52]) is used as a starting point. As shown by FABRIKANT [26] and KARELINA [34] a good approximation to the experimental results is given by an empirical expression for the total excitation free path λ_{exc} :

$$(130) \quad 1/\lambda_{\text{exc}} = (273p/132.8T_n) \cdot \sum_s (1/\lambda_s) \frac{V' - V_s}{V_{ms} - V_s} \exp \left[\frac{V_{ms} - V'}{V_{ms} - V_s} \right],$$

where V' is the potential corresponding to the particle energy. In this approximation two «levels», $s=1, 2$, are used with

$$\lambda_1 = 7.7 \cdot 10^{-2} \text{ m}, \quad \lambda_2 = 2.7 \cdot 10^{-2} \text{ m}, \\ V_1 = 19.25 \text{ V}, \quad V_2 = 20.2 \text{ V}, \quad V_{m1} = 20 \text{ V and } V_{m2} = 28 \text{ V}.$$

If Maxwellian distribution is assumed the number of exciting collisions per unit time and electron becomes for «level» s :

$$(131) \quad Z_s = p \left(\frac{273}{T_n} \right) \int_{v_{fs}}^{\infty} \frac{4}{\sqrt{\pi}} \frac{v^2}{w_e^3} \cdot \frac{v}{A_s} \cdot \frac{V' - V_s}{V_{ms} - V_s} \exp \left[\frac{V_{ms} - V'}{V_{ms} - V_s} - \frac{v^2}{w_e^2} \right] dv,$$

where v is the total velocity of an electron, $w_e = (2kT_e/m_e)^{\frac{1}{2}}$ and $A_s = 132.8\lambda_s$. The total loss κ_e is given by the integrated eq. (131) and eqs. (126)–(129) and (112)–(115):

$$(132) \quad \kappa_e = 2m_e/m_n + \frac{8}{3} \left(\frac{2}{3} \pi \right)^{\frac{1}{2}} \cdot A_{e0} \cdot \left\{ aV_j \left(\frac{7}{4} + \frac{1}{2}x + \frac{3}{2x} \right) \exp[-x] + \right. \\ \left. + \sum_s \frac{1}{A_s} \cdot \frac{V_s}{V_{ms} - V_s} \left[\frac{1 + (xV_s/2V_j) \left(1 + \frac{V_j}{x(V_{ms} - V_s)} \right)}{\left(1 + \frac{V_j}{x(V_{ms} - V_s)} \right)^3} \right] \exp[1-x] V_s/V_j \right\}.$$

The result is shown in Fig. 1 and agrees fairly well with experimental results by BICKERTON [7] and BICKERTON and VON ENGEL [8].

Finally, the longitudinal electric field is obtained from eqs. (123), (124) and (95) as a function of x :

$$(133) \quad E = (96/\pi)^{\frac{1}{2}} \cdot (273p/T_n) V_i (\sqrt{\kappa_e}/x A_{e0}).$$

The factor in front of the right hand member of eq. (133) is somewhat uncertain because it is based upon elementary kinetic methods in the calculation of the frictional coefficients in eqs. (3) and (4). A more rigorous kinetic theory gives a factor $(64/\pi)^{\frac{1}{2}}$ in front of eq. (133) instead of $(96/\pi)^{\frac{1}{2}}$ (VON ENGEL and STEENBEK [25]). However, this source of error should play a minor role in the relative magnitude

$$(134) \quad \Theta = E(B_0 \neq 0)/E(B_0 = 0)$$

of the electric field at varying magnetic field strengths.

Theoretical results for $Rp = 1.94 \text{ N/m} (= 1.46 \text{ cm mmHg})$ and $4.52 \text{ N/m} (= 3.40 \text{ cm mmHg})$ with $T_n = 300^\circ \text{K}$ are shown by the full curves in Fig. 3a and b, as calculated from eqs. (116)–(121), (132) and (134). For the mean free path of ions defined by eqs. (114) and (115) a value $\sqrt{2}$ times that of neutral particles given by KENNARD [35] has been taken. A source of error may be introduced by this value but it does not change the position of the theoretical curve fundamentally; appreciable changes in the rate of diffusion are required to cause a noticeable change in the electron temperature since the production rate Z is a sensitive function of T_e according to eq. (112). In Fig. 3a and b a change of the diffusion coefficient has also been simulated by substituting the function M of eq. (121) by ηM . The value $\eta = 1$ corresponds to the actual situation whereas $\eta = 0.5, 0.1$ and 0.01 (broken lines) give diffusion coefficients which are about twice, ten and hundred times larger than the present in a magnetic field, which is strong enough to satisfy the condition $y^2 \eta M \gg K$. In the present measurements this is the case only for $\eta \geq 0.1$ when the strong fields of the right hand sides of Fig. 3a and b are considered.

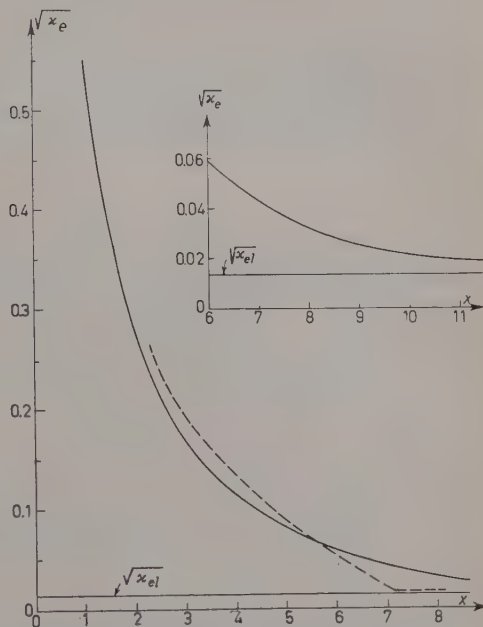


Fig. 1. - Square root of the total fractional loss κ_e of energy of the electrons as a function of T_e . Full line indicates results according to eq. (132), and broken line experimental results by BICKERTON and VON ENGEL.

3.3.4. The experiment.

a) The apparatus. The experimental arrangement is shown in Fig. 2. A discharge tube of inner radius $R = 1$ cm has been placed inside a magnetic coil of four meters length. In one of the runs being made (Fig. 3b) the magnetic field was varied up to $B_0 = 0.53$ Vs/m² ($= 5300$ gauss), corresponding to

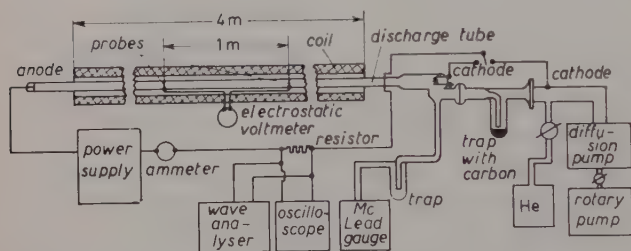


Fig. 2. — Outline of the experimental arrangement. The discharge tube has an inner radius of 1 cm.

a power input of about $3 \cdot 10^5$ W. Since every measurement required only a few seconds time it was sufficient to cool the coil with fans. The tube ends with anode and cathode were both extended far outside of the coil. The diverging field at the coil ends, the large ratio between the tube length and

tube radius and the relatively high pressure used in the experiments (≤ 1.46 mm Hg) make impossible short-circuiting effects of the type discussed by SIMON [66]. Measurements of the longitudinal electric field were made with an electrostatic voltmeter connected between two floating platinum wire probes, one meter apart and both being far from the tube ends. The probes had the shape of circular sectors which followed the tube wall closely. Their connections were screened electrostatically all the way out to the voltmeter. The discharge current was closed through an inductance-free resistor over which the voltage could be examined with an oscilloscope and a wave analyser.

Before the measurements the electrodes were outgassed and the tube run with 180 mA current. Impurities in the helium discharge were easily detected with a small spectroscope. Narrow slits in the coil made observations possible over the entire length of the tube. It was found that the most rapid way to clean the tube from impurities was to place the cathode at the opposite side of the vapor trap filled with carbon (Fig. 2). With a strong current the discharge acted as an ion pump and the gradual disappearance of the impurities could be followed from the anode end to the cathode by means of the spectroscope. Measurements were not performed until the tube was observed to be clean over its entire length.

The pressure was measured with a McLeod gauge.

b) Experimental results. Two series of electric field measurements were made at the pressures 1.47 and 3.26 mmHg as shown by Fig. 3a and 3b. The results at zero magnetic field are given in Table VI together with theoretical results calculated from eqs. (116)–(121), (125) and (133), which are also compared with results by KARELINA [34] for $Rp = 1.47$ cm mmHg and by KLARFELD [36, 37] for $Rp = 3.40$ cm mmHg. The agreement between the experimental results by these authors and the present experiments is as good as can be expected. The present theoretical value of E/p for $Rp = 1.47$ cm mmHg is closer to the experimental than the value

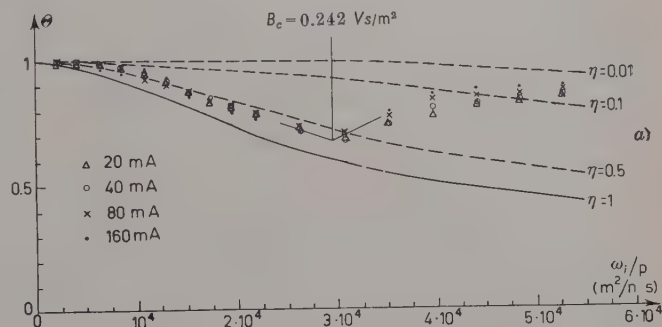
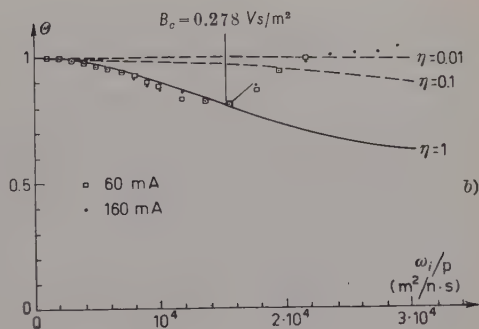


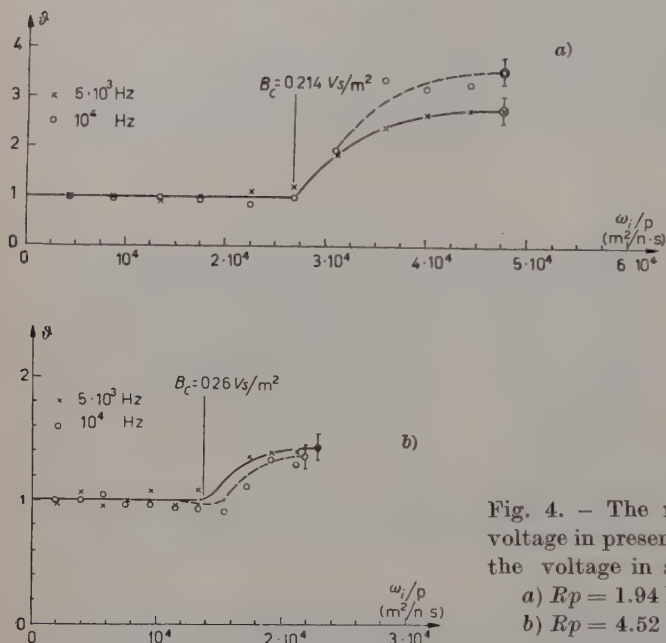
Fig. 3. — The ratio $\Theta = E(B_0)/E(0)$, where $E(B_0)$ is the longitudinal electric field when the magnetic field is present and $E(0)$ the corresponding value without magnetic field. $\omega_i = eB_0/m_i$ is the gyro-frequency of the ions. Experimental results are indicated by marks and theoretical ones by the full curve ($\eta = 1$). A double, a tenfold and a hundredfold reduction of the magnetic contribution to the diffusion coefficient is simulated by the broken lines with $\eta = 0.5$, 0.1 and 0.01 , respectively. a) $Rp = 1.96$ N/m = 1.47 cm mmHg, b) $Rp = 4.33$ N/m = 3.26 cm mmHg.



calculated by KARELINA, but there still remains a discrepancy which partly may be due to an erroneous factor in front of the expression for the mobility.

Fig. 4a and b show the corresponding measurements at $Rp = 1.46$ and 3.40 cm·mm Hg of the relative magnitude ϑ of the noise voltage over the resistor in the discharge circuit. The measurements have been made with a discharge current of 160 mA and at $5 \cdot 10^3$ and 10^4 Hz with the wave analyser adjusted to a band width of 145 Hz. Measurements at lower frequencies

(10^3 Hz) were difficult to interpret; even in the absence of a magnetic field there was a strong and rapidly changing noise voltage. It is seen from Fig. 3



and 4 that the experimental points form a «knee» which indicates that the state of the discharge is changing at a magnetic field $B_c \approx 0.23$ and 0.27 Vs/m² for $Rp \approx 1.46$ and ≈ 3.30 cm mmHg.

Fig. 4. — The ratio ϑ between the noise voltage in presence of the magnetic field and the voltage in absence of the same field.

a) $Rp = 1.94$ N/m = 1.46 cm mmHg,
b) $Rp = 4.52$ N/m = 3.40 cm mmHg.

TABLE VI. — Values of E/p in V/cm mmHg.

Rp (cm mmHg)	I (mA)	Present results		Earlier results	
		Exp.	Theor.	Exp.	Theor.
1.47	20	3.66	5.61	—	—
	40	3.51		—	
	80	3.34		—	
	100	—		3.4	
	160	3.23		—	
3.40	60	1.75	3.20	—	—
	160	1.71		—	
	300	—		1.8	

3.3.5. Discussion.

a) Experimental conditions. In absence of the magnetic field and at the pressures of the present experiments the electron temperature is about $4 \cdot 10^4$ °K and the ion temperature about 1000 °K. From eq. (110)

the values $\bar{\lambda}/R \approx 0.06$ and 0.03 are obtained at $Rp = 1.46$ and 3.30 cm mmHg when T'_i is put equal to $T_e/2$ according to BOHM [10]. With $T'_i \approx T_i$ according to BICKERTON and VON ENGEL [8] the values $\bar{\lambda}/R \approx 0.27$ and 0.14 are obtained which can be regarded as upper limits since the stability of the wall sheath requires $T'_i \approx T_e/2$. Even with $\bar{\lambda}/R = 0.3$ the change in the theoretical value of the electron temperature is only a few percent.

At the lowest pressure and current density used in the experiments the charge density is calculated from eq. (104) to $4 \cdot 10^{16} \text{ m}^{-3}$, corresponding to the Debye distances $h_e = 1.4 \cdot 10^{-4} \text{ m}$ and $h_i = 3 \cdot 10^{-5} \text{ m}$ as given by eq. (14). From eq. (103) $n'/n < 0.2$ at a distance greater than 1 mm ($= 0.1 R$) from the wall. Consequently, the quasi-neutral approximation is valid throughout the major part of the tube. Conditions are improved with increasing current density and pressure; for $I = 0.16 \text{ A}$ and $Rp = 4.33 \text{ N/m}$ the results are $h_e = 1.0 \cdot 10^{-5} \text{ m}$ and $n'/n < 1.0 \cdot 10^{-3}$ at $r = 0.1 R$.

Finally, the smallest radius of gyration of the ions in the present experiments has been $2.8 \cdot 10^{-4} \text{ m}$ (at $B = 0.53 \text{ Vs/m}^2$) which is greater than the largest occurring Debye distance $h_e = 1.4 \cdot 10^{-4} \text{ m}$.

From these considerations is seen that the basic conditions underlying the theory in Sect. 3.3.1-3.3.3. have their correspondence in the present experiments.

b) Conclusions. The left hand parts of the theoretical curves in Fig. 3*a* and *b* show a satisfactory agreement between theory and experiment; the small discrepancies may be due to an error in the mean free paths used in the calculations. An increase in the diffusion coefficient by a factor of ten ($\eta = 0.1$) or more is in any case too large not to be distinguished from the present results. Consequently, the left hand parts of Fig. 3*a* and *b* show that the diffusion is taking place according to the binary collision theory and that a strong reduction in the diffusion coefficient is caused by the magnetic field which traps the particles effectively in its transverse direction. There seems to be no difference between the measurements at varying current densities and from this is concluded that deviations from electric neutrality as well as two-stage processes and recombination do not influence the results noticeably. Correspondingly, the left hand parts of Fig. 4*a* and *b* show no increase in the noise level caused by the magnetic field.

However, when the magnetic field reaches a certain critical value which is about $B_0 = 0.23$ and 0.27 Vs/m^2 at $Rp = 1.94$ and 4.52 N/m the diffusion coefficient starts to increase rapidly and the noise level is suddenly increased at the same time. The deviations between the binary collision theory and the experiments are considerable in this region as shown by the right hand parts of Fig. 3*a* and *b*. In Fig. 3*a* the diffusion coefficient exceeds its value due to the collision theory by more than a factor of ten when the magnetic field exceeds about 0.3 Vs/m^2 and in Fig. 3*b* this occurs at a field strength of

about 0.4 Vs/m^2 . These results strongly support the existence of the «drain» diffusion mechanism suggested by BOHM, BURHOP, MASSEY and WILLIAMS [13]. It should also be observed that the right hand part of Fig. 3a clearly indicates an increase in the diffusion rate at increasing current densities, *i.e.*, at increasing charge densities, n . This also speaks in favour of such a mechanism which is based upon the effect of local electric fields caused by deviations from electric neutrality. Whether the oscillations consist of only a broad spectrum of «electromagnetic turbulence» or include plasma oscillations concentrated around some special frequencies cannot be judged at this stage and requires further investigation. The plasma frequency of electrons is about 10^{10} s^{-1} in the present experiments. It should be pointed out that noise and oscillations in the presence of a magnetic field have also been observed by ÅSTROM [4] and WEBSTER [70] in an electron gas and by BLOCK [11] in model experiments on the auroral discharge.

Finally, the conclusions drawn here are also consistent with the results obtained by BOSTICK and LEVINE [18] for a toroidal discharge in a toroidal magnetic field. These authors find a considerable decrease in the diffusion time as well as the presence of oscillations in a limited range of magnetic field strengths. However, as pointed out by BOSTICK and LEVINE [18] and later by BIERMANN and SCHLÜTER [10] and LEHNERT [44] particle losses are also caused by the gradient in a toroidal magnetic field. Consequently, no definite conclusions can be drawn about the magnitude of the diffusion coefficient in the latter experiment.

The diffusion caused by oscillations and «electromagnetic turbulence» provides a mechanism for ionized matter to slip across a magnetic field. When this mechanism is acting modifications of the present theories of an ionized gas have to be undertaken, both in astrophysics when the motions of magnetic fields and matter are considered, and in the thermonuclear problem when the confinement of a hot gas in a magnetic field is discussed. It is desirable to extend the present investigations to a fully ionized gas in stronger magnetic fields than those being used here as well as to other gases than helium.

4 - Summary.

In the present paper the behaviour of an ionized gas under cosmical and laboratory dimensions is examined by means of dimensionless parameters. In particular, the deviations from electric neutrality and «creeping diffusion» are estimated.

The coupling between plasma and neutral gas is investigated by means of the basic equations for a partially ionized gas. This gives a dispersion relation for plane disturbances of small amplitudes. The effective electrical conductivity

can be deduced from the corresponding damping distance. Expressions for the electrical conductivity in a magnetic field earlier derived by COWLING, SCHLÜTER and PIDDINGTON are obtained as special cases of the present theory. They are shown to be valid only under certain conditions of ionization and coupling between the plasma and the neutral gas.

Agreement is obtained with earlier conclusions by PIDDINGTON and COWLING about the increased dissipation of magneto-hydrodynamic waves in the solar chromosphere and of magnetic fields in cool interstellar clouds.

Magnetohydrodynamic oscillations with wave lengths comparable with the thickness of the ionospheric F_1 -region and with periods comparable with those of « giant pulsations » are damped moderately only if the ionization degree is about hundred times greater inside than outside of the auroral zones.

Two specific examples are given as experimental illustrations to the theory. Firstly, torsional oscillations in a cylindrical « magnetohydrodynamic wave guide » are discussed. It is found that Alfvén waves will exist in an ionized gas in the laboratory only in a high current discharge of relatively large dimensions.

The second example is given by the diffusion processes which take place in a plasma column situated in a longitudinal magnetic field. The balances between the rate of ionization and the losses of charged particles to the walls reflects itself in the electric potential drop along the column. Consequently, a longitudinal magnetic field, which influences the particle diffusion to the walls, will also affect the potential drop. The experiments are found to agree well with the collision diffusion theory in a range of magnetic fields up to a certain critical value. Above this value a marked change occurs which can be interpreted as a sudden and rapid increase in the diffusion coefficient. Simultaneously, the noise level is raised. These results support the « drain » diffusion mechanism earlier suggested by BOHM, BURHOP, MASSEY and WILLIAMS. By this mechanism the particle diffusion across the magnetic field is accelerated by the action of transverse electric fields.

REFERENCES

- [1] H. ALFVÉN: *Nature*, **150**, 405 (1942).
- [2] H. ALFVÉN: *Cosmical Electrodynamics* (Oxford, 1950).
- [3] C. W. ALLEN: *Astrophysical quantities* (London, 1955).
- [4] E. ASTRÖM: *Transactions of the Royal Institute of Technology*, no. 22 (Stockholm, 1948), p. 70.
- [5] E. ASTRÖM: *Ark. f. Fys.*, **2**, 443 (1950).
- [6] W. G. BAKER and D. F. MARTYN: *Phil. Trans.*, A **246**, 36 (1953).

- [7] R. J. BICKERTON: *D. Phil. Thesis* (Oxford, 1954).
- [8] R. J. BICKERTON and A. VON ENGEL: *Proc. Phys. Soc.*, B **69**, 468 (1956).
- [9] L. BIERMANN and R. LÜST: in press (1958).
- [10] L. BIERMANN and A. SCHLÜTER: *Zeits. f. Naturfor.*, **12a**, 805 (1957).
- [11] L. BLOCK: *Tellus*, **7**, 65 (1955).
- [12] D. BOHM: *The characteristics of electrical discharges in magnetic fields*. Ed. by A. GUTHRIE and R. K. WAKERLING (New York, 1949), pp. 77, 95, 12.
- [13] D. BOHM, E. H. S. BURHOP, H. S. W. MASSEY and R. M. WILLIAMS: *The characteristics of electrical discharges in magnetic fields*. Ed. by A. GUTHRIE and R. K. WAKERLING (New York, 1949), pp. 62, 201, 49, 14, 31.
- [14] H. BONDI and T. GOLD: *M.N.R.A.S.*, **110**, 607 (1950).
- [15] W. H. BOSTICK: *Phys. Rev.*, **104**, 292 (1956).
- [16] W. H. BOSTICK: *Electromagnetic phenomena in cosmical physics*. Ed. by B. LEHNERT (Cambridge, 1958).
- [17] W. H. BOSTICK and M. A. LEVINE: *Phys. Rev.*, **87**, 671 (1952).
- [18] W. H. BOSTICK and M. A. LEVINE: *Phys. Rev.*, **97**, 13 (1955).
- [19] T. G. COWLING: *Month. Not. Roy. Astr. Soc.*, **93**, 90 (1933).
- [20] T. G. COWLING: *Month. Not. Roy. Astr. Soc.*, **11**, 114 (1956).
- [21] T. G. COWLING: *Magnetohydrodynamics* (New York and London, 1957).
- [22] C. S. CUMMINGS and L. TONKS: *Phys. Rev.*, **59**, 514 (1941).
- [23] P. J. DICKERMANN: *Conference on extremely high temperatures* (Boston, 1958).
- [24] J. E. DRUMMOND: *Conference on extremely high temperatures* (Boston, 1958).
- [25] A. VON ENGEL and M. STEENBECK: *Elektrische Gasentladungen*, I, II (Berlin, 1932).
- [26] V. A. FABRIKANT: *Compt. Rend. Acad. Sci. U.S.S.R.*, **23**, 891 (1937).
- [27] C. M. FALALIEV: *Comp. Rend. Acad. Sci., U.R.S.S.*, **23**, 891 (1939)
- [28] S. FLÜGGE: *Handb. d. Phys.* (Berlin-Göttingen, 1956), **22**.
- [29] B. N. GERSHMAN, V. L. GINZBURG and N. G. DENISOV: *Usp. Fiz. Nauk*, **61**, 561 (1957).
- [30] A. GUTHRIE and R. K. WAKERLING: *The characteristics of electrical discharges in magnetic fields* (New York, 1949).
- [31] N. HERLOFSON: *Nature*, **165**, 1020 (1950).
- [32] F. HOFFMANN DE and E. TELLER: *Phys. Rev.*, **80**, 692 (1950).
- [33] H. C. VAN DEN HULST: *Int. Union of Theor. and Appl. Mech. and Int. Astr. Union Proc. Symp.* (Paris, 1951).
- [34] N. A. KARELINA: *Journ. Phys. U.S.S.R.*, **6**, 218 (1942).
- [35] E. H. KENNARD: *Kinetic theory of gases* (New York and London, 1938), p. 149.
- [36] B. KLARFELD: *Journ. Techn. Phys. U.S.S.R.*, **4**, 44 (1937).
- [37] B. KLARFELD: *Journ. Techn. Phys. U.S.S.R.*, **5**, 725 (1938).
- [38] A. C. KOLB: *Magnetohydrodynamics*. Ed. by R. K. M. LANDSHOFF (Stanford, 1957), p. 76.
- [39] R. K. M. LANDSHOFF: *Magnetohydrodynamics* (Stanford, 1957).
- [40] B. LEHNERT: *Astrophys. Journ.*, **119**, 647 (1954).
- [41] B. LEHNERT: *Astrophys. Journ.*, **121**, 481 (1955) and *Quart. Appl. Math.*, **12**, 321 (1955).
- [42] B. LEHNERT: *Tellus*, **8**, 241 (1956).
- [43] B. LEHNERT: *Tellus*, **9**, 139 (1957).
- [44] B. LEHNERT: *Nature*, **181**, 331 (1958).
- [45] L. B. LOEB: *Fundamental processes of electrical discharges in gases* (New York, 1939), p. 290.
- [46] I. LUCAS: *Ark. d. Elektr. Übertragung*, **8**, 91, 123 (1954).
- [47] I. LUCAS and A. SCHLÜTER: *Ark. d. Elektr. Übertragung*, **8**, 27 (1954).

- [48] S. LUNDQUIST: *Phys. Rev.*, **76**, 805 (1949).
- [49] S. LUNDQUIST: *Ark. f. Fys.*, **2**, 361 (1950).
- [50] S. LUNDQUIST: *Phys. Rev.*, **83**, 307 (1951).
- [51] R. LÜST and A. SCHLÜTER: *Zeits. f. Astrophys.*, **34**, 263 (1954).
- [52] H. MAIER-LEIBNITZ: *Zeits. f. Phys.*, **95**, 1935 (1935).
- [53] M. MINNAERT: *The sun*. Ed. by G. P. KUIPER (Chicago, 1953).
- [54] W. A. NEWCOMB: *Magnetohydrodynamics*. Ed. by R. K. M. LANDSHOFF (Stanford, 1957).
- [55] S. B. PICKELNER: *Tellus*, **9**, 138 (1957).
- [56] J. H. PIDDINGTON: *Month. Not. Roy. Astr. Soc.*, **114**, 638, 651 (1954).
- [57] J. H. PIDDINGTON: *Month. Not. Roy. Astr. Soc.*, **115**, 671 (1955).
- [58] J. H. PIDDINGTON: *Month. Not. Roy. Astr. Soc.*, **116**, 314 (1956).
- [59] J. H. PIDDINGTON: *Electromagnetic phenomena in cosmical physics*. Ed. by B. LEHNERT (Cambridge, 1958).
- [60] R. POST: see NEWCOMBE [54].
- [61] G. N. ROKHLIN: *Journ. Phys. U.S.S.R.*, **1**, 347 (1939).
- [62] A. SCHLÜTER: *Zeits. f. Naturfor.*, **5a**, 72 (1950).
- [63] A. SCHLÜTER: *Zeits. f. Naturfor.*, **6a**, 73 (1951).
- [64] A. SCHLÜTER: *Electromagnetic phenomena in cosmical physics*. Ed. by B. LEHNERT (Cambridge, 1958).
- [65] A. SCHLÜTER and L. BIERMANN: *Zeits. f. Naturfor.*, **5a**, 237 (1950).
- [66] A. SIMON: *Phys. Rev.*, **98**, 317 (1955).
- [67] L. SPITZER: *Physics of fully ionized gases* (New York and London, 1956).
- [68] P. C. THONEMANN *et al.*: *Nature*, **181**, 217 (1958).
- [69] L. TONKS: *Phys. Rev.*, **56**, 360 (1939).
- [70] H. F. WEBSTER: *Journ. Appl. Phys.*, **26**, 1386 (1955).

INTERVENTI E DISCUSSIONI

— V. FERRARO wondered if it is true to say that the magnetic field gradients are likely to cause a large separation of charge in the plasma and if LEHNERT had considered that.

— B. LEHNERT answered:

It comes out from the terms containing B_0 and b . In some cases I think it would be important. The electrically quasineutral approximation only implies that one puts $n_i \sim n_e$ in the conservation laws. However, it does not imply that $\text{div } \mathbf{E}$ is put equal to zero since even a small relative deviation $|n_i - n_i|/n_{ic}$ may give rise to important electric fields.

— E. WEIBEL wondered what the frequency Ω was.

— B. LEHNERT answered: I have supposed that the whole gas mixture is rotating with a constant Ω . Of course, in the general case there should exist differential rotation as well.

— E. HARRISON asked if B. LEHNERT had assumed the neutral fraction to be constant in the equation of continuity, and that no ionization was taking place in the unsteady state.

— B. LEHNERT replied that the equation of continuity had not been used in the estimations performed. In a discussion on oscillations of small amplitudes given in Section 2'2. the ionization caused by the perturbations was neglected. Further, Dr. LEHNERT replied that if the neutral gas is being ionized continuously, *e.g.* by electron collisions, the conservation laws of matter have to be modified correspondingly. An example is given by the plasma balance in the positive column which is treated in Section 3'3.

— V. FERRARO asked if B. LEHNERT had said that the term $(m_i - m_e)\mathbf{i} \cdot \mathbf{B}/e\varrho$ gives rise to the Hall effect. He had been troubled by this because, if the masses of the ion and the electron were equal this term would disappear. V. FERRARO wondered if this could be explained physically.

— B. LEHNERT's answer was:

If the ion and the electron masses were equal, the mean velocity of the ion gas would become $\mathbf{v} = \mathbf{v} + \mathbf{i}/2en$ and that of the electron gas $\mathbf{v}_e = \mathbf{v} - \mathbf{i}/2en$. Consequently, in a coordinate system which moves with the plasma velocity \mathbf{v} and where an electric field $\mathbf{E} + \mathbf{v} \times \mathbf{B}$ is measured the ion and the electron currents both become equal to $+\frac{1}{2}\mathbf{i}$. The electric Hall fields corresponding to these currents in the magnetic field \mathbf{B} then become oppositely directed and are of the same magnitude; i.e. the total Hall field $(m_i - m_e)\mathbf{i} \cdot \mathbf{B}/e\varrho$ disappears.

— R. LÜST asked:

What magnetic field strengths, and frequencies have you used in your discussion on magneto-hydrodynamic waves in the chromosphere?

— B. LEHNERT answered that he had used a field of 5 gauss and a frequency of 0.1 rad/s, which values are about the same as those applied earlier by PIDDINGTON.

— C. DE JAGER asked if a change of the field strength down to 1 gauss, say, would change Piddington's conclusion about the heating of the chromosphere by the waves.

— B. LEHNERT replied:

This could be possible. The data of the magnetic field strengths are still too uncertain and the values I have used here could merely be considered as illustrations to the theory.

— R. LÜST asked:

Prof. BIERMANN and I have recently reconsidered the damping of waves in the chromosphere. We have assumed lower frequencies than that given in your table and for these frequencies the damping comes about to be quite small. Can this be explained by your theoretical results?

— B. LEHNERT's answer was:

Yes, the dissipation length is approximately proportional to $1/\omega^2$ where ω is the frequency. Consequently, a decrease in ω by a factor of ten or more would make the dissipation length much larger than the depth of the chromosphere.

— K. SCHINDLER asked:

In your theory you have applied an exact treatment of the equations of continuity and of motion. On the other hand, the energy equation has been approximated by the adiabatic relation. How does Joule heating and thermal conduction modify these results?

— B. LEHNERT replies:

For small amplitudes the Joule heating can be neglected in the energy theorem since it consists of a non-linear term proportional to i^2 . However, thermal conduction has not been considered in this treatise, where the sound velocities have been approximated by expressions containing the static equilibrium temperatures and only small deviations from the state are being studied. I quite agree with you, that in a general case thermal conduction may be important and should be taken into account (see also LEHNERT, *Tellus*, 8, 241, (1956) and *Electromagnetic Phenomena in Cosmical Physics* (Cambridge, 1958), p. 51-52).

— F. GIOVANELLI asked if B. LEHNERT's basic assumptions implied that he had excluded the possibility of having sound waves propagated in the ion and the electron gases separately with velocities C_i and C_e respectively.

— B. LEHNERT:

Yes, this is certainly true. By putting $n_i \approx n_e = n$ and $\nabla_p = C^2 \nabla \varrho$ the sound waves in the ion and electron gases are assumed to be propagated with the same wave lengths and phase velocities. A difference would cause charge separation.

— H. C. VAN DE HULST:

Can you make any suggestion about what determines the critical field strength at which deviations from the « binary collision diffusion » are observed?

— B. LEHNERT:

There are yet too few experimental data for such a determination. It is certainly of great interest to investigate how the critical field strength varies with the characteristic dimension, the pressure and the ionization degree. If the « drain » diffusion phenomena suggested here come out to be of importance this would correspond to a decrease in the « effective electric conductivity » and would increase dissipation also in the case of cosmical phenomena.

— G. GOLDSTEIN:

I should like to make two remarks; the first is relative to the diffusion coefficient in the direction across the magnetic field. You have neglected the charge exchange between diffusing positive ions and the neutral atoms. Now, this obviously, cannot be neglected in helium because the cross section of this process is practically the geometric one. My second remark is this: the diffusion of helium ions in helium has shown that the diffusion of molecular ions is much more important than the diffusion of atomic

ions, because the molecular ions are not affected by charge exchange. Consequently molecular ions have a much higher mobility than atomic ions in spite of their greater mass.

— B. LEHNERT:

I quite agree that the effects which you mention exist and that I have neglected them in the simplified theory given here, but I do not think that they will change the results appreciably. They will introduce errors of the same magnitude as those produced by the elementary kinetic theory when this is used for the computation of the collision frequencies. However, only very large changes in the diffusion coefficient are required to give a noticeable change in the potential drop along the tube. An error of a factor of about two in the diffusion coefficient modifies the theoretical results very little.

— E. HARRISON:

Have you neglected the neutral gas pressure gradient in your theory?

— B. LEHNERT:

No, it is taken into account; it appears indirectly in the frictional forces which occur in the equations of motion. I have only assumed that the ionization degree is low and that rather small changes of the neutral density from the constant value are required to produce a pressure gradient which balances the frictional forces. This constant value has been used in the computation of the collision frequencies ν_{in} and ν_{en} .

High Temperature Plasmas.

P. C. THONEMANN

Atomic Energy Research Establishment - Harwell, Berks.

This lectures will be concerned mainly with the experimental methods used in studying plasmas at high temperatures. The methods will be illustrated by describing some of the results obtained with Zeta.

I. - Observation on Turbulent Discharges.

This first chapter describes Harwell studies of turbulent constricted discharges in Argon and Hydrogen. The studies were aimed at finding to what extent containment could be achieved by using the simple pinch effect.

1. - The Bennett relation.

At low pressure ($\sim 10 \mu\text{m Hg}$) and low currents ($< 10 \text{ A}$) positive ions and electrons rapidly diffuse to the tube walls and their lifetime is rarely longer than $20 \mu\text{s}$. This diffusion loss can be reduced by using a confining magnetic field. One such way of achieving this reduction is to use the pinch effect.

By consideration of the radial pressure balance and assuming equal densities of charges we can obtain the Bennett relation [1]:

$$\frac{\mu_0 I^2}{8\pi} = Nk (T_1 + T_2) \quad \text{mks units,}$$

where μ_0 = permeability of free space,
 I = current (amp),
 N = number of particles/meter,
 k = Boltzmann's constant,
 T_1 = ion temperature ($^{\circ}\text{K}$),
 T_2 = electron temperature ($^{\circ}\text{K}$).

This is a general relation which is not dependent on the detailed mechanism of the discharge; expressing the fact that the magnetic energy/unit length is of the same order as the kinetic energy/unit length of the particles. It is not evident that the relation is valid for a simple pinch, if this is macroscopically unstable.

2. - Experimental observations.

The apparatus consisted of a 35 cm bore aluminium torus of 100 cm major diameter, which formed a single turn secondary of an iron cored pulse transformer. The torus was constructed of 6 separately insulated sections.

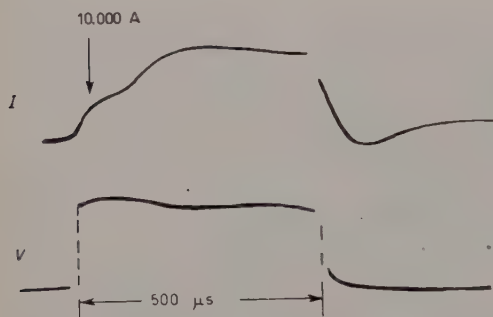


Fig. 1. - Current and voltage oscillograms for Argon discharges of about 10 000 A.

The discharge (10^4 A), having an associated magnetic field of 200 gauss, occurred in Argon or Hydrogen at pressures between 0.2 and 4.0 μmHg with a pulse length of 500 μs as shown in Fig. 1. The marked plateau in Fig. 1 corresponds to formations of the pinch; this behaviour is quite different from fast pinches of the Kurchatov type.

Spectroscopic evidence suggests that impurities do not make an important contribution to the particle density. Argon II and Argon III lines have been seen, though the latter were very weak, indicating that there was little multiple ionization. Image converters and rotating mirror photographs show that the discharge wriggles violently with the velocity of sound in the high temperature gas.

3. - Ion temperature measurements.

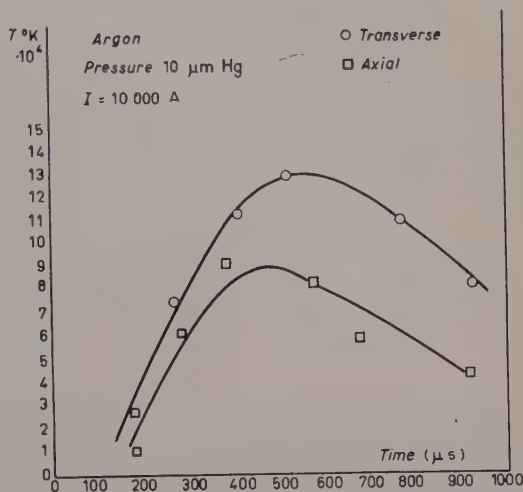
The ion energies are measured from the Doppler broadening of the spectral lines. Any broadening caused by Stark and Zeeman effects can be shown to be negligible.

For temperatures of about 10^5 °K a Fabry-Pérot etalon must be used in conjunction with the spectrometer, however at higher temperature, say 10^6 °K, a simple spectrometer suffices.

It is necessary to separate the broadening due to random thermal motions and that due to bodily movement of the gas. This was done by measuring the broadening in both the axial and transverse radial directions.

The results of this measurement are shown in Fig. 2 from which it is evident that there is appreciable mass motion. In principle this can be done more satisfactorily by examining mixtures of gases of different atomic mass (A). If the broadening is solely due to body motion it is independent of A , whereas if it is caused by the random motion it will decrease as A increases. This has not been done experimentally, largely due to the difficulty of exciting suitable lines simultaneously.

Fig. 2. — Ion temperature showing results for light emerging in the axial direction as well as transverse to the discharge axis.



4. — Electron temperature measurements.

Microwave noise. — In the frequency region where the plasma is behaving as a black body the power radiated (W) is given by

$$W = kT \cdot \Delta f,$$

where k = Boltzman's constant,

T = temperature ($^{\circ}\text{K}$),

Δf = bandwidth of receiver (Hz).

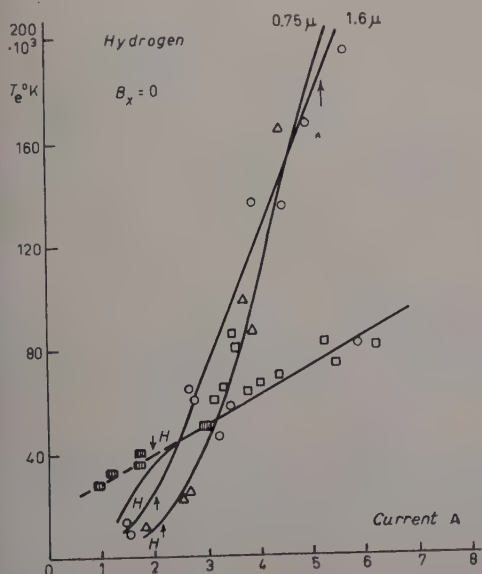


Fig. 3. — Examples of electron temperature measurements using microwave noise emitted by the discharge. Most results were obtained using 8.5 mm wavelength. The results are not reliable if the reflection coefficient is high or the absorption coefficient small. Arrows indicate the limit of reliable measurement. 3 cm observations are shown at the low current end of the 4 μm curve.

Using a suitable microwave horn aerial immersed in the plasma it was verified that incident radiation was absorbed by the plasma and that there were no reflections from the plasma boundary; this was done at wavelengths of 3 cm and 8 mm. The noise power was measured at these wavelengths. The results are shown in Fig. 3.

Double probe method [2]. — The above measurements were checked using a double probe. The electron temperatures were calculated from the voltage-current characteristics and agreed approximately with the microwave measurements.

Resistivity. — If the discharge diameter is known the electron temperature can be calculated from the resistivity formula (3).

5. — Results.

In Argon

$$T_1 + T_2 = 2 \cdot 10^5 \text{ }^\circ\text{K},$$

$$T_1 \approx T_3 \approx 10^5 \text{ }^\circ\text{K}.$$

These results agree approximately with those derived from the Bennett relation.

In Hydrogen there was disagreement, the measured electron temperature being too high, probably because of incomplete ionization leading to a reduced value of N . This is confirmed to some extent by spectroscopic observation on lines in the Balmer series, which are strong throughout the pulse.

Discharge diameters $d = 10 \text{ cm}$ (streak photograph),
 $d = 20 \text{ cm}$ (magnetic probes),
 $d = 25 \text{ cm}$ (electron density, microwave),
 $d = 7 \text{ cm}$ (resistivity equation $T_1 = 10^5 \text{ }^\circ\text{K}$).

Power input. — The power input to the discharge is about 3 eV/atom μs . The total energy absorbed is 45 eV/atom: 20 eV for the ion motion, 10 eV for electron motion and 16 eV for the ionization energy. This gives an energy containment time of 15 μs .

Experiment has shown that only 10% of the total power input reaches the walls as radiation.

For this reason particle collision with the walls must be the dominant loss mechanism. It is to be expected that when the discharge channel approaches the metal wall shock waves will be set up in the channel. The energy of the directed velocity can be converted into thermal motion.

As a consequence of the short containment time, attempts to reach higher temperatures by increasing the current will lead to severe bombardment of the walls and a consequent increase in the concentration of impurities from the walls. This effect limits discharge of this type to currents of less than 20 kiloampere.

6. - Authors.

The electron temperature measurements are the work of A. N. DELLIS, D. LEES and A. P. WILLMORE. The ion temperature measurements are the work of S. A. RAMSDEN and B. JONES. The current-voltage characteristics, the thermo-pile measurements and the magnetic probe measurements are the work of R. CARRUTHERS, T. K. ALLEN and A. N. DELLIS respectively. R. HIDE has carried out the calculations on the shock wave model of the collisions of the current channel with the wall.

II. - Electric and Magnetic Measurements on Laboratory Plasmas.

Laboratory gas discharges are complicated and require a wide range of measurement techniques. The present studies are aimed at determining the gross behaviour of the plasma and not the detailed properties.

A complicating factor is that Saha's equation is not valid, for at least three reasons.

1) The density and dimensions of the plasma are such that nearly all radiation escapes.

2) The life time of the particles is short being determined by wall recombination.

3) The relaxation time for energy exchange between particles is fairly long, thus a Maxwellian velocity distribution may not be established. If it is T_i need not equal T_e .

In hydrogen the relaxation time $t_r = 1/43t_i$ therefore it is usual to assume the electron energy distribution, at least, is Maxwellian.

Plasma confinement. — Confining a plasma of particle density 10^{16} cm^{-3} at about $10^6 \text{ }^\circ\text{K}$ requires a magnetic field (H) of the order of 2 000 gauss which can confine a pressure of

$$\frac{H^2}{8\pi} = 10^6 \text{ dyn/cm}^2.$$

Since the mass density is only about 10^{-10} gm/cm^3 any small pressure unbalance gives rise to large accelerations possibly resulting in shock waves and magnetohydrodynamic disturbances. These phenomena make measurements difficult.

Current flowing and electric fields. — The equivalent circuit diagram for Zeta is as shown in Fig. 4.

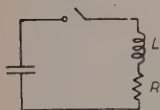


Fig. 4.

The discharge current is measured by a Rogowski coil wound externally round the torus (see Fig. 5).

By consideration of the resistance R and the inductance of the discharge path we have

$$\begin{aligned} V &= RI + \frac{d}{dt} (LI) \\ &= RI + I \frac{dL}{dt} + L \frac{dI}{dt}. \end{aligned}$$

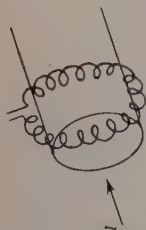


Fig. 5.

The contribution to the electric field from the $I(dL/dt)$ term arises from changes in the configuration of the discharge and may be identified with the mass motion of the plasma. In general the inductance fluctuations are rapid and thus can be distinguished from resistance and current changes. The

voltage and current traces are shown in Fig. 6.

The current curve is smoothed due to the external inductance, which tends to keep the current constant, however marked fluctuations are evident in the voltage curve and a period $100 \mu\text{s}$ can be recognized and the waveform resembles relaxation oscillations.

Electric fields. — The volts per turn are measured by determining the voltage across a circumferential pick-up loop which links the transformer core.

In principle it is possible to measure the electric

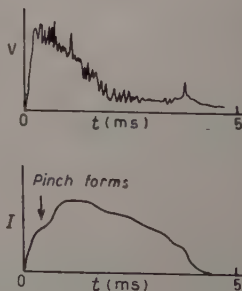


Fig. 6.

field within the plasma by introducing a loop as shown in Fig. 7, and making use of the equation

$$\text{curl } \mathbf{E} = -\frac{d\mathbf{B}}{dt}.$$

Such a measurement is important since the electric field inside a conductor may differ greatly from that exterior to it.

Voltage fluctuations. — Consideration of the excitation of the spark spectrum, particularly the appearance of O V and N IV throughout the pulse suggested that the electron temperature was of the order of 10^6 °K and this temperature was based on an equilibrium process of ionization and volume recombination. At higher temperatures the oxygen ions would be more highly ionized. This was pointed out by Prof. BIERMANN. Other observations supported this conclusion. On the other hand the spectroscopic measure of the kinetic ion temperature of O V and N IV were of the order of $5 \cdot 10^6$ °K. This would be most unlikely unless some mechanism of direct energy transfer to the heavy positive ion was possible. The rapid changes of the plasma configurations suggested by the appearance of the fluctuation of the voltage waveform could give rise to both shock waves and hydromagnetic disturbances. Calculations by R. S. PEASE at Harwell, of the power supplied to the plasma ions through such fluctuations indicated that such a mechanism could account for the observed temperature difference.

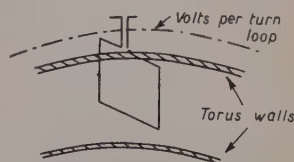


Fig. 7.

Internal magnetic fields. — These can be measured by internal magnetic probes.

The magnetic probe consisted of a quartz tube containing 16 coils each 4 mm diameter with a response time of 5 μ s. The coils have electrostatic screening. Because of the speed of magnetic disturbances in the plasma it would be most desirable to improve the response time to 0.1 μ s. They are calibrated by means of a standard pulsed solenoid. These measurements give information about magnetic fields, the stability of the discharge, the gas pressure, and current density.

To illustrate the information which can be obtained by magnetic probes consider the pinch discharge stabilized by an axial magnetic field. The low pressure gas ($10^{-4} \div 10^{-2}$ mmHg) may be pre-ionized by a R.F. discharge to a low degree of ionization (0.1 \div 1.0 %). When the pulse electric field is first applied the ionization builds up rapidly and a skin current forms. In this case collapse occurs when $B_\theta = B_z$. If the I_z and I_θ currents flow predominates in

a thin skin then:

$$nkT = \frac{H_0^2}{8\pi} - \frac{H_z^2}{8\pi}.$$

Thus from a measure of H_0 and H_z the plasma gas pressure can be derived as a function of the radius.

The total magnetic flux inside the metal tube must be conserved so when collapse occurs the axial magnetic field strength inside the current channel increases (about 10 times).

Simple pinch discharge. — Since the axial currents are maintained by an external source the magnetic energy tends to a maximum, and a constricted discharge increases its length by winding itself into a helix.

The stabilizing effect of an axial magnetic field. — Assume that the axial magnetic flux lies entirely within the cylindrical plasma column.

Since the plasma is a good conductor and decrease of the plasma channel diameter is accompanied by increase in the axial field component (B_z) a restoring force arises which resists the compression. Similarly if a kink develops in a plasma the B_z lines of force are stretched and this leads to a force which tends to restore the plasma to a cylinder.

The axial magnetic field suppresses short wavelength instability efficiently but not the very long wavelengths (*e.g.* the bodily movement of a rigid toroidal plasma column). Eddy currents induced in the surrounding metal walls provide a restoring force for these long wavelengths.

The paramagnetic effect. — In 1956 BICKERTON observed that in a high current toroidal discharge to which an axial magnetic field is applied, the axial magnetic field increases in the interior even though no collapse of the plasma has taken place. It was suggested that this phenomena is due to the different electrical conductivities parallel to and at right angles to the magnetic fields (see SPITZER [3]). This results in a helical current.

This phenomenon has been termed the paramagnetic effect in an ionized gas. It was simultaneously discovered in the USSR and reported at Stockholm in 1958. The total increase due to this and the collapse can be between 10 and 100 times the initial field. An initial seeding field is essential.

Magnetic probe results. — The measured magnetic fields do not show large erratic fluctuations in Zeta, this indicates a quasi stable discharge. There are small fluctuations with a period similar to that observed on the volta-ge trace. B_z is observed to increase with time at the centre of the discharge and to decrease outside the plasma. Fig. 8. shows the variations of B_0 and

B_z with radius. The point where B_θ is zero is the magnetic centre on the discharge. B_z reverses by a small amount outside the plasma column. This can be explained as follows: because of the metal walls no more flux can enter the tube after the discharge collapses and B_z outside the pinch should go to zero. The paramagnetic effect cannot produce any increase in field outside the channel, however instabilities which lead to a helical current channel generate magnetic flux within the helix and cause a reversal of the axial field outside the helix. Thus the appearance of a reversal indicates the existence of helical instabilities.

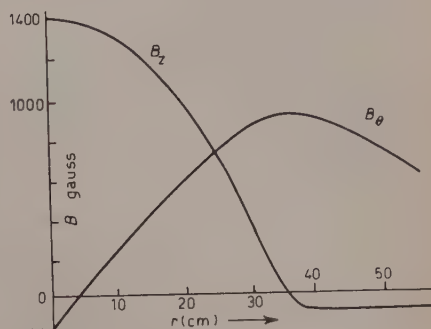


Fig. 8.

Difficulties with probe measurements. — The insertion of a probe into the plasma causes a change in the discharge properties. The resistance is found to increase and the neutron yield falls to a low value, and the intensity of the silicon and oxygen lines increases. The introduction of a second probe near the first does not, however, change the measured magnetic field configuration.

Langmuir probes. — These are used in an attempt to measure electron temperatures and densities.

In its conventional application the potential of the probe relative to the plasma is varied over a range comparable with kT/e , so that incident electrons are retarded. The electron current to the probe is then given by

$$I_e = I \exp [-eV/kT_e],$$

where V is the potential difference between the probe and the plasma. Thus by plotting $\log I$ against V and finding the slope of the curve it is possible to determine T_e .

If the probe is sufficiently negative to reflect all the electrons and collect only positive ions then the ion current (I_2) is given by

$$I_2 = en(kT_i/m_i)^{1/2}.$$

If the probe is small compared to the electron Larmor radius the magnetic field should not have any effect on the characteristic slope.

When the electron temperature is greater than about 200 000 °K it is necessary to vary the probe potential over several hundred volts. The strong positive ion currents tend to cause arcing and the destruction of the probe.

In Zeta the saturation electron current (I_0) rises to 20 000 A/cm² so that the probe should be as small and as well cooled as possible. Even so electric currents of 100 A are measured to probes of area of a few mm².

Largely because of these difficulties no satisfactory results have yet been obtained by this method.

III. - Radiation Measurements on Laboratory Plasmas.

In the second chapter some of the electrical measurements which can be made on a plasma in the frequency range ($0 \div 10^6$) Hz were discussed. The frequency range between 10^7 and the plasma frequency ω_p which is given approximately by $\omega_p = 10^4 n^{\frac{1}{2}}$, where $n =$ electron density, has not yet been explored at Harwell. Therefore we are concerned with measurements in the microwaves and infrared frequencies.



Fig. 9.

As mentioned previously, one expects strong interaction between electromagnetic waves and a plasma at the plasma frequency even when collisions are rare.

The dielectric constant $\epsilon = 1 - (\omega_p^2/\omega^2)$ becomes 0 when $\omega = \omega_p$. Transmission occurs when $\omega < \omega_p$, i.e. $f > 10^4 n^{\frac{1}{2}}$ and no transmission occurs for $f < 10^4 n^{\frac{1}{2}}$, where f is the applied frequency and $\omega = 2\pi f$ transmission measurements can be made as shown simply in Fig. 9.

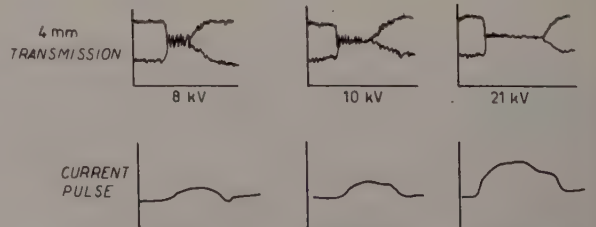


Fig. 10. - Microwave transmission measurements.

It is usual to vary the electron density since variation of the microwave frequency is difficult.

Fig. 10 shows the type of results obtained.

As the current increases the microwave transmission is seen to decrease.

1. - Microwave noise measurements.

The second important measurement is the microwave noise power radiated by the plasma since this gives information regarding the electron temperature. The plasma must appear to behave as a black body, *i.e.*, no reflection no transmission and complete absorption. The condition of no reflection can be achieved by suitably matching the wave guide to the plasma. The measurement of noise power (w) gives the electron temperature (T_1) from the formula $W = kT_1 \Delta f$, where Δf is the bandwidth of the receiver (Hz).

If a standard noise tube is used for comparison Δf need not be known. The receiving antenna (usually a horn) is located in the plasma, and directed along the discharge axis.

Fig. 11. shows the variation of noise power with frequency.

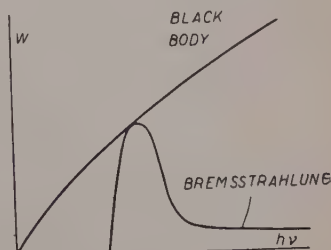


Fig. 11.

2. - Infrared measurements.

For plasma frequencies corresponding to $n > 10^{14}$ microwave equipment is not available and an infrared grating spectrometer can be used. With this technique it should be possible to examine the 1 mm wave length region and to determine the shape of the $W - h\nu$ curve (Fig. 11). The difficulty in this technique lies not in wavelength resolution but in finding a detector with sufficient sensitivity, and time resolution ($< 10^{-2}$ s). Work is now in progress improving the Golay cell detector. No measurements have yet been made.

3. - Visible and ultraviolet region.

Streak photography using rotating mirror, rotating drum or image converter cameras, is valuable to examine plasma displacements. In these methods an image of a slit, illuminated by a cross-section of the discharge, is swept perpendicularly to its length, with time. In Helium discharges a well defined pinched current channel is seen, this expands and hits the walls as the current falls at the end of the discharge. In hydrogen no such channel can be distinguished. This is usually explained by assuming that in the hot regions of the gas the hydrogen is fully ionized and hence emits no light.

If all the light is due to the spark spectra of highly ionized ions one would

expect that the motion of the region of luminosity would correspond to the motion of the positive ions and thus to the current channel. It is difficult to interpret the results because the light need not come from highly ionized ions. More information can be obtained from streak photographs on colour film since the colours help to decide whether or not the light is spark light. It would be very helpful to take streak photographs through narrow band interference filters but as yet the light intensity is too low to permit this.

4. - Line spectroscopy in the visible and ultra violet.

Emission spectra are mainly due to impurity atoms and are of two types. If the electron density $n > 10^{16}$ both continuum and line spectra are emitted but for $n < 10^{15}$ line spectra only are emitted.

In most laboratory discharges the number (N) of electrons/cm is made as small as possible in order to obtain high temperatures, $N=10^{17}$ is the figure commonly obtained, below this figure it is difficult to obtain a discharge. Thus small diameter discharges tend to have large electron densities and emit line spectra and bremsstrahlung continuum, while large diameter discharges have small electron densities and emit predominantly a line spectrum.

5. - Line spectra from Zeta.

The line spectrum from Zeta has been examined with a Hilger medium quartz spectrograph having a dispersion of 20 Å/mm; at low current (50 kA) the spectrum consists mainly of lines from singly ionized atoms, as the current increases, lines from more highly ionized atoms appear, as the current increases still further the lines decrease in intensity.

With a current of 145 kA, in a clean discharge in Zeta with no added impurities very few lines remain. Thus for example the (C III) lines increase to a maximum intensity with increasing current and then grow fainter, the (OV) lines on the other hand appear at 100 kA and increase in intensity and width up to the highest currents.

6. - Ion temperature measurements.

The broadening of the spectral lines in Zeta is due only to the Doppler effect, the other two possible mechanisms of line broadening, the Stark and the Zeeman effects are small enough to be ignored, the first because of the low-densities and the second because of the magnetic fields are small. Ion

temperature measurements in Zeta are concentrated on the (OV) triplet (2781) Å. By measuring the width of this line the mean kinetic energy of the impurity ions can be found, an equilibrium between the (OV) ions and the other plasma ions should be set up in about 80 μ s. So the measurement will give the mean kinetic energy of the plasma ions. There is the possibility that the broadening is due to mass motion of the discharge. In Zeta it has been necessary to rely on magnetic probe and streak photograph techniques to try to exclude this possibility. Information on the mass motion can also be obtained by taking spectrograms, looking first radially and then axially into the discharge. In principle it is possible to distinguish between mass and thermal motion by examining the spectra from ions of different mass, it is difficult however, to excite such spectra simultaneously. It should be easier to do this in the vacuum ultraviolet region of the spectrum.

An attempt has been made to determine the variation of temperature with time. A mechanical shutter was used and arranged to open at various times during the discharge pulse. The results are shown in Fig. 12 but are not sufficiently well resolved to indicate anything other than a mean temperature of about $5 \cdot 10^6$ °K.

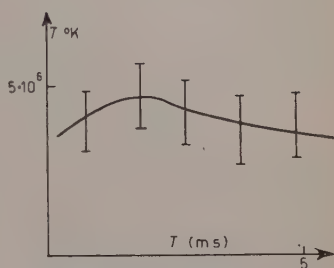


Fig. 12.

The variation of line intensities with time has been determined by using photomultipliers in conjunction with a monochromator, some typical results are shown in Fig. 13.

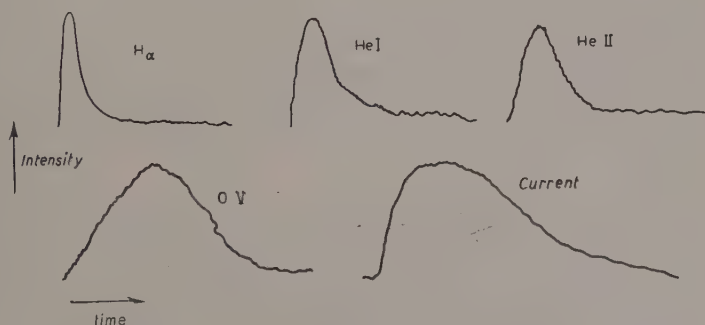


Fig. 13.

The following points are of interest

1) The H_{α} line appears as a well defined spike which disappears at the beginning of the pulse.

2) The He lines behave similarly. The He II peak occurs somewhat later in time than the He I peak.

3) The (OV) line is a suitable choice for ion temperature measurements both because it lies in a convenient spectral range and because it reaches its peak intensity at peak current.

7. - Impurity content.

The actual intensities of the lines are very sensitive to the impurity content of the discharge which is very difficult to control. Such factors as reactions in the gas, reactions with the wall, adsorption on the walls and emission of impurities by the walls all tend to make the impurity content uncertain. The impurity content of the discharge can be obtained from the relative intensities of lines which have known transition probabilities. In a case where the known added impurity was 5% Nitrogen the following results were obtained:

C 5%, N 5%, O 1%, F 10%, Al 8%, Si 2%, *i.e.* total 31%.

These estimates are rather crude and may have a large error.

8. - Electron temperature.

Information concerning electron temperature can be derived from a study of the population of levels of an atom or ion which are excited by electron collision from the ground state. If the level which is excited by electron impact, cannot decay by the emission of radiation to ground state the cross-section for excitation by electron impact is sharply peaked near the threshold. Excitation by electron impact to levels which can return to the ground state in a permitted transition has a different excitation cross-section which

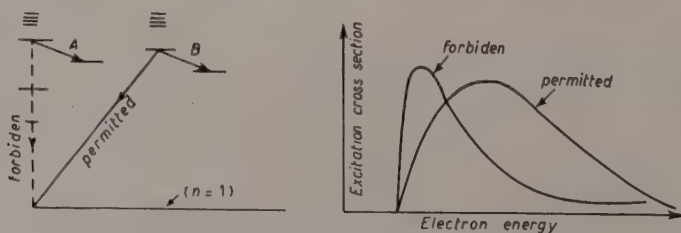


Fig. 14.

varies smooth with electron energy. Thus if both levels are depopulated by permitted transitions to neighbouring levels, the intensity of these lines is a measure of population in the two upper states. The population of the upper levels will therefore be a function of the electron temperature as will be the

ratio of the intensity of the lines arising from transition to neighbouring levels. The convenient lines in He I are 3589 Å and 5016 Å. An example of this type is shown in Fig. 14.

In the plasma produced in Zeta all the helium lines have a low intensity except near the start of the pulse. However a measurement of the relative intensities 400 μ s after the initiation give an electron temperature of $4 \cdot 10^5$ °K. This method can of course be extended to other helium like atoms such as CV whose emission spectrum is well sustained.

9. - Vacuum ultra violet region ((2000 \div 400) Å).

A normal incidence grating vacuum spectrograph was used. The spectrometer was mounted on to the torus through bellows and evacuated to prevent atmospheric absorption. Care was taken to prevent vibration of the spectrograph and a subsidiary experiment checked that no broadening of the lines was produced in this way.

1000 lines have so far been observed but only 400 have been identified.

Calibration of the plates is difficult and because of this no temperatures have yet been derived. The most interesting region will probably be 500 Å to 20 Å where a grazing incidence spectrograph is necessary. No such equipment is yet in operation at Harwell.

10. - X-ray crystal spectrometer ((20 \div 2) Å).

A bent crystal (*e.g.* fluorite) is used to reflect the X-rays through the Bragg angle and focus them on to the photographic plate. Measurements with such an instrument can provide interesting information, particularly using the hydrogen like resonance lines of O VIII and C VI. In addition the bremsstrahlung radiation in this region should give information about the electron temperature.

An attempt has already been made to measure the bremsstrahlung radiation with a xenon filled X-ray proportional counter having a berillium window .008 cm thick. This method has not been successful due to a large flux of high energy X-ray ((20 \div 100) kV) of non-thermal origin.

11. - Total radiation intensity.

This is important. If the plasma is well confined then energy escapes only through radiation and not through particle bombardment of the walls. Measurements of the total radiation are made using a thermopile; 50 mV/W cm² time constant 1.5 s; overall sensitivity 10^{-4} J/cm² for 1 mm deflection.

Particles may make a contribution to the energy measured. However, upper and lower limits to the radiation may be obtained by using thin shielding films (10^{-5} cm) in front of the thermopile which can be removed.

In high current discharges it is always difficult to determine how the energy communicated to the plasma reaches the walls.

Some preliminary figures relevant to Zeta are:

Integrated product $V_{gas} \times I_{gas}$	20 $\cdot 10^4$ joule/pulse
Ohmic losses in gas $I^2 R$	14 $\cdot 10^4$ » »
Total radiant energy (film in)	1.6 $\cdot 10^4$ » »
» » » (» out)	2.7 $\cdot 10^4$ » »

A number of possible modes of energy loss have been left out. For example eddy currents induced in various metal components (*e.g.* tube walls etc.) are estimated to contribute at least an energy loss of $2 \cdot 10^4$ J. If fluctuating magnetic fields of higher frequency are considered this figure may be considerably exceeded.

12. - High energy radiation.

In a high current Deuterium plasma neutrons, protons, X and γ -rays may be produced. These X-rays are due to run-away electrons. A report on this mechanism was given by Dr. A. GIBSON at the Venice Conference 1957. In Zeta the average energy of the X-rays is about 50 keV with occasional bursts 100 keV. About 10^9 X-ray quanta are emitted per pulse.

By inserting a tungsten wire across the discharge plasma and recording the emitted X-rays using a pinhole camera it was shown that the run-away electrons are mainly confined to the central region of the discharge. Using metal targets estimates of the run-away electron current can be obtained (*e.g.* 40 mA per cm^2 in small toruses). The X-rays are monitored with NaI scintillation counters. The neutrons were measured by conventional methods.

1) Using B^{10}F_3 proportional counters mounted in paraffin. The counter was surrounded with two layers of 2 cm thick aluminium to screen out the electric and magnetic fields.

2) An indium anode Geiger counter was used initially to show, beyond doubt, that neutrons were being produced.

3) A plastic scintillator was used to detect the recoil protons produced in it by the neutrons.

It was emphasized that this was an incomplete survey of the field of measurements in high temperature plasmas.

REFERENCES

- [1] W. BENNET: *Phys. Rev.*, **45**, 890 (1934).
- [2] H. MALTER and H. JOHNSON: *Phys. Rev.*, **80**, 58 (1950).
- [3] L. SPITZER: *Physics of Fully Ionised Gases* (New York, 1956) p. 84.

INTERVENTI E DISCUSSIONI

— L. GOLDSTEIN:

Was it possible to identify a lag between the electron temperature and the ion temperature?

— P. C. THONEMANN:

It was not possible because properly time resolved electron temperature measurements could not be made due to fluctuations in the amplitude of the observed signal.

— R. GALLET:

Was it possible to measure electron densities?

— P. C. THONEMANN:

It was possible at the lower density to put limits on the electron density using 8 mm waves. At higher densities (10^{14} electron/cm³) it is necessary to use 4 mm waves.

— L. GOLDSTEIN:

You stated that Saha's equation is not valid because radiation escapes from the gas, but is it not true that the metal walls reflect the radiation?

— P. C. THONEMANN:

The important radiation has a wavelength of the order of 100 Å and only about (4÷10)% could be reflected.

— L. GOLDSTEIN:

Are the Langmuir probe measurements seriously influenced by the secondary electron emission caused by electron and positive ion bombardment?

— P. C. THONEMANN:

Electron emission due to positive ion bombardment is not appreciable but both photoemission and secondary electron emission are important and difficult to estimate.

— D. REAGAN:

Do you have a hollow discharge column in Zeta?

— P. C. THONEMANN:

No, I only used the example of a hollow discharge because it is easy to explain. In Zeta we have a mixed field configuration.

— E. WEIBEL:

Does the axial magnetic field stabilize the discharge?

— P. C. THONEMANN:

Yes, the magnetic probe results show that there are no gross instabilities and this is conformed by streak photographs.

— E. WEIBEL:

Are the magnetic probe results repeatable?

— P. C. THONEMANN:

Yes, the main features do not vary from shot to shot.

— E. WEIBEL:

What is the ratio of B_θ to B_z in Zeta?

— P. C. THONEMANN

I think you are asking if the difference in magnetic pressure will permit any gas pressure. It will, and in fact « nkT » is of the order of

$$\frac{1}{4} \frac{B_z^2}{8\pi}$$

— V. FERRARO:

What is the ratio of the tube to that of the discharge?

— P. C. THONEMANN:

3:1.

— V. FERRARO:

Is the compression of the lines of force uniform?

— P. C. THONEMANN:

Yes.

— A. GILARDINI:

Has a different output been found between a different polarization of the micro-waves used?

— P. C. THONEMANN:

This experiment has not been attempted yet. Great difficulty is experienced in arranging the equipment to get a sensible result at all; this is mainly due to interference.

If you are thinking of the magnetic fields, one must remember that the magnetic field changes with radius from a purely axial to a purely azimuthal one and thus one would not expect any marked polarization.

— A. GILARDINI:

By analogy with cavities when n_e is increasing one finds that the plasma reflects strongly first when the electric field is normal to the axis i.e., when it is in a direction of the density gradient; and secondly when it is parallel to the axis (along which there is no density gradient).

— P. C. THONEMANN:

This experiment should certainly be tried.

— P. AVIVI:

Regarding the disappearance of the spectral lines at high current no lines do appear, or do the lines actually disappear? If so might there not be some energy process involved, and not necessarily an increase in the degree of ionization?

— P. C. THONEMANN:

This is not easy to answer simply. The intensity of the lines observed at low current decreases; then new lines appear. They can be seen on spectrographs, but are only weak. I am sorry that I can only give you qualitative information. Plates taken at the highest currents and in a clean discharge have relatively few lines compared with lower currents.

— R. GALLET:

Can you summarize the present view about the origin of the neutrons?

— P. C. THONEMANN:

The most reasonable interpretation is that they come from a beam of deuterons which are circling round the torus with an energy of about 17 kV. These results have been recently published by B. ROSE *et al.* in *Nature*. The energy was measured by means of a high pressure diffusion cloud chamber, which was collimated to look along the axis. A shift of neutron energy was observed when the discharge current was reversed, this is assumed to correspond to a reversal of the deuteron beam.

The results are explained by assuming that 10^{-6} of the deuterons have this high energy. It is thought that the neutrons are not produced by instabilities because they appear uniformly over the torus and because the magnetic probes show that there are no gross instabilities. ROSE *et al.* have suggested that in the early stages of the discharge, when the electric field is high, deuterons may «run away» in the same way as electrons, and that the beam so established may continue to circulate in the plasma. The particles of this beam will occasionally collide with slow deuterons giving rise to the observed neutron emission.

— T. GOLD:

What is the long wavelength limit to the measurement of total radiation?

— P. C. THONEMANN:

The wavelength must be smaller than the slit width, say about 0.1 mm.

— T. GOLD:

Would you expect a very large amount of radiation beyond this limit?

— P. C. THONEMANN:

We plan to use an infrared spectrograph to determine this.

— T. GOLD:

There must be a large amount of energy still undetected.

— P. C. THONEMANN:

True. It is still a serious problem to determine how the energy comes out. The only hope is to scan the whole electromagnetic spectrum. It is possible of course that most is lost in particle bombardment of the walls.

— D. REAGAN:

How well do you know that 17 kV number? Is there a large error or is it sharply defined?

— P. C. THONEMANN:

This is sharply defined. At a guess the error is ± 5 kV. We have plans under way to measure this more accurately with He III proportional counters.

— A. GIBSON:

I would like to point out that there are objections to the mechanism of neutron emission proposed by ROSE *et al.* In particular it is difficult to see how a 17 keV deuteron beam can be contained, one would expect magnetic containment to depend on the square root of the mass of the particles; thus if 17 keV deuterons can be contained it should be possible to contain 1 MeV electrons. However the X-ray emission from Zeta shows that this is not possible (the X-ray energies are less than 100 keV).

— P. C. THONEMANN:

This has puzzled me. It is difficult to see how the ions can run away in the plasma.

— A. GIBSON:

It is possible for the deuterons to obtain an energy which corresponds to the electron drift velocity. It is possible, but not proved, that there are parts of the discharge where this energy can reach 17 keV.

— R. GALLET:

It is possible that ions could be accelerated in front of the crests of longitudinal plasma oscillations, the ions could thus get high energies.

— P. C. THONEMANN:

There are many of these mechanisms.

— A. GIBSON:

Dr. JUKES at HARWELL has investigated a somewhat similar mechanism using instability waves and it seems to give promising results.

— D. REAGAN:

Have you examined the energies of radially emitted neutrons?

— P. C. THONEMANN:

No, that has not been possible as yet.

— L. BIERMANN:

I do not see any difficulty in containing the deuterons, the Larmor radius is only a fraction of the tube radius.

A discussion followed between BIERMANN, GIBSON, LÜST and REAGAN in which it was emphasized that it is the azimuthal (B_θ) field which is important in producing confinement. The limit placed on deuteron energies by the X-ray observations was again mentioned (see a previous remark by GIBSON).

Microwaves in a Ionized Gas.

A. GILARDINI

Società Industrie Elettroniche - Roma

1. - Introduction.

In all plasma physics, either at high degrees of ionization and at high temperatures, or at low degrees of ionization and at low temperatures, the interpretation and prediction of experimental results require a knowledge of the interaction parameters between electrons, ions and neutral molecules. Measurements in conventional gas discharges make possible a determination of many of them, provided the experimental conditions are properly chosen.

However, only recently the use of microwave methods and of high-purity gases, obtained by new techniques, have led to significant and clean experiments, from which the important interaction parameters could be determined. The success of microwaves techniques in the old field of gas discharges is due essentially to the following reasons.

1) The plasmas, which are produced and maintained by microwave fields, possess the remarkable property, over a very wide range of pressures and container dimensions, of being independent of the electrodes and of the container materials. All ionization phenomena are within the gas and, in all cases where collisions, excitation and ionization data are known from independent beam scattering experiments, theory and experiment can be compared without the necessity of introducing adjustable parameters.

2) In a microwave discharge the purity of the gas is much better maintained, than in d.c. or in low-frequency discharges, because there are no hot electrodes and no liberation of occluded gases at the container walls by bombardment of heavy energetic ions.

3) The measurements of the high-frequency complex conductivity of a plasma permit the accurate evaluation of the electron densities and collision

frequencies. Many interaction parameters can then be inferred from the variation of density with time in a decaying plasma.

4) The electromagnetic noise generated in the microwave region is a measure of the electron temperature.

The best experimental conditions will then be achieved, when for purity reasons the plasma is produced and maintained by microwave fields, and when for accuracy purposes the plasma properties are measured by microwave methods. The use of microwaves for both purposes simplifies also the experimental set-up in most cases. In these lectures I will discuss mostly the experiments which have been performed along these lines at M.I.T. by Prof. W. P. ALLIS, by Prof. S. C. BROWN and by their co-workers. Mention will be also made of the work done along the same lines by the Westinghouse Group and of the work done on points 3) and 4) in d.c. maintained discharges by Prof. L. GOLDSTEIN and his co-workers.

Most of the discussion will be concerned with the production and with the measurements of plasmas of low temperatures and of low degrees of ionization for the following reasons:

- 1) most of the data refer to these classical conditions,
- 2) some of the measured parameters, as for instance the collision frequencies of electrons and ions with neutral gas molecules, are of basic interest also in highly ionized plasmas.

Moreover, the discussion of these plasmas will be most useful insofar as to:

- 1) show the basic phenomena which control the behaviour of microwave generated plasmas,
- 2) indicate the limits within which the electrodes and the container walls do not control the discharge,
- 3) indicate along what directions we may expect to be able to obtain highly ionized plasmas with microwaves.

During the last two years considerable work has been done by the M.I.T. Group with regard to the production of highly ionized microwave plasmas. The aim is not to reach the conditions required by a thermonuclear fusion experiment, but to investigate the fundamental properties of these plasmas. For this reason, most of the efforts have been directed towards the production of a low temperature plasma with a high percent of ionization by working at very low pressures, so that only moderate ion densities are necessary. Considering that this course is mostly devoted to the physics of fully ionized gases

and that I shall make often mention of these new research aims, it seems worth to spend a few more words on this problem now.

We shall specify first the pressure and density ranges of interest for the microwave production and diagnostic of highly ionized plasmas. The electron density n (m^{-3}) which corresponds to the ionization fraction α at the pressure p (mmHg) is:

$$(1.1) \quad n = 3.5 \cdot 10^{22} \alpha p.$$

The maximum density, which can be achieved without too much effort or special set-ups by means of a microwave field, is of the order of the density at which the plasma resonance frequency ($\omega_p/2\pi$) coincides with the field frequency ($\omega/2\pi = f$). At higher densities the dielectric constant, which, neglecting collisions and in usual notations, is

$$(1.2) \quad \epsilon = \epsilon_0 \left(1 - \frac{ne^2}{m\epsilon_0\omega^2} \right) = \epsilon_0 \left[1 - \left(\frac{\omega_p}{\omega} \right)^2 \right],$$

becomes negative and the applied field does not penetrate efficiently inside the plasma. We shall then try to work at pressures such that

$$(1.3) \quad \begin{cases} 3.5 \cdot 10^{22} \alpha p < \frac{m\epsilon_0\omega^2}{e^2} = 1.2 \cdot 10^{-2} f^2, \\ \alpha p < 3.5 \cdot 10^{-25} f^2. \end{cases}$$

To remain in a reasonable pressure range, we must move f well into the microwave region. We then select frequencies between 10^9 and 10^{10} Hz (centimeter wavelength region) and pressures between 10^{-5} and 10^{-3} mmHg; the corresponding densities per cm^3 are in the ($10^{10} \div 10^{12}$) range.

At these pressures the electron mean free path is much larger than the usual plasma dimensions, so that ionization in the gas becomes unlikely and ionization at the walls by secondary effects becomes predominant. In this case we may lose the purity of the gas, typical of the ordinary microwave discharges. Moreover, a very high electric field is required for the gas breakdown.

By using a magnetic field to reduce the ionized particle losses, we can again produce a true gas discharge, namely a plasma controlled only by the ionization in the gas. Moreover, if the frequency of the field for breakdown is chosen very close to the cyclotron frequency, we can produce breakdown with a very low power.

Experiments in the discussed ranges will permit the determination of many interaction parameters, to be used in the design and interpretation of thermonuclear fusion experiments and for the discussion of astrophysical data. I

shall remark that, compared to the determinations made in a thermonuclear experiment, microwave determinations are characterized by being made:

- 1) in a high purity gas,
- 2) in steady state conditions,
- 3) in stable discharges,
- 4) under controlled conditions.

As already said, however, I shall discuss in these lectures mostly ionized plasmas, with low degrees of ionization and with electron temperatures of a few thousand degrees only. I shall give first a general, basic formula for the plasma microwave conductivity, and successively the theoretical expressions for the other basic plasma parameters, which determine the behaviour of a ionized gas (energy gain, distribution function, ionization and excitation frequencies, average energies, etc.). The microwave breakdown condition, both in absence and in presence of a static magnetic field, will then be obtained and compared with the experimental results. A short review of the basic characteristics of the microwave sustained discharges will be also presented. Finally, I shall discuss the problem of measuring electron densities and collision frequencies in resonant cavities.

2. - The plasma microwave conductivity.

We shall derive first a basic general formula for the plasma microwave conductivity as a function of the plasma parameters. This derivation has only the purpose of making the final formulas acceptable; a rigorous demonstration based on the Boltzmann equation, but neglecting long range electron-ion collisions, is given in ALLIS' paper in the *Handbuch der Physik*.

The conductivity of a plasma at high-frequencies has been discussed here also by Prof. FERRARO and Dr. GAILLET, but I need a more general formula, namely a formula valid:

a) when the distribution function is predominantly spherically symmetrical in velocity space, but not necessarily Maxwellian or near to a Maxwellian one,

b) when the electron collision frequency is an arbitrary function of the electron velocity.

We assume here an infinite uniform plasma, whose components are electrons (density n), neutral gas atoms or molecules (density n_0) and singly ionized

atoms or molecules (density n_+). A uniform alternated electric field $\mathbf{E} \exp[j\omega t]$ and a uniform static magnetic field \mathbf{B} are applied to the plasma. We call $f(\mathbf{v}, t)$ the electron distribution function, which is independent of the position in the plasma. In all the cases we shall discuss, the average motion of a single electron can be regarded as the sum of a large random motion and of an oscillatory motion of much smaller amplitude due to the applied field. If we regard the collision effects for this ordered motion as a continuous loss of momentum, this motion becomes a steady state sinusoidal motion, equal for all the electrons having the same speed v ; we indicate its velocity as $\mathbf{v}_s(v) \exp[j\omega t]$. By subtracting this oscillatory velocity from the individual electron velocity \mathbf{v} , we then obtain an ensemble of particle velocities, which represent the random motion, and therefore has a distribution independent of the velocity direction and of time (f_0).

We then have

$$(2.1) \quad \left\{ \begin{aligned} f(\mathbf{v}, t) &= f_0(|\mathbf{v} - \mathbf{v}_s \exp[j\omega t]|), \\ &\cong f_0\left[v - \frac{\mathbf{v} \cdot \mathbf{v}_s}{v} \exp[j\omega t]\right], \\ &\cong f_0(v) - \frac{\mathbf{v} \cdot \mathbf{v}_s}{v} \frac{df_0}{dv} \exp[j\omega t]. \end{aligned} \right.$$

The electric current is due to the electrons and given by

$$(2.2) \quad -e \int \mathbf{v} f(\mathbf{v}, t) d\mathbf{v},$$

where the integration is performed over the entire velocity space. The fundamental alternated component of this current is then

$$(2.3) \quad \mathbf{J} = e \int \mathbf{v} \frac{\mathbf{v} \cdot \mathbf{v}_s}{v} \frac{df_0}{dv} d\mathbf{v}.$$

By using a formula already known from Prof. FERRARO's lectures (eq. (120))

$$(2.4) \quad \int F(v)(\mathbf{A} \cdot \mathbf{v}) \mathbf{v} d\mathbf{v} = \frac{1}{3} \mathbf{A} \int F(v) v^2 d\mathbf{v},$$

we obtain

$$(2.5) \quad \mathbf{J} = \frac{4\pi e}{3} \int_0^\infty \mathbf{v}_s \frac{df_0}{dv} v^3 dv = -en \langle \mathbf{v}_s \rangle,$$

where the brackets indicate the following type of average

$$(2.6) \quad \langle \varphi \rangle = -\frac{4\pi}{3n} \int_0^\infty \varphi(v) \frac{df_0}{dv} v^3 dv.$$

This type of average is in general different from the usual average

$$(2.7) \quad \bar{\varphi} = \frac{4\pi}{n} \int_0^\infty \varphi(v) f_0 v^2 dv,$$

which we shall also use in the future.

To compute \mathbf{J} we must know \mathbf{v}_a . For this we write Newton's law of motion for the average electron of velocity v in the form of Langevin's equation

$$(2.8) \quad m d(\mathbf{v}_a \exp[j\omega t]) = -e(\mathbf{E} + \mathbf{v}_a \times \mathbf{B}) \exp[j\omega t] dt - m\nu_c \mathbf{v}_a \exp[j\omega t] dt,$$

where $\nu_c(v) = \nu_m(v) + \nu_+(v)$ is the total collision frequency for momentum transfer. The quantity ν_m is the collision frequency for momentum transfer between electrons and neutral gas molecules

$$(2.9) \quad \nu_m(v) = n_g v \int q_a(v, \chi) (1 - \cos \chi) d^2\Omega,$$

where q_a is the scattering cross-section for these collisions, χ is the scattering angle, $d^2\Omega$ is the differential of the solid angle and the integration is performed over all scattering angles. Analogously $\nu_+(v)$ refers to collisions between electrons and ions, and is given by a corresponding formula. Neutral molecules and ions are assumed to have very large masses and negligible velocities compared to electrons.

Eq. (2.8) can be written as follows:

$$(2.10) \quad (\nu_c + j\omega - \boldsymbol{\omega}_b \times) \mathbf{v}_a = -(e/m)\mathbf{E},$$

where we have introduced the cyclotron vector:

$$(2.11) \quad \boldsymbol{\omega}_b = (e/m)\mathbf{B}.$$

The solution of (2.10) is obtained by multiplying both sides by $(\nu_c + j\omega + \boldsymbol{\omega}_b \times)$; the result is

$$(2.12) \quad [(\nu_c + j\omega)^2 - \boldsymbol{\omega}_b \times (\boldsymbol{\omega}_b \times)] \mathbf{v}_a = -(e/m)(\nu_c + j\omega + \boldsymbol{\omega}_b \times) \mathbf{E},$$

whence

$$(2.13) \quad (v_c + j\omega)v_{g\parallel} = -(e/m)E_{\parallel},$$

$$(2.14) \quad [(v_c + j\omega)^2 + \omega_b^2]v_{g\perp} = -(e/m)(v_c + j\omega + \omega_b \times)E_{\perp},$$

respectively for the components parallel and normal to the magnetic field.

Substituting eq. (2.13) into eq. (2.5) we determine the complex conductivity of the plasma along the magnetic field:

$$(2.15) \quad \sigma_{\parallel} = J_{\parallel}/E_{\parallel} = \frac{e^2 n}{m} \left\langle \frac{1}{v_c + j\omega} \right\rangle.$$

The conductivity across the magnetic field is determined by substituting eq. (2.14) into eq. (2.5); simple formulas are obtained if we assume the electric field to be circularly polarized. Let \mathbf{i}_x and \mathbf{i}_y be two unity vectors normal to the magnetic field (Fig. 1); a circularly polarized \mathbf{E}_{\perp} field can then be written as

$$(2.16) \quad \mathbf{E}_{\perp} = (\mathbf{i}_x \mp j\mathbf{i}_y)E_{\perp},$$

where the minus and plus signs indicate respectively a right hand and a left hand polarization.

Simple mathematics yields

$$(2.17) \quad \begin{aligned} \omega_b \times \mathbf{E}_{\perp} &= (\mathbf{i}_y \pm j\mathbf{i}_x)\omega_b E_{\perp}, \\ &= \pm j(\mathbf{i}_x \mp j\mathbf{i}_y)\omega_b E_{\perp} = \pm j\omega_b \mathbf{E}_{\perp}. \end{aligned}$$

Eq. (2.14) becomes

$$(2.18) \quad \begin{aligned} [(v_c + j\omega)^2 - (j\omega_b)^2]v_{g\perp} &= -(e/m)(v_c + j\omega \pm j\omega_b)\mathbf{E}_{\perp}, \\ (v_c + j\omega \mp j\omega_b)v_{g\perp} &= -(e/m)\mathbf{E}_{\perp}. \end{aligned}$$

We shall then define two circular conductivities: a conductivity σ_c for the right hand polarization and a conductivity σ_o for the left hand polarization; their expressions are obtained substituting equation (2.18) in (2.5):

$$(2.19) \quad \sigma_c = \frac{e^2 n}{m} \left\langle \frac{1}{v_c + j(\omega - \omega_b)} \right\rangle,$$

$$(2.20) \quad \sigma_o = \frac{e^2 n}{m} \left\langle \frac{1}{v_c + j(\omega + \omega_b)} \right\rangle.$$

When the \mathbf{E}_\perp field is linearly polarized, we can regard it as the sum of two equal and opposite circularly polarized fields, and then define a transverse conductivity σ_\perp in the direction of \mathbf{E}_\perp

$$(2.21) \quad \sigma_\perp = J_x/E_x = \frac{1}{2}(\sigma_c + \sigma_o)$$

and a perpendicular conductivity

$$(2.22) \quad \sigma_\perp = J_y/E_x = \frac{j}{2}(\sigma_o - \sigma_c).$$

These results can be also described in a useful way by introducing a tensor conductivity, defined by

$$(2.23) \quad J_i = \sum_l \sigma_{il} E_l \quad i, l = x, y, z.$$

The matrix of the tensor is then, when the magnetic field is along the z -axis,

$$(2.24) \quad \sigma_{il} = \begin{vmatrix} \frac{1}{2}(\sigma_c + \sigma_o) & \frac{j}{2}(\sigma_o - \sigma_c) & 0 \\ -\frac{j}{2}(\sigma_o - \sigma_c) & \frac{1}{2}(\sigma_c + \sigma_o) & 0 \\ 0 & 0 & \sigma_\parallel \end{vmatrix}.$$

From the complex conductivity the complex dielectric tensor can be derived

$$(2.25) \quad \varepsilon_{il} = \varepsilon_0 \left(\delta_{il} + \frac{\sigma_{il}}{j\omega\varepsilon_0} \right).$$

where δ is the Kronecker's symbol.

A few remarks on the conductivity formulas, we have derived, must now be made.

1) We have assumed a uniform density and a uniform electric field. However, the above formulas give correctly the local conductivity also when the above quantities are changing with position, provided that density and field gradients are not exceedingly large.

2) In the absence of the magnetic field ($\omega_b = 0$) we have only a current in the \mathbf{E} direction, and the scalar conductivity σ is simply given by the parallel value σ_\parallel , which does not contain ω_b (Margenau's formula [1]). The dielectric constant ε is then

$$(2.26) \quad \varepsilon = \varepsilon_0 \left(1 - \frac{ne^2}{m\varepsilon_0\omega^2} \left\langle \frac{j\omega}{v_c + j\omega} \right\rangle \right) = \varepsilon_0 \left[1 - \left(\frac{\omega_p}{\omega} \right)^2 \left\langle \frac{1}{1 - j(v_c/\omega)} \right\rangle \right].$$

In a low pressure plasma and at microwave frequencies, we satisfy very often, over the main part of the f_0 distribution, the condition $v_c^2 \ll \omega^2$. Formula (2.15) becomes then

$$(2.27) \quad \sigma = \frac{e^2 n}{m \omega^2} [\langle v_c \rangle - j \omega],$$

a very well known formula.

3) When v_c is constant,

$$(2.28) \quad \langle \varphi(v_c) \rangle = \varphi(v_c),$$

and we cancel the brackets in all the conductivity formulas.

4) The derived conductivity formulas are rigorously valid only as far as electron-electron collisions can be neglected. This sets limits to the maximum degree of ionization, for which the formulas can be used. We must, however, remark that mutual electron collisions change the conductivities only as a second order effect.

5) Within the above limits the formulas are valid also in the d.c. case ($\omega = 0$). In particular, we obtain in the absence of a magnetic field ($\omega_b = 0$)

$$(2.29) \quad \sigma_{\text{d.c.}} = \frac{e^2 n}{m} \left\langle \frac{1}{v_c} \right\rangle.$$

This can be related to the diffusion coefficient, but not always by the simple Einstein relation. In fact, in the $\omega_b = 0$ case, the free diffusion coefficient for the electrons is:

$$(2.30) \quad D = \left(\frac{v^2}{3 v_c} \right).$$

When v_c is constant, we obtain

$$(2.31) \quad \sigma_{\text{d.c.}} = \frac{3e^2 n}{m v^2} D = \frac{e^2 n}{kT} D,$$

and the same relation can be shown to be always true when the distribution is Maxwellian. Eq. (2.31) is the well-known Einstein relation.

The real and imaginary parts of the circular conductivities are shown in Fig. 2, as a function of ω_b/v_c for a collision frequency independent of velocity.

The collision frequency v_c is in general a complicated function of velocity. Particularly v_m shows large variations with velocity due to the Ramsauer effect at low energies. The theoretical knowledge of the molecular fields is

not, in general, enough accurate for a precise determination of $\nu_m(v)$; we then usually prefer to determine it at very low energies by measuring microwave plasma conductivities under known experimental conditions [2, 3]. At energies

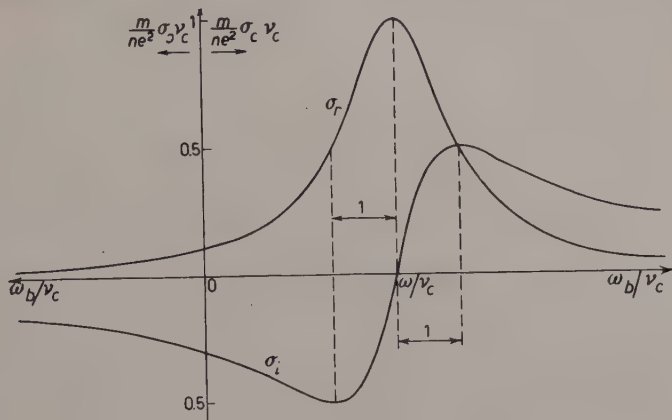


Fig. 2.

larger than about 1 eV, the collision frequency ν_m can be derived from beam scattering experiments.

The collision frequency ν_+ comes in when the ion density in the plasma is sufficiently large. Prof. FERRARO has shown how to compute it according to SPITZER, and I shall use his formula, written in the form

$$(2.32) \quad \nu_+(v) = A \frac{n_+}{v^3} \ln \left(1 + \frac{B\bar{u}^3}{n} \right),$$

where \bar{u} is the average electron energy in eV, $A = 4.04 \cdot 10^5 \text{ m}^6 \text{ s}^{-4}$, $B = 7.1 \cdot 10^{-25} (\text{Vm})^{-3}$.

The average $\langle \nu_+ \rangle$, which enters in eq. (2.27), can be easily computed, according to the definition (2.6); the result is

$$(2.33) \quad \langle \nu_+ \rangle = \frac{4\pi A}{3} f_0(0) \ln \left(1 + \frac{B\bar{u}^3}{n} \right),$$

where we have set $n_+ = n$.

For a Maxwellian distribution

$$(2.34) \quad f_0(v) = \left(\frac{3m}{4\pi e\bar{u}} \right)^{\frac{3}{2}} n \exp \left[-\frac{3mv^2}{4e\bar{u}} \right],$$

the conductivity σ of a low pressure ($\nu_c^2 \ll \omega^2$) plasma [4] will then be

$$(2.35) \quad \sigma = \frac{e^2 n}{m\omega^2} A' \left[\frac{n}{\bar{u}^{\frac{3}{2}}} \ln \left(1 + \frac{B\bar{u}^3}{n} \right) + \langle \nu_m \rangle - j\omega \right],$$

where $A' = 2.7 \cdot 10^{-12} \text{ m}^3 \text{ s}^{-1} \text{ V}^{\frac{1}{2}}$. At low electron energies, as we have in a late afterglow ($\bar{u} = 0.04 \text{ eV}$), $\langle v_+ \rangle$ becomes comparable to $\langle v_m \rangle$ already at moderate electron densities. This condition was then chosen by ANDERSON and GOLDSTEIN [3] for determining $\langle v_+ \rangle$ from plasma conductivity measurements. Theory and experimental results seem to be in fairly good agreement.

3. - Power gain and effective field.

Knowing the plasma conductivity, it is useful to compute the average power gain per electron from the field. This power, in eV per second, will be:

$$(3.1) \quad \frac{1}{en} \frac{1}{2} \text{Re} [\mathbf{E} \cdot \mathbf{J}].$$

Substituting for \mathbf{J} the value given in eq. (2.5) the power becomes:

$$(3.2) \quad -\frac{1}{2} \text{Re} [\mathbf{E} \cdot \langle \mathbf{v}_s \rangle] = -\frac{1}{2} \langle \text{Re} (\mathbf{E} \cdot \mathbf{v}_s) \rangle.$$

The quantity $-(1/2)\mathbf{E} \cdot \mathbf{v}_s$ has a clear physical meaning: it is the power gain of an electron with velocity v , and can be written as $v_c u_c$, u_c being the average energy in eV gained by an electron of velocity v per collision. The average power gain per electron is then $\langle v_c u_c \rangle$.

The energy gain u_c can be easily expressed, as a function of the applied field, by substituting for \mathbf{v}_s the values (2.13) and (2.14) in the definition of u_c :

$$(3.3) \quad u_c = -\frac{1}{2v_c} \text{Re} (\mathbf{E} \cdot \mathbf{v}_s).$$

We obtain

$$(3.4) \quad u_c = \frac{1}{2v_c} \frac{e}{m} \text{Re} \left[\frac{E_{\parallel}^2}{v_c + j\omega} + \frac{(v_c + j\omega)E_{\perp}^2}{(v_c + j\omega)^2 + \omega_b^2} \right] = \\ = \frac{e}{2m} \left[\frac{E_{\parallel}^2}{v_c^2 + \omega^2} + \frac{1}{2} \frac{E_{\perp}^2}{v_c^2 + (\omega + \omega_b)^2} + \frac{1}{2} \frac{E_{\perp}^2}{v_c^2 + (\omega - \omega_b)^2} \right].$$

When v_c is independent of velocity, u_c is independent, too. The power gain per electron is then

$$(3.5) \quad \langle v_c u_c \rangle = v_c u_c = eE_e^2/mv_c,$$

where the field E_e is given by

$$(3.6) \quad E_e^2 = \frac{1}{2} \left[\frac{E_{\parallel}^2}{1 + (\omega/v_c)^2} + \frac{1}{2} \frac{E_{\perp}^2}{1 + (\omega + \omega_b)^2/v_c^2} + \frac{1}{2} \frac{E_{\perp}^2}{1 + (\omega - \omega_b)^2/v_c^2} \right].$$

The field E_e is an equivalent r.m.s. field, called « effective field », which has the important property of taking into account at the same time the frequency and the amplitude of the applied field. At very high pressures, the effective field coincides with the applied field.

4. - The electron distribution function in microwave discharges.

In a highly ionized plasma the distribution function is approximately Maxwellian, due principally to mutual electron interactions. Analogously in the late afterglow of an impulsive discharge, when the decaying plasma has achieved thermal equilibrium with the gas molecules, the distribution is Maxwellian ($\bar{u} = 3kT_g/2e$, T_g being the gas temperature).

In a microwave generated and sustained discharge, at low degrees of ionization, the distribution function may, instead, be very far from Maxwellian. Whereas this distribution should be computed rigorously by solving the Boltzmann equation, we shall here limit our analysis to an approximate evaluation of it. More precisely, we need an accurate knowledge of the shape of f_0 in the high energy tail, in order to compute excitation and ionization rates, and an approximate knowledge of the main body, in order to compute average plasma parameters.

We then write an equation for f_0 , which is accurate in the high energy region, and afterwards we shall use it in determining also the main body of f_0 . This equation is the flux equation in velocity space and says that the rate at which electrons in the high energy region pass a velocity v in the upward direction is equal to the rate of inelastic collisions occurring at velocities higher than v .

The flux rate can be written as the time average of the radial component (in velocity space) of the electron acceleration, multiplied by the distribution function and integrated over a sphere of radius v ,

$$(4.1) \quad \frac{1}{2} \operatorname{Re} \int \left[-\frac{e}{m} (\mathbf{E} + \mathbf{v}_g \times \mathbf{B}) \right] \cdot \left(\frac{\mathbf{v}}{v} \right) \left(-\frac{\mathbf{v} \cdot \mathbf{v}_g}{v} \frac{df_0}{dv} \right) v^2 d^2\Omega = \\ = \frac{1}{2} \frac{e}{m} \operatorname{Re} (\mathbf{E} + \mathbf{v}_g \times \mathbf{B}) \cdot \int \mathbf{v} (\mathbf{v} \cdot \mathbf{v}_g) \frac{df_0}{dv} d^2\Omega.$$

By using the general formula

$$(4.2) \quad \int F(v) (\mathbf{A} \cdot \mathbf{v}) \mathbf{v} d^2\Omega = \frac{4\pi}{3} v^2 F(v) \mathbf{A},$$

we obtain that the flux is

$$(4.3) \quad \frac{4\pi}{3} \frac{e}{m} v^2 \frac{df_0}{dv} \frac{1}{2} \operatorname{Re} (\mathbf{E} \cdot \mathbf{v}_g) = -\frac{4\pi}{3} \frac{e}{m} v_m u_e v^2 \frac{df_0}{dv},$$

having used eq. (3.3) and considered that $v_m \gg v_+$ at low degrees of ionization.

The rate (4.3) must be equal to the rate of inelastic collisions occurring at velocities higher than v :

$$(4.4) \quad \int_0^{\infty} (\nu_x + \nu_i) f_0(v) 4\pi v^2 dv = -\frac{4\pi}{3} \frac{e}{m} \nu_m u_c v^2 \frac{df_0}{dv},$$

where $\nu_x(v)$ and $\nu_i(v)$ are respectively the electronic excitation and ionization frequencies.

By differentiating eq. (4.4) we get:

$$(4.5) \quad (\nu_x + \nu_i) v^2 f_0 = \frac{e}{3m} \frac{d}{dv} \left(\nu_m u_c v^2 \frac{df_0}{dv} \right).$$

The experimental values of $(\nu_x + \nu_i)$ can be written for most gases in the form:

$$(4.6) \quad \nu_x + \nu_i \begin{cases} = 0 & \text{when } y < 1, \\ = \nu_m (h_0 y - h_1) & \text{when } y > 1, \end{cases}$$

where

$$y = (v/v_x)^2 \quad \text{and} \quad v_x = \sqrt{2eu_x/m},$$

u_x being the potential of the first electronic excited state.

At electron velocities larger than v_x (region of inelastic collisions), the solution of equation (4.5) can be written, when ν_m is independent of velocity, as follows [5]:

$$(4.7) \quad f_0 = Cy^{(2a'-3)/4} \exp[-ay] \left(\sum_{n=0}^{\infty} b_n / (ay)^n \right),$$

where C is an integration constant and

$$(4.8) \quad a = \sqrt{(3h_0/2)(u_x/u_c)}, \quad a' = \frac{h_1}{h_0} a, \quad b_0 = 1, \quad b_n = \prod_{r=1}^n \frac{1 - 4(1 + a' - 2r)^2}{32r}.$$

For most gases it is possible to determine a constant ν_m value, which approximates rather well the true collision frequency ν_m over the excitation and ionization regions, so that the above formulas are of very general use.

The constant C is unknown, but the knowledge of the shape (4.7) is sufficient for computing a large number of important parameters, namely all the ratios between average excitation frequencies of two different states or between an average excitation frequency and the corresponding average ionization frequency, etc. These quantities will result functions of u_c and then of E_c/p , ν_m being proportional to the pressure p . Moreover, because of the

exponential nature of f_0 , as given by (4.7), the dependence of these ratios on u_c will primarily be of the type $\exp[Ka] \sim \exp[K'u_c^{-\frac{1}{2}}] \sim \exp[K''p/E_e]$.

For instance, the average number of inelastic collisions per ionization, a quantity we shall need in the future analysis, is

$$(4.9) \quad N_{xi} = \frac{\bar{v}_x + \bar{v}_i}{\bar{v}_i} = \frac{\int_{v_x}^{\infty} (v_x + v_i) f_0 4\pi v^2 dv}{\int_{v_i}^{\infty} v_i f_0 4\pi v^2 dv} \approx A \exp \left[\frac{Bp}{E_e} \right].$$

In Fig. 3, N_{xi} is plotted versus p/E_e for hydrogen and helium and its exponential nature is well demonstrated.

In the energy region $y < 1$, namely at low velocities (region of elastic collisions), eq. (4.5) can be easily solved, but its approximation could be bad, because it does not take into account the diffusion, attachment, recombination and elastic collision

losses, which deplete the flux in velocity space. However, it has been found [6] in the $v_m = \text{constant}$ case, that the solution of eq. (4.5) gives a distribution very close to the actual distribution in all medium pressure discharges, so that we are justified to use it as a first approximation for computing all average plasma quantities.

The integrals to be used in calculating these averages will be limited on the upper side at an equivalent excitation potential u_0 (or velocity $v_0 = \sqrt{2eu_0/m}$), where we assume that the distribution function f_0 for the elastic collision region goes to zero. This potential u_0 is larger than u_x and takes somewhat into account that part of the distribution where inelastic collisions come in.

The conventional average value of a function $\varphi(v)$ is then computed as follows, integrating by parts and substituting $df_0/dv = \text{const}/v_m u_c v^2$ (eq. (4-5)),

$$(4.10) \quad \bar{\varphi} = \frac{\int_0^{v_0} \varphi f_0 4\pi v^2 dv}{\int_0^{v_0} f_0 4\pi v^2 dv} = \frac{\int_0^{v_0} (df_0/dv) dv \int_0^v \varphi(w) w^2 dw}{\frac{1}{3} \int_0^{v_0} (df_0/dv) v^3 dv} = 3 \frac{\int_0^{v_0} (dv/v_m u_c v^2) \int_0^v \varphi(w) w^2 dw}{\int_0^{v_0} (v/v_m u_c) dv}.$$

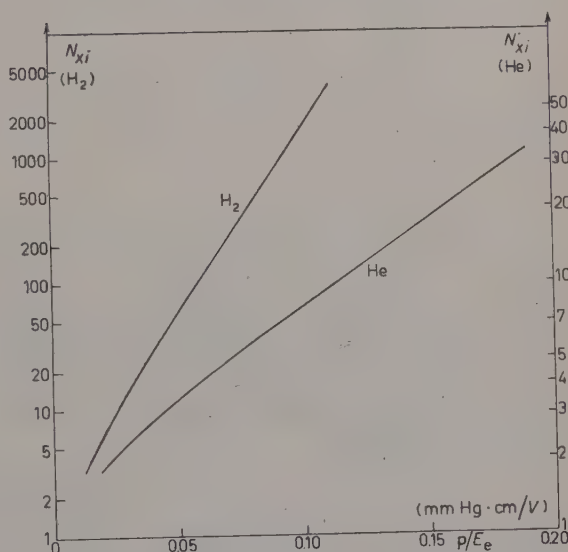


Fig. 3.

Analogously the average $\langle \varphi \rangle$ is computed

$$(4.11) \quad \langle \varphi \rangle = - \frac{(4\pi/3) \int_0^{v_0} \varphi (df_0/dv) v^3 dv}{\int_0^{v_0} f_0 4\pi v^2 dv} = - \frac{\int_0^{v_0} \varphi (df_0/dv) v^3 dv}{\int_0^{v_0} (df_0/dv) v^3 dv} = - \frac{\int_0^{v_0} (\varphi/v_m u_c) v dv}{\int_0^{v_0} (1/v_m u_c) v dv}.$$

When $v_m(v)$ is known, $u_c(v)$ is determined for given applied fields by eq. (3.4). By numerical or analytical methods, the above integrals can thus be computed and the average parameters determined as a function of the applied fields (E , ω , ω_b) and of the gas pressure (p).

The velocity v_0 , at which the extrapolated f_0 for the elastic collision region goes to zero, is found by joining the distribution in the elastic region and the one in the inelastic region. This is done by equating the logarithmic derivative at v_x of the distribution (4.7):

$$(4.12) \quad - \left(\frac{df_0/dv}{f_0} \right)_{v_x} = \frac{\sum_{n=0}^{\infty} (2a - a' + 1.5 + 2n)(b_n/a^n)}{v_x \sum_{n=0}^{\infty} (b_n/a^n)},$$

to the same derivative of the elastic region distribution

$$(4.13) \quad - \frac{(df_0/dv)_{v_x}}{f_0(v_x)} = \frac{(df_0/dv)_{v_x}}{\int_{v_x}^{v_0} (df_0/dv) dv} = \frac{1/v_x^2}{\int_{v_x}^{v_0} (1/v^2) dv} = \frac{1}{v_x^2(1/v_x - 1/v_0)},$$

where v_m has been assumed constant over the extrapolated region. Simple mathematics yields:

$$(4.14) \quad \frac{v_0}{v_x} = 1 - \left\{ \frac{\sum_{n=0}^{\infty} (b_n/a^n)}{\sum_{n=0}^{\infty} (2a - a' + 1.5 + 2n)(b_n/a^n)} \right\}^{-1}.$$

The velocity v_0 is a function of the energy gain u_c , which enters in the above coefficients; within the constant v_m approximation, this velocity, for a given gas, is then a function only of E_c/p .

5. - Energy balance and ionization frequencies.

We have shown how to compute the ratios between different kind of inelastic collision rates (N_{xi} for instance), but not their absolute values. We

shall show now how the average ionization frequency can be determined from the energy balance equation; all other frequencies are then derived from it and the known ratios.

Let us consider a uniform non-diffusing plasma, corresponding to a low degree of ionization, in a gas of atoms without electron attachment, ion recombination and metastable states. The energy balance equation, written on a per electron basis, is

$$(5.1) \quad \langle \nu_m u_c \rangle = u_0 N_{xi} \bar{\nu}_i + \overline{G(v) u \nu_m}.$$

The term on the left is the power gain from the field, the first term on the right is the power lost in inelastic collisions, having assumed that the average energy lost per collision is u_0 , and the last one is the power lost in elastic collisions. The quantity $G(v)$ is the mean fraction of electron energy transferred to the gas molecules, in a collision of an electron of velocity v (in an atomic gas $G = 2m/M$, M being the mass of the atom). The energy transferred to the molecules and the radiated energy are assumed to be dissipated at the container walls.

When diffusion is present and the plasma is in steady state conditions, the energy balance becomes

$$(5.2) \quad \langle \nu_m u_c \rangle = u_0 N_{xi} \bar{\nu}_i + \overline{G u \nu_m} + \frac{5}{3} \bar{u} \bar{\nu}_i.$$

In fact the rate of loss of electrons by diffusion must be equal to the rate of production ($\bar{\nu}_i n$), and each electron lost by diffusion carries on the average the energy $5\bar{u}/3$. The last statement can be shown as follows.

Let us call \mathbf{v}_d the average drift velocity due to diffusion. We then write the distribution function as

$$(5.3) \quad f(\mathbf{v}) = f_0(|\mathbf{v} - \mathbf{v}_d|).$$

It is easy to verify that \mathbf{v}_d is the average drift velocity (all the integrations are performed over the entire velocity space)

$$(5.4) \quad \int \mathbf{v} f(\mathbf{v}) d\mathbf{v} = \int (\mathbf{w} + \mathbf{v}_d) f_0(w) d\mathbf{w} = \mathbf{v}_d \int f_0(w) d\mathbf{w} = \mathbf{v}_d n.$$

The average electron energy is

$$(5.5) \quad \begin{aligned} \bar{u} &= \frac{m}{2en} \int v^2 f(\mathbf{v}) d\mathbf{v} = \frac{m}{2en} \int (\mathbf{w} + \mathbf{v}_d)^2 f_0(w) d\mathbf{w}, \\ &= \frac{m}{2en} \left[\int w^2 f_0(w) d\mathbf{w} + v_d^2 n \right] \simeq \frac{m}{2en} \int w^2 f_0(w) d\mathbf{w}. \end{aligned}$$

The average flux of energy per electron is

$$(5.6) \quad \frac{m}{2en} \int \mathbf{v} v^2 f(\mathbf{v}) d\mathbf{v} = \frac{m}{2en} \int (\mathbf{w} + \mathbf{v}_d)(w^2 + 2\mathbf{w} \cdot \mathbf{v}_d + v_d^2) f_0(w) d\mathbf{w} \simeq \\ \simeq \frac{m}{2en} \left[\mathbf{v}_d \int w^2 f_0(w) d\mathbf{w} + 2 \int \mathbf{w} (\mathbf{w} \cdot \mathbf{v}_d) f_0(w) d\mathbf{w} \right].$$

By means of eq. (2.4) the flux becomes

$$(5.7) \quad \frac{m}{2en} \left(1 + \frac{2}{3} \right) \mathbf{v}_d \int w^2 f_0(w) d\mathbf{w} = \frac{5}{3} \bar{u} \mathbf{v}_d,$$

which is the result we were looking for.

In a gas where ν_m and G are velocity independent, eq. (5.2) becomes

$$(5.8) \quad \nu_m u_c = u_0 N_{xi} \bar{\nu}_i + G \bar{u} \nu_m + \frac{5}{3} \bar{u} \bar{\nu}_i.$$

The average energy \bar{u} is computed from eq. (4.10) with $q = mv^2/2e$ and $\nu_m u_c$ constant:

$$(5.9) \quad \bar{u} = \frac{3m}{2e} \frac{\int_0^{v_0} dv/v^2 \int_0^v w^4 dw}{\int_0^{v_0} v dv} = \frac{3m}{2e} \frac{v_0^2}{10} = \frac{3u_0}{10}.$$

The average ionization frequency $\bar{\nu}_i$ is then

$$(5.10) \quad \bar{\nu}_i = \left(\frac{u_c}{u_0} - \frac{3G}{10} \right) \nu_m / \left(N_{xi} + \frac{1}{2} \right).$$

The values of $\bar{\nu}_i/p$, computed in this way for hydrogen and helium, are plotted in Fig. 4, as a function of E_e/p ($G = 2m/M$).

When attachment and recombination are present, the value $\frac{5}{3}\bar{u}$ for the average energy carried away by each lost electron is no longer correct. However, this term is in most cases only a correction term, and considering our usual ignorance of the energy dependence of these effects, we shall not try to write a better equation. Eq. (5.2) is then assumed correct also in these cases (eventually we could drop the factor $\frac{5}{3}$).

When, as in rare gases, atoms have metastable states with high excitation probabilities, new terms enter in the balance equation. Let us consider a Penning mixture, namely a rare gas contaminated with a small amount of ano-

ther gas with an ionization potential u'_i lower than the metastable level u^* . Let the concentrations be such that each excited metastable collides locally with an impurity atom and ionizes it, releasing the energy difference $(u^* - u'_i)$ mainly to the new free electron. Moreover, the probability, which an electron moving up in energy has to excite the first excitation level (metastable u^*), far exceeds the probabilities to excite successive levels and to ionize. In this approximation $u_0 = u^*$ and \bar{v}_i can be neglected compared to \bar{v}^* , the average excitation frequency of the metastable state. However, this frequency \bar{v}^* can be regarded as an equivalent ionization frequency \bar{v}_{ieq} , from the point of view of the production of new electrons.

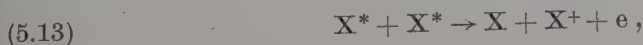
Then, for a Penning mixture, the energy balance equation is

$$\begin{aligned} \langle v_m u_c \rangle + (u^* - u'_i) \bar{v}_{ieq} &= u^* \bar{v}_{ieq} + \frac{2m}{M} \bar{u} \bar{v}_m + \frac{5}{3} \bar{u} \bar{v}_{ieq}, \\ (5.11) \quad \langle v_m u_c \rangle &= u'_i \bar{v}_{ieq} + \frac{2m}{M} \bar{u} \bar{v}_m + \frac{5}{3} \bar{u} \bar{v}_{ieq}. \end{aligned}$$

In the case of helium ($v_m = \text{const}$) contaminated by mercury (the so-called Heg gas), eq. (5.11) gives

$$(5.12) \quad \bar{v}_{ieq} = \left(\frac{u_c}{u^*} - \frac{3}{10} \frac{2m}{M} \right) v_m / \left(\frac{u'_i}{u^*} + \frac{1}{2} \right).$$

Also in the absence of contamination metastable states play an important role in controlling the discharge. In fact, the collision of two metastable states can produce an ionizing event, according to the reaction



which is energetically possible when $2u^* > u_i$, the ionization potential. Moreover, metastables can be ionized by an electron impact during their life time. The effects of these processes could be taken into the energy balance equation. However, we shall not do it here because, whereas there is experimental evi-

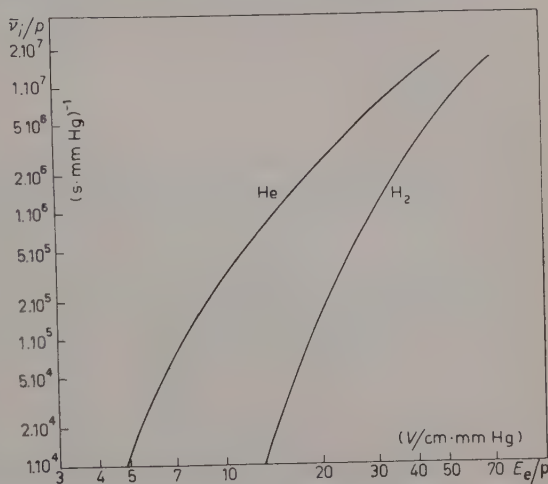


Fig. 4.

dence that the reaction (5.13) plays an important role in determining the characteristics of a microwave discharge in rare gases [7], we do not have enough experimental results, to compare the theory with, and we do not know accurately enough the elementary quantities, which would have to enter in this theory.

6. - The continuity equation and the breakdown condition.

We assume first an ideal gas of atoms, without electron attachment, ion recombination and metastable levels. In a plasma of this gas, the continuity equation for electrons is

$$(6.1) \quad \frac{\partial n}{\partial t} = \bar{v}_i n + \nabla^2 (D_s n),$$

where D_s is an equivalent diffusion coefficient, which in general takes into account also the reduction of the electron diffusion due to the space charge effects.

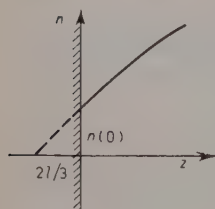


Fig. 5.

Eq. (6.1) has to be solved with the boundary condition $n=0$ at the walls. Rigorously the density would have to be very small at the walls, and to extrapolate to zero in a distance of the order of an electron mean free path. To justify this statement, we may write that the diffusing electron flow is equal to the random flow which would cross the walls in the absence of them, namely (Fig. 5):

$$(6.2) \quad D_s \left(\frac{dn}{dz} \right)_{z=0} = \frac{1}{2} v_c n(0),$$

where l is the mean free path, here assumed constant. In the absence of space charge effects $D_s = l\bar{v}/3$, $v_c = \bar{v}/l$, then

$$(6.3) \quad \left(\frac{dn}{dz} \right)_{z=0} = \frac{n(0)}{(2l/3)},$$

which demonstrates our statement. In the pressure range we shall discuss the mean free path is usually very small compared to the plasma dimensions and the $n=0$ condition at the walls can be used.

We now assume:

- 1) no static magnetic field is present,
- 2) the gas is in a parallelepiped container of sides $L_x L_y L_z$ (Fig. 6),

- 3) the container is in a region of uniform electric microwave field,
 4) at the time $t = 0$, a single electron is present in the position x_0, y_0, z_0 so that

$$(6.4) \quad n(x, y, z, 0) = \delta(x - x_0) \delta(y - y_0) \delta(z - z_0),$$

where δ is a delta-function.

When the electron density is very low, the diffusion coefficient is the free diffusion D (eq. (2.30)). This coefficient and \bar{v}_i are independent of position, and the solution of eq. (6.1) becomes

$$(6.5) \quad n(x, y, z, t) = \sum_{klm} a_{klm}(x_0, y_0, z_0) \sin\left(\frac{k\pi x}{L_x}\right) \sin\left(\frac{l\pi y}{L_y}\right) \sin\left(\frac{m\pi z}{L_z}\right) \exp[\gamma_{klm} t],$$

where

$$(6.6) \quad \gamma_{klm} = \bar{v}_i - D \left[\left(\frac{k\pi}{L_x}\right)^2 + \left(\frac{l\pi}{L_y}\right)^2 + \left(\frac{m\pi}{L_z}\right)^2 \right].$$

As we have seen (Fig. 4), \bar{v}_i is a fast varying function of the applied field, whereas D is not. Let us perform an experiment, where the pressure and the frequency are held constant and the field is increased. At very low fields \bar{v}_i is practically zero, the γ_{klm} are all negative and thus the electron density cannot build-up. As soon as we pass the condition

$$(6.7) \quad \bar{v}_i = D/\Lambda^2,$$

where

$$(6.8) \quad \frac{1}{\Lambda^2} = \left(\frac{\pi}{L_x}\right)^2 + \left(\frac{\pi}{L_y}\right)^2 + \left(\frac{\pi}{L_z}\right)^2,$$

γ_{111} becomes positive and the density increases indefinitely with time. The gas is broken down and eq. (6.7) is the CW microwave breakdown condition.

The quantity Λ is called the container diffusion length and eq. (6.8) gives its value for a parallelepiped geometry. For other shapes it is usually well known from the general theory of particle diffusion. In particular, for a cylindrical container of height L and radius R with flat ends, we have

$$(6.9) \quad \frac{1}{\Lambda^2} = \left(\frac{\pi}{L}\right)^2 + \left(\frac{2.4}{R}\right)^2.$$

In a constant v_m gas (see eq. (5.9))

$$(6.10) \quad D = \frac{\bar{v}^2}{3\nu_m} = \frac{v_0^2}{10\nu_m}.$$

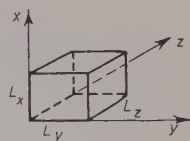


Fig. 6.

Then (Dp) is a function of E_e/p alone; the same was shown to be the case for \bar{v}_i/p . Eq. (6.7) can then be written as

$$(Dp)/(\bar{v}_i/p) = (p\Lambda)^2$$

or:

$$(6.11) \quad (p\Lambda)^2 = F'(E_e/p).$$

Substituting for Dp and v_i/p the values given by eq. (6.10) and (5.10), we obtain

$$(6.12) \quad F'\left(\frac{E_e}{p}\right) = \frac{v_0^2(N_{xi} + \frac{1}{2})}{[10(u_c/u_0) - 3G](v_m/p)^2}.$$

In this expression E_e/p enters in u_c ($= (e/m)(E_e/p)^2/(v_m/p)^2$), u_0 , v_0^2 and N_{xi} . By changing the proper variables, eq. (6.11) becomes

$$(6.13) \quad E_e\Lambda = F''(p\Lambda).$$

This last equation is the equivalent of the Paschen law at microwave frequencies, and is very important because it shows that all breakdown data can be represented on a single plot, provided we use the proper variables.

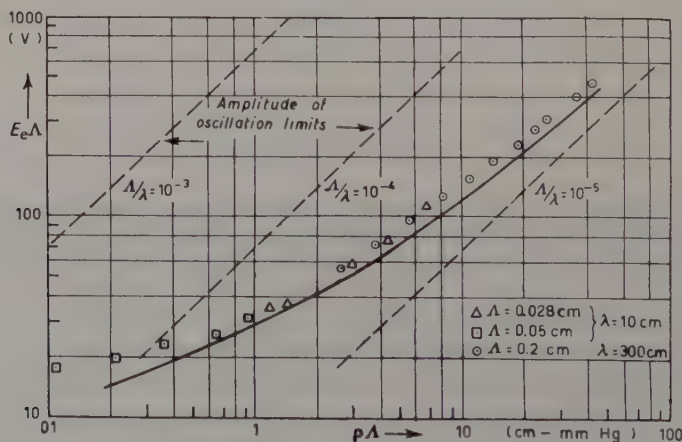


Fig. 7.

Recombination and ionization by metastable-metastable and metastable-electron collisions require high densities to compete comparatively with direct ionization and diffusion and thus they do not enter into the breakdown equa-

tion. The theoretical microwave Paschen curves for hydrogen and helium have then been computed with the above formulas and plotted in Figs. 7 and 8 respectively.

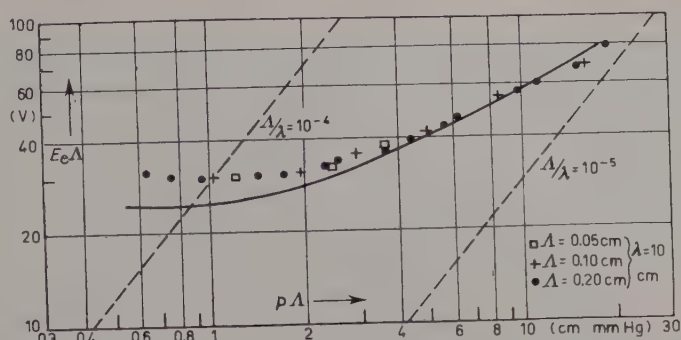


Fig. 8.

When electron attachment is present, as in oxygen, we must add the term $(-\bar{\nu}_a n)$ to the right of eq. (6.1), where $\bar{\nu}_a$ is the average attachment frequency per electron. The most general form of eq. (6.7) is then

$$(6.14) \quad \bar{\nu}_i - \bar{\nu}_a = D/\Lambda^2.$$

In a Penning mixture, eq. (6.7) is still valid, provided we use $\bar{\nu}_{ieq}$ for the average ionization frequency. In the case of the Heg gas, the function F' is

$$(6.15) \quad F' \left(\frac{E}{p} \right) = \frac{v^{*2} \left(\frac{u'_i}{u^*} + \frac{1}{2} \right)}{\left(10 \frac{u_c}{u^*} - 3 \frac{2m}{M} \right) \left(\frac{v_m}{p} \right)^2} = \frac{80.4}{(E_e/p)^2 - 5.2 \cdot 10^4}.$$

The equivalent Paschen law is then (Λ in cm, E_e in V/cm)

$$(6.16) \quad (E_e \Lambda)^2 = 80.4 + 5.2 \cdot (p \Lambda)^2.$$

This curve is plotted in Fig. 9.

If the container has glass walls, the breakdown characteristics can be changed by the persistence of free charges on the walls. Then the metal cavities themselves are used as gas containers. In this case the uniform field condition can be satisfied only by those cavities which approximate a parallel plane geometry, the maximum field being between the plates, normal to them and practically uniform over a region large compared to the plate separation L . The predominant diffusion is then normal to the plates, and the diffusion length is simply $\Lambda = L/\pi$.

Experimental data obtained by ALLIS, BROWN, MACDONALD and REDER under the above conditions in hydrogen [6, 8], helium [5] and Heg [8], are plotted in Figs. 7, 8 and 9.

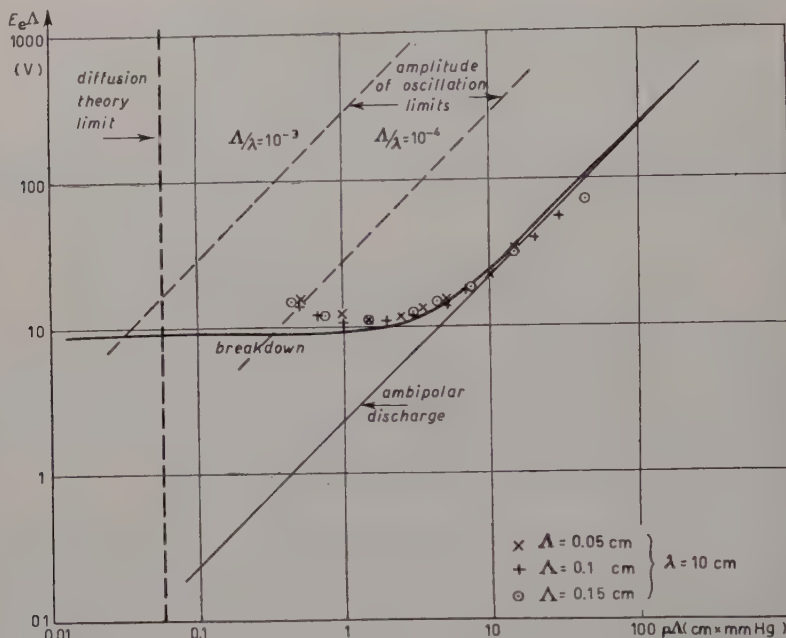


Fig. 9.

The agreement between theory and experiment is fairly good, considering that no adjustable parameter has been used in the theory. A complete agreement at low $p\lambda$ values is obtained, if a better approximation is used for the distribution function, namely if a diffusion term is taken into eq. (4.5). Unfortunately, however, the solution of this generalized eq. (4.5) is not expressible in simple terms, except when v_m is constant. For this reason, we have neglected throughout the additional diffusion term and followed a less exact, but quite general procedure, which is readily usable also when v_m is velocity dependent.

The detailed dependence of the breakdown field on pressure and frequency can be easily derived from the Paschen microwave equation. We shall use for this discussion eq. (6.16), which is analytically very simple; the results are, however, quite general.

By introducing the actual breakdown field E ,

$$(6.17) \quad E^2 = 2 \left(1 + \frac{\omega^2}{v_m^2} \right) E_e^2,$$

eq. (6.16) becomes

$$(6.18) \quad (EA)^2 = \left[1 + \frac{6.3 \cdot 10^3}{(p\lambda)^2} \right] [161 + 10.4(pA)^2],$$

where λ is the free space wavelength in cm.

Here (EA) is a function only of $(p\lambda)$ and (pA) ; this is a quite general result, which by dimensional analysis [9] can be demonstrated true for the microwave breakdown of any gas.

According to (6.18) the breakdown field is directly proportional to the pressure, when this is high, and is inversely proportional, when it is low (Fig. 10). At high pressures the breakdown field is independent of A and λ . At low pressures it decreases, when either A or λ are increasing.

At the breakdown limit (6.7) the building-up time of the discharge is theoretically infinite; if a small over-voltage is used, the building-up time is finite and can be measured as a function of the over-voltage. From this the coefficients \bar{v}_i/p and Dp can be separately derived. The agreement between theory and experiment for hydrogen is very good [10].

The above breakdown theory is correct in the range where diffusion theory is valid: that can be assumed to be where

$$(6.19) \quad A > \bar{l} = \left(\frac{v}{v_m} \right).$$

For hydrogen this means $pA > 2 \cdot 10^{-2}$ cm mmHg, for helium and Hg $pA > 6 \cdot 10^{-2}$ cm mmHg.

Moreover, in order to prevent the walls from controlling the discharge, the amplitude of oscillation of the average electron must be smaller than the dimensions of the container, let us say, be smaller than $L/2$ in the parallel plane case. The amplitude of the oscillation is easily derived by integrating eq. (2.13); assuming v_m independent of velocity, we obtain

$$(6.20) \quad \frac{e}{m} \frac{E}{\omega \sqrt{v_m^2 + \omega^2}} = \frac{e}{m} \frac{\sqrt{2} E_s}{\omega v_m} < \frac{L}{2}.$$

For hydrogen we then have the condition (in usual gas discharge units)

$$(6.21) \quad E_s A < 7 \cdot 10^5 (pA)(A/\lambda),$$

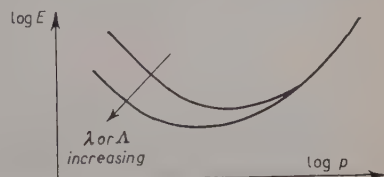


Fig. 10.

and for helium and Heg

$$(6.22) \quad E_e A < 3 \cdot 10^5 (pA)(A/\lambda) .$$

Then, for each value of (A/λ) , we shall have on the Figs. 7, 8 and 9 a straight line, which delimits the validity region as the one on its right side. This shows also that, in order to have a diffusion controlled breakdown, we must use high frequency fields.

When the shape of the cavity does not approximate the parallel plane geometry, the problem is much more difficult, because the field non-uniformity comes in. A theory has been given [11] also for this case, but we shall not discuss it here.

7. The breakdown in a superimposed magnetic field.

When a static magnetic field is present, the diffusion coefficient which enters into eq. (6.1) is no longer a scalar, but becomes a tensor. Referring to the parallelepiped container in a uniform microwave electric field, with a superimposed magnetic field along the z -axis, the continuity equation at low electron densities is:

$$(7.1) \quad \frac{\partial n}{\partial t} = \bar{v}_i n + D_{\perp} \left(\frac{\partial^2 n}{\partial x^2} + \frac{\partial^2 n}{\partial y^2} \right) + D_{\parallel} \frac{\partial^2 n}{\partial z^2} .$$

Here the parallel diffusion coefficient D is equal to the diffusion in the absence of the magnetic field $D (= \bar{v}^2/3\nu_m)$ and the transverse diffusion coefficient D_{\perp} is given by the average $\frac{\bar{v}_m \bar{v}^2/3}{\nu_m^2 + \omega_b^2}$.

The solution of the diffusion equation is still given by eq. (6.5), where now

$$(7.2) \quad \gamma_{klm} = \bar{v}_i - D_{\perp} [(k\pi/L_x)^2 + (l\pi/L_y)^2] - D(m\pi/L_z)^2 .$$

In a constant ν_m gas, like hydrogen and helium, we have the simple relation

$$(7.3) \quad D_{\perp}/D = \nu_m^2/(\nu_m^2 + \omega_b^2) .$$

The CW breakdown condition remains then given by eq. (6.7), provided a modified diffusion length is introduced as follows:

$$(7.4) \quad \frac{1}{A^2} = \frac{\nu_m^2}{\nu_m^2 + \omega_b^2} \left[\left(\frac{\pi}{L_x} \right)^2 + \left(\frac{\pi}{L_y} \right)^2 \right] + \left(\frac{\pi}{L_z} \right)^2 .$$

The effect of the magnetic field on the diffusion is then equivalent to an increase of the container dimensions normal to the field. Analogous formulas can be easily derived for other container shapes.

To discuss the effects of the magnetic field on the breakdown we refer to eq. (6.16), which is still valid for Heg, provided Λ is the modified diffusion length. The magnetic field enters also in the expression for the effective field E_e , according to the general expression (3.6).

The following typical results can be easily checked with the above formulas:

1) when $\nu_m^2 \gg \omega^2$, ω_b^2 , namely at high pressures, the magnetic field does not change the breakdown field in a given experiment;

2) when $E_{\perp} = 0$, the breakdown field decreases with the magnetic field and tends toward a minimum value (Fig. 11), corresponding to $\Lambda = L_z/\pi$;

3) when $E_{\perp} = 0$, at low pressures ($\nu_m^2 \ll \omega^2$) and near cyclotron resonance ($\omega_b \approx \omega$), the effective field becomes

$$(7.5) \quad E_e^2 = \frac{1}{4} \frac{\nu_m^2 E^2}{\nu_m^2 + (\omega - \omega_b)^2},$$

and shows a resonance behaviour as a function of the magnetic field. The diffusion length Λ , instead, changes slowly with the magnetic field, so that the breakdown effective field E_e must remain nearly constant, when the magnetic field is changed through resonance. To hold E_e constant, the actual breakdown field E must thus undergo a sharp decrease at resonance (Fig. 12). In particular, the bandwidth of the breakdown field curve, defined as the separation $\Delta\omega_b$ between the cyclotron frequencies at which the breakdown field

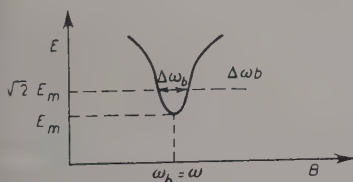


Fig. 12.

is $\sqrt{2}$ times its value at cyclotron resonance will be equal to ν_m and then proportional to, the gas pressure (Fig. 13). If we add the parallel plane geometry conditions $L_y \rightarrow \infty$, $L_x \rightarrow \infty$, the breakdown field in Heg at cyclotron resonance becomes

$$(7.6) \quad E = 2p \left[5.2 + 80.4 \left(\frac{\nu_m/p}{\omega_b} \right)^2 \left(\frac{\pi}{L_x} \right)^2 \right]^{\frac{1}{2}}.$$

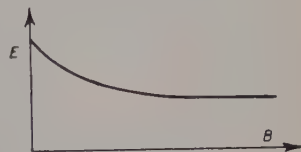


Fig. 11.

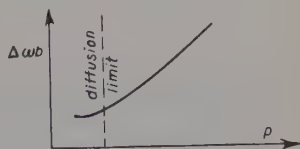


Fig. 13.

In this case the breakdown field is proportional to the pressure (Fig. 14).

All the above behaviours have been observed in Heg [12] and in hydrogen [13].

As we have seen, the breakdown field shows a general trend to decrease when a magnetic field is used, and this is in part due to the reduction of electron diffusion losses. However, the use of a magnetic field can reduce the loss of electrons normal to it, but not along it (end losses). Then we still have a diffusion limit, which prevents us from obtaining an easy breakdown at pressures lower than $(10^{-2} \div 10^{-3})$ mmHg.

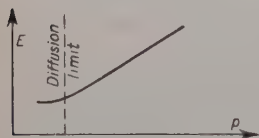


Fig. 14.

We may try to suppress or reduce this loss by a toroidal geometry, or by the use of a non uniform field (magnetic mirror). If the container is made of glass, surprisingly low end losses have been observed experimentally at M.I.T. In this case it is possible to produce and maintain [14] a stable discharge with an extremely low power (mW), at pressures between 10^{-5} and 10^{-3} mmHg, L_z being of the order of 10 cm.

A typical arrangement consists of a cylindrical cavity, oscillating in the TE_{111} mode, with the plasma contained in a quartz tube along the axis, and a B field parallel to the axis. The very low end losses are probably the effect of an electrostatic confinement, due to the fact that the end walls, under electron bombardment, charge up.

8. - Microwave sustained discharges.

The sustained discharge has been less investigated than the breakdown.

Let us assume again an ideal gas, without attachment, recombination and metastable states, placed in a parallelepiped container in a uniform microwave electric field (no static magnetic field is present). Eq. (6.5) gives the initial growing of the density; when densities of the order $(10^7 \div 10^8)$ electrons/cm³ are attained two effects become of importance:

- 1) the diffusion coefficient decreases, due to the space charge effects of the ions, so that γ_{klm} increases and the density tends faster towards infinity,
- 2) the microwave cavity becomes detuned by the change in the dielectric constant, due to the presence of the plasma, and the field E_e decreases.

These two effects will bring the plasma to an equilibrium condition, and in general we shall be able to describe the sustained discharge characteristics by introducing, besides the proper variables $E\lambda$, $p\lambda$, $p\lambda$ (or $E_e\lambda$ and $p\lambda$, when v_m is constant), also the additional proper variable $n_0\lambda^2$, where n_0 is the electron density at the center of the container.

ROSE and BROWN [15] have worked out a detailed theory for hydrogen and for n_0 values low enough, not to perturb the microwave field ($\omega_{p0}^2 = c^2 n_0 / m \varepsilon_0 \ll \omega^2$). Their experimental results show a good agreement with theory.

A simple relation between $E_e A$ and $p A$ can be easily derived, when n_0 is large enough that ambipolar diffusion conditions exist, but ω_{p0}^2 is still much smaller than ω^2 . In fact, the maintaining field condition is, in analogy with (6.7),

$$(8.1) \quad D_a \bar{v}_i = A^2,$$

where D_a is the ambipolar diffusion coefficient

$$(8.2) \quad D_a = D_+ + D_- \frac{\mu_+}{\mu},$$

μ being the electron mobility, D_+ and μ_+ the positive ion diffusion coefficient and mobility.

For hydrogen and Heg we have

$$(8.3) \quad D_+ / \mu_+ = \frac{2}{3} \bar{u}_+$$

$$(8.4) \quad D_- / \mu = \frac{2}{3} \bar{u}$$

and then, the average ion energy \bar{u}_+ being much smaller than \bar{u} ,

$$(8.5) \quad D_a = \frac{2}{3} (\bar{u} + \bar{u}_+) \mu_+ \simeq \frac{2}{3} \bar{u} \mu_+ = \frac{1}{5} u_0 \mu_+.$$

After some straightforward mathematics and with numerical values we obtain from (8.1) for Heg the following equation for the sustaining field in the ambipolar limit (units as in (6.16)):

$$(8.6) \quad (E_e A)^2 = 2.2 \cdot 10^{-3} + 5.2 \cdot (p A)^2.$$

This curve has also been plotted in Fig. 9.

In the case of pure rare gases, there is definite evidence that the maintaining field computed with the above theories is larger than the observed field. Then an additional ionization process, like metastable-metastable collisions, must be assumed present. We shall not discuss it here.

We said at the beginning of this section that the cavity becomes detuned by the plasma and we reach a stationary condition. By retuning the cavity, if no other mechanism would become effective, we could achieve infinite densities. It is however well known that, when we approach the condition $\omega_{p0} = \omega$, the field becomes distorted and does not penetrate efficiently into the plasma.

We can easily see what happens when n_0 is very large ($\omega_{p0}^2 > \omega^2$) in a pa-

parallel plane case, namely when we have an alternated field initially uniform in space between two electrodes (Fig. 15). The total current $j\omega\epsilon\mathbf{E}$ must be z independent, then

$$(8.7) \quad \left[1 - \left(\frac{\omega_p}{\omega} \right)^2 \frac{1}{1 - j(v_m/\omega)} \right] E = \text{const.}$$

The density, and then ω_p^2 , are, under diffusion controlled conditions, continuously increasing away from the walls, with a maximum at the position

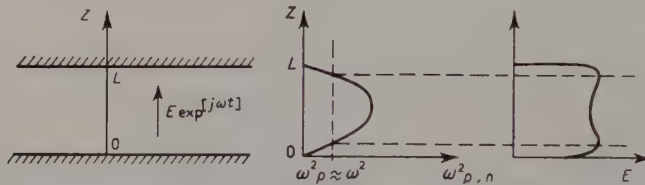


Fig. 15.

$z = L/2$. Then, at two symmetrical z planes, E will have a maximum; ionization and excitation will take place mostly in these two regions, because they vary quite rapidly with the field (see Fig. 4). There are in this case two bright regions, first observed by SCHUMANN [16].

By solving the detailed equations for this case, one finds [17] that the voltage across the electrodes must increase with n_0 , namely that the behaviour which was found at $\omega_{p0}^2 \ll \omega^2$ is here reversed.

No significant data on sustained discharges in magnetic fields are available.

9. - Electron density and collision frequency measurements.

We shall review here only the methods of measuring electron densities and collision frequencies by means of microwaves in resonant cavities, which are the most accurate, and also the most useful, when the plasma has already been generated by a microwave field.

Be $\mathbf{E}_0 \exp[j\omega_0 t]$ and $\mathbf{H}_0 \exp[j\omega_0 t]$ the fields inside a non-degenerate resonant cavity in the absence of the plasma. Be $\mathbf{E} \exp[j\omega_1 t]$ and $\mathbf{H} \exp[j\omega_1 t]$ the fields when the plasma is present. The pulsations ω_0 and ω_1 will then be the complex resonant pulsations without the plasma and with the plasma. Maxwell's equations are:

$$(9.1) \quad \nabla \times \mathbf{H}_0 = j\omega_0 \epsilon_0 \mathbf{E}_0,$$

$$(9.2) \quad \nabla \times \mathbf{E}_0 = -j\omega_0 \mu_0 \mathbf{H}_0,$$

$$(9.3) \quad \nabla \times \mathbf{H} = j\omega_1 \epsilon_0 \mathbf{E} + \boldsymbol{\sigma} \cdot \mathbf{E} \quad (\boldsymbol{\sigma} \text{ is a tensor}),$$

$$(9.4) \quad \nabla \times \mathbf{E} = -j\omega_1 \mu_0 \mathbf{H}.$$

We multiply the first equation by \mathbf{E} , the second by \mathbf{H} , the third by \mathbf{E}_0 and the last by \mathbf{H}_0 ; we add up the first two and subtract the last two, and finally we integrate all over the volume of the cavity. We obtain

$$(9.5) \quad \int_V \nabla \cdot (\mathbf{H}_0 \times \mathbf{E} + \mathbf{E}_0 \times \mathbf{H}) dV = \\ = j(\omega_0 - \omega_1) \int_V (\epsilon_0 \mathbf{E} \cdot \mathbf{E}_0 - \mu_0 \mathbf{H} \cdot \mathbf{H}_0) dV - \int_V (\boldsymbol{\sigma} \cdot \mathbf{E}) \cdot \mathbf{E}_0 dV.$$

The left side vanishes, due to the usual boundary conditions of a perfectly conducting wall, and we obtain

$$(9.6) \quad \omega_1 - \omega_0 = \frac{j \int_V (\boldsymbol{\sigma} \cdot \mathbf{E}) \cdot \mathbf{E}_0 dV}{\int_V [\epsilon_0 \mathbf{E} \cdot \mathbf{E}_0 - \mu_0 \mathbf{H} \cdot \mathbf{H}_0] dV},$$

which gives the shift in the complex pulsation of the cavity when the plasma is present.

At low plasma densities, we can assume that the field configuration is not changed by the plasma, and then set $\mathbf{E} = \mathbf{E}_0$, $\mathbf{H} = \mathbf{H}_0$. Within this approximation and remembering the well known fact that in a microwave cavity the energy stored in the electric field is equal to that stored in the magnetic field,

$$(9.7) \quad \epsilon_0 \int_V E_0^2 dV = - \mu_0 \int_V H_0^2 dV,$$

we obtain

$$(9.8) \quad \omega_1 - \omega_0 = \frac{j \int_V (\boldsymbol{\sigma} \cdot \mathbf{E}_0) \cdot \mathbf{E}_0 dV}{2\epsilon_0 \int_V E_0^2 dV}.$$

This expression is a complex quantity; the imaginary part of it indicates the variation in the half-band width of the cavity ($\mathcal{B}/2$) due to the plasma.

In the absence of a magnetic field and at low pressures ($v_e^2 \ll \omega^2$), the conductivity is a scalar, given by eq. (2.27)

$$(9.9) \quad \sigma = \frac{ne^2}{4\pi^2 m f_0^2} (\langle v_e \rangle - j2\pi f_0),$$

which substituted into (9.8) gives for the shift Δf in the resonant frequency f_0 :

$$(9.10) \quad \frac{\Delta f}{f_0} = \frac{\text{Re}(\omega_1 - \omega_0)}{2\pi f_0} = \frac{e^2}{8\pi^2 m \epsilon_0 f_0^2} \frac{\int_V n E_0^2 dV}{\int_V E_0^2 dV}.$$

Then the frequency shift is a measure of the electron density. The variation in the bandwidth is

$$(9.11) \quad \Delta\mathcal{B} = \frac{e^2}{4\pi^2 m \epsilon_0 f_0^2} \frac{\int \langle v_e \rangle n E_0^2 dV}{\int E_0^2 dV}.$$

When $\langle v_e \rangle$ is constant over the cavity volume, we have

$$(9.12) \quad \langle v_e \rangle = \frac{\Delta\mathcal{B}}{2\Delta f} f_0.$$

This indicates how collision frequencies are measured by microwave techniques [2].

The measurement of a frequency shift gives, according to eq. (9.10), only an average value of the density in the cavity. But, if we measure the frequency shifts of different resonant modes, we can get an idea of the variations of the density through the cavity.

Concerning the applicability of the small perturbation theory, it has been shown [18] that the above assumptions $E = E_0$, $H = H_0$ are acceptable, when the average densities are less than $5 \cdot 10^9 \text{ cm}^{-3}$ at *S* band and $5 \cdot 10^{10} \text{ cm}^{-3}$ at *X* band. The minimum frequency shifts, which can be measured, indicate a minimum measurable density of $2 \cdot 10^7 \text{ cm}^{-3}$ at *S* band and $2 \cdot 10^8 \text{ cm}^{-3}$ at *X* band.

When a static magnetic field, normal to the E field, is present, eq. (9.8) becomes

$$(9.13) \quad \omega_1 - \omega_0 = \frac{j \int_V (\sigma_e + \sigma_o) E_0^2 dV}{4\epsilon_0 \int_V E_0^2 dV}.$$

At low pressures and far from cyclotron resonance, we obtain again for $\Delta f/f_0$ and $\Delta\mathcal{B}$ the same expressions (9.10) and (9.11), except for the multiplying factors $[1 - (\omega_b/2\pi f_0)^2]^{-1}$ and $[1 + (\omega_b/2\pi f_0)^2][1 - (\omega_b/2\pi f_0)^2]^{-2}$ respectively.

When the density increases over the above indicated values, the distortion of the field from the original configuration becomes of importance. Then the frequency shift Δf will not be linearly related to the density, and we can use the measurements of Δf to determine the density only if we have first solved the analytical problem of the new field configuration as a function of the plasma parameters.

However, there is a condition in which we can measure electron densities a few times larger than those corresponding to $\omega_p = \omega$, still using a linear relation between Δf and n . This is the case when, in the absence of the static B field, E is normal to ∇n at any point in the plasma. The reason is that in this condition we do not have large space charge effects, which alter the E field.

This can be easily demonstrated, by writing the continuity equation

$$(9.14) \quad \frac{\partial \varrho}{\partial t} + \nabla \cdot \mathbf{J} = j\omega\varrho + \nabla \cdot (\sigma \mathbf{E}) = j\omega\varrho + \mathbf{E} \cdot \nabla \sigma + \sigma \nabla \cdot \mathbf{E} = 0,$$

where ϱ is the alternated space charge, and using Maxwell's equation,

$$(9.15) \quad \nabla \cdot \mathbf{E} = -\varrho/\varepsilon_0.$$

Substituting (9.15) into (9.14) we obtain

$$(9.16) \quad \left(j\omega - \frac{\sigma}{\varepsilon_0}\right) \varrho = -\mathbf{E} \cdot \nabla \sigma \sim \mathbf{E} \cdot \nabla n.$$

Then ϱ is zero when \mathbf{E} and ∇n are normal.

A typical case is a plasma in a cylindrical container placed along the axis of a cylindrical cavity oscillating in the TE_{011} mode. The density is varying only radially and axially, and the \mathbf{E} field is only azimuthal. BUCHSBAUM and BROWN [19] have found that the relation between Δf and n is linear up to densities corresponding to $\omega_p^2 = 10\omega^2$.

When a magnetic field is present, the conductivity is a tensor and the above result is not in general valid. However, when \mathbf{B} is parallel to \mathbf{E} , and they are normal to ∇n , we shall again have the desired condition. The possibility to satisfy all these conditions is of course dependent on the particular geometry of the experiment.

BIBLIOGRAPHY

- W. P. ALLIS: *Handb. d. Phys.*, **21**, 383 (1956).
 S. C. BROWN: *Handb. d. Phys.*, **22**, 531 (1956).
 L. GOLDSTEIN: *Electrical discharges in gases and modern electronics*, in *Advances in electronics and electron physics*, vol. **7** (New York, 1955).

REFERENCES

- [1] H. MARGENAU: *Phys. Rev.*, **69**, 508 (1946).
 [2] A. V. PHELPS, O. T. FUNDINGSLAND and S. C. BROWN: *Phys. Rev.*, **84**, 559 (1951);
 L. GOULD and S. C. BROWN: *Phys. Rev.*, **95**, 897 (1954); A. GILARDINI and
 S. C. BROWN: *Phys. Rev.*, **105**, 31 (1957).
 [3] J. M. ANDERSON and L. GOLDSTEIN: *Phys. Rev.*, **100**, 1037 (1955); **102**, 933 (1956).
 [4] V. L. GINZBURG: *Žu. Èksp. Teor. Fiz.*, **8**, 253 (1944).

- [5] F. H. REDER and S. C. BROWN: *Phys. Rev.*, **95**, 885 (1954).
- [6] W. P. ALLIS and S. C. BROWN: *Phys. Rev.*, **87**, 419 (1952).
- [7] M. A. BIONDI: *Phys. Rev.*, **88**, 660 (1952).
- [8] A. D. McDONALD and S. C. BROWN: *Phys. Rev.*, **75**, 411 (1949); **76**, 1634 (1949).
- [9] A. D. McDONALD and S. C. BROWN: *Phys. Rev.*, **76**, 1629 (1949).
- [10] M. P. MADAN, E. I. GORDON, S. J. BUCHSBAUM and S. C. BROWN: *Phys. Rev.*, **106**, 839 (1957).
- [11] M. A. HERLIN and S. C. BROWN: *Phys. Rev.*, **74**, 1650 (1948); A. D. McDONALD and S. C. BROWN: *Can. Journ. of Res.*, A **28**, 168 (1950).
- [12] B. LAX, W. P. ALLIS and S. C. BROWN: *Journ. Appl. Phys.*, **21**, 1297 (1950).
- [13] J. L. HIRSHFIELD and H. FIELDS: *M.I.T. Quart. Progr. Rep.* (July 15, 1957), p. 10.
- [14] S. C. BROWN: *Rendiconti del III Congresso Intern. sui fenomeni d'ionizzazione nei gas* (Venezia, 1957), p. 169.
- [15] D. J. ROSE and S. C. BROWN: *Phys. Rev.*, **98**, 310 (1955).
- [16] W. O. SCHUMANN: *Zeits. f. Phys.*, **7**, 121 (1942).
- [17] W. P. ALLIS, S. C. BROWN and E. EVERHART: *Phys. Rev.*, **84**, 519 (1951).
- [18] K. B. PERSSON: *Phys. Rev.*, **106**, 191 (1957).
- [19] S. J. BUCHSBAUM and S. C. BROWN: *Phys. Rev.*, **106**, 196 (1957).

INTERVENTI E DISCUSSIONI

— O. STURROCK:

In eq. (2.1) the $d\mathbf{v}$ on the left side is different from $d(\mathbf{v} - \mathbf{v}_g \exp[i\omega t])$, which must go on the right side, and this gives an additional oscillatory term of the type $\sim f_0 \Delta_0 \cdot \mathbf{v}_g$.

— A. GILARDINI:

The dependence of \mathbf{v}_g on the speed v comes in because we have substituted the discontinuous physical process of collisions with a continuous loss of momentum. Physically any electron in steady state conditions, in the absence of collisions, oscillates with the same amplitude and phase, whatever its random v is. Then the suggested additional term does not exist physically and we shall ignore it. For this reason the present derivation, as I said in the lecture, has the only purpose to make the final formulas acceptable; rigorously they can only be derived by the exact treatment of the Boltzmann equation and of the collision integrals which enter in it.

— L. GOLDSTEIN:

Since even in gases at low degree of ionization, at low temperature and pressure the ion collisions are of some importance, it would be wise to state the limits of validity of the derived formulas.

— A. GILARDINI.

The derived formula for the conductivity contains the ion collision term, which becomes of importance in the afterglow, when the electronic temperature is low. What

we are now discussing is the case of a sustained microwave discharge, where the electron energy is rather high and thus the ion collision term, which contains the term $\bar{u}^{-\frac{1}{2}}$, drops out. This determines the limits of validity.

— L. PENNELEGION:

What is the maximum pressure at which the referred breakdown measurements have been taken?

— A. GILARDINI:

In He this maximum pressure is about 300 mm Hg; in hydrogen measurements at pressures up to the atmospheric have also been taken. At very high pressures, modulation of the average electron energy by the microwave field may be of importance.

Le plasma stellaire.

E. SCHATZMAN

Institut d'Astrophysique - Paris

I. Equations d'état de la matière.

Les propriétés des plasmas sont différentes selon les valeurs des températures et des densités. Nous allons considérer différents domaines correspondant à différentes approximations.

Hypothèse: on peut supposer que l'équilibre thermodynamique est réalisé, ce qui impose:

- une distribution de vitesse suivant la loi de Maxwell;
- une distribution des populations des niveau d'énergie suivant la loi de Boltzmann.

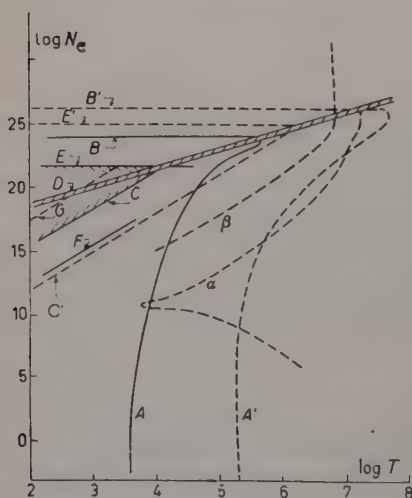


Fig. 1.

avec $\theta = 5040/T$.

1. — Conséquence de la loi de Saha pour l'ionisation.

Pour un gaz parfait nous avons

$$\frac{N_e N_i}{N_0} = \frac{g_i}{g_0} 2 \left[\frac{2\pi m_e}{h^3} kT \right]^{\frac{3}{2}} \exp \left[\frac{-\chi}{kT} \right],$$

g_i et g_0 étant les poids statistiques des ions et atomes neutres. Soit $x = N_i/(N_0 + N_i)$ le degré d'ionisation.

Nous avons

$$\log N_e = \log \frac{1-x}{x} + \log \frac{g_i}{g_0} - \chi\theta + \frac{3}{2} \log T + 15.4,$$

Dans la Fig. 1 on a la représentation de $\log N_e$ en fonction de $\log T$. Les courbes A et A' sont les courbes de demi ionisation pour l'hydrogène et pour l'oxygène 7 fois ionisé.

1.1. *Effet de pression.* — Lorsque les ions se rapprochent, aux densités élevées, l'énergie de l'électron lié, dans un atome, dans le champ de l'ion le plus proche, n'est plus négligeable devant l'énergie d'ionisation χ de l'atome; l'ionisation se produit sous l'effet de la pression. Les distances des ions deviennent de l'ordre du rayon des atomes. Soit a_0 le rayon de l'atome de Bohr, $a = a_0/Z$ le rayon d'un atome; l'effet de pression n'est plus négligeable, si $\frac{4}{3}\pi a^3 N_e \geq 1$ ou encore si

$$\text{Log } N_e \geq 24.2 + 3 \text{ Log } Z,$$

domaine limité par les courbes B (hydrogène) ou B' (oxygène).

1.2. *Comparaison de l'énergie électrostatique du milieu et de l'énergie cinétique des particules.* — L'énergie cinétique par degré de liberté est $\frac{1}{2}kT$, l'énergie potentielle d'un électron, situé à la distance moyenne $[(4\pi/3)N_e]^{-\frac{1}{3}}$ d'un ion, est

$$Ze^2 \left(\frac{4\pi}{3} N_e \right)^{\frac{1}{3}}.$$

Pour que l'équation des gaz parfaits soit valable, il faut:

$$Ze^2 \left(\frac{4\pi}{3} N_e \right)^{\frac{1}{3}} \leq kT,$$

soit

$$\text{Log } N_e \leq 8.9 + 3 \text{ Log } T - 3 \text{ Log } Z,$$

domaine limité par les courbes C (hydrogène) et C' (oxygène).

1.3. *Condition de dégénérescence.* — Il y a dégénérescence lorsque la longueur d'onde de de Broglie associée à l'énergie des électrons devient comparable à la distance des électrons $(\frac{4}{3}\pi N_e)^{-\frac{1}{3}}$. On a

$$\lambda = \frac{h}{m_e v} \simeq \frac{h}{m_e \sqrt{3kT/m_e}} = \frac{h}{\sqrt{3m_e kT}},$$

et le domaine de dégénérescence est défini par

$$\lambda > (\frac{4}{3}\pi N_e)^{-\frac{1}{3}},$$

soit .

$$N_e > 10^{16} T^{\frac{3}{2}}$$

domaine limité par la droite D .

1'4. *Comparaison de l'énergie électrostatique et l'énergie cinétique moyenne dans les cas des gaz dégénérés.* — L'énergie électrostatique moyenne d'un électron, $Ze^2(\frac{4}{3}\pi N_e)^{\frac{1}{3}}$, doit être plus petite que l'énergie cinétique moyenne (qui sera définie plus tard):

$$N_e^{\frac{1}{3}} > Ze^2 \frac{5}{3} \left(\frac{16}{3} \pi \right)^{\frac{1}{3}} \frac{m_e}{h^2}.$$

Cette relation définit un domaine limité par les courbes E (pour $Z=1$) ou E' (pour $Z=8$) (Fig. 1).

Dans la région hachurée (Fig. 1) l'énergie électrostatique ne sera pas négligeable.

Il est utile de mettre en évidence dans le diagramme $\log T$, $\log N_e$, les points représentatifs de l'état physique de l'intérieur des étoiles.

La courbe α est représentative du soleil. La courbe β correspond à une naine blanche typique; 99% de la masse d'une naine blanche typique est dégénéré.

2. — Equation d'état.

Nous partirons du théorème du viriel que nous allons démontrer rapidement pour les gaz classiques (non quantiques).

Soient

$$F_{ix} = m_i \frac{d^2 x_i}{dt^2},$$

les équations du mouvement. Après multiplication per $\frac{1}{2}x_i$, on obtient

$$\frac{1}{2} x_i F_{ix} = -\frac{1}{2} m_i \left(\frac{dx_i}{dt} \right)^2 + \frac{1}{2} \frac{d}{dt} \left(m_i x_i \frac{dx_i}{dt} \right).$$

En moyenne, le deuxième terme du membre de droite tend vers zero si le système est borné.

On obtient ainsi

$$-\frac{1}{2} \overline{x_i F_{ix}} = \frac{1}{2} m_i \overline{\left(\frac{dx_i}{dt} \right)^2}.$$

Si l'on appelle l'énergie cinétique K , l'équation du viriel s'écrit:

$$-\frac{1}{2} \sum \mathbf{r}_i \cdot \mathbf{F}_i = K$$

$\sum \mathbf{r}_i \cdot \mathbf{F}_i$ représente le viriel, introduit par Clausius.

Si les forces dérivent d'un potentiel φ

$$F_{ix} = - \frac{\partial}{\partial x_i} \varphi.$$

Supposons que l'énergie potentielle soit la somme des énergies potentielles mutuelles des particules prises deux à deux, et ne dépendent que de la distance r_{ij} à la puissance $-n$,

$$\varphi = \frac{1}{2} \sum_{ij} \frac{q_{ij}}{(r_{ij})^n}.$$

Si $n=1$, on a la loi de Coulomb. Compte tenu du fait que φ est fonction homogène du degré $-n$, le théorème du viriel peut s'écrire:

$$\frac{1}{2} n \bar{\varphi} + K = 0.$$

Si le système est enfermé dans un récipient, la force introduite par le mur s'écrit $-n \cdot P$, étant P la pression, et \mathbf{n} étant la normale dirigée vers l'extérieur.

La contribution du viriel s'écrira:

$$-\frac{1}{2} \int_s P(\mathbf{r} \cdot \mathbf{n}) dS = \frac{3}{2} PV,$$

en transformant l'intégrale des surface en intégrale de volume.

On obtient alors

$$PV = \frac{1}{3} \sum \frac{p_i^2}{m_i} + \frac{1}{3} n \bar{\varphi},$$

si $n > 3$, les intégrals dans $\bar{\varphi}$ convergent. Pour le cas $n=1$, ROSSELAND (1924) résout le problème des divergences en introduisant la description de Debye-Hückel du milieu ionisé.

Soit χ^{-1} la longueur de Debye; $\Psi = (e/r) \exp[-\chi r]$ le potentiel autour d'un ion. Chaque ion se trouve alors dans le potentiel $(C/r)(\exp[-\chi r] - 1)$, au fond d'une cuvette avec un potentiel $-C\chi$, ($r=0$).

L'énergie de l'ion est alors $-C^2\chi$. Si l'on fait la somme sur tous les ions, les ions ont tous été comptés deux fois, l'énergie totale s'écrit: $-\frac{1}{2} \sum C^2\chi$. En tenant compte de l'expression de la longueur de Debye, on obtient

$$PV = NkT \left[1 - \frac{1}{3} e^2 \frac{(\pi n e^2)^{\frac{1}{2}}}{(kT)^{\frac{3}{2}}} (\sum C_i Z_i^2)^{\frac{1}{2}} \right],$$

N = nombre total des particules libres,

C_i = concentration relative en nombre d'ions d'espèce i .

La parenthèse s'écrit numériquement

$$1 - 10^{-4.4} \left(\frac{n}{T^3} \right)^{\frac{1}{2}} (\sum C_i Z_i^2)^{\frac{1}{2}}.$$

L'énergie électrostatique est inférieure à l'énergie cinétique si

$$\left(\frac{n}{T^3} \right)^{\frac{1}{2}} (\sum C_i Z_i^2)^{\frac{1}{2}} \leq 10^{4.4}.$$

Dans la Fig. 1, la courbe F donnant l'égalité se trouve pour l'hydrogène nettement au dessous de la courbe C . En fait, il paraît évident que l'effet de l'énergie électrostatique est surestimé dans ce traitement.

On peut tenter d'améliorer l'évaluation de la correction en tenant compte des phénomènes collectifs dus aux interactions à grande distance.

3. - Phénomènes collectifs.

Les forces électrostatiques étant à long rayon d'action, les mouvements ne se font pas entièrement au hasard, mais en partie sous la forme de mouvements collectifs que l'on peut représenter comme une propagation d'ondes de fréquences très voisines de la fréquence de plasma (BOHM et PINES).

Le nombre de modes collectifs est celui de modes individuels dépendant de la valeur de χ^{-1} comparée à la distance d des particules: si $\chi^{-1} \sim d$ on a surtout des phénomènes collectifs. Le calcul du nombre des modes collectifs en a été fait par GABOR (*Proc. Roy. Soc., A* (1952)).

Soit k le nombre d'onde de l'onde de plasma, V_p la vitesse de phase, ν la fréquence; le nombre de modes dans l'intervalle $(k, k+dk)$ est:

$$4\pi\nu^2 d\nu / V_p^3 = \frac{1}{2\pi^2} \frac{\omega^2 d\omega}{V_p^3} \quad \omega \text{ pulsation.}$$

Considérons l'équation de dispersion

$$V_P^2 = \frac{3kT}{m_e} \frac{1}{(\omega/\omega_p)^2 - 1}.$$

A chaque mode appartient l'énergie $\frac{1}{2}kT$; donc l'énergie dans $d\omega$ est

$$u_\omega d\omega = \frac{2}{\pi^{\frac{1}{2}} 3^{\frac{1}{2}}} x^2 (x^2 - 1)^{\frac{3}{2}} \frac{N_e^{\frac{3}{2}} e^3}{(kT)^{\frac{1}{2}}} dx, \quad x = \frac{\omega}{\omega_p}.$$

Il n'est pas possible de séparer exactement les modes collectifs des modes individuels; mais GABOR admet qu'on passe assez nettement aux modes individuels pour $x=2$. Aussi l'intégral de 1 à 2 sur ω/ω_x donnera l'énergie moyenne

$$\bar{u} = \int_1^2 u_\omega d\omega = 1.2 \frac{e^3 N_e^{\frac{3}{2}}}{\sqrt{kT}},$$

valeur à introduire dans l'équation du viriel.

En fait, si l'on admet qu'il s'agit d'oscillations sinusoïdales, la moitié de l'énergie peut être considérée comme correspondant à l'énergie potentielle du plasma, et l'autre moitié à l'énergie cinétique. C'est donc $\frac{1}{2}u$ qu'il faut porter dans l'équation du viriel:

$$3PV = K - \frac{1}{2}\bar{u} \quad \text{ou} \quad PV = NkT \left(1 - 10^{-5.7} \frac{N_e^{\frac{1}{2}}}{T^{\frac{1}{2}}} \right),$$

compte tenu de $N_e = (N/2)$ (ionisation complète).

La séparation $\frac{1}{2}\bar{u} = K$ se place selon la courbe G du graphique de Fig. 1, qui est sans doute la plus correcte. Au dessus d'elle on a affaire essentiellement aux phénomènes collectifs. Si l'on admet l'équiparation entre K et φ on peut prendre pour équation d'état approchée:

$$PV = \frac{1}{2}NkT,$$

expression proposée seulement comme valable en ordre de grandeur.

II. Gaz dégénérés d'électrons.

L'étude des gaz dégénérés d'électrons, bien que sortant un peu du programme général de ce Cours sur le plasma, présente un grand intérêt astrophysique, et soulève un certain nombre de questions de principe.

1. — Gaz dégénérés au zéro absolu.

On dénombre facilement le nombre d'états possibles en comptant le nombre de cellules d'extension en phase pouvant être occupées par les électrons. Dans un parallélépipède de côté l_x , l_y , l_z , les longueurs d'onde associées aux composantes des vitesses des électrons sont

$$\lambda_x = h/p_x, \quad \lambda_y = h/p_y, \quad \lambda_z = h/p_z,$$

où p_x , p_y , p_z sont les composantes de la quantité de mouvement.

λ_x est compris un nombre entier de fois dans l_x :

$$\lambda_x = \frac{l_x}{k_x} \quad \text{ou} \quad k_x = \frac{p_x l_x}{h}.$$

Si l'on suppose tous les états occupés jusqu'à une certaine limite,

$$k_0^2 = k_{0x}^2 + k_{0y}^2 + k_{0z}^2,$$

le nombre total d'états est

$$\frac{4\pi}{3} k_0^3 = \frac{4\pi}{3} p_0^3 \frac{l_x l_y l_z}{h^3} = \frac{4\pi}{3} p_0^3 \frac{V}{h^3}.$$

Le spin des électrons étant $\frac{1}{2}$, le nombre d'électrons contenu dans 1 cm^3 au zéro absolu est lié à la limite de Fermi de la quantité de mouvement par la relation

$$N_e = \frac{8\pi p_0^3}{3h^3}.$$

A partir de l'expression relativiste de l'énergie

$$\frac{E}{m_e c^2} = \left(1 + \frac{p^2}{m_e^2 c^2}\right)^{\frac{1}{2}},$$

et du nombre d'électrons dans l'intervalle p , $p+dp$, on calcule aisément la pression P et l'énergie interne d'un gaz complètement dégénéré d'électrons.

En prenant comme variable $x = p_0/m_e c$ on obtient

$$(1) \quad \begin{cases} N_e = \frac{8\pi m_e^3 c^3}{3h^3} x^3, \\ P = \frac{\pi m_e^4 c^5}{3h^3} f(x), \quad f(x) = x(2x^2 - 3)(x^2 + 1)^{\frac{1}{2}} - 3 \operatorname{arctg} \sinh x, \\ U = \frac{\pi m_e^5 c^5}{3h^3} g(x), \quad g(x) = 8x^3[(x^2 + 1)^{\frac{1}{2}} - 1] - f(x). \end{cases}$$

Dans le cas des gaz partiellement dégénérés on doit calculer l'état le plus probable par les méthodes de la statistique quantique.

A titre d'exemple donnons l'expression de N_e et de P :

$$N_e = \frac{8\pi m_e^3 c^3}{h^3} \int_0^\infty \frac{\sinh^2 t \cosh t dt}{\frac{1}{\Lambda} \exp \left[\frac{m_e c^2 \cosh t}{kT} \right] + 1},$$

$$P = \frac{8\pi m_e^4 c^5}{3h^3} \int_0^\infty \frac{\sinh^4 t dt}{\frac{1}{\Lambda} \exp \left[\frac{m_e c^2 \cosh t}{kT} \right] + 1}.$$

Le paramètre Λ est défini par la première de ces équations.

Dans le cas des fortes dégénérescences, on peut calculer des formules approchées, qui permettent de tracer la courbe qui sépare dans le plan $\log T, \log N_e$, la région dégénérée de la région non dégénérée.

On peut avoir une idée de la signification physique de p_0 en comparant le nombre d'onde correspondant au rayon de la sphère occupée en moyenne par chaque électron; on a

$$\frac{8\pi}{3} \lambda_0^3 N_e = 1 \quad \text{et} \quad \frac{4\pi}{3} r_0^3 N_e = 1,$$

donc $\lambda_0 = r_0/2^{\frac{1}{2}}$, la longueur d'onde associée aux particules les plus rapides est de l'ordre de la distance mutuelle des électrons.

Lorsque $x \rightarrow 0$, $f(x) \sim \frac{8}{5}x^5$; si $x \rightarrow \infty$, $f(x) \sim 2x^4$.

Si on applique la formule (1), on peut obtenir la relation masse-rayon pour une sphère entièrement dégénérée. Si on applique l'approximation $f(x) \sim \frac{8}{5}x^5$ pour tout x , on trouve une relation $R(M)$ entre le rayon R et la masse M de l'étoile très différente (Fig. 2) (approximation non relativiste).

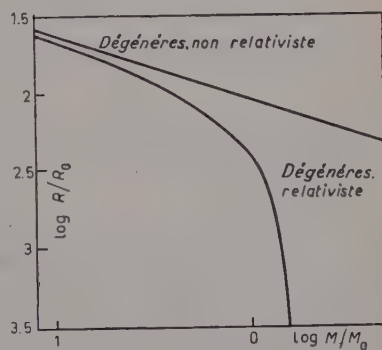


Fig. 2.

EDDINGTON a contesté l'emploi de (1) qui suppose les électrons libres; il affirmait qu'en l'état de collisions permanent, la formule non relativiste pour la pression reste valable même pour x très grand.

On peut répondre à la question posée par EDDINGTON par l'étude des phénomènes collectifs dans les plasmas. Lorsque les phénomènes collectifs sont négligeables, la formule (1), due à STONER et ANDERSON, est valable.

On peut renvoyer à l'article de SINGH (*Ap. Journ.*, **126**, 213 (1957)). Alors que d'habitude on sépare les phénomènes collectifs des phénomènes individuels en cherchant le chemin parcouru par un électron à la vitesse moyenne d'agitation pendant le temps d'une oscillation de plasma, il résulte du travail de SINGH qu'il faut remplacer la vitesse des électrons par la vitesse du mouvement quantifié des électrons piégés dans les cuvettes de potentiel dues aux charges d'espace. On a alors

$$\lambda_D^{-2} = \frac{4\pi N_e e^2}{\hbar \omega_p}.$$

Si on compare la longueur de Debye ainsi obtenue à la distance moyenne entre particules, on trouve

$$\frac{k_D}{k_0} \simeq \frac{10^{-2}}{N_e^{1/12}} < 1.$$

On est amené ainsi à définir une densité minimum limite $N_e > 10^{24}$ au delà de laquelle les phénomènes collectifs sont négligeables. En réalité il y a une certaine incertitude sur le coefficient numérique car on peut aussi comparer l'énergie associée aux modes collectifs à l'énergie cinétique totale des électrons, ce qui peut conduire à une valeur plus petite.

Dans la zone (C) les phénomènes collectifs dominent (Fig. 3). On peut admettre que dans cette région il y a une équipartition entre l'énergie cinétique et l'énergie potentielle des oscillations de plasma dans la région non dégénérée. Cela pourrait conduire à une valeur sensiblement égale à $\frac{1}{2} N k T$. Cette valeur est donnée à titre purement indicatif.

En réponse à une question de DE JAGER on peut considérer des naines blanches ayant épuisé toutes leurs ressources d'énergie (naines noires). Leur courbe représentative dans le plan $\log T$, $\log N_e$ pourrait alors traverser le domaine où les phénomènes collectifs sont importants. En raison du type de variation de la relation

$P/P_{\text{classique}}$ en fonction de la densité, on pourrait s'attendre à des propriétés remarquables de ces naines froides.

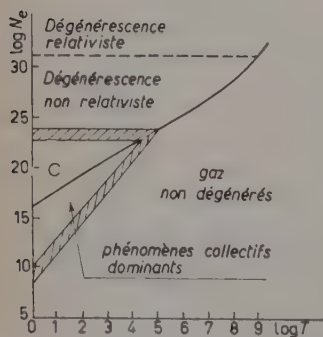


Fig. 3.

III. Influence de l'effet d'écran sur le taux des réactions thermonucléaires.

Afin de situer le problème, rappelons tout d'abord, de quelle façon on calcule ordinairement le taux des réactions thermonucléaires.

Soient deux espèces de noyaux, de masse m_1, m_2 à la même température T , de distribution maxwellienne des vitesses; le nombre de noyaux de vitesse $u_1 v_1 w_1, u_2 v_2 w_2$ est

$$dN_1 dN_2 = N_1 N_2 \exp \left[-\frac{m_1(u_1^2 + v_1^2 + w_1^2)}{2kT} - \frac{m_2(u_2^2 + v_2^2 + w_2^2)}{2kT} \right] \cdot \left(\frac{m_1}{2\pi kT} \right)^{\frac{3}{2}} \left(\frac{m_2}{2\pi kT} \right)^{\frac{3}{2}} du_1 dv_1 dw_1 du_2 dv_2 dw_2.$$

Pour calculer le nombre des chocs spécifiés, on prend comme nouvelles variables la vitesse du centre de gravité

$$u_0 = \frac{m_1 u_1 + m_2 u_2}{m_1 + m_2}, \quad v_0 = \frac{m_1 v_1 + m_2 v_2}{m_1 + m_2}, \quad w_0 = \frac{m_1 w_1 + m_2 w_2}{m_1 + m_2},$$

et la vitesse mutuelle des deux noyaux

$$u = u_1 - u_2, \quad v = v_1 - v_2, \quad w = w_1 - w_2.$$

On a alors

$$\begin{aligned} m_1(u_1^2 + v_1^2 + w_1^2) + m_2(u_2^2 + v_2^2 + w_2^2) &= \\ &= \frac{m_1 m_2}{m_1 + m_2} (u^2 + v^2 + w^2) + (m_1 + m_2)(u_0^2 + v_0^2 + w_0^2). \end{aligned}$$

En faisant l'intégrale sur la vitesse $u v w$, on obtient le nombre des paires de noyaux de vitesse relative $u v w$. On a

$$du_1 dv_1 dw_1 du_2 dv_2 dw_2 = du dv dw du_0 dv_0 dw_0,$$

$$d\mathcal{N} = N_1 N_2 \left(\frac{m_1 m_2}{m_1 + m_2} \cdot \frac{1}{2\pi kT} \right)^{\frac{3}{2}} \exp \left[-\frac{\bar{m}(u^2 + v^2 + w^2)}{2kT} \right] du dv dw.$$

Si σ est la section du choc, le nombre de chocs spécifié par seconde est

$$\begin{aligned} dp &= \sigma |v| N_1 N_2 \left(\frac{\bar{m}}{2\pi kT} \right)^{\frac{3}{2}} \exp \left[\frac{\bar{m}|v|^2}{2kT} \right] 4\pi |v|^2 d|v| = \\ &= \frac{\sigma N_1 N_2}{(\pi)^{\frac{3}{2}}} 4\pi \exp \left[-\frac{E}{kT} \right] \frac{E}{kT} \cdot \frac{dE}{kT} \sqrt{\frac{kT}{2\bar{m}}}. \end{aligned}$$

où E est l'énergie cinétique dans le système du centre de gravité. La section de choc σ peut se mettre sous la forme

$$\sigma = \frac{\sigma_{\text{nuc}}}{E} I(E),$$

où σ_{nuc} est un facteur purement nucléaire, et $I(E)$ est le facteur de pénétration de la barrière de potentiel,

$$I(E) = \exp \left[- \frac{2(2m)^{\frac{1}{2}}}{\hbar} \int_{r^*}^{r_E} \sqrt{U - E} \, dr \right],$$

ou r^* est le rayon du noyau composé, r_E la distance classique d'approche à l'énergie mutuelle E .

Le facteur I est le facteur le plus important, déterminant le taux de réactions entre les noyaux.

Pour calculer le nombre des réactions thermonucléaires par seconde, on doit considérer deux cas.

1) Le cas de la résonance: on a alors pour σ une expression de la forme

$$\sigma_{\text{nuc}} = \frac{\alpha E_i E_j}{(E - E_i)^2 + E_j^2},$$

formule de dispersion de Breit-Wigner.

2) Le cas où il n'y a pas résonance: σ_{nuc} est alors un facteur lentement variable avec l'énergie.

Dans le cas du potentiel de Coulomb, $U = (Z_1 Z_2 e^2)/r$, $E = (Z_1 Z_2 e^2)/r_E$ et par conséquent, en posant

$$I = \exp[-2W], \quad W = \frac{(2m)^{\frac{1}{2}}}{\hbar} (Z_1 Z_2 e^2)^{\frac{1}{2}} \int_{r^*}^{r_E} \sqrt{\frac{1}{r} - \frac{1}{r_E}} \, dr,$$

on peut remplacer r^* par zero dans l'intégrale, ce qui revient à incorporer une constante dans σ_{nuc} . En posant $r = x r_E$, on a

$$W = \frac{(2m)^{\frac{1}{2}}}{\hbar} (Z_1 Z_2 e^2)^{\frac{1}{2}} \left(\frac{Z_1 Z_2 e^2}{E} \right)^{\frac{1}{2}} \int_0^1 \sqrt{\frac{1}{x} - 1} \, dx.$$

L'intégrale vaut $(\pi/2)$, et par conséquent

$$2W = \frac{(2m)^{\frac{1}{2}}}{\hbar} \frac{Z_1 Z_2 e^2}{E^{\frac{1}{2}}} \pi.$$

Trois conclusions peuvent être tirées de ce résultat: les réaction nucléaires se produisent d'autant mieux

- 1) que E est plus grand (températures élevées),
- 2) que les charges $Z_1 Z_2$ sont plus petites,
- 3) que le facteur nucléaire σ_{nucl} est plus grand.

Pour calculer le nombre total des réactions, on calcule l'intégrale

$$\int_0^{\infty} \exp \left[-\frac{E}{kT} - \frac{(2\bar{m})^{\frac{1}{2}}}{\hbar} \pi \frac{Z_1 Z_2 e^2}{E^{\frac{1}{2}}} \right] dE.$$

Le terme dans l'exponentielle possède un maximum très aigu, ce qui permet le calcul de cette intégrale de façon approchée. Le maximum de l'exponentielle est atteint pour:

$$\frac{1}{kT} = \frac{1}{2} \frac{(2\bar{m})^{\frac{1}{2}} \pi Z_1 Z_2 e^2}{\hbar E^{\frac{3}{2}}}, \quad E = \left(\frac{(2\bar{m})^{\frac{1}{2}} \pi Z_1 Z_2 e^2 kT}{2\hbar} \right)^{\frac{2}{3}},$$

l'exponentielle étant $e^{-\tau}$, on a

$$\tau = 3 \left[\frac{\pi^2 e^4 Z_1^2 Z_2^2}{2\hbar^2 kT} \frac{A_1 A_2}{A_1 + A_2} H_0 \right]^{\frac{1}{3}}, \quad (H_0 = 1.66 \cdot 10^{-24} \text{ g}).$$

Par exemple, pour

$$^1\text{H} + ^1\text{H}, \tau = \frac{33.8}{(10^{-6}T)^{\frac{1}{3}}}; \quad ^{12}\text{C} + ^1\text{H}, \tau = \frac{133}{(10^{-6}T)^{\frac{1}{3}}}; \quad ^{14}\text{N} + ^1\text{H}, \tau = \frac{152}{(10^{-6}T)^{\frac{1}{3}}}.$$

Le nombre des réactions par seconde par centimètre cube se met finalement sous la forme

$$p_{ij} = K_{ij} N_i N_j \tau_{ij}^{\lambda} e^{-\tau_{ij}}.$$

Une discussion rapide des différentes réactions possibles, compte tenu des facteurs σ_{nucl} et du rôle de la barrière de potentiel, conduit à retenir les groupes suivantes, d'importance astrophysique

$$\left\{ \begin{array}{l} ^1\text{H} + ^1\text{H} \rightarrow ^2\text{D} + \varepsilon^+ + \gamma \quad (\text{BETHE, CRITCHFIELD}) \\ ^2\text{D} + ^1\text{H} \rightarrow ^3\text{He} + \gamma \\ ^3\text{He} + ^3\text{He} \rightarrow ^4\text{He} + ^1\text{H} + ^1\text{H} \quad (\text{FOWLER, SCHATZMAN}) \\ ^3\text{He} + ^4\text{He} \rightarrow ^7\text{Be} \\ ^7\text{Be} + ^1\text{H} \rightarrow ^8\text{B} \rightarrow ^8\text{Be} \rightarrow 2^4\text{He} \quad (\text{FOWLER}) \end{array} \right\} \left\{ \begin{array}{l} ^1\text{H} + ^{12}\text{C} \rightarrow ^{13}\text{N} + \gamma \quad (\text{BETHE, WEIZSÄCKER}) \\ ^{13}\text{N} \rightarrow ^{13}\text{C} + \varepsilon^+ + \gamma \\ \text{etc...} \\ (\text{connu sous le nom de cycle du carbone}). \end{array} \right.$$

Lorsque, dans les conditions du laboratoire, on part d'un mélange donné à l'avance, on doit considérer avantagement $^2\text{H} + ^2\text{H}$, $^3\text{H} + ^2\text{H}$, $^3\text{H} + ^3\text{H}$ qui ont de très grands σ_{nucl} , et une barrière de potentiel peu importante. Les discussions détaillées de ces réactions ont fait l'objet de nombreuses publications sur lesquelles je ne reviens pas.

Je voudrais examiner maintenant plus en détail certains aspects des réactions thermonucléaires et en particulier le rôle de la charge d'espace. Si l'on considère les équations linéaires du mouvement des ions et des électrons on a

$$N_i m_i \frac{\partial v_i}{\partial t} = N_i Z e E - \text{grad } P_i,$$

$$N_e m_e \frac{\partial v_e}{\partial t} = - N_e e E - \text{grad } P_e,$$

$$\text{div } E = 4\pi e (N_i Z - N_e),$$

et les équations de continuité

$$\frac{\partial N_i}{\partial t} = - N_i \text{div } v_i,$$

$$\frac{\partial N_e}{\partial t} = - N_e \text{div } v_e.$$

En prenant la divergence des deux premiers, on obtient en négligeant les produits des quantités petites:

$$N_i m_i \frac{\partial}{\partial t} \text{div } v_i = N_i Z e \text{div } E - \nabla^2 P_i,$$

$$N_e m_e \frac{\partial}{\partial t} \text{div } v_e = - N_e e \text{div } E - \nabla^2 P_e,$$

et par élimination

$$- m_i \frac{\partial^2 N_i}{\partial t^2} = N_i Z e [4\pi e (N_i Z - N_e)] - \nabla^2 P_i,$$

$$- m_e \frac{\partial^2 N_e}{\partial t^2} = - N_e e [4\pi e (N_i Z - N_e)] - \nabla^2 P_e.$$

Deux approximations peuvent être faites:

1) le fluide d'ions est remplacé par une distribution $n_i = \text{constante}$, ce qui conduit à

$$\nabla^2 N_e - \frac{1}{kT/m_e} \frac{\partial^2 N_e}{\partial t^2} = \frac{\omega_{pe}^2}{kT} (N_i Z - N_e);$$

2) le fluide d'électrons est remplacé par une distribution $N_e = ct_e$, ce qui conduit à

$$\nabla^2 N_i - \frac{1}{kT/m_i} \frac{\partial^2 N_i}{\partial t^2} = -\frac{\omega_{pi}^2}{kT} (N_i Z - N_e).$$

Si l'on considère un ion en mouvement à la vitesse v , on peut obtenir la distribution des charges autour de l'ion, en partant de la solution

$$Ze \frac{e^{-x^2}}{r}$$

et en effectuant une transformation de Lorentz sur la grandeur r' on obtient:

$$r' = \frac{(x - vt)^2}{\sqrt{1 - v^2/c^2}} + y^2 + z^2,$$

où $c^2 = c_e^2 = kT/m_e$ dans le cas des électrons et $c^2 = c_i^2 = kT/m_i$ dans les cas des ions. Dans le domaine des réactions thermonucléaires, la vitesse v des ions, est intermédiaire entre les vitesses c_i et c_e . Examinons donc comment se comporte la charge d'espace autour d'un ion en mouvement. Si $v < c$, la distribution des charges prend l'aspect d'un ellipsoïde aplati; l'applatissement de l'ellipsoïde augmente quand augmente la vitesse. Pour $v > c$, les charges sont distribuées dans un cône, mais la distribution des charges n'est pas influencée par la présence de l'ion à l'avant et à l'arrière de son sens de propagation. Dans le cas de réactions thermonucléaires, dans les conditions usuelles, on pourra admettre que les ions en mouvement sont accompagnés par la charge d'espace des électrons, mais ignorent la distribution des ions, ou plus exactement, vont trop vite pour pouvoir l'influencer.

Dans ces conditions, on pourra admettre, au moins en première approximation, qu'au voisinage d'un ion de charge Z , le potentiel n'est plus coulombien, mais est modifié par la présence des électrons en

$$U = Z_1 Z_2 e^2 \left[\frac{1}{r} - \frac{3}{2} \frac{1}{r_0} + \frac{1}{2} \frac{r^2}{r_0^3} \right],$$

avec

$$\frac{4}{3} \pi r_0^3 N_e = Z.$$

En raison de la charge d'espace, le facteur de pénétration $\Gamma(E)$ va être augmenté, la réaction se trouve facilitée.

IV. Réactions thermonucléaires.

Avant d'étudier le rôle de l'effet d'écran sur les réactions thermonucléaires, je voudrais examiner trois aspects des phénomènes qui se produisent dans un plasma chauffé par les réactions nucléaires.

1. — Parcours moyens.

Les particules produites dans les réactions thermonucléaires sont en général des particules de grande énergie, de l'ordre de plusieurs MeV, c'est-à-dire de plusieurs ordres de grandeurs plus grand que l'énergie thermique des particules constitutives du plasma.

Pour donner une idée de l'ordre de grandeur du parcours moyen de ces particules de grande énergie, nous allons utiliser les formules que Mr. FERRARO a données dans l'étude des collisions entre deux particules.

Pour des particules de masse m_2 , heurtées par une particule de masse m_1 , nous avons la variation de vitesse relative dg dans le temps dt :

$$g \, dg = - \frac{2(Ze^2)^2}{g^2 m_2} \left(\frac{1}{m_1} + \frac{1}{m_2} \right) \frac{2\pi b \, db \, N_2 g \, dt}{b^2 + b_1^2},$$

avec

$$b_1 = \frac{Ze^2}{g^2} \frac{m_1 + m_2}{m_1 m_2},$$

où on déduit immédiatement

$$\frac{g^4}{4} = \frac{g_0^4}{4} - \frac{2(Ze^2)^2}{m_2} \frac{1}{m} l \pi N_2 \log \frac{b_0^2 + b_1^2}{b_1^2}.$$

Si l'on admet que le parcours a lieu toujours dans la même direction, et se termine par $g = 0$, on a

$$l = g_0^4 \left\{ 16\pi \frac{(Ze^2)^2}{m_2} \frac{1}{m} N_2 \log \frac{b_0}{b_1} \right\}^{-1}.$$

Il est commode de mettre en évidence la distance mutuelle entre atomes d'espèce 2, n_2^{-1} , l'énergie cinétique de la particule incidente, $(m/2)g_0^2$ dans le système du centre de gravité. On a alors

$$\frac{l}{r_0} \simeq E_0^2 \frac{m_2}{m} \frac{1}{4\pi (Ze^2/r_0)^2 \log b_0/b_1}.$$

En electron volt

$$\frac{Ze^2}{r_0} = \{10^{-6.85} N_e^{\frac{1}{2}}\} eV.$$

Pour $\log(b_0/b_1)$, (b_0 = longueur de Debye) nous avons en remplaçant g par g_0 ,

$$\log \frac{b_0}{b_1} = \log \left(\frac{4\pi N_2 e^2}{kT} \right)^{-\frac{1}{2}} \frac{E_0}{2Ze^2}.$$

Ce logarithme prend des valeurs de l'ordre de 20.

Pour $N_e \cong 10^{18}$, $r_0 \cong 10^{-6}$, $l/r_0 \cong 10^{11.2}$, $l \cong 10^{5.2} \cong 1$ km. Dans des conditions stellaires, $r_0 \cong 10^{-8.5}$, $l/r_0 \cong 10^{-6.2}$, $l \cong 0.005$ cm. Il est donc évident que dans les réacteurs thermonucléaires les particules chargées de grande énergie qui sont produites seront perdues par le plasma.

2. - Mécanisme d'échange de température.

Considérons maintenant le mécanisme par lequel les particules de grande énergie apportent de la chaleur au plasma. Nous considérons pour cela une particule (2) de vitesse V_2 , grande comparée à la vitesse moyenne V_1 des particules (1) avec lesquelles elle échange de l'énergie. En mettant V_2 le long de l'axe des z , et en appelant ω l'angle de la vitesse V_2 et de la vitesse V_1 , (Fig. 4) on tire aisément des formules de collision données par Mr. FERARO les valeurs des composantes de la vitesse d'une particule (1) après collision:

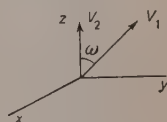


Fig. 4.

$$V_1 \sin \omega - \frac{m_2}{m_1 + m_2} (V_1 \cos \omega - V_2) \delta,$$

$$V_1 \cos \omega + \frac{m_2}{m_1 + m_2} V_1 \sin \omega \delta,$$

avec, pour δ , angle de déviation,

$$\delta = \frac{2Ze^2}{b} \frac{m_1 + m_2}{m_1 m_2} \frac{1}{V_1^2 + V_2^2 - 2V_1 V_2 \cos \omega}.$$

Comme nous supposons $V_2 \gg V_1$, on peut procéder à d'importantes simplifi-

cations et écrire pour les composantes V'_1 :

$$V_x = V'_x,$$

$$V_y = V'_y,$$

$$V_z + \frac{2Ze^2}{bm_1 V_2} = V'_z.$$

La probabilité des valeurs V'_x , V'_y , V'_z est donnée par:

$$\exp \left[\frac{m_1}{2kT} \left\{ \left(V'_z - \frac{2Ze^2}{bm_1 V_2} \right)^2 + V'^2_x + V'^2_y \right\} \right] \left(\frac{m_1}{2\pi kT} \right)^{\frac{3}{2}} dV'_x dV'_y dV'_z \frac{b db}{2b_0^2}.$$

L'intégration sur b , de 0 à b_0 , nous montre que la distribution des vitesses se trouve modifiée au voisinage des vitesses $(2Ze^2/bm_1 v_2)$, qui sont petites. Sans même chercher à intégrer rigoureusement cette densité de probabilité, compte tenu de la distribution des vitesses V_2 , on voit que la distribution des vitesses va se trouver alimentée d'un bout à l'autre de la distribution des vitesses par l'addition d'une petite quantité

$$V_1 \cong \left(\frac{2Ze^2}{b_0 m_1 V_2} \right) \ll \sqrt{\frac{2kT}{m_1}}.$$

Le léger excès dans la distribution des vitesses qui va en résulter (Fig. 5),

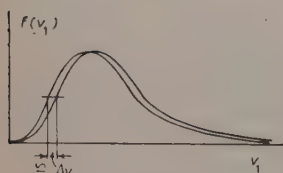


Fig. 5.

va se trouver redistribué par les collisions entre particules (1) sur toute la distribution des vitesses. On notera en particulier que les particules produites par les réactions thermonucléaires étant des particules de grande énergie, modifient peu au passage les vitesses des particules du plasma, et par conséquent chauffent le plasma par addition d'une très petite quantité à toutes les vitesses.

3. - Température des ions et des électrons.

Dans les collisions l'énergie des ions de grande vitesse est transférée aux ions et aux électrons et une portion un peu plus grande de l'énergie aux électrons, si bien qu'*a priori* on devrait s'attendre à trouver une température des électrons un peu supérieure à celle des ions.

Cependant la chaleur produite dans le milieu est rayonnée par les électrons, si bien que les électrons vont être à une température légèrement inférieure à celle des ions. Le calcul du transfert d'énergie des ions aux électrons lorsque

leur température est différente, est un calcul classique (SPITZER, 1941). Il faut naturellement tenir compte exactement de la géométrie des collisions. On trouve alors, approximativement

$$\frac{\Delta E}{\Delta t} \cong \frac{\frac{3}{2}k(T_i - T_e)}{\tau} N_i = N_i \frac{T_i - T_e}{T} \sqrt{3} \omega_p \frac{Z^2 e^2}{b_1} \log \left(\frac{b_1^2}{\mu^2} + 1 \right),$$

en utilisant les notations de FERRARO.

En raison de la grande vitesse des ions produits par les réactions thermonucléaires, leur énergie se répartit à peu près également entre ions et électrons; seule l'énergie apportée aux ions est ensuite transférée des ions aux électrons. On a donc

$$\frac{\Delta E}{E} = \frac{1}{2} Q.$$

Q est proportionnel à n_i^2 , si bien que $T_i - T_e$ ne dépend pratiquement que de la température. A titre d'exemple, en écrivant pour les réactions protons-protons

$$Q = 10^4 \left(\frac{\rho}{100} \right)^2 \left(\frac{T}{14 \cdot 10^6} \right)^4,$$

on obtient approximativement (sans chercher à raffiner sur le coefficient numérique)

$$T_i - T_e \cong 10^{-58} \frac{T^{7/2}}{\log a},$$

même pour une réaction à plus grande section de choc (D-D ou D-T) la différence de température est évanescence.

On sait cependant que dans les décharges à haute intensité la différence $T_i - T_e$ peut être notable; mais il s'agit là d'un effet dû essentiellement à la brièveté du phénomène comparée aux temps de relaxation des ions et des électrons.

4. - Rôle de l'effet d'écran.

Nous revenons ici à l'étude d'un problème plus spécifiquement astrophysique, dans le domaine de densité qui est important. Si l'on modifie, comme nous l'avons déjà dit, le potentiel coulombien par un potentiel dû à une charge l'espace uniformément répartie, on a une nouvelle valeur de la distance classique d'approche. En prenant r_E comme variable, le terme exponentiel peut

s'écrire (E est l'énergie cinétique dans le système du centre de gravité):

$$\exp\left[-\frac{E}{kT}\right] \Gamma(E) = \exp\left[-\frac{Z_1 Z_2 e^2}{kT} \left(\frac{1}{r_E} - \frac{3}{2} \frac{1}{r_0} + \frac{1}{2} \frac{r_E^2}{r_0^3}\right) - \frac{2\pi^2}{h} e(2\bar{m} Z_1 Z_2 r_E)^{\frac{1}{2}}\right].$$

Il a son maximum pour une valeur $r_E \cong r_m$. Introduisons la longueur définie par

$$r_1^3 = \frac{2\hbar^2 e^2 Z_1 Z_2}{m\pi^4 k T^2},$$

et

$$(r_1/r_0) = x.$$

La distance r_m est alors donné par

$$\left(\frac{r_m}{r_0}\right)^3 = 1 + \frac{2}{x^3} [1 - (1 + x^3)]^{\frac{1}{2}}.$$

On a aussi

$$x = \left[\frac{8\hbar^2 e^2 Z_2}{3\pi^3 A k^2 \bar{m}^2} \right]^{\frac{1}{2}} \left(\frac{\rho}{\mu_e T^2} \right)^{\frac{1}{2}}.$$

Le calcul de l'intégrale $\int \exp[-E/kT] \Gamma(E) d(E)$ conduit à un facteur exprimant l'augmentation du taux de réactions thermonucléaires

$$A = f_2(x) \exp[\tau f_1(x)],$$

les fonctions f_1 et f_2 étant définies dans le texte.

Quand x est petit, on peut écrire (faibles densités)

$$A = \exp\left[\frac{\tau x}{2^{5/3}}\right],$$

Quand x est grand on peut écrire (fortes densités)

$$A = 2^{\frac{1}{2}} x \exp\left[\tau \left(1 - \frac{2^{\frac{1}{2}}}{3} x^{-\frac{1}{2}}\right)\right].$$

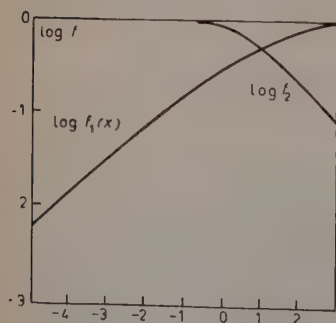


Fig. 6.

La Fig. 6 donne les fonctions $f_1(x)$ et $f_2(x)$ dans une échelle logarithmique.

A titre d'exemple, considérons le cas de la réaction proton-proton. Le facteur d'accroissement A est égal à

$$A = \exp\left[\frac{3.38 \cdot 10^5 \rho^{\frac{1}{2}}}{T \mu_e^{\frac{1}{2}}}\right]$$

Dans le cas solaire, $T = 10^7$, $\rho = 10^2$, le facteur A est très voisin de l'unité; mais le facteur A augmente très vite avec la densité. Dans les conditions typiques d'une naine blanche, $\rho = 10^6$, $T = 10^7$, $\mu_e \cong 2$, $A = 14.6$. Le rôle de ce facteur A est sensible cependant en ce qui concerne la structure interne des étoiles. En effet, considérons rapidement le problème de l'apparition d'une zone convective au centre d'une étoile. On admet ordinairement qu'une zone convective apparaît lorsque la condition

$$\left(\frac{d \log T}{d \log P} \right)_{\text{adiab}} < \left(\frac{d \log T}{d \log P} \right)_{\text{rad}}$$

est satisfaite.

La première quantité est liée au rapport des chaleurs spécifiques et vaut $(\gamma - 1)/\gamma$ dans le cas du gaz parfait. La deuxième quantité est celle qui est effectivement présente dans l'étoile. Dans les régions centrales

$$\left(\frac{d \log T}{d \log P} \right)_{\text{rad}} = \left(\frac{16\pi G c P_R}{\kappa \varepsilon P_G} \right)^{-1},$$

κ coefficient d'absorption par gramme,

ε taux de production d'énergie et par gramme par seconde,

P_G pression gazeuse,

P_R pression de radiation.

Les conditions centrales, donc le débit d'énergie par gramme, dépendent des sources d'énergie.

L'effet d'écran rend moins sensible le débit d'énergie avec variations de température, effet qui n'est pas compensé par la plus grande sensibilité aux variations de densité. Les sources d'énergie se trouvant plus réparties à l'intérieur de l'étoile, ε au centre sera plus petit. La valeur de $(d \log T / d \log P)_{\text{rad}}$ au centre étant abaissée, la condition de stabilité pourra se trouver satisfaite pour des valeurs de la masse des étoiles un peu plus grandes qu'il n'est admis ordinairement. Le résultat a des conséquences sensibles pour l'évolution des étoiles, car il modifie sensiblement le modèle qu'il faut adopter pour décrire la séquence évolutive des étoiles de masse voisine de la masse solaire.

D'autre part, dans le cas du soleil, ce résultat conduit presque certainement à admettre l'absence actuelle de zone convective centrale. Ce problème, a déjà été discuté à Stockholm en 1956, en relation avec la question de l'origine des taches solaires.

V. Influence du cortège sur les réactions thermonucléaires.

Nous avons examiné déjà l'influence du cortège des électrons sur le taux des réactions thermonucléaires entre particules chargées. Trois autres effets doivent être étudiés: influence sur la radioactivité α , sur la radioactivité β , sur la fission spontanée.

1. - Radioactivité α .

Nous avons déjà vu que la charge d'espace des électrons libres, relevait le potentiel électrostatique autour du noyau (Fig. 1). La conséquence en était une plus grande facilité de pénétration de la barrière du potentiel. Au contraire, un niveau de désintégration α va se trouver séparé de l'extérieur du noyau par une plus grande épaisseur de la barrière de potentiel (Fig. 7). La durée de vie de la radioactivité α s'en trouvera augmentée. On pourrait même, à la rigueur, imaginer un niveau α qui serait emprisonné au dessous du niveau de potentiel U_∞ . Nous verrons toutefois que, en pratique, ce cas est inimaginable.

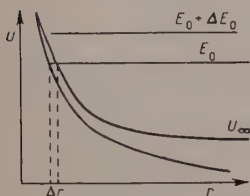


Fig. 7.

En prenant cette fois, comme zéro du potentiel, un certain potentiel à l'intérieur du noyau, nous écrirons

$$U = \frac{Z_1 Z_2 e^2}{r} \left\{ 1 + \frac{1}{2} \left(\frac{r}{r_0} \right)^3 \right\},$$

où r_0 est le volume occupé par Z électrons. Si l'on suppose que r_0 est grand par rapport au rayon du noyau, on peut calculer en première approximation la variation du terme présent dans l'expressoin de la transparence de la barrière de potentiel:

$$\frac{\Delta 2W_\alpha}{2W_\alpha} = \frac{35}{64} \left(\frac{Z_1 Z_2 e^2}{Er_0} \right)^3 = 10^{-38.164} \frac{N_e (Z_1 Z_2)^3}{E_{\text{MeV}}^3}.$$

Pour $Z_1 = 100$, $Z_2 = 2$, $E_{\text{MeV}} \simeq 1$, la période est multipliée par $e = 2.718$ pour une densité de $10^{29.2}$ électrons par cm^3 .

2. - Radioactivité β .

Considérons la transition

$${}^Z\text{X}_A \rightarrow {}^{Z+1}\text{X}_A + \beta^{-1} + \chi_{\text{MeV}}.$$

Si le noyau se trouve plongé dans un gas d'électrons possédant assez d'énergie, la transition inverse

$${}^{Z+1}\text{X}_A + \beta^{-1} + \chi_{\text{MeV}} \rightarrow {}^Z\text{X}_A$$

est possible.

Considérons spécialement les gas dégénérés d'électrons. L'énergie maximum des électrons est donnée par

$$E_{\text{MeV}} = 0.512 \{ [1 + 10^{-19.85} N_e^{\frac{2}{3}}]^{\frac{3}{2}} - 1 \}.$$

Tant que $N_e < 10^{29.8}$ on peut écrire:

$$E_{\text{MeV}} \cong 10^{-20.44} N_e^{\frac{2}{3}}.$$

Soit une radioactivité β d'énergie E . Dès que le nombre d'électrons par centimètre cube N_e est assez grand, la capture β devient suffisante pour contrebalancer complètement la radioactivité; de tels effets n'ont de chance de se produire que si l'énergie de l'émission β est faible.

Par exemple



Il lui correspond une densité $N_e = 10^{28.04}$, très vite atteinte dans les naines blanches.

Aux densités élevées la capture β equilibre la radioactivité β et entraîne une diminution du nombre d'électrons libres. Une des conséquences les plus remarquables de cette propriété est que la compressibilité

$$(d \log P)/(d \log \varrho) = \gamma$$

descend au dessous de la valeur $\frac{4}{3}$ pour N_e assez grand ($N_e > 10^{32}$). On peut montrer en astrophysique qu'une étoile où $\gamma < \frac{4}{3}$ dans une zone suffisamment étendue peut être dynamiquement instable. Elle ne peut osciller, car elle est en équilibre instable. Sans l'effet d'une contraction la pression centrale diminue, si bien que l'étoile ne résiste pas à l'effondrement; inversement, sous l'effet d'une dilatation, la pression centrale augmente au lieu de diminuer, et l'étoile explose.

Ces circonstances se trouvent réunies dans les naines blanches, dès la masse $M = 1.27 M_{\odot}$, ce qui impose une stricte limitation à l'existence des naines blanches.

3. — Fission spontanée.

L'un des exemples le plus remarquable d'atomes subissant la fission spontanée, est celui du Californium ^{254}Cf , de période 55 jours. Cette période est en effet remarquablement courte. Un atome subissant la fission spontanée en 2 atomes Z_1, Z_2 est situé sur un niveau d'énergie assez élevé pour qu'il puisse, par passage sous la barrière du potentiel, se séparer en deux.

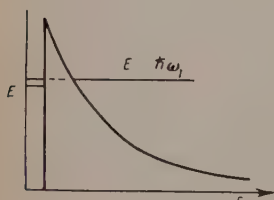


Fig. 8.

Le noyau peut se déformer de différentes façons. Dans la théorie élémentaire de Bohr-Wheeler, la déformation est décrite par une fonction sphérique d'ordre l . A chaque type de déformation correspond une pulsation ω_l , si bien que le niveau de l'atome se trouve en réalité séparé en plusieurs niveaux d'énergie $\hbar\omega_l$ au dessous du niveau E (Fig. 8).

Sous l'effet du nuage d'électrons négatifs qui entourent le noyau la période va être changée, ce qui entraîne un déplacement $\Delta\hbar\omega_l$ du niveau d'énergie sur lequel se produit la fission spontanée. En première approximation on pourra écrire

$$\frac{\Delta\omega_l}{\omega_l} = \frac{1}{2} \frac{2l(l-1)}{2l+1} \frac{4\pi}{3} \frac{Ze}{H_0 A} \sigma \frac{1}{\omega_l^3},$$

où σ est la charge d'espace des électrons au voisinage de la surface du noyau. Si l'on suppose, pour un instant, que la charge d'espace, est due à des électrons uniformément distribués autour du noyau,

$$\sigma = \frac{Ze}{\frac{4}{3}\pi d^3} = eN_e.$$

On aura donc

$$\Delta\hbar\omega_l = \frac{1}{2} \frac{2l(l-1)}{2l+1} \frac{4\pi}{3} \frac{Ze^2}{H_0 A} N_e \frac{\hbar^2}{\hbar\omega_l}.$$

Numériquement

$$\Delta(\hbar\omega_l)_{\text{MeV}} = \frac{l(l-1)}{2l+1} \frac{Z}{A} N_e \frac{1}{(\hbar\omega_l)_{\text{MeV}}} \cdot 10^{-37.222}.$$

Il s'agit encore d'un très petit phénomène sensible seulement aux très hautes densités.

Stellar Atmospheres as a Plasma.

L. BIERMANN

Max Planck-Institut für Physik und Astrophysik - München

1. - General considerations.

1.1. *Equations of motion and Ohm's law.* - In stellar atmospheres the ionized gas may be regarded as having essentially equal densities, N , of ions and electrons. For the case of complete ionization the equations of motion for the two fluids may be written

$$(1_{i(e)}) \quad Nm_{i(e)} \frac{d}{dt} \mathbf{v}_{i(e)} \pm Nm_{\text{red}} \nu (\mathbf{v}_i - \mathbf{v}_e) = \pm eN \left[E + \frac{\mathbf{v}_{i(e)}}{c} \times \mathbf{B} \right] + N\mathbf{K}_{i(e)},$$

where $\mathbf{K}_{i(e)}$, the force per particle, is defined by

$$(2) \quad N\mathbf{K}_{i(e)} = \text{grad } p_{i(e)} + Nm_{i(e)}\mathbf{g}.$$

In these equations the subscript i refers to the ions, the subscript e to the electrons, the \pm is always $+$ for the former and $-$ for the latter, m_{red} is the reduced mass $m_i m_e / (m_i + m_e)$, ν is the mean frequency of collisions between ions and electrons, \mathbf{g} is the gravitational acceleration (or any equivalent acceleration), and the other symbols have the usual meanings. We may assume that there is no polarization of the ions, hence $\mathbf{D} = \mathbf{E}$, and no magnetization, hence $\mathbf{H} = \mathbf{B}$ and all relative charge motion is included in current density. Unrationalized Gaussian (cgs) units are used. It should be unnecessary to discuss farther the derivation and content of these equations in view of the earlier lectures by LEHNERT and FERRARO.

Define the mass velocity

$$(3) \quad \mathbf{v} = (m_i \mathbf{v}_i + m_e \mathbf{v}_e) / (m_i + m_e)$$

and the electric current density

$$(4) \quad \mathbf{j} = eN(\mathbf{v}_i - \mathbf{v}_e).$$

By adding (1_i) and (1_e), one gets the equation for the mass motion

$$(5) \quad N(m_i + m_e) \frac{d}{dt} \mathbf{v} = \frac{1}{c} \mathbf{j} \times \mathbf{B} + N(\mathbf{K}_i + \mathbf{K}_e),$$

where in (1) the substantial derivative is defined in terms of \mathbf{v}_i or \mathbf{v}_e while in (5) and the following equations it is defined in terms of \mathbf{v} . By multiplying (1_i) by m_e , (1_e) by m_i , and combining, one gets

$$(6) \quad \frac{m_i m_e}{eN} \left(\frac{d\mathbf{j}}{dt} + \mathbf{v} \mathbf{j} \right) = e(m_i + m_e) \left[\mathbf{E} + \frac{\mathbf{v}}{c} \times \mathbf{B} \right] \\ + m_e \mathbf{K}_i - m_i \mathbf{K}_e - \frac{1}{Ne} (m_i - m_e) \mathbf{j} \times \mathbf{B}.$$

By neglecting $d\mathbf{j}/dt$ and the terms on the right hand side that are multiplied by m_e , and by eliminating the $\mathbf{j} \times \mathbf{B}$ term with the aid of (5) one gets Ohm's law,

$$(7) \quad \mathbf{j} = \sigma(\mathbf{E}^m + \mathbf{E}^e),$$

where the scalar conductivity is

$$(8) \quad \sigma = \frac{e^2 N}{m_e \nu},$$

the electric field in an inertial frame moving with the plasma is

$$(9) \quad \mathbf{E}^m = \mathbf{E} + \frac{\mathbf{v}}{c} \times \mathbf{B},$$

and the impressed electromotive force is

$$(10) \quad e\mathbf{E}^e = -\frac{1}{N} \text{grad } p_i + m_i \left(\mathbf{g} - \frac{d\mathbf{v}}{dt} \right).$$

There are possible, other, equally good, definitions of \mathbf{E}^e each with a different expression for σ , but the above definition has the advantage that with it the conductivity is a scalar instead of a tensor (see SCHLÜTER, 1950). Where three fluids must be considered, as in the case of only partial ionization *e.g.* in the ionosphere, it is always necessary to use a tensor conductivity (LUKAS and SCHLÜTER, 1953).

This treatment not is based on the assumption that the collision frequency is large compared to the gyro-frequency. SPITZER has shown (*Physics of Fully Ionized Gases*, p. 84) that when the two frequencies are comparable only the conductivities parallel and normal to the magnetic field differ by a factor of about two. No complete treatment has yet been given for the case in which the gyro-frequency is much larger than the collision frequency, but even in this extreme case a description similar to the above is still possible.

The σ of (8) is independent of the magnetic field strength. In some of the alternative formulations of Ohm's law σ decreased with increasing B and hence it was often believed that the presence of a magnetic field would increase the dissipation of energy due to ohmic losses. However this dissipation is caused by collisions and these are not greatly affected by the magnetic field. Thus the magnetic field should not much alter the dissipation.

1'2. *Maxwell's equations.* - In addition to the equations (5) and (7), one has the Maxwell equations

$$(11) \quad \text{curl } \mathbf{B} = \frac{4\pi}{c} \mathbf{j},$$

and

$$(12) \quad \text{curl } \mathbf{E} = -\frac{1}{c} \dot{\mathbf{B}}.$$

In (11) the displacement current is neglected. This is justifiable for most astrophysical applications with the exception of a few cases, *e.g.* where plasma oscillations must be considered. It is useful also to introduce in (12) the electric field in the co moving system, which gives

$$(13) \quad \text{curl } \mathbf{E}^m = -\frac{1}{c} \dot{\mathbf{B}}.$$

Here $\dot{\mathbf{B}}$ is defined by

$$(14) \quad \dot{\mathbf{B}} = \dot{\mathbf{B}} - \text{curl } [\mathbf{v} \times \mathbf{B}]$$

and measures the rate of changes of the flux of \mathbf{B} through an infinitesimal surface element moving and deforming with the fluid.

In most astrophysical applications \mathbf{E}^e is small, σ is very large, \mathbf{j} is bounded, and hence \mathbf{E}^m is small even though the two terms on the right hand side of (9) may be individually large. Thus the electric field in the co-moving system is very small compared to that usually found in a stationary system, and the essential content of (9) is that

$$(15) \quad \mathbf{E} \approx -\frac{\mathbf{v}}{c} \times \mathbf{B}.$$

Therefore the energy density in the electric field is of the order of $(v/c)^2$ times that in the magnetic field. In typical cases this ratio is 10^{-10} and even for high velocities is only 10^{-6} .

1'3. *Numerical examples.* — The conductivity typically varies between about 10^{12} s^{-1} as in cool stellar atmospheres, to 10^{16} s^{-1} as in the corona. For a sun spot with a diameter of about 10^4 km and a magnetic field of about 10^3 gauss , $|\text{curl } \mathbf{B}| \approx 10^{-6}$. Since $\sigma \approx 10^{12} \text{ s}^{-1}$, this gives by (11) and (7) $E^m \approx 10^{-9}$. With $v \approx 3 \text{ km/s}$, (15) gives $E \approx 10^{-2} \gg E^m$. From (12) and (13) it then follows that $|\dot{\mathbf{B}}| \approx 10^{-8} \ll |\mathbf{B}| \approx 10^{-3}$ or 10^{-2} . The observed life of the spot is of the order of days or weeks, *i.e.* 10^5 to 10^6 s so that again $|\dot{\mathbf{B}}|$ is 10^{-3} . Since $|\dot{\mathbf{B}}|$ is so much smaller, the magnetic flux must endure very much longer than the visible spot.

The electric fields due to the gravitational term and the expression for the impressed electromotive forces are given by (10). In the approximation of hydrostatic equilibrium one gets

$$\mathbf{E}^e = \frac{1}{2} \frac{m_i}{e} \mathbf{g} \approx 10^{-15} \mathbf{g}.$$

For main sequence stars one has $E^e \approx 10^{-11} \text{ e.s.u.}$, which is very small compared to $(\mathbf{v}/c) \times \mathbf{B}$. For the sun this gives a potential difference of the order of 1 e.s.u. or 300 V. Using this value of E^e , one gets for the relative charge separation the very small value

$$\frac{n_i - n_e}{n_i} \approx \frac{G m_i^2}{e^2} \approx 10^{-37}.$$

The centrifugal acceleration also, by (10), produces an electric field and charge separation. For rigid rotation these are smaller than the above values by the ratio of the centrifugal to gravitational acceleration. Some kinds of differential rotation, those in which \mathbf{E}^e can not be balanced by a potential field, produce changes in the magnetic fields and hence, by (12) values of \mathbf{E} which may be larger.

2. — Problems of plasma physics in the solar atmosphere.

2'1. *The solar atmosphere.* — At the visible surface of the sun, the temperature is about $6000 \text{ }^\circ\text{K}$, the gas pressure is about 10^5 dynes/cm^2 , the density is 10^{-7} g/cm^3 , and thus the sound velocity is about 6 km/s . The ionization of the hydrogen is only 0.1% or less. The scale height: *i.e.* $H = 1/\text{grad } \ln p$, is about 100 km . The energy transport just above this surface is mainly radiative and the temperature gradient is the radiative one. Immediately

below the visible surface the degree of ionization of the hydrogen rises rapidly. This increases the opacity, *i.e.*, requires a greater temperature gradient to produce the same flux of radiation, and decreases the adiabatic temperature gradient because of the specific heat of ionization. In fact, the radiative temperature gradient becomes larger than the adiabatic one and this leads to instability and turbulence similar to that often observed in the earth's atmosphere. Therefore in the sun and also in cooler stars one has a convective zone in the turbulent state where a substantial part of the heat flux is carried by convection. The effects of this are visible in the granules of the photosphere. These are regions with diameters of about 500 km and a lifetime of a few minutes in which the temperature differs by about 10% from the neighbouring regions. The gas velocities are 1 to 2 km/s. The granules originate in deeper regions where the scale height is probably about 300 km and the pressure is about four times that at the visible surface.

This turbulence draws out the magnetic lines of force and thus feeds energy into the magnetic field provided the field is not so strong that it inhibits the motion. The point at which this occurs is not yet settled because no theory of hydromagnetic turbulence is completely acceptable. There are two schools of thought. According to one there should be approximate equipartition between the magnetic and turbulent energy densities, leading to a field strength of 100 gauss in the sun. On the other hand Babcock's observations yield a field smaller than about 10 gauss in normal quiet regions. ALFVÉN has objected to this conclusion and has argued that a small scale stronger field should be possible if there is a suitable correlation between the magnetic field and the velocities and if this produces some confusion between the Zeeman and Doppler shifts. According to the other school of thought, the magnetic field might however be much weaker than indicated by the equipartition of energy argument.

2.2. Sunspots. — Sunspots are greatly varied in size, shape, and lifetime, but for our purposes it is enough to say that they are cool regions, a moderate size spot having an area of $Q = 10^{18} \text{ cm}^2$, a field strength of about 3000 gauss, and thus a total flux of 10^{21} to 10^{22} gauss cm^2 . This field is reasonably regular, is approximately normal to the surface of the sun at the center of the spot, and leans outwards as the edge of the spot is approached.

The lifetime is of the order of days or weeks. This is very short, compared to the lifetime of the magnetic field due to ohmic losses, which is $\sigma Q/c^2 \approx 30$ years since the lines of force must run through hot regions where the conductivity is $\gtrsim 10^{13} \text{ s}^{-1}$. This suggests that the bundles of lines of force are convected to the surface instead of the field being generated at the site of the spot. Two alternative models are that of Hale, in which one has a closed loop normal to the sun's surface, and the magnetic analogue to that of Bjerknes, in which

a short section of a long tube of force is raised above the sun's surface. Discussion of these points will be found in the *Proceedings of the 1956 Stockholm Symposium on Cosmical Electrodynamics*.

As mentioned above, sunspots are cool and dark, the heat flux being only one fourth or one fifth that of normal regions. Since the energy transport in normal regions is probably by convection and since the purely radiative transport would be much less, a suppression of turbulence by the strong magnetic field provides a possible explanation for the diminished flow of heat.

SCHLÜTER and TEMESVÁRY have developed a model for the internal constitution of sunspots, making the idealizations that the spot is circular, stationary, far from other spots, and in hydrostatic equilibrium. As a preliminary result, there seem to be no contradictions between this theory and our ideas of the internal constitution of the sun, but the theory is still far from complete.

One observation that raises serious difficulties is the Evershed effect. This is an apparent horizontal outflow of gas with a velocity of about 1 to 3 km/s over most of the area of the spot. Thus this flow is across the lines of force, which is inconsistent with one of the main principles of hydromagnetics; namely, that since $\text{curl}[\mathbf{v} \times \mathbf{B}] \neq 0$, the fluid and lines of force move together. One can not assume that the lines of force share this velocity since then there would be large changes in the field in a few hours. It does not seem possible to resolve the paradox by assuming that the outward flow is only of neutral particles, and considering a three fluid model, the coupling of the neutral particles to the ionized particles is found to be too strong even at the very low spot temperatures. Perhaps the solution of the paradox will come only when simultaneous observations of the gas motion, and of the changes in the magnetic field are available. Such observations would be very difficult but should be possible with the available techniques.

2'3. *The heating mechanism of the chromosphere and the corona.* — The chromosphere and particularly the corona are observed to be at much higher temperatures than the lower regions and not to be in local thermodynamic equilibrium. Thus they must be heated by some non-thermal energy source. In recent years the idea has been developed that this source is given by acoustic or pressure waves that originate in the hydrogen convection zone and are damped in the regions to be heated. These waves are caused by the turbulence in this zone which was discussed previously. The energy dissipated as heat by the turbulence is, according to the theory of incompressible turbulence, of the order of v_{turb}^3/l erg/g s, where l is a characteristic length that in the sun is equal to the scale height. This would lead to total dissipation of the turbulent energy in one scale height and hence the conversion to heat of ρv_{turb}^3 erg/cm² s $\approx 10^8$ erg/cm² s (ρ density). Actually the turbulence is not incompressible as the turbulence velocities are 1 to 2 km/s and the velocity of sound, v_s , is about 6 km/s.

Thus pressure waves that propagate outward would be expected. The conversion of turbulent energy into noise had been treated quantitatively by LIGHTHILL (1952), PROUDMAN (1952), and PARKER (1953). If M is the Mach number, the energy that can be converted to noise is of the order of $M^5 \rho v_{\text{turb}}^3$ for isotropic turbulence, and is probably about $M^4 \rho v_{\text{turb}}^3$ for the situation in the sun spot. The best (order of magnitude) estimate that can be made is that $\approx 1\%$ of the energy is diverted from heat to acoustic waves; *i.e.*, 10^6 erg/cm² s. As these waves propagate outward into regions of lower density, the amplitude Δv increases (since the constant energy flux is $\frac{1}{2} \rho \overline{\Delta v^2} v_s$) and when Δv becomes comparable with v_s shock waves develop. These shock waves rapidly transform the acoustic energy into heat. Part of the heat is delivered in the transition layer between the chromosphere and corona and part heats the corona.

We may now raise the question as to what rôle the solar magnetic field plays in this process. Outside the spots Babcock's observations show that the field is of the order of 1 gauss. Thus the Alfvén wave velocity $v_A = B/\sqrt{4\pi\rho}$ is about 10^3 cm/s and $v_A/v_s \approx 0.01$. Under these circumstances the magnetic field has practically no influence on the conversion from turbulent to acoustic energy (KULSRUD, 1953) or on the propagation of acoustic waves in the photosphere; also in the cases of turbulent magnetic fields of the order of 10^2 gauss, associated with the turbulence the influence of such fields on the production of noise would not be excessively large (KULSRUD *l.c.*). It does modify the waves, however in the transition region where v_A becomes comparable with v_s .

2'4. The state of ionization of the solar corona. — One of the principal observable features of the solar corona are the emission lines of highly ionized atoms such as Fe X — Fe XIV and Ni XII — Ni XVI. The potentials for these lines are some hundreds of electron volts (the maximum being some 800 eV) which leads to a corona temperature of the order of 10^6 °K. One can not use the Saha formula to connect the degree of ionization and the density and temperature because the corona is so transparent that the radiation field is essentially characteristic of the photosphere temperature of 6 000 °K. Thus there are very large deviations from thermodynamic equilibrium and we must consider the mechanisms of ionization and recombination in detail. The same situation holds for machines used in thermonuclear research, *e.g.* in Zeta.

There are two mechanisms for ionization. Radiation ionization is proportional to $E_\nu N_i q_{\text{ion}}^\nu$, where E_ν is the intensity of the radiation field at the frequencies of interest which correspond to some 100 eV, N_i is the number of ions per cm³ that have lost i electrons, and q_{ion}^ν is the cross-section for the next ionization of these ions by radiation. Ionization by electron collision is proportional to $N_i N_e v_e \exp[-\chi/kT] q_{\text{ion}}^c$, where N_e is the electron density, v_e is the r.m.s. electron velocity, χ is the ionization potential, and q_{ion}^c is the cross-section for ionization by collision. The exponential factor gives essentially

the fraction of the electrons with sufficient velocity. There are also two processes for recombination, which are just the reverse of the above ionization processes. Radiative recombination is proportional to $N_{i+1}N_e q_{rec}^r$, three-body collisions are proportional to $N_i N_e^2 q_{rec}^c$. But only one of the two processes in each case is important. Ionization by radiation is unimportant both in the corona and in Zeta because E_ν is so small at the frequencies of interest owing to the extremely small optical depth. The densities of the corona and of Zeta are so low that three-body collisions generally are rare under such conditions. Hence the state of ionization is the result of a balance between ionization by collision and two-body recombination. As a consequence, by the rates given above, the electron density drops out and the result depends only on the temperature, contrary to the Saha case. No single temperature will account for all the degrees of ionization observed in the corona. This is probably explained by having different temperatures in different regions in the line of sight. The most detailed recent work on the corona has been done by ELWERTH. A critical point is that the cross-sections are not sufficiently well known either from experiment or theory. A careful combination of the results from both sources of information seems appropriate. The situation is very similar in the experiments on controlled fusion except that there impurities from the walls such as O and Al are important; in addition losses towards the walls may require attention. G. KNORR has just made some calculations of the degrees of ionization to be expected for O, including the non-stationary case.

3. - Hydromagnetic problems of interplanetary space.

3.1. *Isorotation, force-free fields, and the transport of angular momentum.* - FERRARO, and later ALFVÉN, have shown that in a stationary axially symmetrical motion of a highly conducting medium like that near the sun, the stationary state is possible only if the material along the line of force rotates like a rigid body. This follows from the condition that $\text{curl}[\mathbf{v} \times \mathbf{B}] = 0$. This result rises serious astronomical difficulties, as pointed out by ALFVÉN, because if this isorotation extends even as far as the earth's orbit the required velocities become 400 km/s, *i.e.* impossibly large. Where, then, does co-rotation with the sun break down?

LÜST (1952) showed that the point at which the turbulent energy density would balance the magnetic energy density was near the orbit of Mercury and hence suggests that this was the point at which isorotation breaks down.

LÜST and SCHLÜTER (1954) pointed out that force-free fields should be important in this as in other astronomical problems. Such fields should be expected when, as in the neighborhood of the sun, the magnetic energy density is large compared to all the other energy densities. Thus the magnetic field

must be so arranged that the net forces it exerts are small. A force-free field is one in which the magnetic forces are zero and is achieved if the electric current is everywhere parallel to the magnetic field. This requires that $\mathbf{B} \times \text{curl } \mathbf{B} = 0$ and is mathematically equivalent to a problem treated by BELTRAMI half a century ago. LÜST and SCHLÜTER found an axially symmetric force-free field in which the lines of force are closed inside a sphere centered on the sun. The field inside this sphere, which will have a radius of about a third of an astronomical unit, can now rotate with the sun while outside the sphere one can fit a stationary magnetic field that satisfies the desired boundary conditions at infinity, and the rotation does not stretch out any field lines.

The transport of angular momentum from the rotating star to the interstellar medium in this situation was treated by LÜST and SCHLÜTER (1955). It was suggested that the angular momentum is transported by the magnetic field to this spherical boundary and then by turbulent viscosity to the interplanetary medium. (The fact that a field is force-free does not indicate the absence of stresses, it says only that the divergence of the stresses is zero.) In this way it was hoped to explain the fact that the stars observed to have large angular momenta have ages less than about 10^9 years, while older stars are observed to have small angular momenta. But it was only possible to show that in the axially symmetrical case angular momentum would be transmitted by torque-free fields (*i.e.* fields force-free only normal to the meridional plane) differing but little from force-free fields. For axially symmetric, completely force-free fields it was not established whether or not torques could be transmitted. (For the more special case of cylindrical rather than axial symmetry, SCHLÜTER (1957) has shown that force-free fields can transmit torque).

This is only a rough treatment of the problem because corpuscular radiation must almost continuously produce deviations from this idealized stationary state which, however, should be restored fairly rapidly.

3.2. Densities, velocities, and magnetic fields in interplanetary space. — The most stationary feature of interplanetary space is the zodiacal light which is observed between the orbits of Venus and the Earth. This is sunlight scattered from dust and electrons. The amount of each can be determined in principle by observing the intensity and the polarization of the scattered light. The dust is mainly in the ecliptic plane but according to the observations of BEHR and SIEDENTOPF the electrons are not so concentrated and have a density near the earth of about 600 cm^{-3} . The contribution to the polarization of the dust has been reexamined by VAN DE HULST who concludes that the electron density is $(400 \pm 50\%) \text{ cm}^{-3}$. There are, of course, a corresponding number of positive ions. The zodiacal light has not yet given any information on the interplanetary electron velocities.

We know of solar corpuscular radiation mainly from studies of geomagnetic activity and of the aurorae. These show recurrent features with a period of 27 days, corresponding to the synodic rotation period of the sun and interpreted as due to corpuscles originating from limited active regions on the sun. Velocities of 10^8 cm/s follow from the travel time as deduced from the comparison of solar and terrestrial events. This velocity is slightly higher than the thermal velocity in the outer corona. Values for the particle density in corpuscular streams have been deduced by CHAPMAN and UNSÖLD (1949) from the absorption of radio noise that crosses such a stream and from some additional evidence. They deduce local peak values on rare occasions of 10^5 cm $^{-3}$; for more normal situations values of the order of 10^2 to 10^3 cm $^{-3}$ may be derived (not mentioned by the authors). These correspond to particle fluxes of about 10^{13} particles/cm 2 s and 10^{10} particles/cm 2 s, respectively.

Some information can be obtained from cosmic ray data, especially that on the cosmic rays with energies 1 to 30 GeV produced in connection with solar flares. These particles reach places in polar regions that they could not reach if they were not deflected by magnetic fields in interplanetary space. Observations on the 23rd of February, 1956, make this quite certain. From the widths of the impact zones (where the particles arrive with minimum delay) it appears that the source is larger than the visible sun. A source having about the diameter of the co-rotating sphere of magnetic lines of force treated earlier would explain the observations. The delayed onset times at polar stations require some kind of magnetic fields at distances out to a few astronomical units. The sharp onsets in non-polar regions require that there be very little magnetic field between the co-rotating sphere and the earth. The considerable fluctuation in the low energy components (1 to 10 GeV) with the solar cycle seems to require magnetic clouds throughout most of the solar system, these clouds being stronger or more irregular when the sun is most active.

3'3. *Comet tails.* — The solid nuclei of comets have probably diameters of the general order of 1 to 10 km composed of dust grains held together by frozen gases. These nuclei are not visible; but when they approach the sun the gas evaporates producing a surrounding coma and a tail. The coma is composed of dust and gas and has a diameter of about 10^4 to 10^5 km. There are three types of tails. Type I tails are directed nearly radially away from the sun and are composed of ions such as CO^+ , N_2^+ , and presumably others that are difficult to observe owing to the spectral distribution of the resonance bands. Type II and III tails are much more curved and are composed of neutral molecules such as CN, C_2 , and of dust. The curvature of type II and III tails suggests that the material is accelerated away from the sun by light pressure with an acceleration of the order of the local solar gravity. The straightness of the type I tails and the accelerated motions sometimes observed in bright

knots gives accelerations away from the sun ordinarily about 10^2 times the local solar gravity. At times, as in Comet Morehouse, Comet Halley, Comet 1942 *g* and others, this can rise to 10^3 or 10^4 . These accelerations can not be due to light pressure, which falls short by several powers of 10, because of the low oscillator strength of the transitions in question, and hence another mechanism is required. The particle density in the tail is not well known, but the CO^+ alone may be about 10 particles/cm³ in a bright tail. It has been proposed (L. BIERMANN, 1951) that the solar corpuscular radiation accelerates the gas in type I comet tails. This will also explain the ionization. The only alternative explanation for the latter is ionization by ultraviolet light, which would require an intensity exceeding the black body value by $10^5 \div 10^7$, and recent rocket observations exclude this. The ionization is rather produced by charge exchange, a cross-section of 10^{-15} cm² which is supported by laboratory experiments being easily sufficient to explain the observed rates of development of ion structures in comets. One mechanism of coupling that may produce the acceleration is the ordinary friction between the ionized gases which is effective, if the electron is of the order of 10^7 . (The unionized type II and III tails would not be accelerated by this mechanism.) CHAPMAN suggests however, that, with an essentially static interplanetary gas heated from the solar corona, the electron temperature should be 105 °K, in which case the frictional coupling mechanism would fail. But a solar magnetic field like that described above would greatly reduce the thermal conductivity and hence lower the temperature in the interplanetary space. Also if there is to be any solar corpuscular radiation, it will sweep away any static interplanetary gas, and, in fact, as mentioned already, the interplanetary gas contributing to the zodiacal light seems to be just the outward flowing solar corpuscular radiation (L. BIERMANN, 1957). In addition, collective phenomena of some sort or entrained magnetic fields might enhance the coupling between the solar corpuscular radiation and type I tails.

This model in its general lines is supported by the fact that recurrent accelerations of bright knots are seen separated by the period of rotation of the sun as seen from the comet. There is also correlation between geomagnetic phenomena which should be produced by the solar corpuscular radiation, and accelerations in comets, when they are so situated that they might be expected to be in the corpuscular beams.

The structure of comet tails often suggests that magnetic fields may be present. For example, one often sees streamers containing fine structures whose radii are 10^3 km and whose lengths are as much as some 10^5 to 10^6 km. If the temperature were even as low as 300 °K, thermal motions would increase greatly the diameter before they attained such lengths. Magnetic fields along the streamers would suppress the expansion. Sometimes one can see structures that appear like a helix seen in perspective. These may be due to

force-free magnetic fields. Sometimes the accelerations are reasonably far from radial. Perhaps the magnetic conditions are different from cloud to cloud, but these observations have not been worked out.

Finally, it does seem that the observations on comet tails exclude the possibility of co-rotation of the gaseous interplanetary medium in the neighborhood of the earth (outside, of course, that region in which there must be co-rotation with the earth itself owing to the geomagnetic field).

BIBLIOGRAPHY

1) *General considerations.*

H. ALFVÉN: *Arkiv f. Fysik* (1942).

A. SCHLÜTER: *Zeits. f. Naturforsch.*, **59**, 72 (1950).

L. SPITZER: *Physics of Fully Ionized Gases*, (New York 1956).

T. G. COWLING: *Magnetohydrodynamics*, (New York, 1957).

2) *Plasma physics in the solar atmosphere.*

G. KUIPER: *The Sun* (Chicago, 1954).

Proceedings of the 1956 Stockholm Symposium on Cosmical Electrodynamics (IAU, in press).

L. BIERMANN: and R. LÜST, *Non-thermal Phenomena in Stellar Atmospheres*, in *Compendium on Stellar Astronomy*, vol. 6 (in press).

3) *Hydromagnetic problems of interplanetary space.*

H. ALFVÉN: *Arkiv f. Fysik* (1943).

R. LÜST and A. SCHLÜTER: *Zeits. f. Astrophysik*, **34**, 263 (1954).

R. LÜST and A. SCHLÜTER: *Zeits. f. Astrophysik*, **38**, 190 (1955).

L. BIERMANN: *Zeits. f. Astrophysik*, **29**, 274 (1951).

L. BIERMANN: *Observatory*, (June 1957).

INTERVENTI E DISCUSSIONI

— C. DE JAGER:

Is the life time of a granule long enough to allow equipartition to be set up between the turbulent and magnetic energies?

— L. BIERMANN:

The conductivities are such that one can speak with some confidence of frozen-in magnetic fields. Under these circumstances one might expect that if turbulence continues for a very long time (though being short compared to the life of the sun), a state should be reached where there would be this equipartition. This view is supported to some extent by the theoretical work of FERMI, of BATCHELOR, of SCHLÜTER and myself, and of CHANDRASEKHAR; but the subject is so difficult that the theory is not yet in a final state. The evidence from Babcock's measurements is against this conclusion anyhow at first sight, but the resolution is not as fine as the structures found by Schwarzschild and the conclusion may have to be revised.

— G. GOLDSTEIN:

Is not the situation in the machine very different from that in the corona because of the electron losses to the walls in the machine?

— L. BIERMANN:

Yes, this is certainly right. Perhaps Dr. THONEMANN could say something about the conditions in the machines.

— P. C. THONEMANN:

We are still trying to find out whether the walls are playing a part or whether the lower electron temperature suggested by Dr. BIERMANN is the important factor. A complicating factor is that we see progressive stages of ionization of oxygen emitted from the wall. We see the O V and O VI but do not know the final state.

— THONEMANN, FERRARO, GIOVANELLI, DE JAGER and BIERMANN discussed the influence of the magnetic forces on the height of the visible «surface» in the spots relative to the surroundings, here the gas pressure (according to the contribution of SCHLÜTER and TEMESVÁRY to the Stockholm symposium, 1956) is lower than in the same geometrical level in the photosphere.

— T. GOLD:

In connection with corpuscular radiation and force-free fields, I can see that as a first approximation one should work out the force-free fields. But it seems to me that static fields in which gas pressure significantly affects the shapes are to be worked out next, since the gas pressures in the solar atmosphere are large enough to do this. Thirdly, since the observed variations with time are large, the transient state is important. These dynamical field shapes may vary greatly from the static shapes and be the ones actually observed. After all the geomagnetic records show activity more than half the time.

— L. BIERMANN:

Yes, the dynamical state is certainly important. PARKER has considered an ideal case in which the gas streams out radially from the sun. When one considers the interaction between these corpuscular streams and solar magnetic fields, one gets electric fields which produce a coupling with the comet tails. Cometary observations do not seem to favour this model, at least in the region between Venus and Mars.

— T. GOLD:

The co-rotating sphere must be greatly disturbed by the outstreaming corpuscular radiation.

— L. BIERMANN:

Certainly, it is intended only as an idealization describing the average conditions.

— GOLD and BIERMANN discussed the extent to which fields connected to the sun would give angular momentum to the corpuscular material coming out while Biermann felt that there should be a co-rotating inner region.

— T. GOLD:

The interaction mechanism between the corpuscular streams and the material in the comet tails has always puzzled me. The magnetic interaction is very attractive; but since the acceleration would be normal with the magnetic field, this requires an unacceptably accurate alignment of these fields.

— L. BIERMANN:

That is perfectly correct. Ordinarily friction should provide the coupling, as indicated in the lecture. But magnetic fields might at times play an important rôle and explain some of the observed phenomena.

— R. GALLET:

I would like to make two remarks about the corpuscular radiation. The observations from the whistlers indicate that at least 50% of the time the space near the earth has a filamentary structure since when we have good recording conditions each whistler is propagated along several discrete paths. Second, the observed VLF (very low frequency) radiation, which is different from the whistlers, is sometimes easily explained as originating from a stream of material that comes steadily for several hours with a velocity that may be roughly 3000 km/s. More often the observations are to be explained as due to small bunches of corpuscular radiation, with diameters of several 100 km, and velocities of 10^4 km/s. It seems clear that the corpuscular stream is broken up into droplets and accelerated near the earth. The whistler data give an average electron density out to 3 earth radii of about 5000 per cm^3 which is larger than the value you give for interplanetary space. It seems clear that this is to be regarded as an extension of the earth's atmosphere since the gradient in the density shows that the density is proportional to r^{-3} . The scale height shows that the gas is ionized hydrogen.

— L. BIERMANN:

Does the transit time from the sun to the earth support the high velocity of 10^4 km/s?

— R. GALLET:

No, the high velocity arises only in the neighborhood of the earth. We attack only secondary effects, such as those connected with aurorae. There is a good correlation between flashes in the aurorae and the bursts of the VLF noise.

— V. FERRARO:

I think that the spectroscopic observations of Meinel along the lines of force confirm the high velocities.

— R. GALLET:

Yes, when one includes the spiraling around the lines of force these observations give particle velocities of 10^4 km/s.

— V. FERRARO:

Is not 10^4 km/s too high a velocity because it gives too great a penetration of the earth's atmosphere?

— R. GALLET:

A velocity of 10^4 km/s is needed for penetration to 100 km.

— C. DE JAGER:

BLACKWELL has shown recently that the interplanetary gas is of solar origin and is drifting away from the sun. Since the distribution of polarization seems to be symmetric around the ecliptic rather than the solar equator, it is suggested by BLACKWELL that the dust produces much of the polarization and that the gas density is less by a factor of 10 than the usual figure. I do not know if this is right and would like your opinion. Secondly, does the sharpness of the onset times for the solar flare cosmic rays support a low value of the interplanetary gas density?

— L. BIERMANN:

As to the first question, I think that Dr. van de Hulst's discussion two years ago yielded the value of the electron density which I used. I do not know if the data would admit a substantially lower density.

— H. C. VAN DE HULST:

Not if the theory is right.

— L. BIERMANN:

As to the second point, the sharpness of the onset times have been discussed by LÜST and SIMPSON. If there are no interplanetary magnetic fields, the gas density is too low by perhaps 10^9 to produce any noticeable absorption. The influence of magnetic fields is complicated. First, the cosmic rays appear to come not from the visible sun, but from a larger region that could be the co-rotating sphere. Second, there seem to be some magnetic fields which SIMPSON puts at about 1.5 astronomical units from the sun, which reflect the cosmic rays back. This is, however, too simple a model. Perhaps Dr. LÜST has some comment on recent improvements of the model.

— R. LÜST:

There has been no progress in understanding the situation. The simple assumption of Simpson, Meyer, and Parker was just an assumption to enable them to analyse a complicated situation and they never held that it was a close approximation to the actual situation.

— C. DE JAGER:

Should the reflecting cloud be spherical or toroidal?

— R. LÜST:

The only thing needed to explain the observations is some kind of cavity that will store some of the cosmic rays for times up to 12 hours.

— E. SCHATZMAN:

What is the time scale for the exchange of angular momentum between the star and the interstellar medium? Is it the same for all types of stars? If it is always comparable with the contraction time of average stars, the angular momentum of light *F*, *G* and *K* stars could be carried away but that of heavy *A* and *B* stars could not.

— L. BIERMANN:

This depends on the magnetic field strength; cf. the papers of LÜST and SCHLÜTER.

— E. SCHATZMAN:

Matter ejected from the star would carry away angular momentum. If it interacts with a co-rotating magnetic field, only a very small loss of mass is needed to explain the deceleration of the rotation.

— R. LÜST:

TER HAAR showed that any reasonable loss of mass would not produce enough deceleration.

— E. SCHATZMAN:

But he did not include the effects of a magnetic field, which could impart angular momentum to the gas after it left the star.

— P. J. KELLOG:

Observations at Iowa and at Minnesota of X-rays in conjunction with aurorae provide information on the corpuscular streams. The theoretical work of CHAPMAN and FERRARO allows one to deduce particle velocities of the order of $(3000 \div 4000)$ km/s and particle densities of only 1 or 0.1 per cm^3 if the X-rays come from the full stream striking the earth.

— T. GOLD:

In connection with Dr. Schatzman's question, it seems important to note that stars differ enormously in surface conditions, and the outflow of matter and hence of angular momentum should vary enormously from one type of star to another. Perhaps some sharp change in the detailed surface conditions explains the sharp break in the curve of angular velocity.

— L. BIERMANN:

There is a point that occurs to me in connection with some of the earlier questions. The earth's magnetic field and the entrained material should co-rotate with the earth out to some cut-off surface, just as the sun's field does. The analysis of cosmic ray data by Dr. ROTHWELL indicates that out to 2 or 3 earth's radii the magnetic field is essentially as deduced from surface measurements. Thus, the co-rotation should end at some more distant point.

The Interstellar Plasma.

H. C. VAN DE HULST
Sterrewacht Leiden

I. - The Observational Data.

Plasma physics, as defined in other lectures at this Summer School, is applicable to the interstellar gas, if

- a) there is ionized gas between the stars,
- b) there are magnetic fields in the interstellar space.

Evidence on these points can be derived from classical, *i.e.*, optical astronomy, from radio-astronomy, and to some extent also from cosmic ray studies. In this first lecture we shall review the pertinent observations.

1. - The geography of the Universe.

Table I gives an idea of the orders of magnitude of some quantities with which we are dealing. We shall be especially concerned with the gas dispersed

TABLE I. - *Basic properties and dimensions.*

	Geometry		Internal velocities		Number density
	size (cm)	shape	systematic	random	atoms/cm ³
A star (Sun)	10 ¹⁰	sphere	—	—	10 ²⁴
A solar system	10 ¹⁶	flat	30 km/s (Earth)		10 ³
A galactic system	10 ²³ = 30 kpc	disk + halo	200 km/s (rotational)	10 km/s	1
The Universe	10 ²⁸	—	up to <i>c</i>	500 km/s	10 ⁻⁴

Conversion; 1 kpc = 1 kiloparsec = 3.25 · 10²¹ cm, 1 km/s = 1 kpc/10⁶ year.

in the galactic system. However, we must realize that there may be transfer of matter from stars into the interstellar gas, or conversely, and from the latter to the universe.

2. – Populations in the Galaxy.

The material in the galactic system is divided over stars, gas and dust in the following approximate percentages.

	Stars	Gas	Dust
Total system	98 %	2 %	< 1 %
Near the sun	75 %	25 %	< 1 %

We should like to study the distribution of this material in six-dimensional ordinary and velocity space. However, not all data can be measured equally well. The position on the sky can be measured with high precision but any distance estimate usually is inaccurate. The velocity of a star or gas cloud in the line of sight can be measured with ease from the Doppler effect, but the motions across the line of sight can be established only for nearby stars.

In spite of these limitations in the observations one important fact has emerged: not all combinations of velocity and space distribution occur. Instead, two fairly distinct groups (populations) are seen. The stars of the two populations differ also by their chemical constitution and other physical characteristics. Briefly, the properties are as follows.

Population I = Disk population = Young population. – The motion of stars and gas clouds of this population occurs in nearly circular orbits in the disk. Motions perpendicular to the disk and motions causing deviations from circularity are only about 10 km/s. The distribution in space is very flat, with average deviations from the galactic plane of about 0.1 kpc. The distribution inside this flat disk is not homogeneous but shows irregularities and spiral arms. Some stars of this population occur strikingly in nests (technical term: associations).

Explanation: After the Galaxy had formed, the gas motion settled to the state of minimum energy consistent with a given angular momentum *i.e.* to a rapidly rotating flat disk. The stars which formed from the gas at any time between that moment and now have to partake in this general motion. Stars formed very recently (0 to 10 million years ago) can still be seen near the nest where they were hatched.

Population II = Halo population = Old population. — Stars of this population that happen to pass in our neighbourhood have no tendency to move in the disk or to describe a circular orbit. The space distribution is only moderately flattened. Average distance from plane = 5 or 10 kpc. Most objects belonging to this population are fairly strongly concentrated towards the galactic centre. No spiral structure, no interstellar clouds.

Explanation: The stars which formed before the gas settled to a disk-shaped system are still seen in very nearly the same orbits as they had at birth.

Note: There are intermediate forms and other significant criteria not mentioned in this brief description. In recent discussions up to 6 or more populations have been distinguished.

A schematic picture of disk and halo is given in Fig. 1.

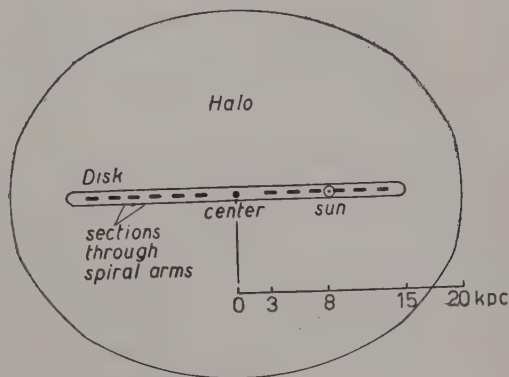


Fig. 1. — Schematic drawing of the Galaxy.

3. — Observational data about the interstellar gas.

The overall properties reviewed above cannot be readily inferred from what we see at our single observing point, the sun. The picture has been pieced together from much patient and ingenious work by a large variety of methods. We shall not further discuss the stars but shall briefly summarize where the data on the gas come from.

Optical data can be obtained in the range $(2 \div 0.3) \mu\text{m} \div 3000 \text{ \AA}$. Recently, rocket observations have been made in the 1300 \AA region. Within the disk, visibility extends to about 2 kpc, because of scattering by the interstellar dust, which amounts to a factor 5 or 10 on 1 kpc, in the average. For this reason it was formerly thought that the sun was in the centre of the Galaxy. The following gaseous objects are observed:

a) *Shells*, which are concentric with a star, and were clearly blown off by this star. Masses of the order of 1 solar mass, or smaller. The matter in the shell will eventually become part of the interstellar gas. One example, the Crab nebula, will be discussed in detail.

b) *Heavy nebulae*, which consist of highly irregular masses of gas, mixed with a small amount of dust. In bright nebulae we find hot stars, responsible

for ionization and excitation of the gas. The same nebulae usually show dark spots, due to the absorption of light by overlying dust clouds. The density of the nebulae is of the order of $(10^2 \div 10^3)$ atoms/cm³. Total masses up to 10^4 solar masses. Famous example: the Orion nebula.

c) *Emission regions*, which are similar to nebulae, but fainter, so that special techniques are required for their observation. Density 10 atoms/cm³.

d) *Clouds producing absorption lines*. The absorption of Ca⁺ and other lines can be observed in the spectra of bright stars and are distinguished as interstellar in spectroscopic binary stars. The existence of separate absorption components with different Doppler shifts points to the existence of separate clouds. These are probably clouds in which hydrogen is ionized (H II regions). They may be similar to c), above. H I regions cannot be observed, except for the suspicion that in most dark dust clouds the hydrogen is unionized.

Radio data are obtained from all over the Galaxy as dust absorption is absent. The radiation can be either continuous or in the 21 cm hydrogen line. Continuous radiation can be distinguished in «thermal» and «non thermal» radiation. The main properties are summarized in Table II.

TABLE II. — *Mechanisms of galactic radio emission.*

		from	mechanism
Continuous radiation	thermal, predominant at short λ , e.g. 10 cm	emission regions in disk	free-free
	non-thermal, predominant at long λ , e.g. 3 m	halo + disk	probably synchrotron
Line emission	<div> <div></div> <div>hyperfine-structure line of atomic H at 21 cm</div> </div>	HI regions in disk	spontaneous transition

4. — Mapping of spiral arms.

Let us investigate the possibility to make a map of the Galaxy with its spiral arms in the ordinary 3-dimensional space. We call

r = distance from the sun,

l = longitude along the galactic plane,

b = latitude from the galactic plane,

v_r , v_l and v_b the corresponding velocities.

The quantities which can be measured directly, are l , b and v_r . Clearly, the problem is to find r . This is done as follows.

Emission region (HII): from the optical brightness of the stars involved. This method is confined to the « visible range » of roughly 2 kpc and, even there, often uncertain. Nevertheless some parts of the nearer spiral arms were first mapped by this method in 1950.

HI regions: by a conversion of the measured v_r (Doppler effect) into r (distance). This conversion is based on the assumption that both the cloud and the sun make circular orbits around the galactic centre. It can be shown (Fig. 2) that

$$v_r = \{\omega(R) - \omega(R_1)\} R_1 \sin l',$$

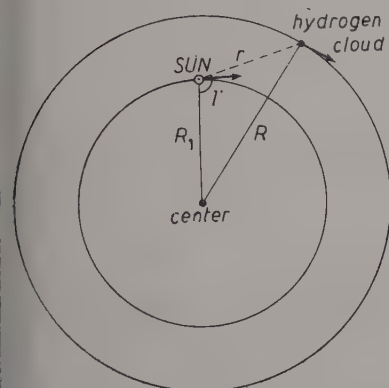


Fig. 2. — Differential galactic rotation.

where l' = reduced longitude and ω is the angular velocity of rotation at the distance R from the centre. The function $\omega(R)$ is connected with the gravitational potential, and thus with the density distribution.

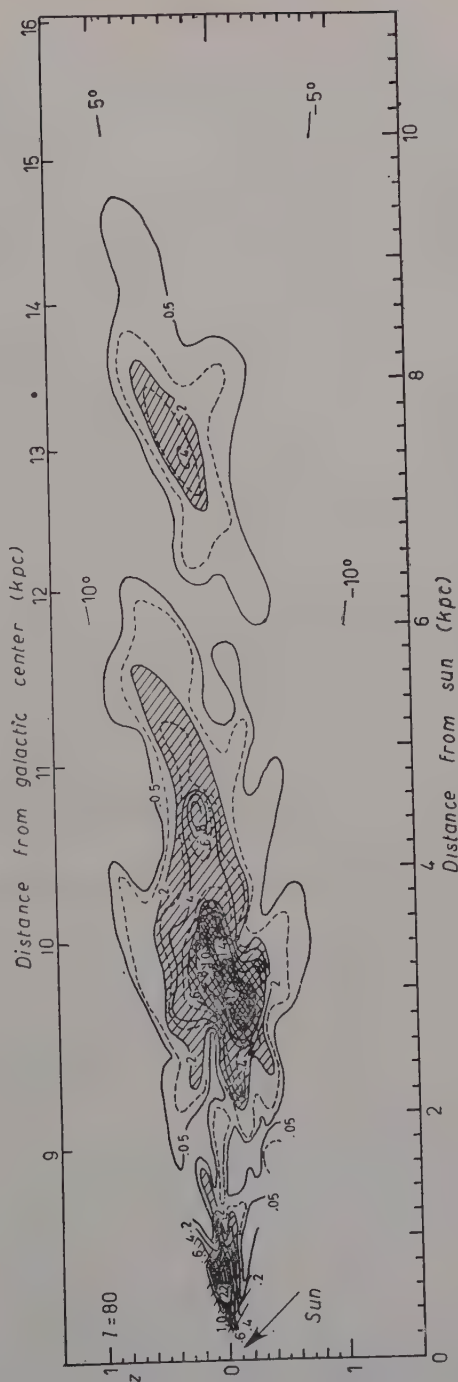


Fig. 3. — Contours of constant density of atomic hydrogen in a plane through the sun perpendicular to the galactic plane at longitude 80° . The densities range from 0.05 to 1.6 atoms/cm³. The plane cuts through three spiral arms. [From G. WESTERHOUT, *Bull. Astron. Nether.*, **13**, 201, no. 475 (1957)].

There are methods to find this function. Once this function is known for the galactic system R and thus r (0, 1 or 2 values) can be derived from the measured v_r .

Observations of the 21 cm line and consequent mapping of the spiral arm have been extensively pursued, mainly in the Netherlands, since 1951. It was found that forbidden velocities (on the above assumptions) are virtually absent; the ambiguity (2 values of r) that arises for $R < R_1$ was resolved by studying the latitude distribution. The space density of atomic hydrogen was quantitatively mapped in 3 dimensions over all of the sky visible from Holland with a resolution of the order of $(0.2 \times 0.2 \times 0.5)$ kpc. This is sufficient to see the spiral arms in detail but not to observe individual clouds. Fig. 3 shows a sample cross-section through three spiral arms. Corresponding research on the Southern sky has since been made at Sydney.

The 25 meter telescope at Dwingeloo put in operation in 1956 gives an angular resolution of 0.56° . With this telescope the brightest extragalactic systems M 31 (Andromeda nebula), M 33, M 101, etc., were found to behave similarly to our Galaxy. The Magellanic Clouds studied in Australia appear to have relatively more hydrogen gas, in agreement with their stronger Population I.

Another phenomenon discovered at Dwingeloo is the expanding motion of hydrogen gas in the nuclear region of our Galaxy (see Part. V).

II. — Mechanisms of Radio Emission.

5. — Units and definitions in radio astronomy.

For a black body of absolute temperature T , the brightness as a function of the frequency ν is given by the Raleigh-Jeans law:

$$B = \frac{2kT\nu^2}{c^2},$$

where T is the real temperature of the body. For an arbitrary body we can define a brightness temperature T_b according to the formula:

$$B = \frac{2kT_b\nu^2}{c^2}.$$

The units of B are $\text{erg}/(\text{cm}^2 \text{ s sr Hz})$ or more commonly $\text{W}/(\text{m}^2 \text{ sr Hz})$.

For an arbitrary source the flux density is defined by integrating the bright-

ness over the solid angle:

$$S = \int B d\Omega,$$

The units of S are $\text{erg}/(\text{cm}^2 \text{ s Hz})$ or more commonly $\text{W}/(\text{m}^2 \text{ Hz})$.

A few consequences of these formulae are:

a) Any brightness (this is the same thing as in traditional astrophysics would be called surface brightness) can be expressed by an equivalent brightness temperature, whether the mechanism of emission be thermal or not.

b) This brightness temperature has to be $> 1^\circ\text{K}$ or $> 0.1^\circ\text{K}$ (with present receivers) to be measured at all. Small radiotelescopes can do this equally well as big ones provided the source fills the entire antenna beam.

c) The ease of detecting a « point source » increases as the square of the telescope diameter.

6. - Thermal radiation.

As is customary in radio astronomy, we shall restrict the use of the name « thermal radiation » to free-free transitions (bremsstrahlung) from a thermal, ionized gas. The emissivity per unit volume, ε , is given by

$$\varepsilon = \kappa B(T) = \frac{4}{3} \left(\frac{2}{\pi m^3 k T} \right)^{\frac{1}{2}} \frac{L}{c^3} N^2 \quad \text{erg/cm}^3 \text{ s sr Hz},$$

where κ is the absorption coefficient per unit length, given by

$$\kappa = \frac{4e^6 N^2}{3(2\pi)^{\frac{1}{2}} / m k T)^{\frac{3}{2}} c v^2} \quad \text{cm}^{-1}.$$

The relation $\varepsilon = \kappa B$ is Kirchhoff's law. In the formula for κ , the reduction of the absorption coefficient by stimulated emission is included.

The factor L is a logarithmic factor, related but not identical to the one which appears in expressions for electrical conductivity (see lectures of Prof. FERRARO). The difference is in the fact that the upper impact parameter under the logarithm may be the Debye shielding distance but may also be v_{thermal}/v , for the pulse emitted by a too slow encounter simply does not contain the highest frequencies.

As a consequence of these formula the brightness of a layer of finite thickness l , becomes

generally: $B = B(T)(1 - e^{-\tau})$, where $\tau = l\kappa$,

for small τ this reduces to $B = \tau \cdot B(T) \sim \nu^0$,

for large τ this becomes $B = B(T) \sim \nu^2$.

7. - Evidence for the existence of non-thermal radiation.

Already in 1931 galactic radiation at long waves (15 m) has been observed. The corresponding T_b in the brightest parts is of the order of $500\,000^\circ$, which is too high for thermal radiation.

Point sources, discovered in 1946 and later, give various spectra, most of which are outside the range permitted by thermal radiation. For example, we have:

Sun (approximately)	$S \sim \nu^2$	black body;
Orion nebula at high ν and other emis- sion regions in entire range	$S \sim \nu^0$	thermal, small τ ;
Crab nebula	$S \sim \nu^{-0.5}$	} non-thermal.
Cygnus A, Cassiopeia A, etc.	$S \sim \nu^{-0.8}$	

The situation is illustrated in Fig. 4. Although accurate measurements on an absolute scale are difficult to attain, it is quite clear that the spectrum of most sources runs against the slope prescribed by the theory of thermal radiation. Also, the known size of some of the discrete sources gives a high brightness temperature, which cannot be thermal. For instance, at $\lambda = 10$ m

the quiet sun is very nearly a thermal source with diameter $35'$, $T_b = 10^6$. The source Cas A has a flux density S which is 10 times higher $= 4 \cdot 10^{-22}$ MKS units, in spite of the fact that its diameter is only $5'$, so that its solid angle is 50 times smaller than the sun. Consequently, $T_b = 50 \cdot 10 \cdot 10^6 = 5 \cdot 10^8$, approximately.

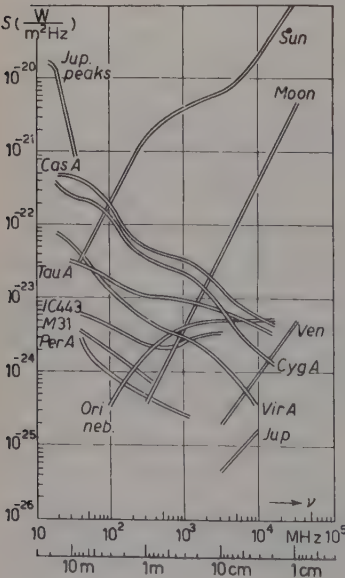


Fig. 4 (prepared for this publication by Miss A. Ross and the author). - Flux densities of some bright radio sources as a function of the frequency, drawn by interpolation between the most reliable measurements. The range of each curve in frequency indicates the actual range of the measurements. Thermal radiation from Venus and Jupiter has been reduced to mean inferior conjunction and mean opposition distance, respectively.

8. - Theory of synchrotron radiation.

This effect has often been mentioned in lectures at this summer school as it is important both for laboratory investigations and in the cosmos. Its possible importance for solar radio astronomy was first suggested by KIEPENHEUER. Later ŠKLOVSKIJ (1952) invoked it for the galaxy and for point sources; the Russian school calls it magnetic bremsstrahlung.

Principle: An electron moving in a homogeneous magnetic field describes a helical orbit. The centripetal acceleration in this orbit causes the emission of radiation, according to classical theory. Let us take for convenience a circular orbit. The angular velocity and radius are given by:

$$\omega_H = \frac{eH}{E}, \quad \frac{1}{R} = \frac{eHc}{Ev}$$

where

$$E = \text{energy of the electron} = \frac{m_0 c^2}{\sqrt{1 - v^2/c^2}}.$$

The units are the conventional gauss units: electrostatic for e and electromagnetic for H .

As the motion is strictly periodic with circular frequency ω_H (gyrofrequency), the emitted spectrum consists of discrete peaks at frequency ω_H and its harmonics. Two limiting cases may be distinguished.

a) If $v \ll c$ (non-relativistic electrons), the only frequency emitted is ω_H .

b) If $E \gg m_0 c^2$, i.e., $v \approx c$ (relativistic electrons), a great number of harmonics are emitted, in practice defining a continuous spectrum of a characteristic form illustrated in Fig. 5. The reason for this is that, similar to the well known effect of aberration, the emitted energy is sent mainly in and near the direction of momentary flight of the electron in its orbit. Consequently, any fixed observer receives only short pulses of energy, which upon Fourier analysis give a large number of harmonics.

The properties of the radiation emitted by an electron in a helical orbit are quite similar to that emitted in a circular orbit, namely for relativistic

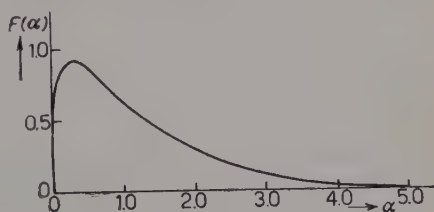


Fig. 5. — Characteristic spectrum of synchrotron radiation by electrons of one velocity. Intensity is plotted versus frequency in dimensionless units. [From J. H. OORT and TH. WALRAVEN: *Bull. Astron. Nether.*, **12**, 285, no. 462 (1956)].

velocities: emission only in very narrow cone around tangent of orbit, linear polarization with electric field \parallel acceleration, *i.e.* $\perp H$, practically continuous spectrum. Let us now define the numerical values. If we call

m = rest mass of an electron,

e = charge of an electron,

c = velocity of light,

H = magnetic field,

E = total electron energy,

R = radius of orbit,

θ = pitch of helix,

$F(x)$ = the function presented in Fig. 5,

we have:

	c.g.s. units	E in eV
Ratio mass/Rest mass	$\gamma = \frac{E}{mc^2}$	$\gamma = 1.95 \cdot 10^{-6} E$
Radius of orbit	$R = \frac{E}{eH}$	$R = 3.33 \cdot 10^{-3} E/H$
Characteristic frequency	$\nu_c = \frac{3}{2} \gamma^3 \nu_H = \frac{3eE^2 H \cos \theta}{4\pi m^3 c^5}$	$\nu_c = 1.64 \cdot 10^{-5} E^2 H \cos \theta$
Emission per unit frequency band	$P(\nu) = \frac{\sqrt{3} \cdot e^3 H \cos \theta}{mc^2} F\left(\frac{\nu}{\nu_c}\right)$	$P(\nu) = 2.34 \cdot 10^{-22} F\left(\frac{\nu}{\nu_c}\right) H \cos \theta$
Total radiation loss	$W = \frac{2c}{3} \left(\frac{e}{mc^2}\right)^4 H^2 E^2 \cos^2 \theta$	$W = 6.0 \cdot 10^{-27} E^2 H^2 \cos^2 \theta$
Time for energy loss from ∞ to E	$t = \frac{3m^4 c^7}{2e^4 H^2 E \cos^2 \theta}$	$t = 2.7 \cdot 10^{14} (H \cos \theta)^{-2} E^{-1}$

Some representative examples, that may illustrate the orders of magnitude involved, are given in Table III. All values have been computed for electrons. Protons give weaker radiation ($\sim m^{-1}$) and have a much longer life-time ($\sim m^4$).

The characteristic times for energy loss are quite large in all cases mentioned, except for hard electrons in cosmic rays (which are just wiped out) and for the electrons giving the optical radiation in the Crab nebula (which have to be replenished somehow).

TABLE III. — *Representative examples of synchrotron radiation.*

	E (eV)	$H \cos \theta$ (G)	R	ν_c	t
Synchrotron	$7 \cdot 10^7$	$5 \cdot 10^3$	46 cm	$4 \cdot 10^{14}$	0.14 s
Solar electrons	$3 \cdot 10^8$	1	100 km	$1.5 \cdot 10^{14}$	1 day
Cosmic-ray electrons in the Galaxy	{ soft $3 \cdot 10^{10}$ hard $3 \cdot 10^{18}$ radio 10^8	10^{-5}	2/3 astr. unit	$1.5 \cdot 10^{11}$	10^{14} s
		10^{-5}	0.3 kpc	$1.5 \cdot 10^{27}$	10^6 s
		10^{-3}	3000 km	164 MHz	10^5 years
Crab nebula	{ opt. $2 \cdot 10^{11}$ $3 \cdot 10^9$	10^{-3}	1/20 astr. unit	violet light	50 years
Halo of Galaxy		10^{-6}	2/3 astr. unit.	150 MHz	10^{17} s

Note that the energy loss $dE/dt \sim E^2$ gives rise to a finite time to bring the energy from ∞ to E . For non-relativistic electrons the more familiar exponential decay occurs with an energy decay time

$$\tau = \frac{3}{4} \frac{m^3 c^5}{e^4} (H \cos \theta)^{-2} = 2.6 \cdot 10^8 (H \cos \theta)^{-2}.$$

In a thermonuclear machine with $H = 10^4$ gauss we must use for average electrons (10^4 eV) the non-relativistic formula, which gives $\tau = 3$ s, and for the high-energy tail of the distribution (10^6 eV) the relativistic formula: $t = 3$ s. This seems in either case an important loss.

III. — The Crab Nebula.

9. — Observational data on the shell.

About 1770 MESSIER made a list of nebulae and other fuzzy objects so that comet hunters would not be disturbed by them. Number 1 of this list is the Crab nebula. The first identified radio source (Tau A) was this same object.

Optical observations (photography, spectroscopy, photo-electric photometry) show that it consists of two parts:

- 1) a shell, consisting of filaments, which gives an emission line spectrum.
- 2) an inner mass that is fuzzy but not amorphous, and which gives a continuous spectrum.

The shell has a normal nebular spectrum, from which an electron temperature $T_e = 15\,000^\circ\text{K}$ and an electron density $N_e = 10^3\text{ cm}^{-3}$ has been derived.

The transverse angular expansion can be measured by comparing old photographs with recent ones, and the radial expansion can be measured from the Doppler shift. If we assume that the radial and transverse expansion-velocities are equal, we can derive the actual dimensions and the distance of the nebula. From the transverse expansion we can extrapolate backwards and find that the nebula originated about 1000 years ago. It is most likely to be identified with the supernova of 1054, known from Chinese sources.

The radial velocity measured by Doppler splitting gives a velocity of 1150 km/s; the distance is 1 kpc or 2 kpc, the corresponding longest diameter is 1.8 pc. or 3.6 pc. The uncertainty is in the question whether the expansion velocity in the line of sight equals that at the end of the major axis (true form = oblate spheroid) or at the end of the minor axis (true form = prolate spheroid).

Bright knots in the spectral lines can be identified with individual filaments; their radial velocities give a 3-dimensional picture of the filaments, showing that they are located in the outside of the nebula. The mass of the shell is 0.1 to 1 solar mass.

10. - Observational data on the inner part.

The visual continuous spectrum is white and does not give much of a clue to its physical explanation. The first surprising fact came from radio observations

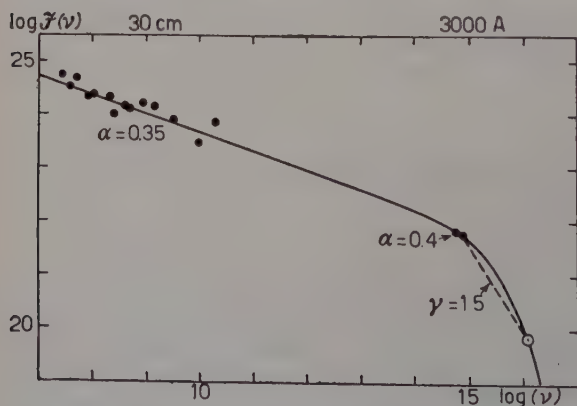


Fig6. . - Combined radio and optical spectrum of the inner part of the Crab nebula. [From L. WOLTJER: *Bull. Astron. Nether.*, 14, 39, no. 483 (1958)].

which yield a value of $S(\nu)$ which is a factor 1000 higher than the value found in the visual region. The radio and the visual continuous spectrum appear to lie on the same straight line, the slope of which corresponds to what we now call a typical non-thermal spectrum. A significant point in the ultraviolet was computed by WOLTJER from the maximum amount of ionizing radiation that reaches the shell. Fig. 6, which may be considered

as an extension of Fig. 4, shows all of these data.

ŠKLOVSKIJ suggested that synchrotron radiation is responsible for both

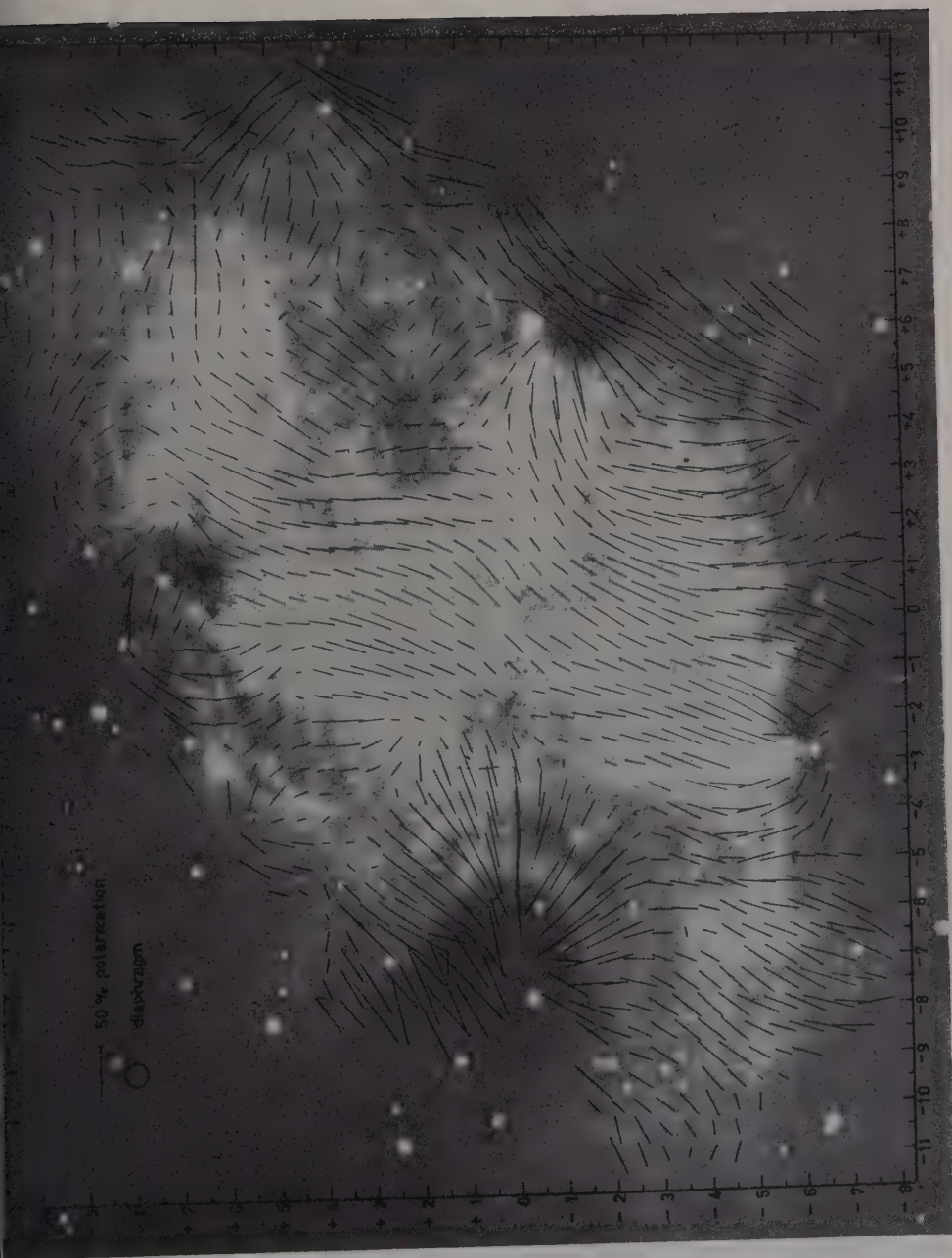


Fig. 7. - The Crab nebula. Measured polarization of the visual continuum superposed on a photograph of this continuum taken without polarizing filter. Each bar presents the direction of the electric vector and the degree of polarization, with maximum values about 60%. [From L. WOLTJER; *Bull. Astron. Nether.*, **13**, 301, no. 478 (1957)].

radio and the optical spectrum. A crucial test would be the optical polarization. This test was made in Russia, then in Leiden, then at Mount Palomar. Nearly 100% linear polarization was found in many places. The most detailed map of the optical polarization has been made by WOLTJER from Palomar plates. Fig. 7 shows this map printed on the reproduction of a Palomar photograph of the inner part of the Crab nebula taken without polarization filter.

The radio observations of the Crab nebula presumably all refer to the inner part, as the shell emission must be negligible. The radio polarization is absent or small in the meter waves. Probably it is cancelled by the Faraday effect. A small percentage (7%) has recently been found at $\lambda = 3$ cm.

The radio size of the Crab nebula has been measured in Dwingeloo and elsewhere by employing occultations by the moon. The full sizes, obtained by optical and radio observations, are about equal, but the light has a marked concentration towards the centre whereas the radio brightness fills the nebula more homogeneously.

11. - Synchrotron radiation and energy spectrum.

Before we review the attempts to explain these highly intriguing properties of the Crab nebula, two subjects of a more physical character have to be discussed in this section and the next one.

From Section 8 we know the emission spectrum of mono-energetic electrons. Now, if the energy distribution is given by

$$N(E) dE = k E^{-\gamma} dE,$$

then the spectrum emission per unit volume found by elementary integration over all energies is

$$\varepsilon(\nu) = \text{const} \times H^{\frac{1}{2}(\gamma+1)} \nu^{-\frac{1}{2}(\gamma-1)} = \text{const} \times H^{\alpha+1} \nu^{-\alpha},$$

The precise expression for the constant is irrelevant to us. But it is important to note that the expressions

$$\alpha = \frac{1}{2}(\gamma - 1), \quad \gamma = 2\alpha + 1$$

give a direct relation between the exponent of the energy spectrum, γ , and the exponent of the radio spectrum, α .

Some actual values may illustrate this relation:

		α	γ
Crab nebula	{ radio light	0.35	1.7
	{ ultra-violet light	1.5	4.0
Galaxy, non-thermal radiation		0.65	2.3
Cosmic rays	{ soft	—	1.5
	{ hard	—	$2.5 \div 3.0$

12. — Force-free fields.

Definition: a force-free field is a magnetic field with the current parallel to the field, *i.e.*, a field in which the Lorentz force is zero:

$$\mathbf{B} \times \text{curl } \mathbf{B} = 0.$$

The trend of astrophysical research in recent years is to consider force-free fields of great importance in the explanation of cosmical phenomena. The initial argument put forward by LÜST and SCHLÜTER was mainly intuitive: any situation in which a tenuous gas carries a strong magnetic field, so that the inertial forces and gas pressure gradients are smaller by order of magnitude than the gradients of magnetic pressure, can be maintained only if the magnetic force vanishes, or nearly vanishes. Very recently WOLTJER and CHANDRA-SEKHAR have derived a number of exact theorems, showing indeed the unique importance of force-free fields for certain equilibrium configurations. We shall very briefly summarize the basic properties.

There exist three possibilities to realize a force-free field:

trivial case:	$\text{curl } \mathbf{B} = 0,$	
simple case:	$\text{curl } \mathbf{B} = \alpha \mathbf{B}$	($\alpha = \text{constant}$),
general case:	$\text{curl } \mathbf{B} = \alpha \mathbf{B}$	(α depends on the position).

The simplest example is a field expressed in rectangular co-ordinates, in which at any level, $z = \text{constant}$, the field is homogeneous and parallel to the steps of a winding stair case:

$$H_x = \cos \alpha z, \quad H_y = \sin \alpha z, \quad H_z = 0.$$

A similarly simple example in cylindrical co-ordinates was given by LUND-QUIST. The lines of force are helices with pitch decreasing with increasing radius. These examples are force-free fields with $\alpha = \text{constant}$ and so is the

set of solutions in spherical co-ordinates first given by LÜST and SCHLÜTER. At present also the complete solution for constant α in spherical co-ordinates is known. No examples have been worked out in which α is a function of position.

Theorems on boundary conditions:

1) If we require the absence of currents outside the volume V , and $\mathbf{B} \rightarrow 0$ at infinity, a fully force-free field is impossible.

2) A force-free field can be contained within a volume V by a surface current on the surface S enclosing V , in such a manner that no currents flow outside V and $\mathbf{B} \rightarrow 0$ at infinity.

Theorems of L. WOLTJER:

1) The force-free fields with $\alpha = \text{constant}$ are among the fields with maximum magnetic energy $\int H^2 dV$ for a given mean square current density $\int |\text{curl } \mathbf{B}|^2 dV$.

2) The force-free fields with $\alpha = \text{constant}$ are among the fields with minimum ohmic dissipation for a given magnetic energy (and $\sigma = \text{constant}$).

3) Force-free fields with constant α represent the state of lowest magnetic energy in a closed system.

4) Hydromagnetic equilibrium in the absence of fluid motions requires a force-free field with constant α .

These theorems are mentioned here for their intrinsic interest but it should be clear that a proper understanding cannot be gained from these brief formulations. The reader is invited to consult the original papers. Whereas theorems (1) and (2) derived by CHANDRASEKHAR and WOLTJER lead to the equation

$$\text{curl}(\text{curl } \mathbf{B} - \alpha \mathbf{B}) = 0, \quad \alpha = \text{constant},$$

theorems (3) and (4) give the more restricted result

$$\text{curl } \mathbf{B} - \alpha \mathbf{B} = 0, \quad \alpha = \text{constant}.$$

The condition $\alpha = \text{constant}$, first introduced merely for mathematical simplicity now follows from physical considerations.

13. - The magnetic field of the Crab nebula.

Let us first make an order-of-magnitude estimate of the field strength. Suppose we wish to consider electron acceleration only at the explosion,

1000 years ago. Then the decay time (from Section 8) is

$$t = 3 \cdot 10^{14} H^{-2} E^{-1} \geq 3 \cdot 10^{10}.$$

The electrons giving optical radiation have

$$\nu = 1.6 \cdot 10^{-5} H E^2 = 1.5 \cdot 10^{15}.$$

So

$$\left. \begin{array}{l} H^2 E \leq 10^4 \\ H E^2 = 10^{20} \end{array} \right\} \text{ which gives } \left\{ \begin{array}{l} H \leq 10^{-4} \text{ gauss} \\ E \geq 10^{12} \text{ eV} \end{array} \right.$$

It is estimated that the actual values lie close to these limits. Assuming H much larger gives a short life time. OORT and WALRAVEN have made computations with $H = 10^{-3}$ G, and have taken account of the gradual losses of energetic electrons during the 1000 years. WOLTJER has also taken H somewhat higher, $H = 3 \cdot 10^{-4}$ G, but he introduces an acceleration mechanism that at the present time is still strong enough to overcome the radiation losses of all electrons with $E < 10^{12}$ eV. Some evidence for the operation of such an acceleration is in the moving ripples near the centre observed on photographs by BAADE. On the other hand, to make H even lower would require even more energetic electrons, and would give trouble with the interstellar fields, which are estimated to be of the order of 10^{-5} G.

We now consider the problem of the different sizes obtained by radio and optical measurement of the nebula. There are two alternatives:

a) The energy spectrum is the same through the nebula. The magnetic field in the outer parts is so weak that optical frequencies are not measured there.

b) The magnetic field is the same through the nebula. The energy spectrum of relativistic electrons is different in different parts of the nebula in this sense, that the cut-off energy is lower in the outer part. WOLTJER shows that possibility b) is in better agreement with the colour observations.

A further problem of great interest is the geometry of the magnetic field, WOLTJER supposes that it resembles the lowest model of force-free field that can be contained in a sphere. Some support to this idea is given by the large scale symmetry in the polarization measurements, with an S -shaped twist. The net polarization to be expected in such a field, which has a different direction in different volume elements along the line of sight, comes to the right order of 20%. The surface current needed is identified with the filamentary shell. Unlike the inner part, the shell is indeed massive enough to take up the outward Lorentz force. In spite of the impression from a photograph in continuous light, the nebula as a whole must be pictured as a rather empty shell. The well-defined filaments in the shell probably are current channels contracted by pinch effect.

Having gone so far into the interpretation of the Crab nebula we encounter new intriguing problems.

Where does the magnetic field come from? Where do the relativistic electrons come from? These questions have been very much in discussion and have not really been settled. The best work is probably that of WOLTJER, who has proposed that the magnetic field has resulted from some dynamo mechanism in early years after the explosion, and that electrons are produced by radioactive decay of the debris of the supernova explosion. Certain other ideas have been put forward by PIDDINGTON and by the Russians.

IV. - Interstellar Matter in our Vicinity.

14. - Temperature of the interstellar gas.

Interstellar matter has been studied for half a century, but most of this time only a relatively small vicinity of the sun ($r < 1$ or 2 kpc) could be observed. And still, our most detailed observations and computations refer to this particular region of the galactic disk.

The first problem is the temperature. There is absolutely no reason why there should be thermodynamical equilibrium in interstellar space. Instead of a furnace with walls all at the same temperature we roughly have:

10^{14} part of wall has $T \approx 10^4$ °K (stellar disks)

rest part of wall has $T \approx 0$ °K (interspace).

Before talking about a temperature at all we should first make plausible that the degrees of freedom of a certain subsystem have so many mutual interactions that within it a temperature can be defined. We then have to count patiently all gains and losses of energy to find the temperature of this subsystem in the stationary situation. Table IV gives three examples (temperatures all in degrees Kelvin). The values in this table are (with some changes) taken from SPITZER's work.

The only comment to be made to the first line of this table is that actual dust particles in space probably are poor infrared radiators, because they are so small. They may have $T = 10$ °K or 20 °K.

Further it should never be assumed that excitation or ionization temperatures are anywhere near the computed kinetic temperatures. Saha's law just does not hold. Instead, we should equate the number of ionizations and recombinations, which may occur by different processes. The same remark

for exactly the same reasons has been made earlier in this course for the ionization equilibrium in the corona and in Zeta.

TABLE IV. — *Temperature equilibrium of interstellar matter.*

	Subsystem	Gains	Losses	T	Relaxation time
Black test body	internal degrees of freedom	absorption of visual radiation	emission of infrared rad.	3°	—
Gas in H II region	random motions of electrons, protons and atoms (equipartition within 1 month)	ionization of H-atoms by UV radiation budget:	excitation of O^+ and O^{++} ions by electrons 10^{-24} erg/s cm^3	10000° ($n_e = 1 \text{ cm}^{-3}$)	10^5 years
Gas in H I region	random motion of electrons, ions and atoms (similar)	ionization of C atoms, heating by cloud collisions budget:	excitation of low levels by electrons 10^{-28} erg/s cm^3	125° ($n_H = 1 \text{ cm}^{-3}$)	10^7 years

The basic reason for the existence of H II and H I regions is that the ultra-violet quanta (from hot stars) that are large enough to ionize hydrogen are exhausted by absorption before they reach certain volumes of space which, consequently, remain neutral. Only the longer-wave radiation can penetrate into these H I regions and can still ionize C and a few other elements of low ionization potential, which, however, are less abundant than H by a factor 10^4 . This means that a volume of H II gets and spends in its yearly energy budget about 10^4 times what the same volume of H I gets and spends.

Initially, SPITZER arrived at 50 degrees as the most probable value for H I. But the 21 cm wave length observations showed 125° as the better value. So a new source of heating had to be found, for which collisions between clouds are now held responsible.

The relaxation times, computed as the ratio of energy content to energy budget, are still relatively small compared to times of evolution. So the stationary case may be well approached, except for H I regions where heating may come by sudden jerks. They may resemble a man with many rich aunts and uncles who does not keep a regular budget but inherits money at irregular intervals and then spends most of it fast and the rest gradually.

The most important consequence of the factor 100 in temperature between H II and H I region is the large pressure differences which are set up.

Let us for a moment call the smothered-out density and temperature of H I regions, as observed at 21 cm, the « normal » state of the interstellar gas. Then,

by order of magnitude, $n=1$, $T=10^2$, $nT=10^2$. If a new star is formed inside such a region, the star will reach the stage of evolution where it begins to emit quanta ionizing the hydrogen. They tend to form an H II region with $n=1$, $T=10^4$, and $nT=10^4$. But this situation is highly instable. The strong pressure of the hot gas will compress the cold gas and try to change it into an equal pressure gas with $n=10^2$, $T=10^2$ and $nT=10^4$. Naturally such an end condition is not reached, but, instead the H I regions start to expand and break up into smaller, somewhat compressed units. There is good support, both in the observed motions and in the photographed forms of emission nebulae that this picture is correct in broad lines. It also gives a natural explanation of why the clouds are continuously formed again. It seems that these events provide the basic process by which nuclear energy (in the hot star) may be fed directly into the motions of the interstellar clouds. At the same time, conditions in the compressed H I regions may be favorable for the formation of even more new stars.

Observational checks: All of this is mainly theory based on difficult estimates of cross-sections, densities, etc. It has taken several years before the temperature computations of SPITZER were taken quite seriously by himself and by other astronomers. Now there are several observations confirming at least in general lines the correctness of the theoretical picture derived above.

In the denser than average H II regions a direct temperature determination may be made from line intensity ratios of O III and other ions. Also the radio brightness of nearby H II regions at 3.5 meter (optically thick) comes in the correct order. The much smaller value for H I regions has been inferred from the saturation value of line intensity in certain regions. It may be noted that, if no absorption or self-absorption occurs, the temperature does not come into the formula for the intensity of the 21 cm line. Finally, the existence of expanding cloud complexes and of expanding associations of stars lends greater claim of reality to the idea of expanding H II-regions. The phenomena are extremely complex and still very imperfectly understood.

15. - Motions in the interstellar gas.

One might think: why not use Doppler broadening to measure the temperature? The answer is that the thermal motions are relatively small compared to the fluid velocities or cloud velocities. The usual statistical studies of the Ca^+ and Na absorption lines and of H emission line at 21 cm all give 5 to 8 km/s for the root mean square velocity component in the line of sight. The widths of individual components in Ca^+ give somewhat lower values (3 to 4 km/s) but the resolution is uncertain. The finest data are from the H line in absorp-

tion in four bright radio sources. There the value is $(1.2 \div 1.9)$ km/s, corresponding to $T = 200^\circ$ to 400° , if the motion is interpreted as thermal motion. This beautifully confirms the low temperature of H I regions but as seen above, it is likely that the real temperature is of the order of 125° , or in places still lower. All further motions have to be interpreted as fluid motions.

As it is quite common to see separate displaced components of the absorption lines, both in Ca^+ and in H, the fluid motions may be interpreted as separate clouds moving with their own speeds. The sizes of these clouds are still a matter of some debate. Ordinary estimates are $(10 \div 30)$ pc. All of these data refer again to the galactic disk in our vicinity.

What keeps these clouds going and what determines their peculiar shapes? If left alone, they would run into each other and gradually disperse. Much thought has been devoted to this question. I shall postpone a review of this subject until we have seen more of the magnetic fields and spiral arms.

16. - Interstellar magnetic fields. Observational evidence.

How can we measure or detect a magnetic field in an inaccessible place? Some possibilities in a roughly decreasing order of directness of proof are:

- A) Zeeman effect (as in sunspots),
- B) Polarization of synchrotron radiation (as in Crab nebula),
- C) Forms suggesting lines of force (as in corona of sun),
- D) Birefringence (radio circular birefringence = Faraday effect),
- E) Dichroism (optical linear dichroism = interstellar polarization),
- F) Phenomena for which we cannot find any other explanation.

For the interstellar gas, A and B have not yet been measured but probably are within the range of present observing techniques. On C there is little evidence except for planetary nebulae, which sometimes have very peculiar shapes. Also D is unobserved but it will bother us very much in trying to measure B. Under F fall the, historically oldest, arguments on the existence of magnetic fields to keep the cosmic rays within the Galaxy. They are discussed in the lecture by Dr. DAVIS. Altogether, the present situation, except for effect E, is one of very scarce evidence. I shall now discuss two points in somewhat greater detail.

Interstellar polarization. - It was discovered by accident in 1949 that distant stars have linearly polarized light. The effect is clearly correlated with the extinction by interstellar dust and must be interpreted as a difference in the numerical extinction value for different directions of polarization. Such an effect can, in principle, be caused by non-spherical dust grains oriented in a

magnetic field. I shall entirely skip the possible theories both for the dynamics of the orientation effect and for the optics of the resulting polarization. We just assume on the basis of these theories that the following three directions coincide:

direction of maximum electric vector of observed light,
preferred direction of minimum axis of grains (as projected on sky),
direction of magnetic field (as projected on sky).

So far several thousand stars have been observed. This means that we have maps of the projected field lines. Two rather different samples are illustrated

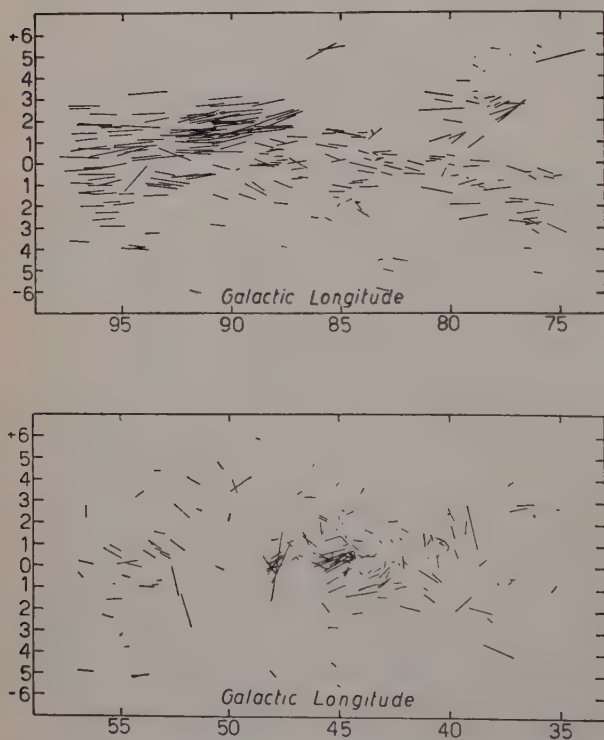


Fig. 8. — Measured interstellar polarization in two fields. Top: longitudes $75^\circ \div 95^\circ$ with good alignment. Bottom: longitudes $35^\circ \div 55^\circ$ with poor alignment. Each bar presents the direction of the electric vector and degree of polarization, with maximum values about 10%. [From W. A. HILTNER: *Ap. Journ. Suppl.*, 1, no. 24 (1956)].

in Fig. 8. Generally, the field is fairly regular on a large scale and by no means turbulent with a small scale of 10 pc or so. More particularly, it appears to be parallel to the galactic plane in the fields where the alignment is good. For example, near $l=90^\circ$ (Fig. 8-A) it is very well aligned with deviation angles of 5° only. At other longitudes (Fig. 8-B) it is highly erratic.

It has been claimed, first by CHANDRASEKHAR and FERMI, that this means that a spiral arm is a continuous tube of force. Some bulges in the lines of force then are due to the cloud motion inside the arm. This would explain that in looking sideways at the arm the field would be regular with a limited play in the directions and in looking along the arm it would seem erratic.

We shall return to the dynamics of this model in the last lecture. Right now I wish to state that the observational support is present but weak. There

is a tendency of this sort but it is difficult to judge if it is general, also because in the neighbourhood of the Sun, to which these data refer, the map of the spiral arms is still fairly incomplete. On a still smaller scale there is plenty of evidence of connection with the structure of individual filamentary nebulae, *e.g.*, in the Pleiades and in the North America nebula, which may again tend to mask the structure of the field on the scale of a spiral arm.

Another promising attack on the galactic magnetic field are the attempts to measure the *polarization of the continuous radioemission of the Galaxy*. You have heard the theory. If the background is due to synchrotron radiation, it must be 100% polarized in any volume element. But the actual measurements made so far give a polarization less than 1%. This may be due to

1) addition of thermal (unpolarized) radiation; this is negligible unless we are right near the galactic plane in a short wave length.

2) addition of emission in many elements along the line of sight and in the width of the beam, which have different directions of \mathbf{H} .

3) addition of radiation in many frequencies that suffer different Faraday effect.

In spite of these drawbacks it is an exciting thought that perhaps the field has enough of a large scale to be measured. Table V gives an idea of the possibilities.

TABLE V. — *Specification of attempts to measure polarization of galactic background.*

	Beam	Band (MHz)	(MHz)	T_b	pT_b	p
RAZIN (1956)	20°	0.4 — 1.2	200	75°	3°?	0.04?
THOMSON (1957)	25°	4	160	400°	< 4°	< 0.01
DWINGELOO (plan)	2°	1 and 10	400	30°	(± 0.3)	(± 0.01)

In the bottom line the accuracies that can perhaps be reached are indicated. The number of radians by which the plane of polarization is turned is

$$\varphi = 2.36 \times 10^4 \frac{N H l \cos \theta}{\nu^2} \quad (\text{c.g.s.}).$$

With $l = 500 \text{ pc} = 1.5 \cdot 10^{21}$, $N = 0.1$, $H \cos \theta = 10^{-5}$, $\nu = 4 \cdot 10^8$, this gives $\varphi = 220$. So the precaution of taking $\Delta f/f = 1/400$ is very essential.

V. - The Interstellar Plasma Throughout the Galaxy.

17. - Spiral arms.

The mass of the Galaxy is estimated at 10^{11} solar masses, the total mass of the gas in it at $1.5 \cdot 10^9$ solar masses = 1.5 %. We have seen that the present motions of stars and gas in the disk are almost precisely motions in circular orbits under the influence of gravitational forces only. This holds for distances to the center which are more than 3 kpc. The absence of systematic deviations from circular motions is illustrated by the fact that the direction of the center, derived from the study of differential motions in the solar neighbourhood coincides exactly with that derived from the space distribution of Population II stars.

With the sun's distance $R_1 = 8.2$ kpc from the center of the Galaxy and the sun's velocity of 220 km/s, we find a revolution period of $2.3 \cdot 10^8$ years, which makes more than 30 revolutions during the age of the Galaxy ($8 \cdot 10^9$ years).

In this disk are the spirals arms. They are primarily places of high gas concentration. In this gas new stars are formed continually, which make spiral arms conspicuous on photographs of other galaxies. The gravitational potential suffers very little distortion from the presence of a spiral arm.

Our present knowledge about these arms is inconsistent. At one side we have made maps based on the hypothesis that each cloud of hydrogen atoms moves in a circular orbit governed by gravitation only. On the other hand we know that the spiral arms are first of all a phenomenon in the gas and may quite well be governed by forces or gas dynamics of magnetic fields. A further support of this view comes from the fact that the differential rotation in the absence of the other forces will wind up the arms beyond recognition in few revolutions. So we feel uncomfortable about these maps based on the 21 cm data and should like to interpret them with more certainty.

The first definite suggestion about magnetic fields in the spiral arms was made by CHANDRASEKHAR and FERMI. The spiral arms would form a long tube of force in which selfgravitation balances the sum of the pressures due to cloud motions and the magnetic field; this part of the theory seems not acceptable. Further, they suggested that local deviations in the lines of force by an average angle α would be caused by the gas motion with velocity v . If, for instance, we equate these values to the amplitudes in a standing hydromagnetic wave, we have

$$v^2 = \frac{H^2 \alpha^2}{4\pi \rho}.$$

With the values (revised by SPITZER): $v = 7$ km/s, $\alpha = 0.13$ rad, $\varrho = 2 \cdot 10^{-24}$ g/cm³, this gives $H = 2.6 \cdot 10^{-5}$ gauss.

This theory ignores the differential rotation entirely. Also it does not tell us about any forces that might hold a spiral arm together lengthwise. Therefore, Mr. WENTZEL has tried at Leiden to make computations about a simple model in which we start with a magnetized, isolated cloud with diameter $\frac{1}{2}$ kpc, which is gradually drawn out into a spiral arm. The stretched lines of force then react back on the cloud and oppose further stretching but so far there is little indication that this effect is really important.

18. - Expanding motion near the galactic nucleus.

A quite unexpected discovery has come out of the 21 cm line measurements at Dwingeloo. At angles smaller than 25° from the galactic center the line profiles have very long but faint wings. It is as if a very strongly broadened line were added to the ordinary profile. This must be due to motion of the gases in the central region of the galaxy, where R is smaller than 3 kpc. Initially, these motions were interpreted as turbulent motion. With the new telescope more details were seen and it was soon discovered that one of the strongest details in it corresponds to an arm taking part in a motion of rotation plus expansion. The expansion component is 53 km/s, as seen from the absorption line that this arm cuts out in the continuous spectrum of the source at the galactic center. At present, almost all the time during which the galactic center is above the horizon at Dwingeloo is devoted to a further study of this problem. It appears that expansion in this central region is a general phenomenon, which is not confined to one arm. We find absorption in the central source at all frequencies corresponding to negative velocities (approach, 0 to -150 km/s) but none at the corresponding positive velocities.

So far, this motion is entirely unexplained. If the average velocity of expansion is 100 km/s, the travel time from 0 to 3 kpc is only $3 \cdot 10^7$ years. Under gravitational forces alone the material would soon fall back, but, since we do not see it fall back, it seems more likely that very strong non-gravitational forces are at work. But the supply of energy and of mass at the center then is a very severe problem; the average density of H in this region is of the order of 0.4 cm^{-3} , i.e., about half of what it is further out. If there is no new supply of mass, for instance through the halo, the mass in the nuclear region would barely suffice for this process to go on through the age of the Galaxy.

19. - Halo theories.

We have thought about the halo as containing relativistic electrons emitting the continuous radio noise. We need only $N_e = 10^{-12} \text{ cm}^{-3}$ if $H = 10^{-5}$ gauss. A halo has also been observed around the Andromeda nebula giving the same order-of-magnitude estimates. This leaves the region virtually empty, just like the inside of the Crab nebula. However, the next question is if there cannot be a real (ordinary) ionized gas in this halo. There are some reasons in the observations, notably in the continued existence of clouds to assume some kind of pressure equilibrium between the halo gas and the «normal gas». SPITZER suggests that, for instance, $n = 10^{-4}$, $T = 10^6 \text{ }^\circ\text{K}$, and $nT = 10^2$. There would be absolutely no way to observe this gas directly. On the less drastic assumptions, $n = 10^{-2}$, $T = 10^4 \text{ }^\circ\text{K}$ and $nT = 10^2$ made by PIKELNER, there still should be a fair proportion of neutral H, which the observations do not seem to confirm. Moreover, in order to bring the gas with $T = 10^4 \text{ }^\circ\text{K}$ to high distances above the galactic plane, PIKELNER has to assume strong fluid motions of 100 km/s, in this gas. It is difficult to see how these motions can be prevented from degrading into thermal motion.

Direct observations do not tell us anything about the magnetic field in the halo, except that it must be there to make synchrotron radiation possible. Now, it is interesting that the recent radio observations show that the non-thermal component of galactic radio-emission is not equally strong throughout the halo. There is a marked concentration to the disk so that the emission per unit volume near the disk may be about 10 times that at $z = 10 \text{ kpc}$. From the spectral law: $B \sim \nu^{-0.6}$ and the theory given earlier we find that $\varepsilon \sim NH^{1.6}$.

This still leaves two possibilities: does H or N increase near the disk? GINZBURG has solved this dilemma by assuming that $N \sim H$. The field far up in the halo should then be about $\frac{1}{3}$ of the field in the disk. The qualitative ground for the assumption $N \sim H$ may be found in the consideration that the electrons probably are accelerated or supplied in or near the disk, in a region of big H . The pitch of their orbits increases if they move to smaller H and, consequently, the number density drops. (This gives a decrease but not an exact law $N \sim H$.)

Some considerations on the shape of the halo magnetic field must be made. Nothing about it is known. The few simplest suggestions that we might make do not work. Assume, e.g., a big ring current around the galactic system, yielding a poloidal field and any cosmic rays that are formed will move outward and escape from the galactic system. This leads to difficulties that will be discussed further by Dr. DAVIS. On the other hand, if we take mainly toroidal lines of force in the halo, parallel to the disk, and if in addition we think that the angles of pitch in a weak field are fairly strong, another

problem arises. In these circumstances, when looking into the halo, we should never see an electron moving into our direction. Hence we could never receive any synchrotron radiation at all from the polar caps, which is contrary to the observations.

20. - Energy budget of the interstellar gas as a whole.

Like the preceding subject, the magnetic fields in the halo, this question is intimately connected with the origin of the cosmic rays. So a complete discussion is not needed at this time.

The problem became acute when it was realized that the clouds will run into each other, be heated, and radiate the energy away, so that there is a severe loss from the kinetic energy of the interstellar medium. It was first believed that the differential rotation (galactic) could supply this by means of some turbulent phenomenon. It is now thought, however, that the supply of energy must come from the expanding H II region, *i.e.*, from nuclear power.

If this is correct, the budget would consist of one main source of loss (by collision between clouds) and one main source of income (the expanding H II regions). Both would amount to 10^{39} erg/s over the entire Galaxy. However, the situation is far from clear. In some theories, cosmic rays account for even 10^{40} erg/s extracted from the gas motions, which is clearly impossible when there is no additional gain. There might well be further gains, because the expanding motion near the center gives us some reason to believe that there is a process, magnetic or otherwise, which feeds huge amounts of energy directly into the large-scale motion of the Galaxy. The kinetic energy carried away by the gas expanding from the center is estimated at 10^{40} erg/s. A similar amount would be available if we could use up ten percent of the energy contained in the rotation of the interstellar gas.

BIBLIOGRAPHY

References to the world-wide literature on the topics of these lectures may be found in the following reports.

Report commission 34 on interstellar matter, in *Trans. Intern. Astron. Union*, **9** (Meeting Dublin 1955) and **10** (Meeting Moscow 1958), Cambridge.

H. C. VAN DE HULST and J. M. BURGERS ed.: *Gas dynamics of cosmic clouds*, I.A.U. Symposium, no. 2 (Amsterdam, 1955).

H. C. VAN DE HULST ed.: *Radio astronomy*, I.A.U. Symposium, no. 4 (Cambridge, 1957).

R. N. THOMAS and J. M. BURGERS: *Rev. Mod. Phys.*, **30**, 911 (1958).

R. N. BRACEWELL ed.: *Radio astronomy*, in *I.A.U. Symposium*, (Stanford), in preparation.

The *Bulletins* of the Astronomical Institutes of the Netherlands (B.A.N.) contain the full publications of Dutch work on the 21 cm line (no. 452, 458, 475, 480), on the continuous radio emission (no. 472, 488) and on optical studies of the Crab Nebula (no. 462, 478, 483).

The new papers on force-free fields referred to in the Section III are: S. CHANDRASEKHAR and L. WOLTJER: *Proc. Nat. Ac. Sci.*, **44**, 285 (1958) and L. WOLTJER: *Proc. Nat. Ac. Sci.*, **44**, 489 and 833 (1958).

INTERVENTI E DISCUSSIONI

— L. S. GOLDSTEIN:

By using different frequencies and measuring the corresponding ratios of the deflection, the Faraday effect may be eliminated entirely.

— H. C. VAN DE HULST:

In principle this works well, but in order to measure anything at all we require a narrow bandwidth.

— T. GOLD:

The 3° for an interstellar black test body is badly known. The contribution of the stars in the galaxy is fairly well known, but extragalactic sources, especially for a long wavelength, are poorly known. Different cosmological theories give different results; the radiation of particles should be investigated in the laboratory. The uncertainty in temperature may amount to a factor of 10.

— H. C. VAN DE HULST:

The most naive cosmological model of an euclidean space homogeneously filled with galaxies without red shift would give 10^{14} times more radiation than we get from the galaxy. My impression is that as soon as red shift is introduced the extragalactic contribution becomes negligibly small, but other models might give other results.

— L. BIERMANN:

The computed energy density of the extragalactic space is about 10^{-2} times the interstellar energy density and this computation seems confirmed by observations made in France. It does not seem likely that the introduction of other cosmological models would change the extragalactic energy density by a factor of more than 100, so that the interstellar energy density will not change by more than a factor of 2.

— B. LEHNERT:

If the clouds have a magnetic field reaching outside them, would the collision be simply elastic without heating?

— H. C. VAN DE HULST:

There is no direct observational evidence for such collisions but theoretically they seem possible.

— T. GOLD:

With the new radio-observational techniques the Zeeman effect of the 21 cm line could be measured even if it is as small as 10^{-5} G.

— L. BIERMANN:

It is known that there is a considerable exchange of mass between the stars and the gas and it is estimated that the loss of mass by the stars is about one solar mass per year for the whole galaxy. The figures for the gas density given by you are considerably lower than those adopted formerly. My problem is: can these exchanges of gas explain the apparent contradiction that the spiral arms should be young for one reason and old for another?

— H. C. VAN DE HULST:

There is little to say about this. OORT once suggested that spiral arms might grow on one side and lose matter on the other, but this suggestion has never been worked out.

— V. FERRARO:

On the basis of the general motion of the gas, the toroidal component of the magnetic field would be expected to be somewhat larger than the poloidal component.

— H. C. VAN DE HULST:

So: in the disk, parallel to the disk. Would the dynamo theory also predict something about the field outside the disk?

— V. FERRARO:

The field would perhaps be weak, because the field is confined to the regions where there are generators.

— H. C. VAN DE HULST:

That would make it difficult to understand the non-thermal radiation.

Propagation and Production of Electromagnetic Waves in a Plasma (*).

R. GALLET

National Bureau of Standards, Boulder Laboratories - Colorado

Electromagnetic waves can be produced in a plasma either by thermal or non-thermal mechanisms. Thermal radiation emitted by a plasma is due primarily to the bremsstrahlung of the random motion. The theory for this is well developed and explains the solar thermal noise emitted by the photosphere as well as from the chromosphere and the corona.

The non thermal mechanisms of emission of electromagnetic waves are of four types:

a) Čerenkov mechanism. Relatively slow particles crossing a plasma can produce this type of radiation because a plasma is much more dispersive than a common dielectric. The refractive index can then be very large and the phase velocity very small. Radiation of this type has never been observed neither in nature nor in the laboratory.

b) Synchrotron mechanism. Radiation is produced in this case by high energy particles in a magnetic field.

c) Travelling wave tube mechanism. If a beam of particles with velocity v moves in the presence of an electromagnetic wave of phase velocity $V_p = v$, then either the beam or the wave can increase its energy at the expenses of the other.

d) Shock waves mechanism. Shock waves may produce oscillations which in turn will radiate. The efficiency of this mechanism is low.

The mechanisms a) and b) involve motion of individual particles; mechanisms c) and d) involve instead collective motions.

Natural plasmas emit mainly non-thermal radiation. With the exception of the radiation of the quiet sun which is of thermal type we have the following examples of non-thermal radiation:

(*) Notes taken during the lectures and reorganized by the direction of the Course.

1) *Radio bursts from the planet Jupiter.* These bursts have the following interesting properties:

- a) They are quasi-monochromatic sources (bandwidth approx. 0.5 MHz)
- b) They are emitted in pulses of high energy (10^{18} ergs-pulse). For the emission of the entire planet, the integrated average rate is roughly 1 pulse/s.
- c) They exhibit a high frequency cut-off at about 30 Hz.

These radiations are certainly not due to lightning discharges since lightning shows a great range of frequency and does not have energy comparable to the Jupiter bursts.

2) *Solar bursts.* — All types of solar bursts that are already well observed are non-thermal emissions. Recently another important type of transient emission has been discovered by the group headed by DENISSE in Paris and has been called type IV bursts. It consists of the emission of an intense continuum (a very large band of frequencies between about 500 and 200 MHz) that appears after some strong solar flares. The duration of emission is of the order of one hour. Interferometric observations have shown that they take place far out above the solar surface, within the corona. From their polarization and other properties they show, they are believed to be due to *synchrotron* radiation from a steady cloud of very energetic particles.

3) *Galactic radio-emission.* — Increasing evidence indicates that the general galactic radio emission by interstellar gas is non-thermal as indicated by observations on frequencies less than 50 MHz. For instance, at 9 MHz the equivalent temperature is 10^6 °K and at 1 MHz it is 10^8 °K.

4) *Aurorae.* — Aurorae frequently emit electromagnetic radiation.

The propagation of electromagnetic waves in a plasma can explain two new phenomena discovered only recently although the fundamental information concerning the first one is contained in the Appleton-Hartree equation which has been known for more than 25 years. These phenomena are:

1) Whistlers.

2) Very low frequency emission also known as VLF emission.

Both are very low frequency phenomena; whistlers are trains of waves in the kHz range propagating along the earth's magnetic field with high dispersion and low velocity; VLF emission results from the mass motion of ionized clouds of particles in the outer ionosphere at 2 or 3 earth's radii distance.

A third application of the propagation theory of an electromagnetic wave in a plasma has a bearing on the problem of determining the properties of a dense laboratory plasma. In fact the electronic density and the electronic temperature of a dense plasma can be measured with microwaves whose frequency is lower than both the plasma frequency and the gyrofrequency.

I. - Propagation of Electromagnetic Waves in a Plasma.

1. - General relations for continuous waves and for a wave packet.

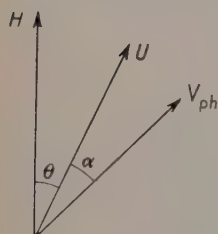
1) Homogeneous plasma. No refraction case. The refractive index n is a function of the frequency ω , of the angle between the direction of the magnetic field H and the direction of the phase propagation θ , and of three parameters of the medium: the plasma frequency, the gyrofrequency and the collision frequency. Then we have:

$$n = F(\omega, \theta, \omega_H, \omega_p, \nu),$$

where $\omega = 2\pi f$ = angular frequency of the radio wave;

θ = angle defined previously;

$\omega_H = 2\pi f_H = \frac{eH}{mc}$ = gyrofrequency of the electron in the magnetic field;



$$\omega_p^2 = (2\pi f_p)^2 = \frac{4\pi N_e e^2}{m} = \text{plasma frequency};$$

ν = collision frequency;

e is given in esu, H in gauss.

The following numerical relations for N_e and f_H are often useful:

$$f_H = 2.800 \cdot 10^6 H \quad \text{Hz} \quad (H \text{ in gauss}),$$

$$N_e = 1.24 \cdot 10^{-8} f_p^2.$$

Fig. 1. H = magnetic field; U = group velocity; V_{ph} = phase velocity.

For the moment we will ignore the effects due to ions. This involves restricting our range to those frequencies where ω is much greater than the ion-gyrofrequency. When the opposite restriction holds, hydromagnetic waves occur. If we consider a pulse (i.e. a wave-packet of plane parallel waves, limited in time or in space extension) propagating in the direction θ , the group velocity U is:

$$U = \frac{c}{n'},$$

where n' is given by

$$n' = n + \omega \frac{dn}{d\omega},$$

The direction of U is the direction of energy propagation.

The energy travels in a direction different from the direction of phase propagation; we call this the ray direction. If α is the angle between the group velocity U and the phase velocity V_{ph} , then $\operatorname{tg} \alpha$ is given by

$$\operatorname{tg} \alpha = \frac{1}{V_{ph}} \frac{dV_{ph}}{d\theta} = -\frac{1}{n} \frac{dn}{d\theta}.$$

The wave packet travels in the ray direction with velocity u

$$u = U \sec \alpha.$$

We define the group ray refractive index m' as

$$m' = \frac{c}{u} = n' \cos \alpha.$$

When these expressions for the direction of propagation of the energy are applied, we find for certain frequency ranges below the plasma and the gyro-frequency, that the direction of propagation of the energy is confined within a narrow cone centered on the lines of force of the magnetic field. Hence, for certain frequencies the lines of force may act as guides for the radiation.

2) Inhomogeneous plasma. In an inhomogeneous plasma, both H and N will vary from point to point. Consequently there will be *refraction*. The refractive properties are given by the equation for the curvature (Fig. 2):

$$\frac{d\varphi}{ds} = -\frac{1}{V_{ph}} \frac{dV_{ph}}{dN} = \frac{1}{n} \left(\frac{dn}{dN} \right),$$

N being the vector normal to the phase trajectory tangent to the wave front.

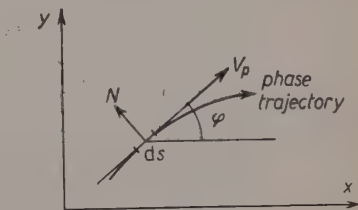


Fig. 2.

2. - General relationships between ε , σ , n , κ .

If we have a plane, sinusoidal wave propagating in the direction of the x axis, in a plasma with absorption coefficient per unit length, κ , and refractive index n , the wave is described by:

$$E = E_0 \exp[-\kappa] \exp \left[i\omega \left(t - \frac{n}{c} \right) \right].$$

This can be written in the form

$$E = E_0 \exp \left[i\omega \left(t - \frac{m}{c} x \right) \right],$$

where m is the *complex refractive index* defined by

$$m = n - ig,$$

where the *absorption index* g is

$$g = \frac{\kappa c}{\omega}.$$

This wave must be a solution of Maxwell's equations; and consequently of the telegraphic equation:

$$\nabla^2 E = \frac{\epsilon \mu}{c^2} \frac{\partial^2 E}{\partial t^2} + \frac{4\pi \sigma \mu}{c} \frac{\partial E}{\partial t}.$$

This condition leads to the following equations (taking $\mu = 1$)

$$n^2 - g^2 = \epsilon, \quad ng = \frac{2\pi\sigma}{\omega}.$$

These may be solved for n and g , to obtain

$$n = \sqrt{\frac{\epsilon}{2} + \sqrt{\frac{\epsilon^2}{4} + \frac{4\pi^2\sigma^2}{\omega^2}}}; \quad g = \sqrt{\frac{\epsilon}{2} - \sqrt{\frac{\epsilon^2}{4} + \frac{4\pi^2\sigma^2}{\omega^2}}}.$$

These equations give n and g as functions of σ and ϵ which in turn must be evaluated from a microscopic theory of the plasma.

The following are some useful approximations:

$$(1) \quad \sigma^2 \ll \frac{\epsilon^2 \omega^2}{16\pi^2}.$$

This approximation gives for V_{ph}^2

$$V_{ph}^2 = \frac{c^2}{n^2} = \frac{c^2}{\epsilon} \left[1 - \left(\frac{2\pi\sigma}{\epsilon\omega} \right)^2 \right].$$

For $\sigma = 0$; $V_{ph}^2 = c^2/\epsilon$ which corresponds to

$$n = n_0 = \sqrt{\epsilon}, \quad \text{the classical result.}$$

V_x can also be written

$$V_{ph} = \frac{c}{n_0} \left[1 - \frac{1}{2} \left(\frac{\kappa c}{n_0 \omega} \right)^2 \right].$$

2) For $\sigma^2 \gg (\epsilon^2 \omega^2)/16\pi^2$ (the case of a strongly conducting medium)

$$V_{ph} \simeq \frac{c}{(2\pi\sigma/\omega)^{\frac{1}{2}}}.$$

This shows that for ω very small, V_{ph} is proportional to $\omega^{\frac{1}{2}}$.

3. - Dispersion laws.

In general σ and ϵ are functions of ω , which depend on the particular mechanisms of interaction between the electric field of the wave, on the one hand, and the charges and fields of the medium on the other hand.

For σ we have the relationship for the conduction current

$$j = \sigma E,$$

σ generally being a function of E may be considered to be independent of E for small field strengths. However σ depends in an indirect way on the field strength since E influences the electron temperature T_e which is often much larger than the ion temperature T_i , and σ depends on T_e .

In a gas, j is given by the equation

$$j = n_1 e_1 \bar{C}_{o_1} + n_2 e_2 \bar{C}_{o_2},$$

where 1 = ions,

2 = electrons,

° indicates average values.

For $n_1 = n_2 = n$ and $e_1 = -e_2 = e$

$$j = ne(\bar{C}_{o_1} - \bar{C}_{o_2}).$$

In general \bar{C}_{o_1} is much smaller than \bar{C}_{o_2} as we will show; so we ignore the ion conductivity and write for j

$$j = -ne\bar{C}_{o_2}.$$

In order to show that $\bar{C}_1 \ll \bar{C}_2$ we make use of the approximate equations

$$\bar{C}_1 \simeq \gamma_1 \tau_1,$$

$$\bar{C}_2 \simeq \gamma_2 \tau_2,$$

where γ is the acceleration of the particles between collisions

$$\gamma_{1,2} = \frac{eE}{m_{1,2}},$$

and τ is the collision time given by

$$\tau_{1,2} = \frac{l}{\bar{C}_{1,2}},$$

l being the mean free path, and \bar{C} the average velocity.

Using the kinetic theory relationship

$$\bar{C}_{1,2} = \frac{3kT_{1,2}}{m_{1,2}},$$

one obtains

$$\frac{\bar{C}_1}{\bar{C}_2} = \left(\frac{m_2}{m_1}\right)^{\frac{1}{2}} \left(\frac{T_1}{T_2}\right)^{\frac{1}{2}} \ll 1.$$

The problem now is to obtain \bar{C}_2 as a function of E using kinetic theory. From an elementary statistical theory we obtain

$$\sigma = \frac{Ne^2}{kT} D_{12},$$

where D_{12} is the diffusion coefficient of electrons with respect to ions.

$$D_{12} = \frac{1}{3} l \bar{v}, \quad \bar{v} = \left(\frac{8kT_e}{\pi m}\right)^{\frac{1}{2}}.$$

The formula for σ can be expressed as

$$\sigma = \frac{N_e e^2}{m} \frac{1}{\nu},$$

where ν is the collision number; ν is determined from the kinetic theory.

When E is sinusoidally time dependent (in the absence of an external magnetic field)

$$E_0 = E_0 \exp [i\omega t].$$

The solution of the Boltzmann equation gives for the average velocity a solution of the form

$$\bar{C}_e = v_0 \exp [i(\omega t + \varphi)].$$

There we have a velocity in phase with the field, $v_0 \cos \varphi$ which determines σ , and a component in quadrature $v_0 \sin \varphi$ which determines ε .

In this way, one obtains:

$$\varepsilon = 1 - \frac{\omega_p^2}{\omega^2 + \nu^2}; \quad \sigma = \frac{\nu}{4\pi} \frac{\omega_p^2}{\omega^2 + \nu^2} \quad \text{and} \quad \kappa = \frac{\nu}{2c} \frac{1 - \varepsilon}{n},$$

or approximately, if $g^2 \ll n^2$,

$$\kappa = \frac{\nu}{2c} \frac{1 - n^2}{n}.$$

We can also express κ as

$$\kappa = \kappa_0 \frac{1}{1 + (\omega/\nu)^2},$$

where

$$\kappa_0 = \frac{\omega_p^2}{2cn} \frac{1}{\nu}.$$

INTERVENTI E DISCUSSIONI

— A. GILARDINI:

Is the formula relating σ with D_{12} valid only if the distribution is Maxwellian?

— R. GALLET:

No, it is a more general relationship. However the one relating σ with $1/\nu$ is valid only for ν constant.

II. – The Emission of Radio-Waves by the Planet Jupiter. An Enigma.

1. – Introduction.

The emission of radiation from Jupiter is certainly a plasma phenomenon, and this is the reason to present it in this series. The exact mechanism of emission is still unknown. However, the observations have shown that the emission consist of pulses, each one with a narrow frequency band-width. The band-width is of the order of 0.5 MHz which makes $\Delta f/f$ about 2.5 %. Also the general spectrum of the emission is sharply limited towards a maximum frequency of the order of 30 MHz.

The discovery is due to BURKE and FRANKLIN of the Carnegie Institution in the year 1955.

Soon after this discovery a systematic program of observations paralleling theoretical work was undertaken by the author at the National Bureau of Standards Boulder Lab. (Colorado), with the very valuable experimental help from K. BOWLES who designed the equipment and took a most active part in the observations.

Research performed with two independent phase-switching interferometers observing simultaneously at 18 and 20 MHz have shown the main characteristics of the emission which will be discussed below.

The purpose of the research were as follows:

- 1) Nature of the emissions (intensity, spectrum, etc.).
- 2) Localization of the sources on the planet.
- 3) Determination of the rotational period of Jupiter.
- 4) Studies of the Jovian ionosphere.

2. – Main features of the planet Jupiter.

The main features of the surface of the planet are well known from optical observations; the band structure and the red spot appears clearly on photographs.

Useful data are summarized below:

- Diameter: $140\,000\text{ km} = 11 \times \text{Earth's diameter}$.
- Distance: 5 astronomical units.
- Rotational period: $9^{\text{h}} 55^{\text{m}} 40^{\text{s}}, 632$.
- Mass: $300 \times \text{Earth's mass}$.
- Density: 1.3 (very nearly that of the Sun).
- Central pressure: $40 \cdot 10^6$ atmospheres.
- Temperature of the visual surface: about 150°K .
- Composition of the bulk: solid Hydrogen.
- Composition of the atmosphere: mainly Hydrogen and perhaps Helium, plus CH_4 and NH_3 visible spectroscopically.

The determination of the rotational period is a very complex problem because visual observations refer to the atmospheric cloud system and reveal currents of different speeds and time variations of the rotational period for a given current; even the most permanent visual feature, the red spot, presents a conspicuous long term variation in its period. Therefore the value of the period indicated above corresponds roughly to an average rotational period of the visible surface and is the conventional value, called the System II, adopted by the international ephemerides, but no object of the surface rotates which such a period.

The equatorial regions move with a larger speed: their period is about $9^{\text{h}} 55^{\text{m}}$. Both periods refer of course to the atmosphere of the planet since the solid bulk is masked by the clouds and is invisible to the observer.

The precision of determination of a rotational period is rather high. A difference of one second in the rotation period relative to the adopted System II represents a longitude displacement of $8^\circ, 88$ after one year. The object rotating with that period will present itself in the central meridian with nearly $15''$ difference with respect to the time computed in the System II. The radio emission shows sharp peaks of activity, as a function of the longitude of the central meridian, as evidenced by the recurrence of the reception after an integral number of rotations. The system of these peaks, called longitude profile, is essentially maintained from one year to another. The best rotation period deduced from the recurrence is $9^{\text{h}} 55^{\text{m}} 29^{\text{s}}, 6$; nearly 11 seconds shorter than the System II. After one year this corresponds to observations of the same peak $2^{\text{h}} 45^{\text{m}}$ before the time computed from the System II. The precision in the comparison of two longitude profiles one year apart is of the order of $(4 \div 5)^\circ$; consequently using all the available radio observations, which extend over a period of 6 years, we are able to determine a rotational period with a precision of about 0.1 s.

Concerning the constitution of the planet, from the values of density and pressure given before we can infer that the main bulk of Jupiter must be composed of solid Hydrogen mixed with small quantities of other light elements. In the atmosphere we have spectroscopic evidence of the existence of the molecules CH_4 and NH_3 . The latter must be crystallized at the low temperature indicated.

The temperature is obtained by different methods: infrared and centimeter waves thermal radiation, thermodynamic computation for the pressure of equilibrium between the vapor and the crystals of CH_4 and NH_3 at the cloud level. The temperature has a value that differs seriously from that obtained considering thermal equilibrium with the solar radiation, which amounts to 103°K . RAMSEY recently has discussed the constitution of the planet and arrived to the conclusion that the internal temperature may very well be as high as 10000°K .

3. - Characteristics of the radio emission.

The observations on 18 MHz and 20 MHz have been performed during more than 2 years. Only in winter and at night the observations can be carried out satisfactory. In daytime the augmentation of ionization in our ionosphere and the increased rate of interference produces many difficulties (see Table I).

The direction of the planet is well determined by the lobes of the interferometer.

The radiation of Jupiter appears to be composed of pulses each having a duration of two or three seconds; the reception period commences abruptly in both frequencies and lasts for a time which does not exceed two hours.

The pulses exhibit a strong grouping tendency over periods of several minutes, separated by quiet periods also of several minutes. High speed records resolving each pulse, made in the two frequencies simultaneously, have never shown a simultaneity in the bursts; no frequency drift has been observed and also the groups of pulses observed in both the frequencies differ considerably and are not necessarily simultaneous.

A second type of burst has also been observed; their duration is of the order of few $1/100$ of a second and its occurrence is very rare.

On the average the activity is higher on 18 MHz than on 20 MHz. The ratio of percentage of time of observation when the radiation was received at 20 MHz and 18 MHz was 0.5 in 1956 and 0.6 in 1957.

The peak energy of the pulses is about $10^{-20} \text{ W m}^{-2} \text{ Hz}^{-1}$. The maximum observed value was $4 \cdot 10^{-20}$. For comparison a typical value for a well de-

tectable radio source is $10^{-24} \text{ W m}^{-2} \text{ Hz}^{-1}$. A solar burst of $10^{-18} \text{ W m}^{-2} \text{ Hz}^{-1}$ is already a very strong event and is quite rare.

TABLE 1. - *Gross statistics of the synoptic record at National Bureau of Standard.*

		Fre- quency	Series		Notes
			1956	1947	
A 1	Total recording time available expressed in hours	$\left\{ \begin{array}{l} 20 \text{ MHz} \\ 18 \text{ MHz} \end{array} \right.$	$\left\{ \begin{array}{l} 605 \text{ h} \\ 494 \text{ h} \end{array} \right.$	$\left\{ \begin{array}{l} 30 \\ 590 \end{array} \right.$	Total: 2100 h of records
2	Total recording time available expressed in degrees of longitude	$\left\{ \begin{array}{l} 20 \text{ MHz} \\ 18 \text{ MHz} \end{array} \right.$	$\left\{ \begin{array}{l} 21926 \\ 17909 \end{array} \right.$	$\left\{ \begin{array}{l} 21248 \\ 14948 \end{array} \right.$	
3	Number of observational nights during the period	$\left\{ \begin{array}{l} 20 \text{ MHz} \\ 18 \text{ MHz} \end{array} \right.$	$\left\{ \begin{array}{l} 70 \\ 62 \end{array} \right.$	$\left\{ \begin{array}{l} 114 \\ 103 \end{array} \right.$	
4	Efficiency: mean length in longitude observable per night	$\left\{ \begin{array}{l} 20 \text{ MHz} \\ 18 \text{ MHz} \end{array} \right.$	$\left\{ \begin{array}{l} 313^\circ \\ 289^\circ \end{array} \right.$	$\left\{ \begin{array}{l} 186^\circ \\ 145^\circ \end{array} \right.$	
5	Mean time duration in hours	$\left\{ \begin{array}{l} 20 \text{ MHz} \\ 18 \text{ MHz} \end{array} \right.$	$\left\{ \begin{array}{l} 8.63 \\ 7.97 \end{array} \right.$	$\left\{ \begin{array}{l} 4.13 \\ 4.00 \end{array} \right.$	
6	Average number of opportunities to have each longitude in the central meridian	$\left\{ \begin{array}{l} 20 \text{ MHz} \\ 18 \text{ MHz} \end{array} \right.$	$\left\{ \begin{array}{l} 61.8 \\ 50.0 \end{array} \right.$	$\left\{ \begin{array}{l} 59.1 \\ 41.9 \end{array} \right.$	
7	Middle date of the observational period	$\left\{ \begin{array}{l} 20 \text{ MHz} \\ 18 \text{ MHz} \end{array} \right.$	$\left\{ \begin{array}{l} 13 \text{ Feb.} - 14 \text{ Jan.} \\ 16-17 \text{ Feb.} - 14 \text{ Jan.} \end{array} \right.$		
8	Weighted mean epoch (determined by emission)	$\left\{ \begin{array}{l} 20 \text{ MHz} \\ 18 \text{ MHz} \end{array} \right.$	$\left\{ \begin{array}{l} 9 \text{ Feb.} - 24 \text{ Jan.} \\ 16-17 \text{ Feb.} - 26 \text{ Jan.} \end{array} \right.$		
B 1	Percentage of time Jupiter is emitting	$\left\{ \begin{array}{l} 20 \text{ MHz} \\ 18 \text{ MHz} \end{array} \right.$	$\left\{ \begin{array}{l} 8.49 \\ 16.94 \end{array} \right.$	$\left\{ \begin{array}{l} 6.13 \\ 10.6 \end{array} \right.$	
2	Average Zurich sunspot number during observational period	$\left\{ \begin{array}{l} 20 \text{ MHz} \\ 18 \text{ MHz} \end{array} \right.$	$\left\{ \begin{array}{l} 108 \\ 111 \end{array} \right.$	$\left\{ \begin{array}{l} 159 \\ 158 \end{array} \right.$	

Taking into account the distance of Jupiter, the amount of power received has to be multiplied by a factor of 25 for comparison with that from the sun. Therefore the power normally received from Jupiter is comparable with the strongest received from the sun and it is much more frequent. The total energy

per pulse at the planet in a bandwidth of 0.5 MHz has a value of the order of 10^{18} ergs.

In order to establish a scale of energy let us compare the emission of Jupiter with some geophysical and man-made phenomena.

The efficiency of the radio emission for all known natural phenomena—lightning, solar flare, explosions—is small, always less than 10^{-5} . Therefore if the efficiency for the conversion in radio waves at Jupiter is comparable, it is easy to see that the production of each pulse requires at least 10^{23} ergs. On the earth the only comparable phenomena of explosive nature are the big volcanic explosions, earthquakes and the H bomb (see Table II).

TABLE II.

Man-made		Geophysical	
« A » Bomb (20 kilotons TNT)	$8 \cdot 10^{20}$ erg	Total energy in a lightning discharge	$2 \cdot 10^{17}$ erg
« H » Bomb (5 megatons)	$2.1 \cdot 10^{23}$	Integrated radio energy from a lightning discharge	$2 \cdot 10^{12}$
« Z.E.T.A. » pulse	$2 \cdot 10^{12}$	Largest volcanic eruptions	10^{24}
		Largest earthquake	10^{25}
		Atmospheric waves from Krakatoa explosion	10^{24}
		Kinetic total energy of atmosphere	$8 \cdot 10^{27}$

4. — Other important properties deduced from observations.

4.1. *Nature of the sources.* — The comparison of longitude profiles from one year to another year not only furnishes a precise value of the rotation period as indicated above, but it gives also important information on the physical structure of the giant planet. The fact that the sources are fixed, relative to each other in longitude, indicates that they are at the surface of the solid body. The permanency of their activity over several years is a very important characteristic. The activity is fluctuating over periods of some days or weeks. The most active source was observed 50% of the available observation time over a period of several months in 1956 on the frequency of 18 MHz, when the

source was in the central meridian of the planet, a very high activity indeed. The true activity of the sources may even be larger because, as it will be indicated below, transmission effects in the ionosphere of Jupiter limit the reception time for purely geometric reasons.

From what has been said about the duration, intensity, narrow band-width spectrum of the radio pulses, it seems that the radiation mechanism, with its well defined frequency, involves some sort of plasma resonance, and some sort of explosion. The change of frequency from burst to burst indicates that the plasma involved is not of constant density. If shock waves were produced high in the atmosphere and propagated within the ionosphere of Jupiter exciting radiation at the local plasma frequency, drift should be produced. This effect, which was expected by the author at the start of this work, has never been found. Therefore the best image which can be formed is that of a certain number of discrete regions exhibiting a sort of volcanic activity which produces extremely large shock waves. The shock fronts are responsible for both the presence of the ionization and the production of radiation.

Until now no valid correlation with phenomena observed visually has been obtained.

4.2. *Ionosphere of Jupiter.* — It is not intended here to discuss this question in details. But strong evidence for the presence of the ionosphere and the measurements of its properties has been obtained from the following phenomena.

The reception time during a given observation is always much smaller than one complete half rotation from Jupiter (nearly 5^h), and its average duration is of the order of one hour, though quite variable. Generally the beginning and the end of the reception for a given source have a quite abrupt cut-off. The reception time is centered very close to the passage in the central meridian, and naturally it is the last property which permits to obtain a well defined longitudinal profile with sharp peaks as a function of longitude. Therefore the radiation is limited to a more or less open cone above the source which, because of the rotation of Jupiter, sweeps the space. The reception is possible only when the earth is inside the cone. Such a cone is well known in ionospheric propagation for waves of frequency greater than the ionospheric critical frequency. All the observations are compatible with this hypothesis.

When solar activity increases the critical frequencies of the ionosphere increase also, and for a given frequency the angular aperture of the observed cone decreases, reducing the observing time on the earth. Such an effect has been found for both frequencies. From 1956 to 1957 the solar activity has increased considerably and the observed Jupiter's activity, either for each particular source or for the total average activity, has been reduced to about 60%. More

over the theory shows that the effect should be less sensible for a higher frequency; the observed relative diminution at 20 MHz was significantly less than at 10 MHz as expected.

The presence of a ionosphere gives the hope to be able to distinguish, by polarization measurements, the ordinary and extraordinary rays propagated through the ionosphere, and to obtain the difference of their critical frequencies.

This quantity will give a direct and precise measurement of the magnetic field of Jupiter. It should be possible to measure this magnetic field at each separated source. Circular polarization of the radiation from Jupiter has already been observed.

INTERVENTI E DISCUSSIONI

— C. DE JAGER

Could not the bandwidth be smaller than 0.5 MHz?

— R. GALLET:

No! Simultaneous observations over too wide a frequency range can not be made with the apparatus employed, aerial dipole and a bandwidth of 0.4 MHz. When observations are made within this band, a good parallelism is observed; but at an interval of 2 MHz apart the correlation between pulses is zero.

— K. O. KIEPENHEUER:

Do you use an interferometer to lower the background noise?

— R. GALLET:

Yes, and also to carry out a continuous observation.

— P. C. THONEMANN

Is there any reason to believe that volcanic explosions on the earth give rise to such a narrow bandwidth radiation?

— R. GALLET:

Shock waves from explosions do emit some of the radio emissions which have been observed. I believe that the energy produced by volcanic eruptions is sufficient and of the type required and that some radio emission could be detected. I used for the phenomena observed on Jupiter the word « volcanic » in a general sense, owing to the lack of a better expression.

— C. M. BRAAMS:

Can you give us an idea of the order of magnitude of the energy involved in atmospheric phenomena, such as may be produced by a hurricane?

— R. GALLET:

A sound question! Of course, it is difficult to make an accurate estimate, but the energy of one lightning flash is of the order of 10^{17} erg. In a very large thundercloud, over one or two hours at the rate of one pulse/s, the total energy spent is about 10^{21} erg. In a large region like a hurricane perhaps it is as much as 10^{23} erg. I am referring to the kinetic energy only; however the potential energy and heat energy may amount to one thousand times these values.

— E. SCHATZMAN:

There are graphs by MAUNDERS which show that the Sun's activity is localized. Would it be possible to derive a model for Jupiter similar to those already derived for the Sun near the solar surface?

— R. GALLET:

We shall be able to tackle the problem experimentally. We know already that the pulses are circularly polarized, so we are certain we are observing a magnetic field on Jupiter. From the observation of irregularities in this field measured for the different sources and the variation in the rotational period, we may perhaps be able to deduce some information about the internal structure of Jupiter. I will not commit myself on these possibilities presently.

— H. C. VAN DE HULST:

In the geophysical phenomena only lightning flashes have a short duration, while the others last longer. Does the small time constant observed not favour this explanation of the phenomenon on Jupiter?

— R. GALLET:

No! The spectrum is not that of a lightning discharge. The shape of the pulse is also not a simple one, such as presenting an exponential decay. On the other hand during volcanic eruptions the explosions are quite short, few seconds, similar to that observed.

— V. FERRARO:

Are radio waves produced when a terrestrial volcano explodes?

— R. GALLET:

I hope it will be possible to carry out experiments to test this question.

III. – On the emission of Electromagnetic Waves by Plasma Oscillations.

The subject of this lecture concerns the problem of emission of electromagnetic waves by plasma oscillations. We shall discuss two points, namely:

- 1) Is the emission possible? and
- 2) What is the coupling mechanism that permits it?

It is normally accepted that the solar radio bursts are produced by such a mechanism.

1. – Survey of the characteristics of solar radio emission.

As a reference the flux of the « Quiet Sun » between 30 and 300 MHz is equivalent to that of a black body at an apparent temperature T_b of 10^6 °K. The following relation is given by van de Hulst:

$$S = \int B d\Omega; \quad B = 2kT_b\nu^2/c^2.$$

For the Sun $d\Omega = 6.8 \cdot 10^{-5}$ steradian, therefore

$$S = 1.9 \cdot 10^{-27} T_b / \lambda^2. \quad (\text{MKS units}).$$

The following Table III of flux ($\text{W m}^{-2} \text{Hz}^{-1}$) is useful for comparison purposes.

TABLE III.

Source	300 MHz	100 MHz	30 MHz
Quiet Sun	$1.9 \cdot 10^{-21}$	$2.1 \cdot 10^{-22}$	$1.9 \cdot 10^{-23}$
Crab Nebula	—	$1 \cdot 10^{-23}$	—
M. 31 (Andromeda)	—	$2 \cdot 10^{-24}$	—

The range of observation for the burst activity of the Sun extends from 3000 MHz to 50 MHz. The maximum peak intensity received is somewhere near 100 MHz perhaps more nearly 80.

The range of power flux is $(10^{-22} \div 10^{-15}) \text{ W m}^{-2} \text{Hz}^{-1}$, a very large range indeed.

Bursts of power 10^{-18} are quite rare and of 10^{-16} exceptional. Only one burst of a peak power greater than 10^{-15} was observed (Australia, 8 March 1947).

Few statistics of the number of bursts as a function of amplitude have been collected but they do not cover adequately the intensities larger than 10^{-19} .

A burst of a peak power $10^{-16} \text{ W m}^{-2} \text{ Hz}^{-1}$ gives at the Sun $7 \cdot 10^6 \text{ W Hz}^{-1}$. The bandwidth, at a given moment, is quite narrow and may be $(2 \div 3) \text{ MHz}$ near 100 MHz . Therefore the total instantaneous power will be $(14 \div 21) \cdot 10^{12} \text{ W}$ or about 10^{20} erg radiated per second per pulse. The emissive surface may be of the order of $10^4 \cdot 10^4 \text{ km} = 10^{18} \text{ cm}^2$. Hence the emission is about $100 \text{ erg s}^{-1} \text{ cm}^{-2}$.

For comparison the integrated thermal radiation of the Sun is:

— Photosphere: $6.3 \cdot 10^{10} \text{ erg s}^{-1} \text{ cm}^{-2}$.

— Total corona radiation: $6.3 \cdot 10^3 \text{ erg s}^{-1} \text{ cm}^{-2}$.

So even the strongest burst at the Sun gives a radiated radio energy which is small compared to the normal radiation from the Sun. However, considering that radio emission takes place on a localized level, the energy emitted as radio waves becomes an important factor. Moreover one must assume a conversion factor smaller or of the order of 10^{-5} between the energy source (kinetic) and the radiation. The mechanical energy involved in the disturbance is considerable compared with the coronal radiation.

The three different types of emission, on an energy scale, are summarized below:

1) *Quiet Sun* (the lowest power). Purely thermal radiation due to free-free transitions.

2) *Slowly varying component* (order of magnitude $(10 \div 100)$ times that of the quiet Sun). Thermal radiation related to «plage» or Sun spot activity which heats up and augments the density of the corona. Also free-free transition emission.

3) *Bursts*: 4 types have been recognized:

Type I. *Noise storm* (circularly or elliptically polarized). A combination of small bursts (pips) plus enhancement of the continuum. Above «noisy» spots. Frequency range: about 50 MHz between 100 and 300 MHz . Pips observed at 160 MHz have a bandwidth of about $(2 \div 3) \text{ MHz}$ and last for about 0.1 s . Average duration between pips during a typical noise storm was 0.25 s . The energy is less certain. Perhaps this is a phenomenon of instability due to plasma oscillations, but it is difficult to reconcile this idea with the fact that these pips exhibit high circular or elliptic polarization.

Type II. *Slow drifts*. Range of frequency $(40 \div 600) \text{ MHz}$, randomly polarized.

Type III: *Fast drift* (few seconds). Randomly polarized.

Type IV. A very smooth continuum lasting for about one hour, circularly polarized. Radiation probably due to synchrotron radiation by a cloud of relativistic particles, high in the solar corona. Quite exceptional after exceptional flares.

2. - Coupling mechanism between plasma oscillations and electromagnetic waves.

Observations show the following main properties: a narrow frequency band is received at a given time, while the band can be drifting in frequency as a function of time. Secondly they seem to support the idea that the frequency coincides with, or is very near to, the plasma frequency.

A shock wave or a stream of particles seems to be able to excite and amplify plasma oscillations; however the detailed mechanism of this excitation will not be discussed now.

We have to understand the manner in which electromagnetic waves can be radiated by the plasma oscillations. Therefore we should study the coupling mechanism between plasma oscillations and electromagnetic waves.

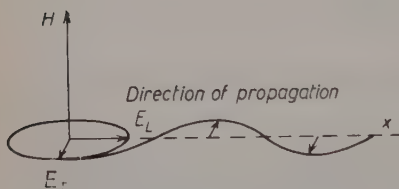


Fig. 3.

Consider the structure of a longitudinal plasma oscillation. The oscillatory motion of the electrons is in the direction of propagation. In the presence of a weak magnetic field (Fig. 3), the longitudinal magnetic component does not affect the motion. The transverse magnetic component, however, will produce a perturbation normal to the direction of propagation and to the magnetic field.

Therefore the electric motion produces a small electric vector with the properties necessary for the production of an electromagnetic wave. The mode of the propagation of this wave is the extraordinary transverse mode.

However the existence of a transverse electric field is not sufficient to produce a radiated electromagnetic wave. The electromagnetic wave can be built up only if a condition of coherence between the two waves is satisfied. The two waves should be in phase over an appreciable length l , extending over many wave lengths. Therefore the coupling will exist if it is possible to find a frequency for which the two waves will have the same wavelength.

When this assumption is made we see that the direction of the radiation will be confined to a narrow cone in the direction of propagation. In all other directions destructive interference takes place.

Plasma oscillations are such that their phase velocity, $V_{ph, P.O.}$, is larger than, but of the same order of magnitude as, the root mean square thermal electron

velocity u in the plasma. The dispersion law can be written in a form which defines a refractive index μ such as

$$V_{ph.P.O.} = \frac{u}{\mu}.$$

The coupling condition is essentially

$$V_{ph} = \frac{c}{n} = \frac{u}{\mu} \quad \text{or} \quad \mu = n\beta \quad \text{with} \quad \beta = \frac{u}{c};$$

β is always very small. Besides, $\mu < 1$; it is 0 at, or near, ω_p and increases for $\omega > \omega_p$. In order to satisfy the above condition n should be large.

Consider the dispersion law for electromagnetic waves in the case of a transverse magnetic field. The refractive index n is represented in Fig. 4, for zero collision number.

The branch of interest in the coupling problem is the transverse extraordinary wave,

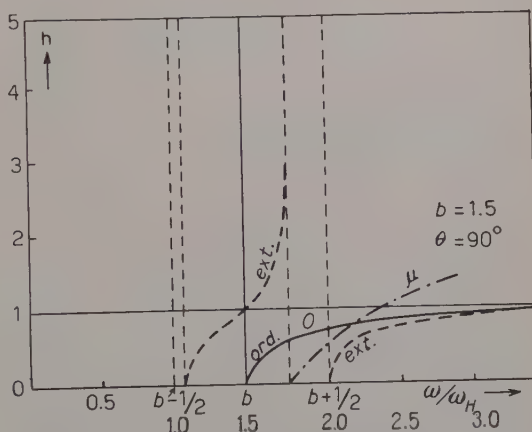


Fig. 4. - $b = 1.5$; $\theta = 90^\circ$; ord \equiv ordinary ray; ext \equiv extraordinary ray.

$$n = 0 \quad \text{at} \quad \omega_0 = \left(\omega_p^2 + \frac{\omega_H^2}{4} \right)^{\frac{1}{2}} - \frac{\omega_H}{2},$$

$$n = 1 \quad \text{at} \quad \omega = \omega_p,$$

$$n = \infty \quad \text{at} \quad \omega_\infty = (\omega_p^2 + \omega_H^2)^{\frac{1}{2}}.$$

The law of dispersion of the plasma oscillations is less straightforward. Several formulae given by different authors have to be considered.

a) BOHM and GROSS give the following expression, valid only for ω near ω_p ,

$$\omega^2 = \omega_p^2 + \frac{3kT}{m_e} \kappa^2,$$

with

$$\kappa = \frac{2\pi}{\lambda} \quad \text{and} \quad \omega_p^2 = \frac{4\pi n e^2}{m}.$$

The dispersion is directly function of temperature. In this case

$$\mu = \left(1 - \frac{\omega_p^2}{\omega^2}\right)^{\frac{1}{2}}.$$

The law is exactly the mathematical form of the refractive index of electromagnetic waves n for the ordinary ray.

b) The more general formula given by GABOR is

$$\left(\frac{\omega}{\omega_p}\right)^2 \left[\left(\frac{\omega}{\omega_p}\right)^2 - 1 \right] = u^2 \left(\frac{\omega}{\omega_p}\right)^2.$$

This formula is also given by M. BAYET. With refractive index μ the formula is equivalent to

$$\mu = \left(\frac{\omega^2}{\omega_p^2} - 1\right)^{\frac{1}{2}}.$$

This expression is valid for ω not limited to the neighborhood of ω_p . The inferior limit of ω is ω_p and the upper one is due to the fact that $\lambda_{\min} \simeq D$ (Debye distance); this corresponds to $\omega_{\max} \simeq 2\omega_p$. Therefore plasma oscillations are possible only within a frequency band above ω_p , quite limited in frequency.

The superiority of this new law appears when the group velocity is computed. With the first law the group velocity is such that

$$\mu\mu' = 1.$$

Therefore the limiting value of the group velocity when ω increases is u . But more detailed considerations, such as those developed by GABOR, show that the group velocity should go towards zero when ω increases above $2\omega_p$; the energy cannot propagate for waves of wave length smaller than the Debye distance.

c) These two laws however do not consider the effect of a magnetic field. For a small magnetic field (perturbation treatment) BOHM and GROSS, as well as SEN, give the following dispersion law:

$$\omega^2 = \omega_p^2 + \omega_H^2 + \frac{3kT}{m} \omega^2 \left(1 + 3 \frac{\omega_H^2}{\omega_p^2}\right),$$

or

$$\mu^2 = \frac{1}{1 + 3/b^2} \left[1 - \frac{\omega_p^2 + \omega_H^2}{\omega^2}\right],$$

with $b = \omega_p/\omega_H$.

The law is general however; it is the extension of the first law valid only for ω near the critical frequency. The refractive index μ is zero for the critical frequency $\omega_{\infty} = (\omega_p^2 + \omega_H^2)^{\frac{1}{2}}$, where the refractive index n is infinite.

It results that the two curves of refractive indices for electromagnetic waves and for plasma oscillations have no common frequency besides ω_{∞} . Therefore the coupling condition $\mu = n\beta$ is *not fulfilled under such conditions*.

But the real physical conditions are more complex.

The role of collisions upon the dispersion laws for electromagnetic waves and plasma oscillations has been neglected. In presence of collisions n is not infinite for ω_{∞} , but has a maximum slightly before that frequency, has still a large value at ω_{∞} , and keeps very small but finite values on the right. The absorption coefficient increases very rapidly near ω_{∞} and has a large maximum value after ω_{∞} . For the plasma oscillations μ is not zero any more at ω_{∞} and keeps small but finite values on the left, with a large absorption coefficient. Therefore the frequency domains of the two types of waves *overlap*, and have the proper behavior to satisfy in general the coupling condition within a narrow band of frequency. Hence it is the collisions which are primarily responsible for the positive effect searched. The collisions produce also a negative effect by heavy absorption.

It is seen that the efficiency of the energy transfer will always be low. Moreover if the collision number becomes too large, not only the absorption becomes prohibitive but the maximum value for n does not attain values large enough for satisfying the coupling condition, and the energy transfer is suppressed.

Last, but important, the dispersion laws considered above for plasma oscillations are valid only for a maxwellian electronic velocity distribution function. In the center of a shock front, where the conditions are favorable to excitation of plasma oscillation, the velocity distribution function is strongly different from the maxwellian one. This modifies considerably the dispersion law, which in general will extend on the left of ω_{∞} , even without the effect of collisions. To the contrary the dispersion of electromagnetic waves is, to the first order, not affected by the shape of the velocity distribution function.

In conclusion it is seen that coupling is in general possible for a narrow frequency band near ω_{∞} : The energy transfers is of low efficiency, due to heavy absorption. The coupling is due primarily to the presence of a weak magnetic field, and is depending on collisions and departures of the velocity distribution function from the maxwellian one.

INTERVENTI E DISCUSSIONI

— C. DE JAGER:

Does bandwidth agree with observations?

— R. GALLET:

Length has to be quite short.

— G. RIGHINI:

What about the « u » bursts?

— R. GALLET:

I do not want to discuss these at present. They have a duration of a few seconds and a bandwidth very similar to that of Type III bursts.

— C. DE JAGER:

What is the distinction between « u » bursts and Type III bursts?

— R. GALLET:

I do not believe that till now a good explanation of the « u » bursts has been given.

Plasma Confinement by External Magnetic Fields.

J. G. LINHART

CERN P.S. Division - Genève

It is generally appreciated that the practical utilization of power from thermonuclear reactions depends on the perfection of insulation of the thermonuclear fuel from all sinks of thermal energy [1,2]. The most efficient method of achieving this is to confine the fuel, which at the temperatures suitable for fusion reactions appears in the form of a fully ionized gas, by strong magnetic fields. These magnetic fields can be generated either by currents in the ionized gas itself [3], or by currents in conductors outside the gas [4] or by both [5].

In this lecture we shall be concerned with the confinement of plasma by magnetic fields generated by currents outside the plasma.

Such a magnetic field configuration is often called a magnetic bottle. The loss of heat energy from plasma confined in such a bottle is mainly due to

- a) particle losses,
- b) bremsstrahlen and cyclotron radiation.

The loss *b*) has been discussed elsewhere [6] and does not depend on the form of the magnetic bottle.

The loss *a*) can be divided into two categories:

- a) particle loss due to plasma instabilities;
- b) particle loss due to collisions between particles leading to plasma diffusion out of the magnetic bottle.

We shall concentrate mainly on the diffusion loss through the holes in the magnetic bottle. We shall develop an approximate theory and apply it to two particularly simple magnetic bottles. (The diffusion loss at right angles

to the walls of a flux-tube is due mainly to electron-positive ion collisions and has been discussed elsewhere [7]).

We shall discuss the results in connection with thermonuclear applications.

I. - General Considerations.

1. - Magnetic bottle containing hydrogen plasma.

Let us consider a simple magnetic bottle formed by coaxial magnetic mirrors facing each other (Fig. 1) and containing hydrogen plasma. Let us assume that at time $t=0$ the velocity distribution of both electrons and protons is maxwellian with a temperature T . It can be shown that as the magnetic moment of each particle is invariant between two successive collisions

$$(1) \quad \frac{\sin^2 \theta}{B} = \text{const},$$

where θ is the angle between the velocity vector \mathbf{v} and the B -line belonging to the guiding centre of the particle.

In absence of collisions particles for which

$$(2) \quad (\sin^2 \theta)_{z=0} < \frac{B(z=0)}{B(z=z_1)} = b,$$

will leak through the magnetic mirrors. Those for which

$$(3) \quad (\sin^2 \theta)_{z=0} > \sin^2 \alpha = b$$

will remain within the bottle.

One can, therefore, consider the plasma between two magnetic mirrors as a mixture of two gases. The first, say gas A , in which all the particles obey eq. (3) and are, therefore, fully confined. The second, gas B , in which particles obey eq. (2) and, therefore, are not confined.

If collisions between particles occur, than the loss from the magnetic bottle containing a mixture of A and B is determined by the magnitude of collision-induced transitions from A to B and B to A (Fig. 2). This interchange of particles between the gases

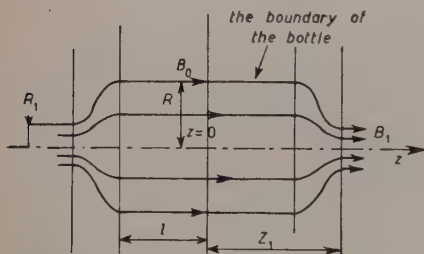


Fig. 1.

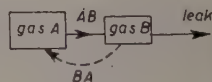


Fig. 2.

A and B can be represented by a diagram in the velocity space (Fig. 3).

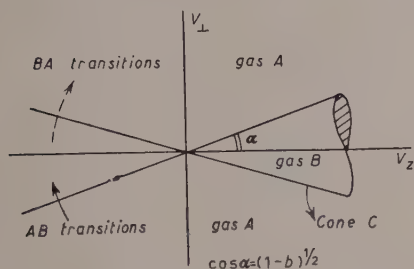


Fig. 3.

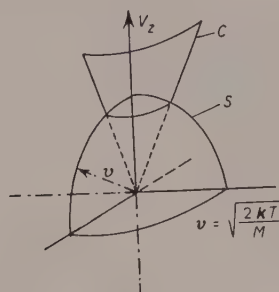


Fig. 4.

If the apex angle α is small then the probability that a large angle collision between two protons belonging to the gas A will result in transfer of one of them to the gas B is approximately (Fig. 4)

$$\kappa = \frac{\text{surface of spherical sectors cut out by the cone } C}{\text{surface of a sphere } S},$$

$$\kappa \simeq \frac{1}{2} \sin^2 \alpha,$$

and using eq. (3) one has

$$(4) \quad \kappa = \frac{1}{2} b.$$

The factor b may be evaluated as follows

$$b = \frac{B_0}{B_1} = \left(\frac{R_1}{R} \right)^2.$$

The transfer AB occurs, therefore, at a rate

$$(5) \quad \frac{dn_{A^-}}{dt} = - \frac{\bar{n}_{A^+}}{\tau} \kappa$$

where n_A is the density of the gas A and τ is the corresponding mean collision time.

The gas A is, of course, composed of equal number of electrons and protons and we should, therefore work out separately

$$\frac{dn_{A^-}}{dt} \quad \text{and} \quad \frac{dn_{A^+}}{dt}.$$

eq. (5) suggests, that the loss of protons from A is smaller than that of electrons. However, the actual loss of plasma from the magnetic bottle is determined by the loss of protons. The electrons are then held by the electric field of the protons. Thus τ can be taken as the mean time between proton-proton collisions and this is [7, pag. 78]:

$$(6) \quad \tau = \frac{11.4}{d \ln A} \frac{T^{\frac{3}{2}}}{n} \simeq \frac{T^{\frac{3}{2}}}{n}.$$

With this eq. (5) becomes

$$(7) \quad \frac{dn_A}{dt} = -\frac{1}{2} \frac{n_A n}{T^{\frac{3}{2}}} b \quad (\text{part/cm}^3, \text{ s}).$$

Also with our assumption that $\alpha \ll 1$ one has $n_A \gg n_B$ and therefore $n_A \sim n$. Thus

$$(7a) \quad \frac{dn_A}{dt} = -\frac{1}{2} \frac{n^2 b}{T^{\frac{3}{2}}} \quad (\text{part/cm}^3, \text{ s}).$$

The loss of plasma is then given by eq. (7a).

The corresponding loss of energy is

$$(8) \quad W = \frac{3}{2} kT \int_{\Omega} \frac{dn_A}{dt} d\Omega \quad (\text{erg/s}),$$

where Ω is the volume of the bottle.

An average energy loss per cm^3 is

$$(9) \quad W_0 = \frac{3}{4} k \frac{n^2}{T^{\frac{3}{2}}} Bb \quad (\text{erg/cm}^3, \text{ s}),$$

and using the definition of b in terms of bottle-geometry one has

$$(10a) \quad W_0 = \frac{3}{4} k \frac{n^2}{T^{\frac{3}{2}}} \left(\frac{R_1}{R} \right)^2 \quad (\text{erg/cm}^3, \text{ s}).$$

The loss of A -particles due to small angle collisions is more severe than the large angle loss given by eq. (10). The effect of the small angle collisions is to produce a diffusion of particles on the surface of the sphere S . The boundary Γ of the loss cone C can be regarded as a sink of particles, the equator

of S will then be a locus of maximum density (Fig. 5). The flux of particles across I is then proportional to

$$\left[\ln \frac{B_1}{B_0} \right]^{-1}.$$

The energy loss can be shown to be equal to

$$W'_0 = \frac{3}{4} k \frac{n^2}{T^{\frac{1}{2}}} \left[\ln \frac{1}{b} \right]^{-1}.$$

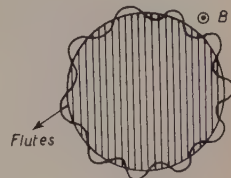


Fig. 5

The diffusion loss from the simple bottle discussed so far may be expected to be inferior to the loss due to flute-instability. This instability will occur in magnetic bottles in which

$$(11) \quad \int_s \frac{ds}{R_c r B^2} > 0,$$

where the integration is along a field line through the bottle and R_c is the radius of curvature of the flux line.

An example of magnetic bottle which, according to this criterion, should not exhibit a flute-instability is a quadrupole magnetic field (Fig. 6). The diffusion loss should then be the only appreciable particle loss from a plasma confined in such a bottle.

There are three holes in the quadrupole bottle. It is obvious that the large aperture of the central cylindrical gap G will permit the largest leak. One can again solve the problem of loss by the approximate method of the two-gas model.

The allocation of velocity space to the gases A and B is asymmetric if $B_2 \neq B_1$.

It can be shown that

$$(12) \quad \frac{B_1}{B_2} \equiv \frac{R\delta}{r_0^2}.$$

where B_1 , respectively B_2 , are the field strengths in the axial aperture and in the gap respectively.

In order that $B_1 = B_2$ one must make

$$(12a) \quad g = r_0 \left(\frac{r_0}{R} \right),$$

which encounters technological difficulties if $R/r_0 \gg 1$.

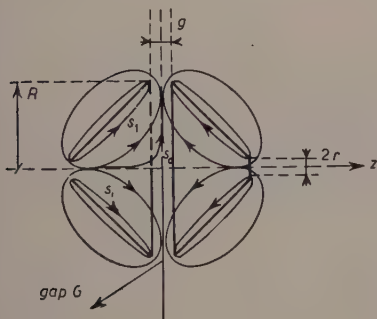


Fig. 6.

Also the apex angle of the cone C dividing the velocity space changes from zero for the rectangular field-line S_0 to some finite value for the field line S_1 tangential to the coils. Along any flux-tube between S_0 and S_1 one encounters a field minimum B_{\min} . An approximate expression for an average value for B_{\min} is

$$(13) \quad \overline{B_{\min}} = \frac{\pi r_0^2 B_1}{\pi(R/2)^2} = 4 \left(\frac{r_0}{R} \right)^2 B_1,$$

and we get for

$$(14) \quad \overline{b} = \frac{\overline{B_{\min}}}{B_2} = 4 \left(\frac{r_0}{R} \right)^2 \frac{Rg}{r_0^2} = 4 \frac{g}{R}.$$

With this the loss of energy from a cm^3 of the confined plasma is found in the same way as in the case of a simple bottle and it is

$$(15) \quad w_0 = W_0 + W'_0 = \frac{3}{4} k \frac{n^2}{T^{\frac{1}{2}}} \left[4 \frac{g}{R} + \left(\ln \frac{R}{4g} \right)^{-1} \right] \quad (\text{erg}/\text{cm}^3, \text{s}).$$

2. - Conclusions.

In order that the magnetic bottles described here could be used to confine plasma in thermonuclear reactors, the energy loss given by equations (10a,b) and (15) must be appreciably less than the nuclear output [2]. For the TD reaction running at a temperature $T \sim 10^9$ ($^{\circ}\text{K}$) one has for the output power density [1]

$$(16) \quad w_N = \frac{1}{2} n^2 \langle \sigma v_{\text{DT}} \rangle_{\text{av}} \cdot \varepsilon \quad (\text{erg}/\text{cm}^3, \text{s}),$$

where

$$\langle \sigma v_{\text{DT}} \rangle_{\text{av}} \sim 10^{-15} \quad (\text{cm}^3/\text{s}), \quad \varepsilon \sim \frac{1}{4} \cdot 10^{-4} \quad (\text{erg}).$$

Therefore

$$(16a) \quad w_N = \frac{1}{8} \cdot n^2 \cdot 10^{-19} \quad (\text{erg}/\text{cm}^3, \text{s}).$$

Let us form a ration between the nuclear output density and the energy loss density for the quadrupole bottle of Fig. 6.^o Thus

$$(17) \quad \frac{w_N}{w_0} = \eta.$$

Using eq. (15) one gets

$$(18) \quad \eta \sim \left[\frac{g}{R} + \frac{1}{4} \left(\ln \frac{R}{4g} \right)^{-1} \right].$$

Thus at these very high temperatures the energy loss due to particle diffusion is small compared with the nuclear output.

It thus appears that magnetic bottles with holes can be considered as means of plasma confinement for thermonuclear processes provided the plasma confinement is a stable one.

II. - The Problem of Runaway Electrons in Plasma.

We shall analyse some of the more important effects resulting from the application of an electric field E to an infinite volume of uniform plasma. As the electrons have a much smaller mass than the positive ions their velocity will be affected by the field E much more than that of the ions. Let us observe the motion of a single electron through plasma. Its equation of motion is

$$(1) \quad m\dot{v} = eE = F_e - F_p,$$

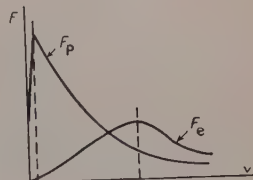


Fig. 7.

where F_e is the friction force due to collisions with electrons, F_p is the friction force due to collisions with positive ions.

These two forces are velocity-dependent as shown in Fig. 7.

They can be represented by the following formulae (1)-(3):

$$(2) \quad \begin{cases} F_e = 8\pi A \frac{n_e}{v^2}, & \text{for } v \gg \sqrt{\frac{2kT_e}{m}} = S_e, \\ F_e = 19An_e \frac{v}{S_e^3}, & \text{for } v < S_e \end{cases}$$

$$(3) \quad \begin{cases} F_p = 4\pi A \frac{n_p}{v^2}, & \text{for } v \gg \sqrt{\frac{2kT_p}{M}} = S_p, \\ F_p = 19An_p \frac{v}{S_p^3}, & \text{for } v < S_p, \end{cases}$$

where

$$A = \frac{e^4 \ln A}{m}.$$

The force F_p is not a true friction force as it causes a deflection of the velocity vector, rather than diminishing its magnitude.

The criterion for decoupling an electron in the velocity space follows from

equation (1) and it is at time $t = 0$,

$$(4) \quad eE \geq (F_e + F_p) \cos \varphi \quad \text{and} \quad \frac{\delta}{\delta t} [eE - (F_e + F_p) \cos \varphi] \geq 0.$$

where φ is the angle between \mathbf{v} and \mathbf{E} (Fig. 8). Let us consider the case in which $v > S_e$ and $n_e \sim n_p = n$ and let us evaluate equation (4) for $v_x = S_e$, $v_y = 0$,

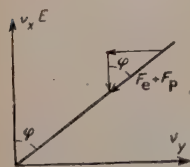


Fig. 8.

$$(5) \quad E \geq 12 \frac{e^3 \ln \Lambda}{2k} \frac{n}{T_e} \quad (\text{V/cm}),$$

or taking $\ln \Lambda \sim 10$

$$(6) (*) \quad E \geq 4.5 \cdot 10^{-8} \frac{n}{T_e} \quad (\text{V/cm}).$$

Example: $n = 10^{12}$ el./cm³, $T_e = 10^4$ °K $\rightarrow E > 4.5$ V/cm.

This electric field is then capable of decoupling electrons whose representative points in velocity space lie above the contour C (Fig. 9).

Let us now calculate the portion Δn of n which is decoupled by a given field E . This is

$$(7) \quad \Delta n = \int_{v_x=v}^{\infty} \int_{v_y=0}^{\infty} n(v_x v_y) 2\pi v_y dv_y dx,$$

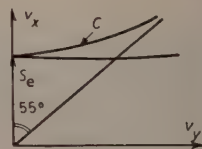


Fig. 9.

where v follows from equation (5). Assuming that $n(v_x v_y)$ was originally Maxwellian one gets

$$(7a) \quad \Delta n = \frac{2\pi n}{(2\pi k T/m)^{3/2}} \int_v^{\infty} \int_0^{\infty} \exp [(-v_x^2 - 2v_y^2)/S^2] v_y dv_y dv_x.$$

The double integral can be written as follows:

$$I = S^3 \int_0^{\infty} \exp \left[\left(-\frac{2v_x^2}{S^2} \right) \frac{y_y}{S} \right] \left[\int_{v_x v_y/S}^{\infty} \exp \left[\left(-\frac{v_x^2}{S^2} \right) \right] d \frac{v_x}{S} \right] d \frac{v_y}{S}.$$

(*) A similar formula is derived by considering the growth of the mean free path of an electron due to the acceleration (eE/m) (see Appendix I).

A slightly optimistic estimate of n is obtained if $v(v_y) = v(0) = v_0$. Then

$$I = S^3 \frac{\sqrt{\pi}}{2} \left[1 - \varphi \left(\frac{v_0}{S} \right) \right] \frac{1}{4} \int_0^\infty \exp[-x] dx = S^3 \frac{\sqrt{\pi}}{8} \left[1 - \varphi \left(\frac{v_0}{S} \right) \right],$$

where $\varphi(v_0/S)$ is an error function (*).

As

$$v_0^2 = 12\pi \frac{e^3 \ln A}{m} \frac{n}{E},$$

one gets

$$(8) \quad \frac{\Delta n}{n} = \frac{1}{4} \left[1 - \varphi \left(\sqrt{\frac{E_c}{E}} \right) \right],$$

where E_c follows from equation (6).

The graph of this function is plotted in Fig. 10.

The decoupling process will be well established within a time equal to a few mean collision times for the electrons. As the mean collision time is

$$(9) \quad t_{\text{coll}} \sim \frac{1}{40} \frac{T_e^{3/2}}{n} \quad (\text{s}),$$

the decoupling time is of the order of

$$(9a) \quad t_d \sim \frac{1}{10} \frac{T_e^{3/2}}{n} \quad (\text{s}).$$

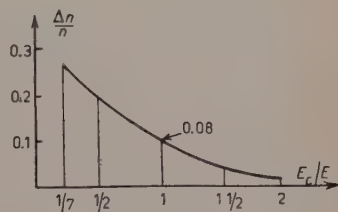


Fig. 10.

Example: $n = 10^{12}$, $T_e = 10^4$ °K $\rightarrow t_d \sim 1/10$ μ s.

The length of the decoupling time corresponds to a certain spread in velocity Δv of the decoupled electron stream. This is

$$(9b) \quad \Delta v \sim \frac{1}{2} \frac{eE}{m} t_d \quad (\text{cm/s}).$$

Using equations (6) and (11) one gets

$$(9c) \quad v \sim 0.4 \cdot 10^7 \sqrt{T_e} \quad (\text{cm/s}).$$

(*) The value of I is not critically dependent on the form of the contour C .

In most cases $T_e \sim 10^4$ and therefore

$$(9d) \quad \Delta v \sim \frac{1}{2} \cdot 10^9 \quad \text{cm/s}.$$

This corresponds to an electron energy of 70 eV or a kinetic temperature of $5 \cdot 10^5$ °K.

Owing to collisions the velocity distribution of those electrons that did not run away will not remain cut off by the curve C as shown in Fig. 9; these electrons will cross the boundary C and they too will be decoupled by the field E .

APPENDIX I.

The mean free path approach to the problem of runaway electrons.

The expression for the mean free path of an electron in plasma is given by

$$\lambda = \frac{(mv^2)^2}{\pi e^4 n \ln \Lambda} \quad (\text{cm}).$$

The velocity which the electron acquires in an electric field E is

$$v = \frac{eE}{m} t \quad (\text{cm/s}).$$

The length of path traversed due to this accelerated motion is

$$x = \frac{1}{2} vt \quad (\text{cm}).$$

It is evident that the mean free path of an electron in accelerated motion grows as t^4 , whereas the path actually traversed only as t^2 . If, therefore, an average particle does not suffer a collision before λ/x reaches unity it will not be involved in a collision at any time after that. Thus

$$\frac{\lambda}{x} \simeq \frac{1}{5\pi m} \frac{E^3}{n} t^2 = 1,$$

from which

$$t = \left(\frac{5\pi m}{E^3} n_e \right)^{\frac{1}{2}} \quad (\text{s}).$$

If this t is shorter than

$$t_{\text{coll}} \sim 0.03 \frac{\sqrt{m}(kT)^{\frac{1}{2}}}{e^4 n},$$

then the electrons will be decoupled. The decoupling field E_c follows from

$$t = t_{\text{coll}},$$

and it is

$$E_c \sim 3.8 \cdot 10^{-8} \frac{n}{T} \quad (\text{V/cm}).$$

III - Plasma Wave Guides.

1. - Wave equation.

We shall now derive the wave equation of electromagnetic oscillations on a cylinder of plasma and apply this to three different confinements of such a cylindrical plasma by magnetic fields. These are (Fig. 11.):

a) $B_x I_\theta$ pinch in which $(e/mc)B_x \gg \omega_p$.

b) $I_x B_\theta$ pinch.

c) A combined $B_x I_\theta$ and $I_x B_\theta$ pinch.

At the end of each of these paragraphs we shall briefly discuss the application of the corresponding confinement for radiation compression.

The general wave equation describing harmonic electromagnetic oscillations in a current carrying medium is

$$(1) \quad \text{curl curl } \mathbf{E} - \frac{\omega^2}{c^2} \mathbf{E} = -4\pi j \frac{\omega}{c^2} \mathbf{i}.$$

If this medium is plasma the currents at microwave frequencies are due almost completely to the electron motion. Let us use, therefore, the equation of motion for the electron gas component of the plasma. This is [8]

$$(2) \quad \frac{\partial \mathbf{V}}{\partial t} = -\frac{e}{mc} (c\mathbf{E} + \mathbf{V} \times \mathbf{B}) - \frac{1}{nm} \text{grad } p_e.$$

We shall assume that the ordered velocity of the electrons is larger than the mean thermal speed and that the h.f. component of the \mathbf{B} field is small compared to the steady field. In this case the pressure term in equation (2) can be neglected. Multiplying eq. (2) by $-en$ we get an equation for the current density $\mathbf{i} = -en\mathbf{V}$

$$(2a) \quad \frac{\partial \mathbf{i}}{\partial t} = \frac{e^2 n}{m} \mathbf{E} - \frac{e}{mc} \mathbf{i} \times \mathbf{B}.$$

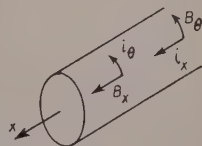


Fig. 11.

Let us use the following symbols

$$\omega_p = \sqrt{\frac{4\pi e^2 n}{m}} = \text{plasma frequency},$$

$$\omega_c = \frac{e}{mc} \mathbf{B} \equiv \text{cyclotron frequency vector}.$$

With these eq. (2a) becomes (for a harmonic oscillation of angular frequency ω)

$$(3) \quad j\omega \mathbf{i} = \frac{\omega^2 p}{4\pi} \mathbf{E} - \mathbf{i} \times \omega_c.$$

We shall be interested in wave propagation on plasma cylinders, let us, therefore, rewrite equations (1)–(3) in cylindrical co-ordinates x, r, θ . Furthermore we shall restrict ourselves to problems in which $\partial/\partial\theta = 0$.

The wave equation (1) thus becomes

$$(1a) \quad \frac{\partial^2 E_x}{\partial x \partial r} - \frac{\partial^2 E_x}{\partial x^2} - \frac{\omega^2}{c^2} E_r = -4\pi j \frac{\omega}{c^2} i_r,$$

$$(1b) \quad \frac{1}{2} \frac{\partial^2 r E_r}{\partial x \partial r} - \frac{1}{r} \frac{\partial}{\partial r} r \frac{\partial}{\partial r} E_x - \frac{\omega^2}{c^2} E_x = -4\pi j \frac{\omega}{c^2} i_x,$$

$$(1c) \quad \frac{\partial}{\partial r} \frac{1}{r} - \frac{\partial r E_\theta}{\partial r} - \frac{\partial^2 E_\theta}{\partial x^2} - \frac{\omega^2}{c^2} E_\theta = -4\pi j \frac{\omega}{c^2} i_\theta.$$

The equation for current density, considering only B_θ and B_x field is

$$(3a) \quad j\omega i_x + i_r \omega_{c_\theta} = \frac{\omega_p^2}{4\pi} E_x,$$

$$(3b) \quad j\omega i_r - i_x \omega_{c_\theta} + i_\theta \omega_{c_x} = \frac{\omega_p^2}{4\pi} E_r,$$

$$(3c) \quad j\omega i_\theta - i_r \omega_{c_x} = \frac{\omega_p^2}{4\pi} E_\theta.$$

Let us now consider three simple situations which can be described by these equations.

a) *Confinements by a strong B_z field.* We shall assume that the field B_z is strong enough to prevent an appreciable r.f. current flow in the radial and azimuthal direction. Let us also assume that the r.f. pattern varies with x

as $\exp [jkx]$. Then equation (1a) gives

$$(1a') \quad E_r = jk \left(\frac{\omega^2}{c^2} - k^2 \right)^{-1} \frac{\partial E_x}{\partial r},$$

whereas equation (3a) gives for the current density

$$(3a') \quad j\omega i_x = \frac{\omega^2 p}{4\pi} E_x.$$

Substituting these into equation (1b) we get

$$(4) \quad \frac{1}{r} \frac{\partial}{\partial r} r \frac{\partial E_x}{\partial r} + \left(\frac{\omega^2}{c^2} - k^2 \right) \left(1 - \frac{\omega_p^2}{\omega^2} \right) E_x = 0.$$

Comparing this equation with a wave equation in a dielectric medium one finds that the plasma behaves as an anisotropic dielectric with

$$\epsilon_r = 1, \quad \epsilon_x = 1 - \frac{\omega_p^2}{\omega^2}.$$

The solution of equation (4) is

$$(5) \quad E_x = a \cdot J_0(|\chi|r),$$

where

$$(5a) \quad \chi^2 = \left(\frac{\omega^2}{c^2} - k^2 \right) \left(1 - \frac{\omega_p^2}{\omega^2} \right).$$

The corresponding solution for H_θ can be obtained from the second Maxwell's equation. Thus

$$(6) \quad [\text{curl } \mathbf{E}]_\theta = -j \frac{\omega}{c} H_\theta.$$

Using equation (1a) one has

$$H_\theta = \frac{j\omega/c}{(\omega^2/c^2) - k^2} \frac{\partial E_x}{\partial r},$$

or

$$(7) \quad H_\theta = -j \frac{a(\chi)(\omega/c)}{(\omega^2/c^2) - k^2} J_1(|\chi|r).$$

Assuming that the space outside the plasma cylinder is vacuum, the solution

of the wave equation for $r = r_0$ and for a guided cylindrical wave is

$$(8) \quad E_x = b \cdot K_0(|\chi_0|r),$$

$$(9) \quad H_\theta = -j \frac{b |\chi_0| (\omega/c)}{(\omega^2/c^2) - k^2} K_1(|\chi_0|r).$$

The constants a and b are obtained from the condition that the E_x and H_θ components must be continuous functions of the radius. Thus at the boundary of the plasma cylinder

$$(10) \quad a J_0(|\chi|r_0) - b K_0(|\chi_0|r_0) = 0,$$

$$(11) \quad a |\chi| J_1(|\chi|r_0) - b |\chi_0| K_1(|\chi_0|r_0) = 0.$$

The secular equation of this system is

$$(12) \quad \frac{J_0(|\chi|r_0)}{J_1(|\chi|r_0)} = \frac{|\chi|}{|\chi_0|} \frac{K_0(|\chi_0|r_0)}{K_1(|\chi_0|r_0)}.$$

This can be written as

$$(12a) \quad \frac{J_0(|\chi|r_0)}{J_1(|\chi|r_0)} = \left(\frac{\omega_p^2}{\omega^2} - 1 \right)^{\frac{1}{2}} \frac{K_0(|\chi_0|r_0)}{K_1(|\chi_0|r_0)}.$$

It is useful to introduce the following system of non-dimensional quantities,

$$(13) \quad \xi = \frac{\omega_p^2}{\omega^2}, \quad \kappa = \frac{k^2 c^2}{\omega_p^2}, \quad \varrho = r_0 \frac{\omega_p}{c} = 2\sqrt{\nu}.$$

With this equation (12a) becomes

$$(12b) \quad \frac{J_0\{[4\nu(1-1/\xi)(\xi-\kappa)]^{\frac{1}{2}}\}}{J_1\{[4\nu(1-1/\xi)(\xi-\kappa)]^{\frac{1}{2}}\}} = \left(\frac{1}{\xi} - 1 \right)^{\frac{1}{2}} \frac{K_0\{[4\nu(\kappa-\xi)]^{\frac{1}{2}}\}}{K_1\{[4\nu(\kappa-\xi)]^{\frac{1}{2}}\}}.$$

The curve representing the dispersion equation (12b) could be plotted in a ξ, κ co-ordinate system. One has

$$(14a) \quad \xi = \frac{\omega^2}{\omega_p^2} = \frac{(2\pi c)^2}{\lambda^2 4\pi(e^2 n/m)} = \left(\frac{\pi r_0}{\lambda} \right)^2 \nu^{-1}.$$

$$(14b) \quad \kappa = \frac{K^2 c^2}{\omega_p^2} = \frac{(2\pi c)^2}{\lambda^2 g 4\pi(e^2 n/m)} = \left(\frac{\pi r_0}{\lambda g} \right)^2 \nu^{-1}.$$

During a radial contraction of the plasma cylinder ν and λg remain constant. Thus in following a curve corresponding to a particular value of ν (see Fig. 12) one can find the relationship

$$\lambda = \lambda(r_0; \lambda g, \nu),$$

where λg and ν are parameters.

If the radial compression ratio is

$$\eta = \frac{r_{01}}{r_{20}} = \sqrt{\frac{\kappa_1}{\kappa_2}},$$

the frequency multiplication becomes

$$(15) \quad g = \frac{\lambda_1}{\lambda_2} = \sqrt{\frac{\xi_2}{\xi_1}} \cdot \eta = \sqrt{\frac{\xi_2 \kappa_1}{\xi_1 \kappa_2}}.$$

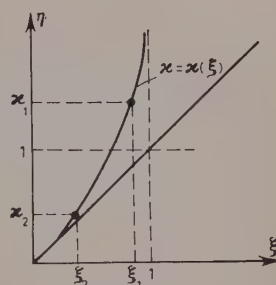


Fig. 12.

Since $\kappa_1/\kappa_2 > \xi_1/\xi_2$ it follows that

$$(16) \quad \eta > g > 1,$$

λ and r_0 may be expressed as functions of ξ and κ . Thus

$$(17) \quad \lambda = \lambda g \sqrt{\frac{\kappa}{\xi}} \quad \text{and} \quad r_0 = \lambda g \frac{\sqrt{\nu \kappa}}{\pi}.$$

From these, and with the help of the $\kappa = \kappa(\xi)$ curves one can plot curves (Fig. 13) representing

$$\lambda = \lambda(r_0).$$

As the plasma cylinder is radially compressed, λg remains constant and one would expect that when $r_0 \ll \lambda g$ the r.f. power flows mainly outside the plasma guide and $\lambda \rightarrow \lambda g$. This is confirmed from the $\kappa = \kappa(\xi)$ curves and from the equation

$$\frac{\lambda g}{r_0} = \frac{\pi}{\sqrt{\kappa}}.$$

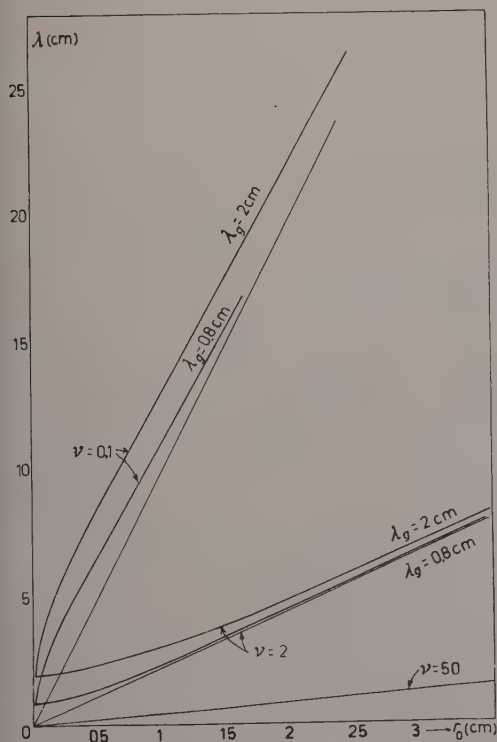


Fig. 13.

Thus as $\kappa \rightarrow 0$ one obtains

$$\frac{\kappa}{\xi} \rightarrow 1 \quad \text{and} \quad \lambda \rightarrow \lambda g.$$

When the plasma guide expands r_0 becomes larger than λg and one would expect that the character of the oscillations should become similar to the Langmuir electron oscillations. This is indeed so, as when $\lambda g/r_0 \rightarrow 0$, $\kappa \rightarrow \infty$ and this is possible only if $\xi \rightarrow 1$, *i.e.* $\omega \sim \omega_p$, the Langmuir plasma frequency. In this case the wavelength that can be propagated follows from eq. (4a). This gives

$$\frac{\lambda}{r_0} = \frac{\pi}{\sqrt{\nu\xi}}.$$

For $\xi \rightarrow 1$ one obtains $\lambda = r_0(\pi/\sqrt{\nu})$, a relationship connected with the existence of the stray fields outside the plasma.

The efficiency of a radiation compression process can be associated with a function

$$(18) \quad \frac{\Delta\lambda/\lambda}{\Delta r_0/r_0} = f,$$

where $\Delta\lambda$ and Δr_0 correspond to some $\Delta\xi$.

This may be also written as

$$(18a) \quad f = \frac{\lambda}{r_0} \frac{d\lambda/d\xi}{dr_0/d\xi} = \frac{\sqrt{\nu\xi}}{\pi} \cdot \frac{(d/d\xi)\sqrt{\kappa/\xi}}{\sqrt{\nu/\pi}(d/d\xi)\sqrt{\kappa}}$$

and therefore

$$(18b) \quad f = 1 - \frac{1}{\xi} \frac{\kappa}{d\xi/d\kappa},$$

for $\xi \rightarrow 0$, $\kappa/\xi \rightarrow 1$ and $d\kappa/d\xi = 1$. Therefore

$$f(\xi = 0) = 0.$$

f can be also expressed in terms of r_0 and λ as

$$(18c) \quad f = \frac{r_0^2}{\lambda^2} \cdot \frac{d(\lambda^2)}{d(r_0^2)},$$

As $\xi \rightarrow 1$ there is $\lambda^2/r_0^2 \rightarrow \pi^2/\nu$ and $d(\lambda^2)/d(r_0^2)(\pi^2/\nu)$.

Therefore

$$f \rightarrow 1.$$

It is obviously important to choose such ν which will permit an efficient radiation compression. This can be done with the help of curves for $\lambda(r_0)$ plotted in Fig. 13. Often a decisive parameter will be the initial and final frequency, *e.g.* one may desire a frequency multiplication from the *S*-band into the *X*-band. From Fig. 13 it is obvious that such a frequency shift cannot be efficiently effected with a $\nu = 0.1$ guide, but $\nu = 2$ will be appropriate. On the other hand a $\nu = 20$ guide requires a too large initial radius (*i.e.* the dimension corresponding to *S*-band).

Let us also consider the effect on the r.f. field pattern of creation of new plasma (by ionising collisions) within a plasma guide whose radius r_0 remains constant.

Let us assume that ν changes from ν_1 to ν_2 where $\nu_1 < \nu_2$. If the original state is represented by a point $\xi_1 \kappa_1$ in the $\xi \kappa$ diagram (Fig. 6a) and the final state by a point $\xi_2 \kappa_2$ it follows from equations (14), (14a) that

$$\frac{\xi_1}{\xi_2} = \frac{\lambda_2^2 \nu_2}{\lambda_1^2 \nu_1}, \quad \frac{\kappa_1}{\kappa_2} = \frac{\nu_2}{\nu_1}.$$

The frequency shift is again given by equation (15)

$$g = \frac{\lambda_1}{\lambda_2} = \left(\frac{\xi_1 \kappa_2}{\xi_2 \kappa_1} \right)^{-\frac{1}{2}}.$$

The curves representing the change in ν for $r_0 = \text{const}$ are shown in Fig. 14. From these it is obvious that an increase in κ results in an increase of the frequency of the guide mode.

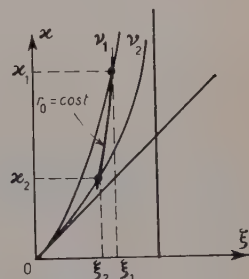


Fig. 14.

b) Confinements by the B_θ -field of a steady current through plasma in the x -direction. In this case the electric field of an *E*-mode is everywhere perpendicular to the steady magnetic field B_θ (see Fig. 15). Provided that

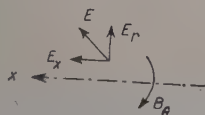


Fig. 15.

$$\omega_{cp} < \omega < \omega_c,$$

where ω_{cp} is the proton synchrotron frequency, two types of currents can flow. One is a Hall current, the other is a polarization current. These follow from equations (3abc) remembering that

$\omega_{c_x} = 0$. Thus

$$(19a) \quad j\omega i_x + i_r \omega_{c\theta} = \frac{\omega_p^2}{4\pi} E_x,$$

$$(19b) \quad j\omega i_r - i_x \omega_{c\theta} = \frac{\omega_p^2}{4\pi} E_r.$$

Thus (putting $\omega_{c_x} = \omega_c$)

$$(20a) \quad i_x = \frac{1}{4\pi} \frac{\omega_p^2}{\omega_c^2} \left(1 - \frac{\omega^2}{\omega_c^2}\right)^{-1} (j\omega E_x - \omega_c E_r),$$

$$(20b) \quad i_r = \frac{1}{4\pi} \frac{\omega_p^2}{\omega_c^2} \left(1 - \frac{\omega^2}{\omega_c^2}\right)^{-1} (j\omega E_r + \omega_c E_x).$$

The plasma behaves, therefore, as a medium of dielectric constant

$$(21a) \quad \varepsilon = \varepsilon_x = \varepsilon_r = 1 + \frac{\omega_p^2}{\omega_c^2} \left(1 - \frac{\omega^2}{\omega_c^2}\right)^{-1},$$

and whose conductivity tensor has diagonal components

$$(21b) \quad -\sigma_{rx} = \sigma_{rx} = \frac{1}{4\pi} \frac{\omega_p^2}{\omega_c^2} \left(1 - \frac{\omega^2}{\omega_c^2}\right)^{-1}.$$

One could substitute equations (20a) and (20b) into the corresponding wave equations (1abc). However, as ω_c is a function of r and for some value of r $\omega_c = \omega$, these equations are difficult to simplify and solve. Some progress can be made by simplifying the geometry of the problem.

Let us consider an infinite plasma with $\omega_{c_x} = \omega_c$, $\omega_{c_y} = \omega_{c_z} = 0$.

Let there be a wave $E = E \exp [j(\omega t + kx)]$ and $(\partial/\partial y) = (\partial/\partial z) = 0$. The E_z component can be neglected as that belongs to a transversal wave unaffected by the field B .

The equation 3 becomes

$$j\omega i_x = \frac{\omega_p^2}{4\pi} E_x - i_y \omega_c,$$

$$j\omega i_y = \frac{\omega_p^2}{4\pi} E_y + i_x \omega_c,$$

from which

$$(22a) \quad i_x = \frac{1}{4\pi} \frac{\omega_p^2}{\omega_c^2} \left(1 - \frac{\omega^2}{\omega_c^2}\right)^{-1} (j\omega E_x - \omega_c E_y),$$

$$(22b) \quad i_y = \frac{1}{4\pi} \frac{\omega_p^2}{\omega_c^2} \left(1 - \frac{\omega^2}{\omega_c^2}\right)^{-1} (j\omega E_y + \omega_c E_x).$$

These currents are a mixture of polarization currents and of Hall currents similar to those of equations (20ab). The wave equation can be developed as follows

$$\text{curl } E = z_0 \frac{\partial E_y}{\partial x},$$

$$\text{curl} \left(z_0 \frac{\partial E_y}{\partial x} \right) - y_0 \frac{\partial^2 E_y}{\partial x^2} = y_0 k^2 E_y,$$

Therefore, the component wave equations become

$$(23a) \quad -\frac{\omega^2}{c^2} E_x = -j \frac{\omega}{c^2} \left(\frac{\omega_p}{\omega_c} \right)^2 \left(1 - \frac{\omega^2}{\omega_c^2} \right)^{-1} (j\omega E_x - \omega_c E_y),$$

$$(23b) \quad k^2 E_y - \frac{\omega^2}{c^2} E_y = -j \frac{\omega}{c^2} \left(\frac{\omega_p}{\omega_c} \right)^2 \left(1 - \frac{\omega^2}{\omega_c^2} \right)^{-1} (j\omega E_y + \omega_c E_x).$$

From the second one one gets:

$$E_x = \frac{j c^2}{\omega \omega_c} \left[\left(\frac{\omega_c}{\omega_p} \right)^2 \left(k^2 - \frac{\omega^2}{c^2} \right) \left(k - \frac{\omega^2}{\omega_c^2} - \frac{\omega^2}{c^2} \right) \right] E_y.$$

Substituting this into equation (23a) one obtains

$$(24) \quad \frac{\omega_p^2}{\omega_c^2} = - \left\{ \left(\frac{\omega_c}{\omega_p} \right)^2 \left(k^2 - \frac{\omega^2}{c^2} \right) \left(1 - \frac{\omega^2}{\omega_c^2} \right) - \frac{\omega^2}{c^2} \right\} \left\{ 1 - \frac{\omega^2}{\omega_c^2} + \frac{\omega_p^2}{\omega_c^2} \right\}.$$

Put

$$\frac{\omega_p^2}{\omega_c^2} = a, \quad \left(\frac{c}{\omega_p} \right)^2 = \eta, \quad \left(\frac{\omega}{\omega_p} \right)^2 = \xi.$$

Equation (24) can now be written as

$$(24a) \quad a = - \{ (\eta - \xi)(1 - a\xi) - a\xi \} \cdot (1 + a - a\xi),$$

from which

$$(25) \quad \eta = \frac{\xi(1 + a - a\xi)^2 - a}{(1 - a\xi)(1 + a - a\xi)}.$$

Let us plot $\eta = \eta(\xi)$ for different a . The phase velocity of the wave is then (Fig. 16)

$$(26) \quad v_p = \frac{\omega}{k} = \frac{\sqrt{\xi}}{\sqrt{\eta}} \cdot c \quad \text{and} \quad \frac{v_p}{c} = (\text{tg } \gamma)^{-\frac{1}{2}}.$$

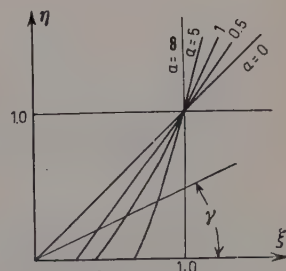


Fig. 16.

The dimensionless variables ξ , η , and a may be also expressed as

$$(27) \quad \xi = \frac{(2\pi c/\lambda)^2}{4\pi e^2 n/m}, \quad \eta = \frac{(2\pi c/\lambda g)^2}{4\pi e^2 n/m}, \quad a = \frac{4\pi e^2 n/m}{e^2 B^2/m^2 c^2}.$$

Writing $n = (N/\frac{1}{2}Y^2)$, where Y is a characteristic dimension of the plasma in the direction transversal to x and putting $N(e^2/mc^2) = \nu$ one gets

$$(28) \quad \xi = \left(\frac{Y}{\lambda}\right)^2 \nu^{-1}, \quad \eta = \left(\frac{Y}{\lambda_g}\right)^2 \nu^{-1}, \quad a = 2\pi m c^2 (YB)^{-2} \cdot N.$$

It follows from the $\eta(\xi)$ diagram that there is a region of propagation, especially for weak magnetic fields, in which the phase velocity is substantially different from c .

Let us now consider a slab of plasma of thickness y (see Fig. 17). Let us assume that a wave described by the dispersion relation (24a) propagates within the slab and is reflected from the boundary at an angle α . Such a reflection is possible only if $\omega < \omega_p$.

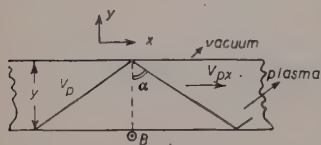


Fig. 17.

In such a case the phase velocity V_{px} of this wave along the x -axis will be greater than V_p given by equation (26). It thus appears possible to make $V_{px} = c$, if one could choose originally a $\eta(\xi)$ corresponding to $V_p < c$. However,

waves in this velocity region possess $\omega < \omega_p$ and therefore cannot be guided within the plasma slab.

If, on the other hand, the plasma slab is placed between two metal surfaces, one could use the $v_p < c$ region of the η , ξ plane for propagation.

If now the separation of the metal surfaces which is also the transversal dimension Y of the plasma is decreased, the frequency ω will increase and $v_p \rightarrow c$ along a curve in the $\eta(\xi)$ plane corresponding to a particular a . As n changes in the same way as B^2 it follows that $a = \text{const}$.

It seems plausible that the propagation of waves on a plasma cylinder formed by $B_0 i_x$ pinch will exhibit a behaviour similar to that of a plasma slab.

c) *Confinement by a helical $B_0 B_x$ field.* This confinement seems suited for a three-dimensional compression of a radiation guided by a cylinder of plasma.

Let us again simplify the situation, mainly because a general wave equation corresponding to this case is difficult to interpret and let us assume that

$$\frac{\omega_c}{\omega} \gg 1,$$

and also that $\lambda g < 2r_0$.

The physical meaning of these assumptions is that $\mathbf{i} \parallel \mathbf{B}$ and that most of the r.f. energy flows through the plasma. The equation for the electron current is, therefore

$$i_{||} = -\frac{e^2 E_{11}}{m\omega},$$

where (Fig. 18)

$$(29) \quad E_{11} = E_x \cdot \cos \psi$$

and the kinetic energy of the r.f. motion of an electron is

$$(30) \quad W_{ek} = \frac{e^2 E_{11}^2}{2m\omega^2} = \frac{e^2 E_{\infty}^2}{2m\omega^2} \cos^2 \psi.$$

The kinetic energy within a $\lambda_g/2$ segment of the beam is therefore

$$(31) \quad W_k = \frac{1}{2} \frac{e^2 E_x^2}{2m\omega^2} \cos^2 \psi \cdot \pi r_0^2 \frac{\lambda_g}{2} \cdot n.$$

This changes every π/ω (s) into an electric energy (*)

$$(32) \quad W_e \simeq \frac{1}{2} \pi r_0^2 \frac{\lambda_g}{2} \frac{E_x^2}{8\pi}.$$

From the equality $W_k = W_E$ we get

$$\omega^2 = \frac{4\pi e^2 n}{m} \cos^2 \psi,$$

or

$$(33) \quad \omega = \omega_p \cos \psi .$$

Thus as one decreases the angle ψ , ω increases as $\cos \psi$. If this did not involve any change in the radius r_0 of the plasma cylinder, one could interpret this change of ω as a result of a compression in the x -direction (or rather an untwisting in the θ -direction).

However as such a change in ψ could be effected only by changing the ratio of B_z/B_θ a change of radius r_0 must also occur. If, *e.g.*, B_z is rapidly increased, one may expect that r_0 and ψ will decrease and the r.f. field will, therefore, experience a three-dimensional compression.

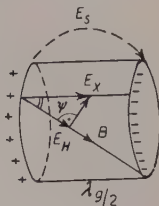


Fig. 18.

(*) If one takes into account the energy stored in the stray fields E_s , eq. (34) becomes a dispersion equation for this mode.

APPENDIX II

The Q of a plasma resonator.

The h.f. current density in an infinite and uniform plasma is

$$(A.1) \quad i = \frac{ne^2E}{m\omega} \frac{\nu_c/\omega}{(\nu_c/\omega)^2 + 1} - j \frac{ne^2E}{m\omega} \frac{1}{(\nu_c/\omega)^2 + 1},$$

where ν_c is the collision frequency of electrons. The energy stored per unit volume is

$$(A.2) \quad W_s = \frac{1}{2} mn \left(\frac{eE}{m\omega} \right)^2 = \frac{1}{2} n \frac{e^2 E^2}{m\omega^2}.$$

The energy dissipated

$$(A.3) \quad W_d = \frac{1}{2} \operatorname{Re}(i) \cdot E = \frac{1}{2} \frac{ne^2 E^2}{m\omega} \frac{\nu_c/\omega}{(1 + (\nu_c/\omega)^2)}.$$

One can define an effective Q of such plasma as a ratio

$$(A.4) \quad Q = \frac{wW_s}{w_d} = \frac{\frac{1}{2}n(e^2E^2/m\omega)}{\frac{1}{2}n(e^2E^2/m\omega)(\nu_c/\omega)} \left\{ 1 + \left(\frac{\nu_c}{\omega} \right)^2 \right\}.$$

For large ω/ν_c one gets

$$(A.4a) \quad Q \approx \omega/\nu_c.$$

If the degree of ionisation is larger than 1% and if the r.f. velocity is smaller than the mean thermal speed, then the collision frequency is

$$(A.5) \quad \nu_c = 50 \frac{n}{T^{\frac{1}{2}}}.$$

Therefore

$$(A.4b) \quad Q \approx \frac{\omega T^{\frac{1}{2}}}{50n}.$$

For adiabatic compression

$$\frac{T^{\frac{1}{2}}}{n} = \text{const},$$

and it is in our case

$$\frac{T_0^{\frac{1}{2}}}{n_0} \approx 0 \dots \times 10^{-6}.$$

Thus finally

$$(A.4c) \quad Q \sim 0.02 \cdot 10^{-8} \omega = 2 \cdot 10^{-8} \omega.$$

Ex.: for $\omega = 2 \cdot 10^{11}$ one gets $Q = 0.4 \cdot 10^4$.

When the r.f. velocity is larger than the mean thermal speed, *i.e.* when

$$\frac{eE}{m\omega} > \frac{\sqrt{2kT}}{m},$$

i.e. for

$$E > \frac{\omega}{e} \sqrt{2kTm},$$

and as $T \sim 10^4$

$$(A.6) \quad E > 10^{-10} \quad (\text{ab. V/cm}).$$

The collision frequency is

$$(A.7) \quad \nu_c = 10^{-31} \left(\frac{\omega}{E} \right)^3 n \quad (\text{cal/s, rad/s, ab. V/cm, el/cm}^3),$$

and consequently

$$(A.8) \quad Q = 10^{34} \frac{E^3}{n\omega^2} \quad (\text{ab. V/cm, el/cm}^3, \text{rad/s}).$$

We shall be dealing with initial plasma densities of the order of 10^{12} el/cm³ and initial angular frequencies of the order of 10^{11} rad/s. A feasible field strength is about 100 ab. V/cm. Thus it follows that the order of magnitude of Q is 10^7 . The collision frequency in this case is of the order of 10^5 . If there are also neutral molecules, then the collision frequency between an electron and neutral molecules is

$$\nu_n = \frac{eE}{m\omega} \alpha \cdot 10^{-16} \cdot n_n,$$

where α is usually of the order of unity. Thus

$$(A.9) \quad \nu_n \sim 50 \frac{E}{\omega} n_n.$$

Let us form a ratio of

$$(A.10) \quad \frac{\nu_c}{\nu_n} = 2 \cdot 10^{-36} \left(\frac{E}{\omega} \right)^4 \frac{n}{n_n}.$$

This ratio is of the order of unity for the above mentioned quantities if

$$n_n = 2n,$$

i.e. if the degree of ionisation is about 50%.

It has been shown that during an adiabatic two-dimensional compression of a plasma guide

$$E^{\frac{2}{3}}/\omega = \text{const.}$$

It thus follows that the Q corresponding to electron-proton collisions (eq. (8)) varies as $\omega^{\frac{2}{3}}$ during the compression, whereas the Q -factor corresponding to the electron-neutrals collisions varies as

$$Q_n = \frac{1}{50} \frac{\omega^2}{En_n} \alpha \omega^{\frac{2}{3}},$$

during the same compression. For high temperature plasma the Landau damping must be also considered as a source of r.f. loss.

REFERENCES

- [1] R. F. POST: *Rev. of Mod. Phys.*, **28**, 338 (1956).
- [2] J. G. LINHART: *Nuclear Engineering*, **2**, 60 (1957).
- [3] P. C. THONEMANN, E. P. BUTT, R. CARRUTHERS, A. N. DELLIS, D. W. FRY, A. GIBSON, G. N. HARDING, D. E. LEES, R. W. P. MCWHIRTER, R. S. PEASE, S. A. RAMSDEN and S. WARD: *Nature*, **181**, 217 (1958).
- [4] L. SPITZER: *Nature*, **181**, 221 (1958).
- [5] S. J. ROBERTS and R. J. TAYLER: *AERE* rep. T/R 2138; *AERE* rep. T/R 2264.
- [6] W. HEITLER: *Quantum theory of radiation*, (Oxford 1954).
- [7] L. SPITZER: *Physics of fully ionized gases* (New York, 1956), p. 36.
- [8] L. SPITZER: *Physics of fully ionized gases* (New York, 1956), p. 73.

INTERVENTI E DISCUSSIONI

— R. LÜST:

Your calculations have been carried out at fusion temperatures. But at lower temperatures the energy losses are much more severe and if you actually have to heat an originally cold plasma, the bottle will be empty before the high temperature region will be reached.

— J. G. LINHART:

I agree with you that we have to apply some reasonably fast heating mechanism. The losses at lower temperatures are so high that a zero energy reactor will not be possible below $130 \cdot 10^6$ °K (D-T-reaction). One has to heat the plasma to this temperature during, say, $1 \mu\text{s}$. I think that there are mechanisms by means of which one can heat up a plasma in this order of time.

— F. R. SCHWARZL:

In your calculation you have assumed that the mean free path of the particles must be at least of the order of magnitude of the bottle dimensions. If you look on the other hand to the other extreme, that you have a very large number of collisions, one gets the same formula as you but the confinement factor α is left out for there are as many particles thrown out from A to B as from B to A and in consequence the magnetic configuration comes not in any longer, and you don't have a bottle at all.

— J. G. LINHART:

I agree, as soon as there is an appreciable transfer from B to A as well, the usual magnetohydrodynamic equations are valid and the confinement is virtually independent of the bottle geometry.

— F. R. SCHWARZL:

This seems to me an interesting example of a case, where the equations of magnetohydrodynamics give quite an opposite result to the single particle model. One should be careful therefore in using the magnetohydrodynamic equations for the description of high temperature plasmas.

— J. G. LINHART:

I quite agree with you. Many people have recognized this and it was especially appreciated in the study of instabilities in high temperature plasmas with anisotropic velocity distributions because very often one gets different results depending on whether one treats this using the distribution function or whether one uses the magnetohydrodynamic model.

— F. C. THONEMANN:

I think you will find that even in the last vacua conceivable one gets a loss of particles by charge exchange which exceeds by far the loss through the end of the bottle.

— J. G. LINHART:

I seem to recollect that a vacuum of the order of 10^{-6} is required for the two losses to be equal, however, this difficulty would enter into any confinement project.

— L. S. GOLDSTEIN:

I imagine that when you are accelerating the runaway-electrons quite a number of collisions with the gas will occur.

— J. G. LINHART:

Not really, the whole acceleration is accomplished in about $8 \mu\text{s}$ so that during this period the scattering due to the neutrals is negligible.

— L. S. GOLDSTEIN:

What kind of gas did you use?

— J. G. LINHART:

We used several gases, from hydrogen to mercury. The mechanism seems to work best in argon, the reason being not so much the decoupling effect of the runaways described here, but the fact that one can produce uniform plasmas at lower pressures in argon than in other gases.

— L. S. GOLDSTEIN:

Probably you get the runaway electrons easier in argon because of the Ramsauer minimum.

— J. G. LINHART:

Yes, I agree, that might have an effect.

— H. WILHELMSSON:

What is the order of magnitude of the magnetic field owing to the plasma currents?

— J. G. LINHART:

The initial current of 300 A corresponds to about 100 G, but when at the end of acceleration there remains only 1/10 A the earth's magnetic field strength is probably higher than the field of the relativistic beam.

— H. C. VAN DE HULST:

Is that right that the field pattern is similar to that in an infinite plasma in the limit in which most of the field is concentrated within the plasma?

— J. G. LINHART:

Yes, there remains only a small stray field at the boundaries of the plasma.

— L. S. GOLDSTEIN:

I think the gas ought to be completely ionized and of high temperature before squeezing?

— J. G. LINHART:

It would be helpful if the electron temperature were very high, but even for an ordinary gas discharge plasma the Q -factor of a plasma resonator is reasonably high. One can write $Q \approx \omega T_e^{\frac{3}{2}} / 50n$, and for $\omega = 2 \cdot 10^{11}$, $T_e = 10^4$, $n = 10^{12}$ one gets $Q \sim 4000$, which is not bad. The effect of the neutrals is negligible if the degree of ionization exceeds 15%.

— O. STURROCK:

You have used for the wave guide pattern the small amplitude theory, but on the other hand you propose to use high field strengths.

— J. G. LINHART:

The linear theory is applicable if

$$\lambda g \gg A = \frac{eE}{m\omega^2};$$

during the compression the electric field becomes high, but the frequency ω increases too and it can be shown, that if the criterium is satisfied before the compression, it also holds in the pinched state.

Optical and Radiophenomena Associated with a Solar Activity Centre.

C. DE JAGER

Sterrewacht Sonnenborgh - Utrecht

1. - The first part of the life history of an activity centre.

A solar activity centre is a region of enhanced activity, as a rule not greater than 0.1 to 0.2 times the solar diameter. In this region most transient solar phenomena are observed, such as faculae, sunspots, flares, surges, spot-prominences, coronal condensations.... There are many kinds of activity centres (CA); most of them live short, some stay longer and may reach the state of complete development. In this paper we discuss the «ideal», fully developed CA as it was for the first time described by KIEPENHEUER in 1952. It has a lifetime perhaps of the order of 200 days, but only the first 30 days, when the CA is at maximum activity, are of importance for the present discussion.

The first indications that a CA is going to be born are given by magnetic field measurements. In an optically quiet region of the sun's disk a weak field originates (some Gauss) that rapidly increases in area and strength. After some hours (sometimes only after some days) one of the coarse H α -mottles in the magnetic region elongates and becomes fairly bright; somewhat later it decreases in brightness while it grows at the same time. Sometimes two brightness maxima occur, which correspond to regions of opposite magnetic polarity of the so-called BM (Bipolar Magnetic) region. After some days the «leading spot» originates in the west end of the region, followed, after some days, at the east end, by the «following spot» which is often smaller than the leader and has an opposite magnetic polarity.

At this moment the first phase in the life of the CA can be considered as being ended. Simultaneously with the growth of the BM field and of the faculae the intensity of the coronal radiation at 5303 Å (Fe XIV) has increased. The bright coronal area has about the same extension as the facular

field. The occurrence of this line, with its ionization potential of 355 eV points to a somewhat increased temperature in the corona (about 10^6 °K). Not many details are as yet visible in the corona.

With the establishment of the bipolar spot character a period of greater activity starts. Small unstable «spot filaments» (or «spot prominences») occur, which are first orientated more or less around the faculae, later they tend to point towards the leading spot of the group. The spot group increases in size and in number of components; the first flares occur. As GIOVANELLI showed, already 20 years ago, the occurrence of flares is correlated with changes in the position or in the number of spots in the groups. Flares are not apt to occur when the spot group has its maximum size (which happens after 10÷15 days), but rather when the group is growing or decaying, and flares occur most often in spot groups with a complex magnetic character. It is known that spots are parts of the BM region where the magnetic field strength is much greater than in the surroundings. A BM region has a field of some Gauss, in a spot it ranges between some hundreds and 4500 gauss. So it seems rather certain that flares are due to changings in the magnetic fields of spot groups.

This second phase is the period of greatest activity of the CA. It ends after 20 to 30 days, when the spot group has disappeared. The relation between flares and coronal activity in this phase will be discussed in Sect. 3.

The second phase is followed by a period of decreased activity in the life of the CA. The BM region increases in size; the field strength starts to decrease, some solar rotations later. Also the facular field continues to grow in size, not in brightness, and later gradually disintegrates. This phase of the development will not be treated in this paper.

2. - The coronal extension of a moderately active CA.

The enhancement of the 5303 Å radiation in the corona above a CA indicates an increase of the temperature in the coronal parts of the CA. Other information about this part of the sun can be derived from the radio-spectrum. Eclipse observations, but especially the observations made with the great modern interferometer aerials have shown that CA's emit an enhanced thermal radiation, especially at dm and short metre waves; the radiation reaches its top intensity not when the spots are at maximum development but later when the facular area is at the top of its development. In a moderately active CA the temperature is above 10^6 °K and the density is also increased, the precise values depending on the state of development.

That the rather stable ray and arch structures, shown to us on the magnificent film taken by R. B. DUNN, require a magnetic explanation seems

unquestionable. To what extent the motions occurring in coronal active regions are regulated by magnetic fields can be best shown with the prominences. There are two types of prominences, the *spot prominences*, short lived, small active ones, which occur close to the spots in activity centres, and secondly the long stable *quiescent* ones, which may exist for many months, and which occur as a rule at the high latitude border of a CA, and sometimes in a «dark lane» which divides an old activity centre in two parts.

These latter prominences perhaps represent an equilibrium configuration between the external magnetic and the internal turbulent energies: with the usual prominence values $N_{\text{proton}} = N_{\text{electron}} = 2 \cdot 10^{10} \text{ cm}^{-3}$ and with $v_{\text{turb}} = 5 \text{ km/s}$, and assuming this energy equal to $H^2/8\pi$ one obtains $H = 0.2 \text{ gauss}$, an acceptable value for the borders of the BM regions. This is more or less the basis of Kippenhahn and Schlüter's prominence theory in which is assumed that the quiescent prominences are supported by the horizontal or slightly concave parts of the field. The field is somewhat depressed by the occurrence of the prominence and this leads to a stable configuration.

The sunspot prominences obviously occur in regions of greater fields. An assumed field strength of 3 gauss would lead to a magnetic energy density more than hundred times the value for the quiescent prominences. So, the motions of spot prominences are regulated by hydromagnetic laws.

3. — The coronal condensations and the flares.

The highest temperatures and greatest densities occur in the *coronal condensations*. Following Waldmeier's definition we speak of «permanent» and «sporadic» condensations. The latter occur in the first. The permanent condensations may persist for days, sometimes longer; they have the greatest electron densities $((0.5 \div 2) \cdot 10^{10} \text{ cm}^{-3})$ and often show the 5694 Å line (Ca XV; 814 eV), the line of highest excitation potential of the solar spectrum. The occurrence of this line is correlated with flares; brightness maximum is attained some time (average: 0^b.5) after the occurrence of a flare. The electron temperature in the centre of a condensation is between 2 and $5 \cdot 10^6 \text{ }^\circ\text{K}$.

The sporadic condensations occur in the permanent ones. They emit mainly the 5303 Å line, are short lived and show structures, similar to the knot, loop and funnel prominences observed in H α . The most remarkable phenomenon is that these 5303 Å structures often coincide in place with the H α structures, so that one gets the impression that the cool objects are embedded in the hotter ones, or reversely (which of the two is inside is difficult to say but it seems that it is the prominences). The sporadic condensation are related to the flares but in a less strict sense than the yellow emission regions.

The sporadic condensations show us how a highly excited solar region suddenly can cool down to temperatures of the order of 10^4 °K.

A *flare* is one of the high-lights in the life of a CA. Their *forms* have been shown to us by Dr. GIOVANELLI. Their *temperatures* are 10 000 to 15 000 °K, their electron *densities*, are high, about $2 \cdot 10^{13} \text{ cm}^{-3}$. Most flares originate in the high chromosphere but they extend slowly: the average heights are 15 000 to 20 000 km, well inside the corona. Other flares find their origin right in the low corona, so that the question might be posed whether flares should be considered as suddenly cooled coronal regions or rather as suddenly heated chromospheric regions. (The latter is the usual concept.) But this is not the most important problem: the temperature variations are accompanied by sudden and much more drastic *density* changes. The temperature of a flare exceeds hardly that of the upper chromosphere and is only 10^{-2} that of the corona, but the flare's electron densities exceed that of the chromosphere by a factor $10^{3.5}$ and that of the corona by a factor $10^{4.5}$. So the problem of the flares is to explain how in some minutes the density can increase by such a factor.

The solution could perhaps be found in recent observations of SEVERNY who explained flares as a collapse of the plasma. Magnetographic observations showed that flares originate in a neutral region between the spots. The appearance of the flares seems to lead to a contraction of the surrounding fields. When the contraction of the field lines around the neutral region is sufficiently high, the magnetic forces which tend to contract the plasma increase more rapidly than the pressure; the plasma collapses. A contraction of 0.1 to 0.01 (corresponding with density variations of 10^3 to 10^6) can perhaps be reached. During the contraction shock waves are produced which may account for dynamic phenomena observed during and after the flare.

4. - The radioemission of flares.

There is so much diversity in the radio phenomena that accompany flares that it seems hopeless to systematize. Nevertheless, let us draw a picture of the «ideal», fully developed radio spectrum occurring together with flares and

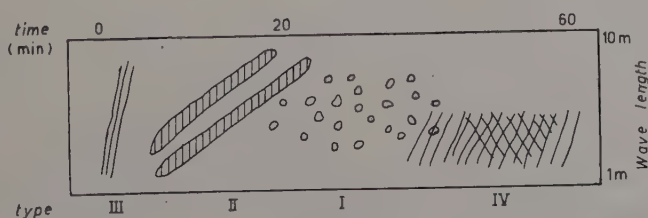


Fig. 1.

let us forget for this moment that this ideal case occurs in reality only for one case in 10^2 or 10^3 .

The succession in time is: III, V, II, I, IV. Some of the properties are listed below:

Type	Other design.	$\Delta f/\Delta t$ (MHz)	Polariz.	Bandwidth (MHz)	Time of occurrence	Remarks
III		$f/4.5$	mainly polariz.	$20 \div 40$	start of flare	often in groups
II	outburst	0.2		$20 \div 40$	main phase of flare	
I	stormburst	no	mainly polariz.	some MHz	end of flare	numerous dur- ing noise storm
IV	enhancement of base level		mainly polariz.	broad	end of flare	

The type V bursts are shortlived enhancements of the base level at long wavelengths; they occur after type III bursts.

Some problems, related to the emission of these types of radio transients will be discussed shortly.

The *stormbursts* do not show an appreciable frequency shift but might still be associated with motion of matter since it has been found that flares followed by noise storms are often followed by geomagnetic storms. An investigation of weak noise storms has shown that the stormbursts often occur in groups (only 10% occur singly). An average group consists of 2 to 3 strong members and a greater number of smaller ones; each group lasts for 10 seconds or less. These groups in turn cluster together; these supergroups last for 10 to 20 minutes. The time profiles are asymmetric; they rise rapidly and fall more slowly. In the spectrum they have a small bandwidth; the bandwidth and the duration are:

at 100 MHz	4 MHz	—
164 »	4 »	0.2 s
200 »	6 »	0.35 »
400 »	12 »	0.2 »

Remarkable is that $\Delta f/f$ is nearly constant as a function of frequency and that it is virtually equal to the width of a strictly monochromatic line widened by the thermal Doppler motions of an electron gas of 10^6 °K. This poses the problem of the contribution of thermal motions of a plasma to the profile of a burst emitted by plasma oscillations.

In any case, whatever the widening mechanism may be, this result shows that the density range $\Delta N_e/N_e$ that contributes to the stormburst emission is small as compared to $(\Delta f/f)^2 \approx 0.07$. Let us put $\Delta N_e/N_e = 0.02$, then with current coronal models one finds that the emitting clouds have diameters smaller than 200 to 600 km. A lower limit to the « cloud » diameter is found by assuming that a pip is emitted by an electron cloud oscillating in a strictly ordered way, and that the average kinetic energy of the cloud is transferred into oscillation energy; in that case the diameter is of the order of 10 cm.

The *type III bursts* are strongly asymmetric in time. At 200 MHz they fall into several groups with halfwidths ranging from 0.4 s to 1.5 s. The pips of longest duration are rare and occur only in the first part of a flare. If we assume that they are due to plasma oscillations, then these oscillations must decay exponentially by collisions, with $\lambda = 4.2 \cdot 10^3 N_e T^{-3/2}$. Assume further that N_e is determined by the plasma frequency, then T can be found. It appears to range between $2.6 \cdot 10^6$ and $7 \cdot 10^6$ °K. This shows that the pips occurring in the first phase of a flare are emitted by regions with temperatures of about $5 \cdot 10^6$ °K.

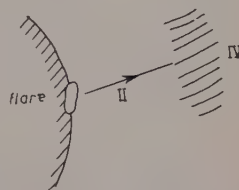


Fig. 2.

Still higher temperatures must occur in the regions emitting the *type IV bursts*. The phenomenon has been known for a long time to radioastronomers, who called it an « enhancement of the base level ». DENISSE and co-workers realized that one was dealing here with a particular kind of solar radio emission. The type IV bursts can be best observed when the flare is at the sun's limb. One sometimes observes that the flare is followed by a type II burst showing tangential motion away from the sun. Then a large spot is formed at some distance to the limb ($0.5 R_\odot$). This spot may last for an hour; it emits the continuous radiation that is now called a type IV burst. The emission can be explained as due to synchrotron radiation of relativistic electrons, by taking $N_e = 4 \cdot 10^{22}$, $E = 3$ MeV, $H = 1$ gauss. The observed duration of the type IV bursts (1 hour) is of the same order as the life times of electrons of 3 MeV in a region with an electron density of 10^8 cm^{-3} .

It is perhaps useful to summarize in this connection some other phenomena that point to high temperatures in the corona after a flare. These phenomena are observed at shorter wavelengths:

1) The 5694 \AA emission (Ca XV, 814 eV) occurs after flares in the corona; maximum intensity is reached half an hour after a flare.

2) Recent rocket observations of the X-ray radiation related to flares have shown, that the existence of a flare produces a hardening of the solar X-ray radiation. The quiet sun does not emit X-rays at wavelengths below 8 \AA , but during flares this limiting wavelength shifts towards shorter values to reach 1.5 \AA during the strongest flares. This indicates ionization temperatures of the order of $10^7 \text{ }^\circ\text{K}$. No X-ray measurements have as yet been made *after* flares but the observations that are now made from Sputnik III might throw more light on this problem.

3) Cosmic radiation bursts reach their maximum intensity after flares; the time differences are:

Flare of	Time difference
28- 2-1942	1 h
7- 3-1942	1
25- 7-1946	2.5
19-11-1949	0.5
23- 2-1956	0.2

It is by no means sure that this radiation is emitted by the same regions which emit the type IV bursts or that this radiation is really emitted after the flare, but the possibility should be kept open.

Dynamical Features of the Chromosphere.

C. DE JAGER

Sterrewacht Sonnenborgh - Utrecht

In this paper the chromosphere is treated primarily from the descriptive point of view. Some theories on the dynamics of the chromosphere are briefly mentioned, and a discussion of the energy balance of the chromosphere is included, but for a more detailed theoretical treatment reference is made to Dr. BIERMANN's lectures.

1. - Generalities.

The chromosphere is a sheet of plasma, 5000 to 10000 km thick, in which temperatures of 4000 to 40000 °K occur, enclosed between 1) a cool and denser, practically neutral gas (the photosphere), with at the surface a temperature of 4500 to 4600 °K, and rapidly increasing with depth, and 2) a hot tenuous plasma, the corona ($T=10^6$ °K). The thermal and mechanical properties of the

chromosphere are determined by 1) the incoming photospheric flux of radiation, but especially by 2) the mechanical energy flux coming from the deep photosphere; further, in its upper part by 3) the downward heat con-

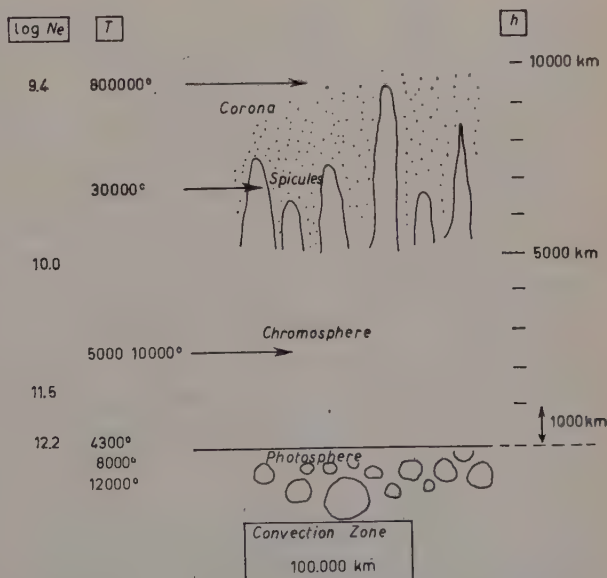


Fig. 1.

duction from the corona, while 4) its general structure is further determined by the gravitational field of the sun. 5) The rôle of magnetic fields in determining the chromospheric structure is still obscure (Fig. 1).

2. — Thermal properties.

That our knowledge of the chromosphere is relatively scanty results partly from the fact that its spectrum can only be observed well during a solar eclipse. The chromosphere emits a line spectrum; the continuous spectrum is faint. With a slitless spectrograph the so-called flash spectrum is obtained. It gives the integrated intensity E in the emission lines for chromospheric heights greater than the projected height of the moon's limb above that of the sun. The reduction of E to the surface brightness F is not difficult and demands only very precise observations. The step from F to the emission ε per element of volume presupposes knowledge of the relative variation of ε with height, while moreover the influence of self-absorption must be eliminated. If these steps have been made, then $\varepsilon = N_m A_{mn} h\nu_{mn}$, where N_m is the number of particles in the upper quantum state. Then, eventually, there remains the interpretation of N_m in terms of—say—electron temperatures and particle densities. The chromosphere is not in thermodynamic equilibrium, so Boltzmann's and Saha's laws cannot be applied and the detailed equilibrium has to be investigated between all atomic levels between which transitions are possible. The influence of collisions on this equilibrium has naturally to be taken into account as well as the influence of the radiation field, which consists of two parts: the external field, from the photosphere and corona, and the internal field, generated by the gas itself. Then, for each level the number of incoming transitions is put equal to the number of outgoing transitions, yielding N equations with N unknowns; N is the number of levels, incorporated in the computations; the unknowns are the populations of these N levels. Obviously the intensity and frequency distribution of the own chromospheric radiation field greatly depends on the solution of the system, so that the solution has to be obtained in several approximations. A fairly complete quantitative discussion has not yet been published but some approximated solutions have been obtained for hydrogen and helium. A very extended series of computations of the hydrogen equilibrium between temperatures of 6 000 °K to 100 000 °K has been started at the observatories of Uccle (Belgium) and Utrecht. Use is made of electronic computers and it is hoped that the results are available within one or two years.

The various temperature determinations for the chromosphere do not yet fully agree, but one of the results found with good certainty is, that in the region about 2 000 km above the photosphere, the helium and the hydrogen

data point to temperatures of $10\,000^\circ\text{K}$ or perhaps somewhat more, whereas data from metal lines and from the continuous spectrum indicate that the temperatures are between $4\,000$ and $7\,000^\circ\text{K}$. Optical data from other lines and referring to other heights complete this picture and the conclusion seems inevitable that the low chromosphere, at least above $1\,000$ km is inhomogeneous showing a temperature distribution of the two main kinds of elements as the curves *h* and *c* in Fig. 2.

For the moments we do not yet discuss the explanation of these two kinds of elements but it should be remarked that if the chromosphere is inhomogeneous and consists of two kinds of elements the elements can only exist at two well defined temperatures, for which a preliminary thermodynamic-equilibrium computation yielded $6\,000^\circ\text{K}$ and $20\,000^\circ\text{K}$. At other T values these elements are not stable: a slight increase

of the temperature, due to an injection of energy would correspond to a decrease of the emission of radiation, hence to a further increase of T , ..., etc., and mutatis mutandis for the reverse process. These two temperatures correspond fairly well with the average values of each of the curves *c* and *h* of Fig. 2.

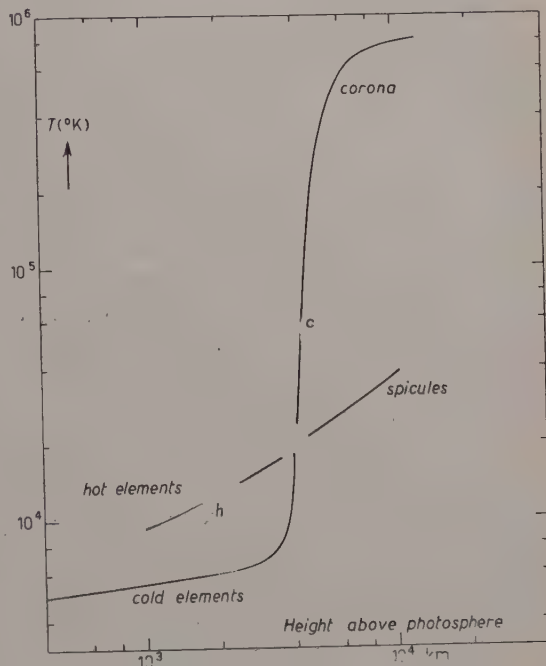


Fig. 2.

3. - Mechanical properties.

The temperature inhomogeneities, described above could only be discovered after a long and detailed treatment of chromospheric spectra, but a direct look at the chromosphere through a $\text{H}\alpha$ filter and through a quiet atmosphere shows immediately the inhomogeneities of the upper chromosphere. The spicules (Fig. 1) have diameters of 500 to $1\,000$ km, lifetimes of 3 to 5 min, and are mainly visible between $5\,000$ and 10^4 km above the photosphere. They penetrate from the chromosphere into the corona and are typical low-temperature

objects since they emit H α light: their temperatures seem to rise from about $2 \cdot 10^4$ °K at 5 000 km to about $5 \cdot 10^4$ °K at 10 000 km. They go upward with approximately constant velocity, then stop (abruptly?), 40% of them then fade away. About 25% of the descending ones first stay at maximum height for about one minute.

Two fundamental problems are, whether these high chromospheric inhomogeneities have perhaps to do with the inhomogeneities of the low chromosphere, and if so, with which of them they have to be associated. These problems can be solved by the investigation of spectroheliograms. Spectroheliograms are sharp monochromatic images of the sun. As a rule they are made in the light of Fraunhofer lines; since the absorption coefficients in these lines are great, a set of spectroheliograms, made in various lines or in various parts of the same line can yield pictures of the sun in various chromospheric levels, thus permitting to deduce a three-dimensional image of the chromosphere. Metal line spectroheliograms give information on the levels between 0 and 1 000 km; Ca⁺ lines show regions between 500 and 3 000 km; H α spectroheliograms go up to 5 000 km.

There is a wide and bewildering diversity between the aspects of different kinds of spectroheliograms but a closer investigation shows (Table I) that on all spectro- heliograms the following three main structures occur:

TABLE I.

Structure	Diameter or characteristic length	Life time	Doppler velocities
fine mottling	1 000 km	5 min	20 km/s ?
coarse mottling	5 000 ÷ 8 000 km	0.5 d (?)	
network	50 000 km	days (?)	0.14 to 1.0 km/s

These three structures can be seen nicely on a Ca⁺ spectroheliogram, but it is essential that they appear on all chromospheric pictures, but they may appear bright in one line and dark in another; their relative intensities differ from line to line and differ also between wing and centre of a line profile.

The fine mottles, which can be best seen in Ca⁺ occur also in H α but are only well visible in the line centre. They do occur in the wings but can hardly be discovered between the much intenser coarse structures. If the given average life times of the fine mottles is correct one is tempted to identify them with the spicules as seen from above. This identification then, leads to the following conclusions: *a*) the spicules occur only above the 1 500 km level, since fine mottles have not been observed on spectroheliograms referring to the low chromosphere; *b*) the hot elements of the low chromosphere are the basis of

the spicules, a conclusion which is based on the observed intensities of the fine mottles in different spectral lines.

The coarse mottling and the network, formed by these mottles are composed of fine mottles. They are related to upward and downward motions in the chromosphere. At the 4 000 km level (wings of H α) the coarse mottles descend with an average velocity of 1.1 km/s with respect to the mean level, and the regions between the mottles ascend with about half that velocity.

This velocity increases with height, as follows from the following Table II.

TABLE II.

Height above photosphere	Source	$\langle \xi^2 \rangle^{\frac{1}{2}}$
— 100 km	middle strong metal lines	0.16 km/s
+ 500 »	strong metal lines	0.4 »
2000 »	H β	0.6 »
4000 »	H α	1.1 »

The differences in brightness between the coarse mottles and their surroundings are perhaps due to a difference of about 200 °K in their excitation temperature; the mottles being hotter. An alternative possibility is that the microturbulence in the mottles is by about 5 km/s greater than in the surroundings.

4. — The chromospheric energy balance and the heating of the corona.

In Dr. BIERMANN's lecture it was shown that mechanical energy is transported through the lower chromosphere to be dissipated on the way and in the corona. If ξ_i is the average turbulent velocity component at a given height, the flux of mechanical energy is equal to $(\frac{1}{2}\rho\xi_i^2)c$, where c is the velocity of sound. So without dissipation of energy ξ_i should increase proportional to $(\rho c)^{-\frac{1}{2}}$, till $\xi_i \approx c$; at about that level energy dissipation would start at a much greater rate. The various observations of the turbulent velocities in the chromosphere show consistently that $\xi_i = 2.7$ km/s at $h = 0$; it increases with height till 10 km/s at 1500 km and 15 km/s between 3 000 and 4 000 km. So $\xi_i = c$ between 1 000 and 2 000 km and the question might be posed whether this is the reason that fine mottles are not visible on spectroheliograms referring to lower chromospheric heights. It is another confirmation of the viewpoint that the fine mottles are perhaps due to shock waves in the chromosphere, and thus have to be considered as the bases of the spicules.

In the table below, the mechanical energy flux is given, as computed with the given turbulent velocity components and with the known densities of the chromosphere. It is compared with the photospheric radiation flux, which is hardly absorbed. The other columns will be explained further in this section. The Table III gives log flux in $\text{erg cm}^{-2} \text{s}^{-1}$. The arrows show the direction in which the flux progresses.

Table III.

h (km)	Phot. rad. flux	Mechanical flux	Emission of rad.	Heat conduction
100	10.8	8.7	8.7	
1 000	10.8	7.1		
4 000	10.8	5.9 ↓	6.3	
Transition layer	10.8		5.4	4.6 ↑
Corona	10.8 ↓		4.5	— ↑

Although the mechanical flux (3rd column) is much less than the photospheric radiation flux, it is very important for the understanding of the chromospheric structures. In the fourth column the (roughly estimated) emission of radiation of the chromosphere is given. These values should be compared with those in the 3rd column. The agreement at 100 km is purely accidental: at that height a great part of the chromospheric radiation is due to photo-excitation and -ionization by photospheric light. That, however, at 4 000 km the mechanical flux and the line emission are about equal, shows that in the medium chromosphere about half of the mechanical flux serves for the heating of the chromosphere; the other half is transported further upward and will be dissipated in higher levels. (The lines emitted at the 4 000 km level are mainly excited by collisions).

At about 5 000 km the chromospheric temperature suddenly increases to very high values. This can be understood. The dissipation of energy may be assumed to take place in an interval about equal to the scale height; in the medium chromosphere the scale height is about 1 000 km, hence the dissipation per cm^3 is about $10^{-2} \text{ erg cm}^{-3} \text{s}^{-1}$. On the other hand the gas radiates away $1.8 \cdot 10^{-21} N_e T^{-\frac{1}{2}} \text{ erg cm}^{-3} \text{s}^{-1}$ (mainly free-free and free-bound transitions of hydrogen and helium), and for an assumed temperature of $10^4 \text{ }^\circ\text{K}$ (not very essential) this value decreases below that of the dissipated energy for $\log N_e = 9.7$. This value of the electron density occurs slightly above 4 000 km. So, at about that height a steep increase of temperature must set in.

Before considering in detail the $T(h)$ relation above 4000 km, a few words on the mechanisms of energy transport and dissipation in the low and medium chromosphere. In the low chromosphere we have:

a) Transport by *sound waves*: up to about 1500 km.

Dissipation may occur it two ways:

b) Dissipation by *shock waves*: this mechanism seems to start already at about 1500 km and produces the fine mottling and the spicules.

c) Dissipation by *Alfvén waves*. In a half ionized gas energy will be dissipated by the drag of the oscillating plasma on the neutral gas. PIDDINGTON estimated that this mechanism would be sufficiently efficient to dissipate a flux of $10^6 \text{ erg cm}^{-2} \text{ s}^{-1}$. This mechanism can be efficient in the cool elements near 4000 km, where these elements are about half ionized.

5. - The transition layer between chromosphere and corona.

For the *heating* of the corona a flux of $10^6 \text{ erg cm}^{-2} \text{ s}^{-1}$ is available, but the energy *losses* in the form of radiation (mainly metal line radiation below 100 Å) are smaller: only $10^{4.5} \text{ erg cm}^{-2} \text{ s}^{-1}$. So the greater part of the incoming flux must be lost in another way. There are two mechanisms:

A part of the energy is lost by the evaporation of high energy particles from the corona and leads to a continuous flux of particles from the sun. As PICKELNER showed, if the average temperature of the corona would rise to above $1.6 \cdot 10^6 \text{ }^\circ\text{K}$, the corona would be lost fairly rapidly by evaporation. The average temperature is lower, somewhat below $10^6 \text{ }^\circ\text{K}$, but also at this temperature there will be a continuous loss.

The other part of the energy is conducted backward to the chromosphere. The $T(h)$ relation in the transition region is mainly determined by the conduction equation

$$(1) \quad \pi F_c = K dh/dT.$$

In this transition region the backward conducted energy is finally lost by the emission of ultraviolet line radiations.

The $T(h)$ relation in the transition region can be determined observationally by means of radio-observations of the quiet sun. Such observations show that the surface brightness of the disk centre, expressed in temperatures, increases from 5600 °K at a wavelength of 4 mm to nearly $10^6 \text{ }^\circ\text{K}$ at 10 m. Since the cm wave radiation comes mainly from the chromosphere and the metre waves come from the corona, this shows the increase in temperature between these two regions. The centre-limb intensity distribution shows that

at 4 mm the solar intensity profile is virtually rectangular with no brightness difference between centre and limb; at 1 to 3 cm a limb brightening becomes perceptible which becomes very important (2 to 3 times the central disk intensity) at 10 to 20 cm. For longer wavelengths the limb brightening decreases again, to shift somewhat towards the disk centre at metre waves. This limb brightening is essentially an equatorial brightening, at the poles it is absent, indicating different $T(h)$ relations for the polar and equatorial parts of the corona.

On the basis of a $T(h)$ curve, recently derived from such radio-data is possible to determine the conductive energy flux πF_c occurring in the equation (1). This flux appears to be of the order $10^{5.6}$ erg cm⁻² s⁻¹ in the upper part of the transition region, hence, is only slightly smaller than the mechanical flux fed into the corona.

The last problem to be treated here, is what happens to this energy. It seems probable that this energy is emitted in the ultra violet. Rocket spectra of the sun, obtained at altitudes above 100 km show a wealth of emission lines in the range (900÷1700) Å. It is mostly lines of high ionization potential; the electron temperatures necessary to produce their state of ionization range between 8000 °K (Si I) to 140000 °K (O VI). The strongest line, Ly α , is emitted by regions with an electron temperature of about 40000 °K. The total energy emitted in these lines will be only slightly greater than the energy emitted in Ly α , and will be about $10^{5.4}$ erg cm⁻² s⁻¹, hence of the same order as the energy conducted backward. The fluxes computed in this section are included in the Table III.

Solar Disturbances Producing Type II Radio Bursts.

R. G. GIOVANELLI

*Commonwealth Scientific Industrial Research Organization
Division of Physics - Sydney*

Solar radio bursts of type II are characterized by a steady decrease in frequency over a period of a few minutes [1]. This has generally been interpreted as due to the passage of an ejected particle stream through the corona at a velocity of the order of 500 km/s, exciting plasma oscillations whose frequency is proportional to $N_e^{\frac{1}{2}}$.

By combining the measured frequency (and so the electron concentration) with the coronal electron-height distribution given by the Allen-Baumbach formula, the observed frequency time curve yields the height-time curve and thus the velocity.

The situation is somewhat complicated by the frequent observation of a pair of frequencies, presumably the plasma frequency and its second harmonic, in type II bursts. On theoretical grounds it is expected that in the case of a spherically symmetrical corona these two frequencies will be observed only when the source is within about 20° of the centre of the disk; for if the source occurs beyond this distance, rays emitted at the fundamental plasma frequency will be so refracted in the corona that they will not escape towards the earth [2].

Type II bursts are relatively infrequent though it is known that they are associated with chromospheric flares. During 1956-1957, 15 type II bursts were observed by WILD and his collaborators at days to Dapto during times of good solar observation in Sydney. Comparison of records yields the results shown in Table I [3].

In all cases but one, some form of dark hydrogen activity or ejected matter was seen: the exception was a diffusely expanding flare of a type also known to eject particle streams.

The type II bursts associated with limb events showed no harmonic structure, and comparisons have been made with the observed prominence

height-time plots on the assumption that the emission has been: 1) at the fundamental plasma frequency, and 2) at the second harmonic.

TABLE I.

Cause	Number of case
Ejected prominence at limb	2
Surge at limb	2
Disappearing filament (followed by flares) on disk	2
Flare on disk.	7
Probably flare	1
Probably ejected prominence.	1
<i>Total</i>	15

The results have been inconclusive, two events favouring the second harmonic, three the fundamental. If, as expected, the emitted radiation is in fact the second harmonic, this necessitates at least one of the following additional assumptions for the three exceptional cases:

a) the ejected particle stream extended beyond the region in which the prominence was observed; this is quite possible, and requires testing with longer exposure photographs in future observations;

b) a lower electron density than given by the Allen-Baumbach formula;

c) departures from spherical symmetry; this is by no means unexpected since the corona shows a strong structure of bright streamers and dark lanes; and therefore possesses considerable density variations. Making use of some additional data, it has been found that in general, both fundamental and second harmonics are observed in events whose bases lie at distances ≤ 0.8 of the solar radius from the sun's centre; one harmonic alone, presumably the second, is found in events originating further from the centre of the disk; this can be explained only by departures from spherical symmetry.

The limb prominence observations yield good minimum estimates of velocities along the trajectories. In the five cases available these were 350, 500, ≥ 200 , 650 and 250 km/s. These all exceed the velocity of sound in ionized hydrogen at 10^6 °K, which is about 160 km/s. It is also interesting that two of the five limb events were surges in the same activity region on a day when a number of other surges of velocity below the speed of sound failed to stimulate type II bursts.

In summary 1) it can be asserted that particle streams of different origin

can stimulate the emission of type II bursts; 2) in all limb events the streams have had velocities exceeding that of the sound in the corona; 3) the fundamental plasma frequency escapes from much nearer the limb than expected on the basis of a spherically symmetrical corona.

REFERENCES

- [1] J. P. WILD: *Aust. Journ. Sci. Res.*, A **3**, 399 (1950).
- [2] J. P. WILD, J. D. MURRAY and W. C. ROVE: *Aust. Journ. Phys.*, **1**, 439 (1954).
- [3] R. G. GIOVANELLI and J. A. ROBERTS: *Aust. Journ. Phys.*, **11**, 353 (1958).

Flare Surges, Puffs and Type III Bursts.

R. G. GIOVANELLI

*Commonwealth Scientific Industrial Research Organization
Division of Physics - Sydney*

1. - Flare surges.

During some flares, dark patches of hydrogen can be observed ejected from the same activity region with velocities of the order of 50 km/s or more. These are known as surges, and at the limb may be traced outwards for perhaps 10^5 km or more. Questions arise as to their mode of origin, direction of motion, and physical conditions such as T_e and density.

1.1. *Relationship between flare and surge* [1]. - Cinematograph studies of flare surges using an H α filter show clearly that the surge comes out of the flare region itself, and not from some other part of the same spot group. Usually the surge can be seen on the disk starting either in contact with or even superimposed on the flare; sometimes there is a gap between flare and surge, though the surge moves away from the flare (Fig. 1). Nevertheless, the surge does not usually move radially away from the centre of the flare; it may travel tangentially. It is found, in fact, that the directions of surges, projected on the disk, are initially almost radially away from the nearest major sunspot. The surge probably lies in a vertical plane containing the local magnetic field direction. However, available observations do not show the line of sight component of the surge velocity, so that we do not know whether a surge follows lines of force exactly.

About one flare in five is associated with a dark surge on the disk. There is no well established connection between the size of a flare and its ability to produce a surge, and in fact the very tiniest flares, of area $20 \cdot 10^{-6}$ of the sun's hemisphere, are about as efficient as the largest.

In many cases the first traced of a surge appears to be the diffuse bright expansion of the flare; this can be detected in 80% of events where the flare area exceeds $40 \cdot 10^{-6}$ of the sun's hemisphere, and therefore probably occurs

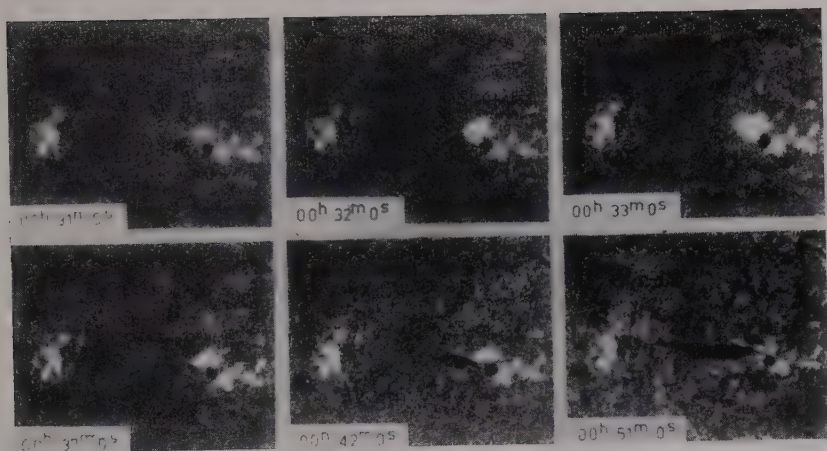


Fig. 1. — Flare-surge of 4-7-1957. Between 0032 and 0033 the flare showed a sudden diffuse expansion, which was followed by the ejection of a dark surge away from the neighbouring sunspot; this is clearly visible on the photographs at 0042 and 0051.

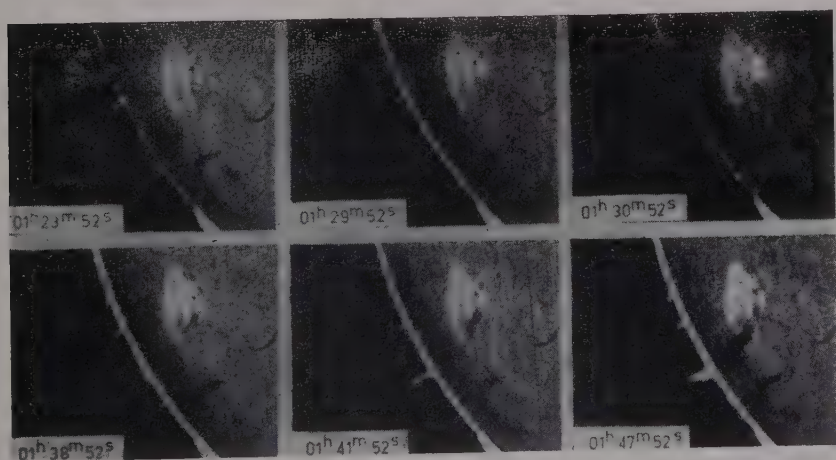


Fig. 2. — Flare-surge of 18-5-1956. This flare expanded suddenly between 0129 and 0130. A dark surge could be seen in the same position at 0138. In the above photographs the link has been given an enhanced exposure with respect to the disk, and the bright spike marking the trajectory of the particle streams emitted by the flare, and visible on the photographs at 0141 and 0147, was in reality very faint. The hemisphere can be seen unobstructed between the spike and the dark surge showing that the outer parts of the particle stream are highly transparent.

in all flare surges. As a rule, the diffusely expanded part of the flare contracts or disappears, and the dark surge follows soon afterwards.

Study of events on the disk and at the limb shows that the expansion of the flare occurs at the initial stages of ejection of a particle stream. The bright ejection fades and disappears because it is then highly transparent, but the invisible stream continues outwards, and can be detected against the black sky background if it crosses the limb (Fig. 2). In the meantime, further back along the particle stream, an opaque region develops and moves outwards along the stream, this being the customary dark surge.

1.2. *Physical conditions in surges.* — The physical explanation of these changes in appearance is as follows. The transparency of the stream shortly after ejection is due to the small number of neutral atoms present, presumably because the degree of ionization is high; and this requires a high initial temperature, probably in excess of 10^4 °K, but somewhat uncertain as there is inadequate knowledge of the density. The development of an opacity at any point in this stream indicates an increase in the number of 2-quantum atoms present, and this implies an increase in the neutral atom concentration. But theory and observation both show that surges expand during ejection, whence the neutral atom concentration increases only if T_e falls. So T_e must be falling where H α opacities are developing.

On the other hand, there are a few instances where part of the flare is itself ejected, severing contact with the main bulk of the flare. One of these ejections occurred at a velocity of 350 km/s, and yet increased in brightness during flight. This necessitates an increase in temperature so that, in some cases at least, a heating mechanism operates after ejection.

2. — Puffs and type III bursts.

In a type III burst [2] the frequency decreases rapidly in a few seconds, the accepted cause being a disturbance passing through the solar corona at a velocity of the order of $c/10$.

LOUGHHEAD, ROBERTS and McCABE [3] found that (60÷70)% of type III bursts occurred during the lifetimes of flares of apparent area exceeding about $20 \cdot 10^{-6}$ of the sun's hemisphere, but that rather less than one flare in four is associated with a type III burst. This low figure indicates a difference in degree or type between various flares. But as over $\frac{2}{3}$ of the bursts are associated with tiny flares of apparent area below $40 \cdot 10^{-6}$ of the sun's hemisphere, flare size alone is not the determining factor.

Surges occur about as frequently with flares as do type III bursts; about one flare in 4 or 5 produces a surge. In 48 flare surges, type III bursts were

found during 29% of the flares, whereas they occurred during only 18% of 246 flares not observed to be accompanied by surges. This increase is, however, not statistically significant.

Some flare surges appear to be of an explosive character. During a minute or so the flare may expand rapidly, ejecting a particle stream as explained earlier. Usually, but not always, this expansion or «puff» occurs at the out-break of the flare. In other flare surges the initial bright expansion is much more diffuse and indefinite, and these are not included here as «puffs». Its violent and sudden nature suggests that a puff is the indentifiable flare characteristic most likely to be associated with type III bursts. A short list of flares showing clear, indisputable puffs has been prepared and compared with times of type III bursts. The following Table I shows the numbers of puffs with bursts occurring within 2 minutes of the time of the puff.

TABLE I.

Flare area ($\cdot 10^{-6}$ hemisphere)	0—40	> 40	Total
Number of flare puffs	14	13	27
Puffs with type III bursts	11	7	18

Two-thirds of the puffs are associated with type III bursts, a result of high statistical significance. No significance can be attached to the apparent decrease in frequency of association as the flare area increases.

With one exception, all the above flares produced dark surges on the disk. Thus the puffs produce two types of ejection: one a relatively low speed particle stream at a velocity of the order of 50 km/s or more, the other a high speed disturbance with a velocity of the order of $c/10$.

It is by no means clear whether puffs are the only type of flare which can excite type III bursts; for the majority of flares associated with these bursts are too small to be resolved properly on available records.

REFERENCES

- [1] R. G. GIOVANELLI and M. K. McCABE: *Aust. Journ. Phys.*, **11**, 353 (1958).
- [2] J. P. WILD, J. A. ROBERTS and J. D. MURRAY: *Nature*, **173**, 532 (1954).
- [3] R. E. LOUGHHEAD, J. A. ROBERTS and M. K. McCABE: *Aust. Journ. Phys.*, **10**, 483 (1957).

The Observability of Hydromagnetic Phenomena on the Sun.

K. O. KIEPENHEUER

Fraunhofer Institut, Freiburg i. Br.

1. - Introduction.

One is rather sure today, that most of the variable phenomena observable on the sun's surface are influenced by magnetic fields. For this reason we might call them all hydromagnetic phenomena.

Our knowledge about these phenomena is based exclusively on what we can see or measure by means of telescopes in the optical and radio range. It is the subject of this lecture to give you an idea of the accuracy of observations and of their more or less fundamental limitations which are brought in by our own atmosphere. If we want to deduce the physical properties of the outer layers of the sun, which we can reach optically, such as density, temperature, turbulent velocity and magnetic field, we have first to obtain a spectrum of this very part of the solar atmosphere, which we want to study. Until recently the observing programs of this kind were mostly based on the assumption, that the sun's atmosphere is quite homogeneous and therefore a spectrum taken from a region of say 10 000 km in diameter will represent reasonably the state of things in this part of the sun. But more and more it is found by the observers, almost in all layers of the solar atmosphere, that there is no homogeneous or even smooth distribution of density, temperature etc. Instead a kind of fibrous structure is found, the dimension of which is of the order of the one known since very long in the photosphere called granulation. To obtain reliable information about the nature of these structures—which altogether build up the solar atmosphere—we have to get spectra of individual structures, the dimensions of which often are only of the order of 1" or about 750 km. In this way the observation of solar hydromagnetic phenomena will depend and will be disturbed strongly by seeing conditions, which unfortunately at day time are much worse than at night, because of the sun's heating effect on our atmosphere. In fact we reach at day time on the average only 1/10 of the resolving power obtained in stellar work at night.

Before discussing the effect of seeing on the observation of the different solar phenomena, here some more general informations about these limitations of solar work.

Seeing (Fig. 1). A good telescope of about 10 cm aperture resolves theoretically about 1" of arc, an objective of 20 cm should give 0".5. However because of scintillation this theoretical resolution will be reached in solar work only during a very small fraction of the available observing time. Even on a well sited observatory there will be only minutes per day or per week, which permit to photograph details of 1" or to follow such details over more than a few seconds of time.

It is noteworthy in this connection that (Figs. 2a, 2b) the best photographs of solar granulation obtained by JANSSEN [1] in 1885 at Meudon are still the best ones. Their resolution is of the order of 0".7. Some progress has been made recently by several workers in France, England and the States by photographing the sun from unmanned balloons some 20 or 30 km above the ground [2]. They show a somewhat better resolution. But it is quite clear that it will be extremely difficult to do basic spectroscopic work from such a ballon. The dimensions of the spectrograph and the need to hold the sun's image on the slit with an accuracy of the order of 1" during several seconds of time at least will be almost prohibitive. The same will be true for the use of artificial satellites in this connection.

To a certain, but rather small extent there is some hope to weaken the effect of scintillation by using photoelectric guiding of the telescope. The time constant of such a device has to be however very small, of the order 0.1 second or less. Such methods can be applied only to small regions of the solar disk.

2. - Measurements of magnetic fields.

Only the Zeeman effect of certain suitable Fraunhofer lines has shown to give reliable results. For the field of sunspots, which are of the order of 500 to 3 000 gauss visual and photographic methods have been in use for almost 50 years now. They are based on the line displacement, which is of the order

$$\Delta\lambda \sim 4.7 \cdot 10^{-5} H \lambda^2 \sim 1.3 \cdot 10^{-5} H \text{ (Å)}$$

(for the green iron line λ 5250) and which allows to measure the spot fields with an accuracy of about ± 100 gauss. This corresponds roughly to 1/25 of the line width.

Much more sensitive methods have been developped during recent years

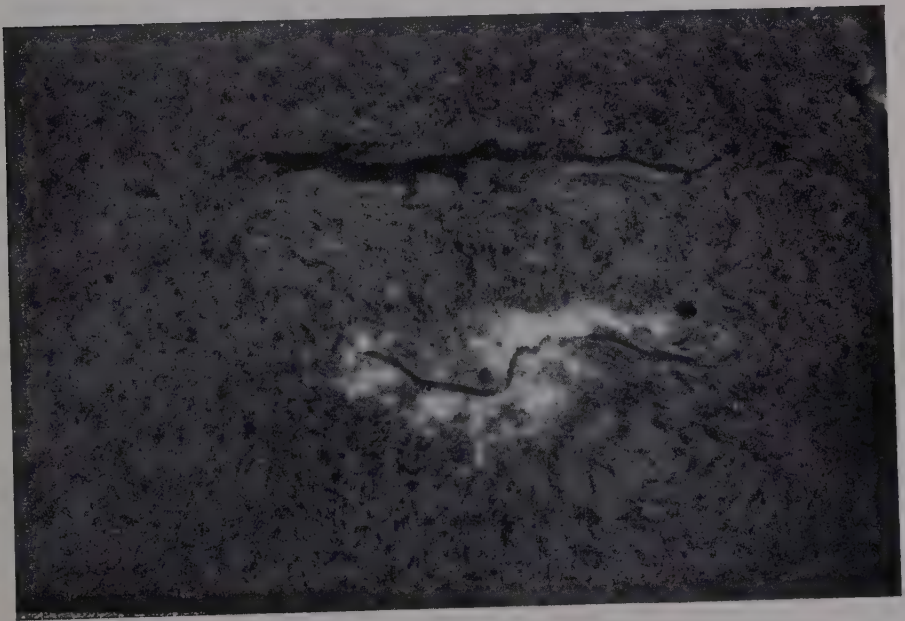
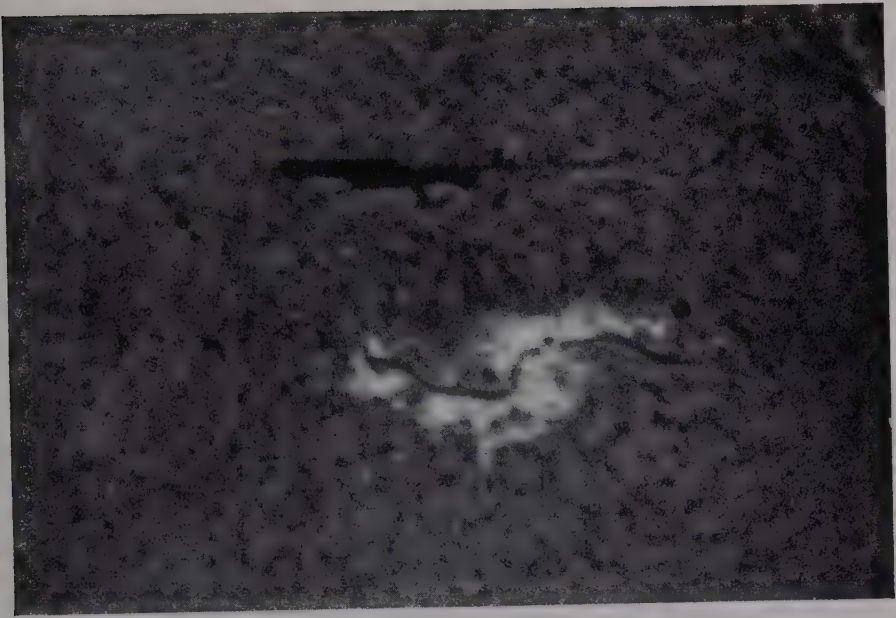


Fig. 1. — The influence of seeing on the visibility of chromospheric structures: H α -filtergrams taken with bad seeing (top) and good seeing (below). The smallest details detectable are in the upper picture of the order of 4000 km, in the lower of 1500 km.

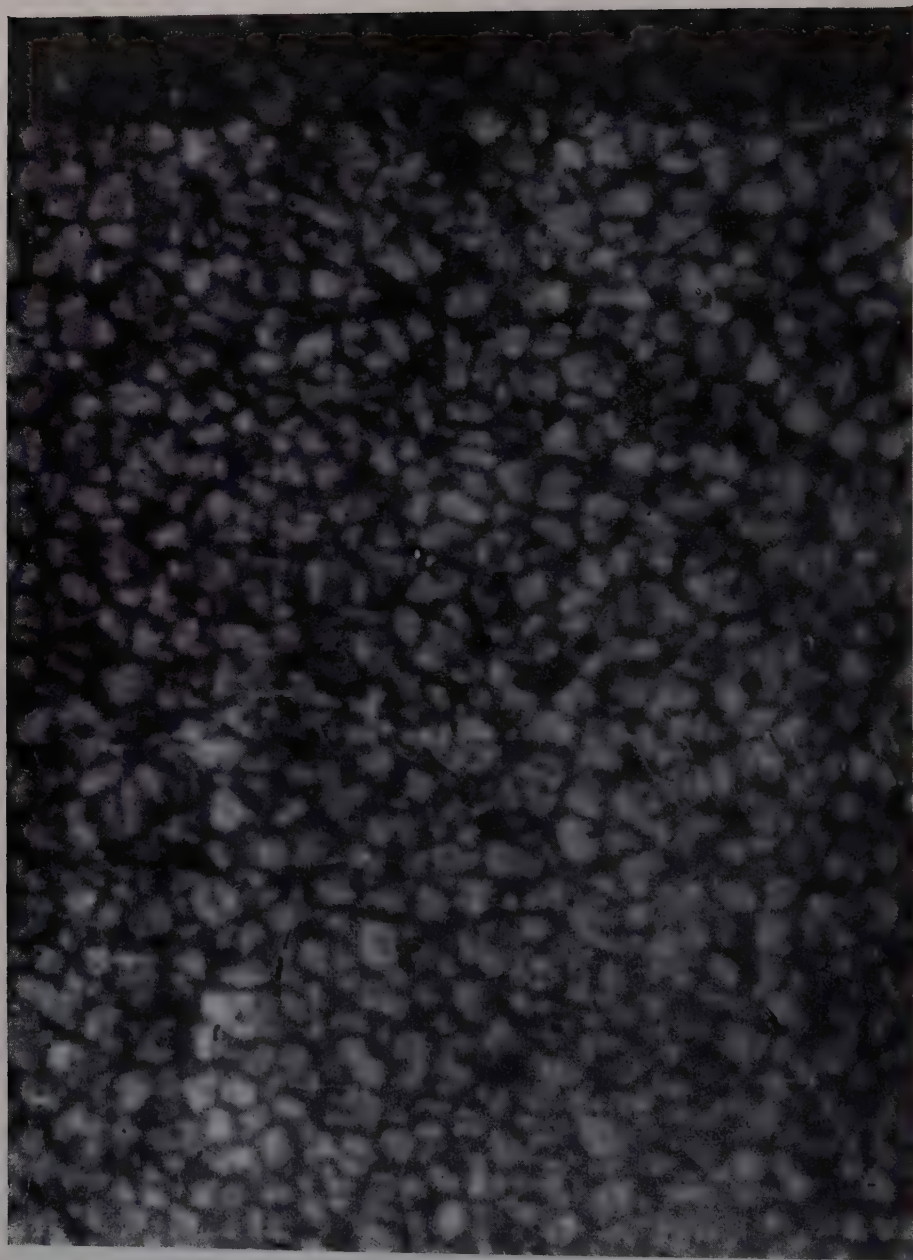


Fig. 2a. — Solar granulation. JANSSEN's best photo (1885).

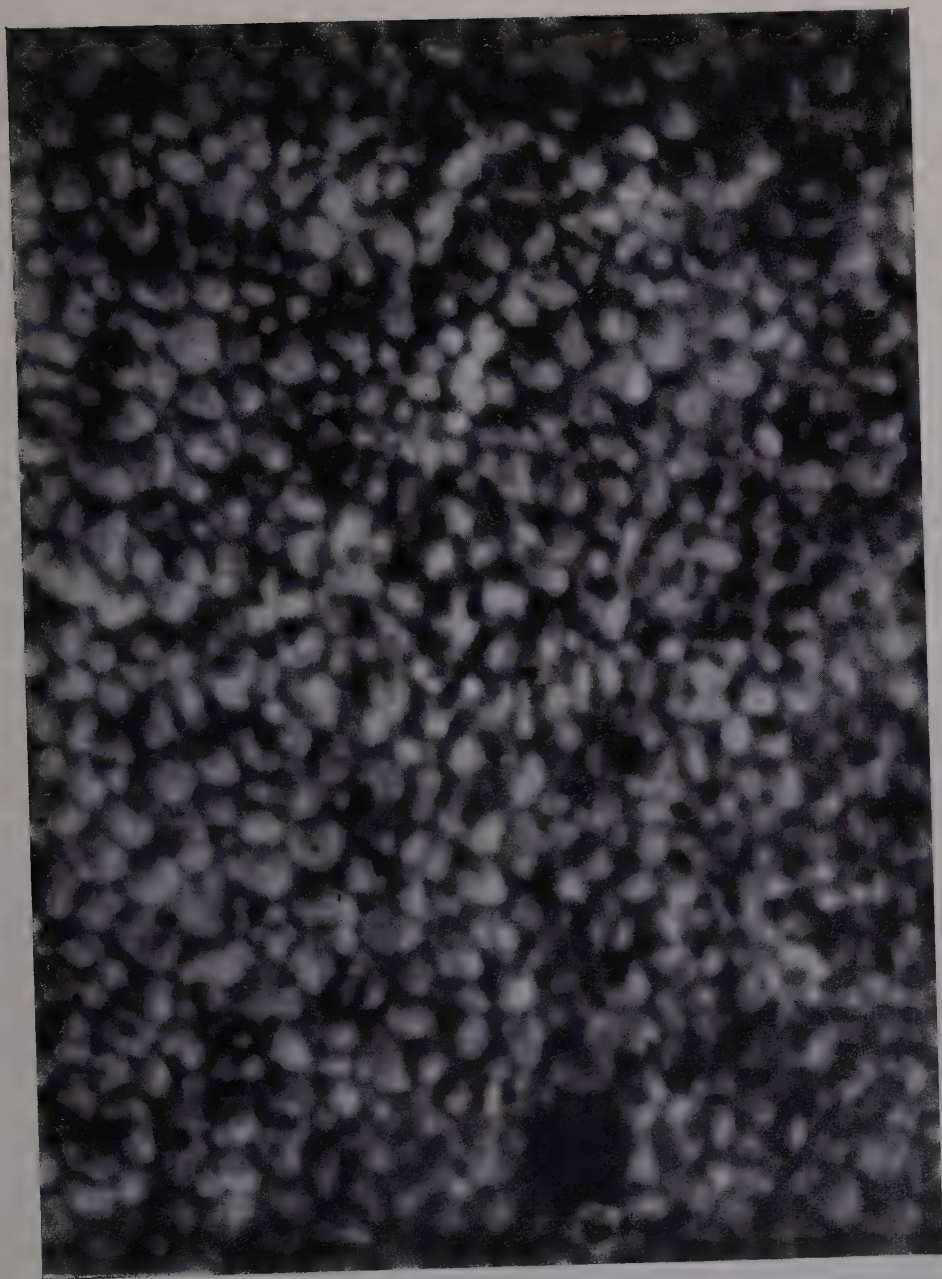


Fig. 2b. - Solar granulation. Photograph taken from an unmanned balloon at about 30 km height.

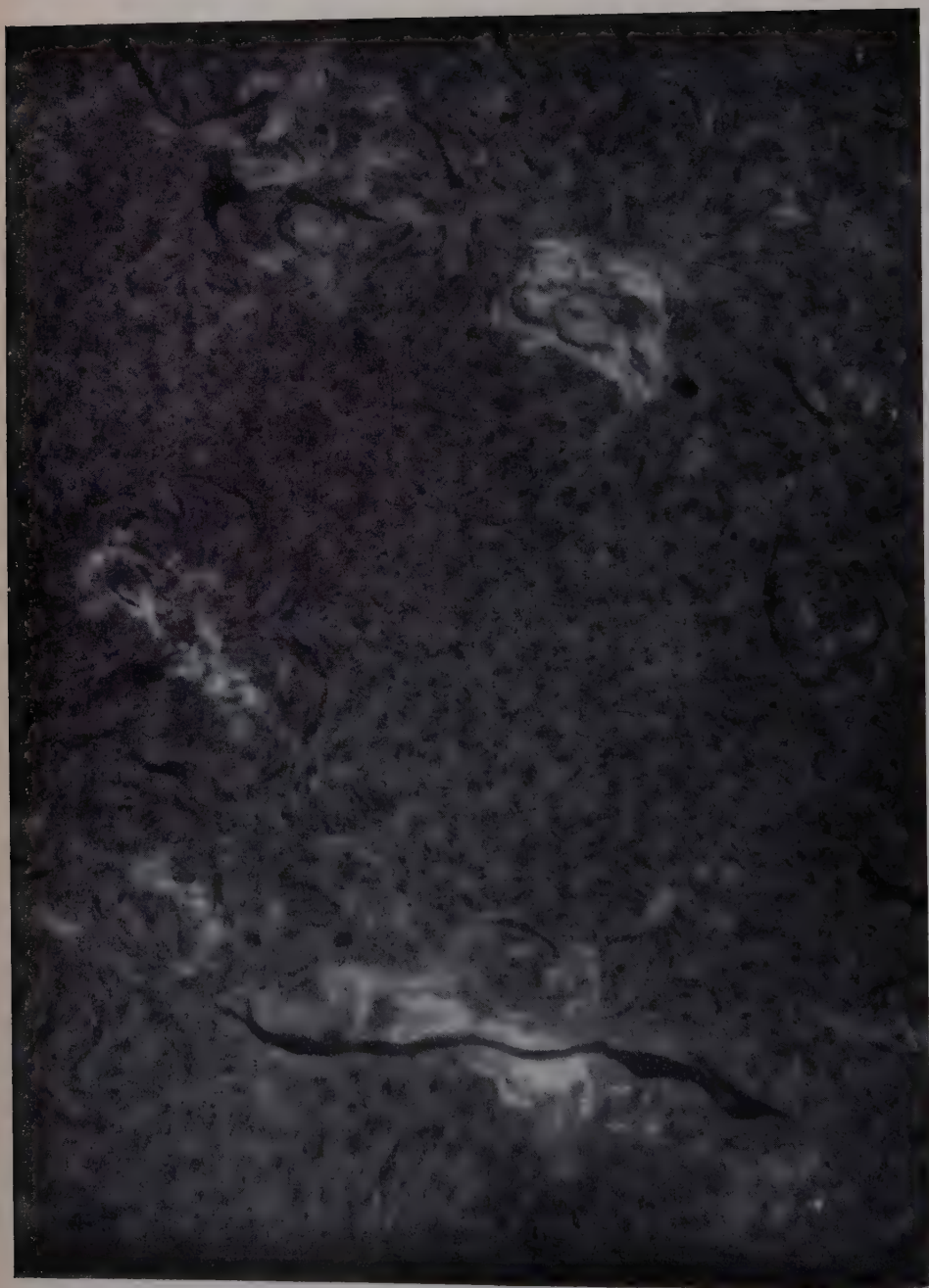


Fig. 3. — Chromospheric structures in an active region. It can be seen very well how the granular structure away from sunspots (center of image) is transformed into a characteristic pattern in the vicinity of sunspot groups (upper left, lower right). H α -filtergram of the Fraunhofer Institut (Observatory Anacapri) November 13, 1957).

by using photoelectric procedures [3]. They do measure more the polarization arising in the wings of a magnetic line, than its displacement. This polarization p —in the case of the longitudinal effect the two wings show opposite circular polarization—will be of the order

$$p = (1 - R)^2 \frac{\Delta\lambda}{w},$$

where $\Delta\lambda$ is the Zeeman displacement, R the residual intensity in the line and w its width. Again for the iron line $\lambda 5250$ one obtains numerically

$$p \sim 3 \cdot 10^{-4} H,$$

which amounts to about 3‰ for a field of 10 gauss. The smallest field still detectable will therefore be reached, when the random fluctuations of the photocurrent within the time interval t will be of the order $\Delta E/E$. These fluctuations amount at least to \sqrt{N}/N , N being the total number of photoelectrons available within the time t . In this way the smallest detectable field will depend on the amount of light which is available in the wing of the line and on the quantum efficiency η of the multipliers used.

One obtains

$$H_{\min} \approx \frac{w}{(1 - R)^2} \frac{1}{\sqrt{\eta} \frac{dt}{D}},$$

where d is the diameter of the spot which scans the solar surface and D is the diameter of the objective of the telescope. The result is that for a scanning spot of about 1" (geocentric) in diameter and an objective of 20 cm only a field of 10 to 20 gauss can be detected, when using a time constant of 1 s. The use of a bigger objective would not help, because then the definition of the sun's image would suffer because of seeing. The measurement of the *transverse* Zeeman effect is unfortunately still less good. So we have to state in a general way that there are set quite serious limitations to the measurement of magnetic fields on the sun, which let it seem rather improbable that we will be able to detect magnetic fields within such small structures as photospheric granules, small chromospheric filaments and prominence streamers.

All results hitherto obtained on magnetic fields outside sunspots relate to dimensions of the scanning spot which are large as compared to a granulum. The famous magnetograms of H. D. BABCOCK [3] are recorded with about 70", some russian magnetograms with 10" to 20". They all are smoothing out the fine details of the solar magnetic field.

Recently also some work has been started independently in Russia and Australia to measure the Zeeman effect of $H\alpha$ and K, both lines being formed in the chromosphere. From such measurements the magnetic field in the chromosphere will be obtained.

3. - Review of solar phenomena.

In the following résumé only a few remarks about solar phenomena will be made. Mostly I will deal with the limitations of observation. Some new observations still to be carried out will be mentioned.

Photospheric granulation. As a consequence of the bad visibility and the relative short life time of single solar granules but also because of missing efforts we have very little good information about the life time of granules, its variations close to sunspots and in undisturbed regions of the sun. We know very little about the structure of a single granule and nothing about its internal magnetic field. Very little is known also about the relations between the photospheric structures and these of the overlaying chromosphere.

Sunspots. Apart from some important studies of spot spectra very little has been done during the last 50 years to obtain better information of the visible structure of the sunspot, and this in spite of the fact that almost all observatories have equipment to do this kind of work. The following information should have priority.

How is a young spot developping in an undisturbed region of granulation?

How develops the magnetic field of such a small spot?

How the penumbra of a spot is formed and how does it interact with the surrounding granulation and the chromospheric structures above?

How does the spot field penetrate into the surrounding photosphere and chromosphere?

What is the correct shape (fine structure) of the umbral and penumbral field of the sunspot and how does it vary with time?

Especially the last two questions could be answered by using modern photo-electric equipment, which has proved already very valuable when measuring small fields.

Chromospheric structures (Fig. 3). since a few years we have a wealth of detailed direct and also spectroscopic information about the great variety of phenomena occuring in the solar chromosphere, as there are: small long lived dark features like cypress trees, narrowing toward their tops (2 000 km in diameter and about 4 000 km high); spicules which are bright spikes shooting outward, very well to be seen on the sun's limb, hardly detectable on the sun's surface.

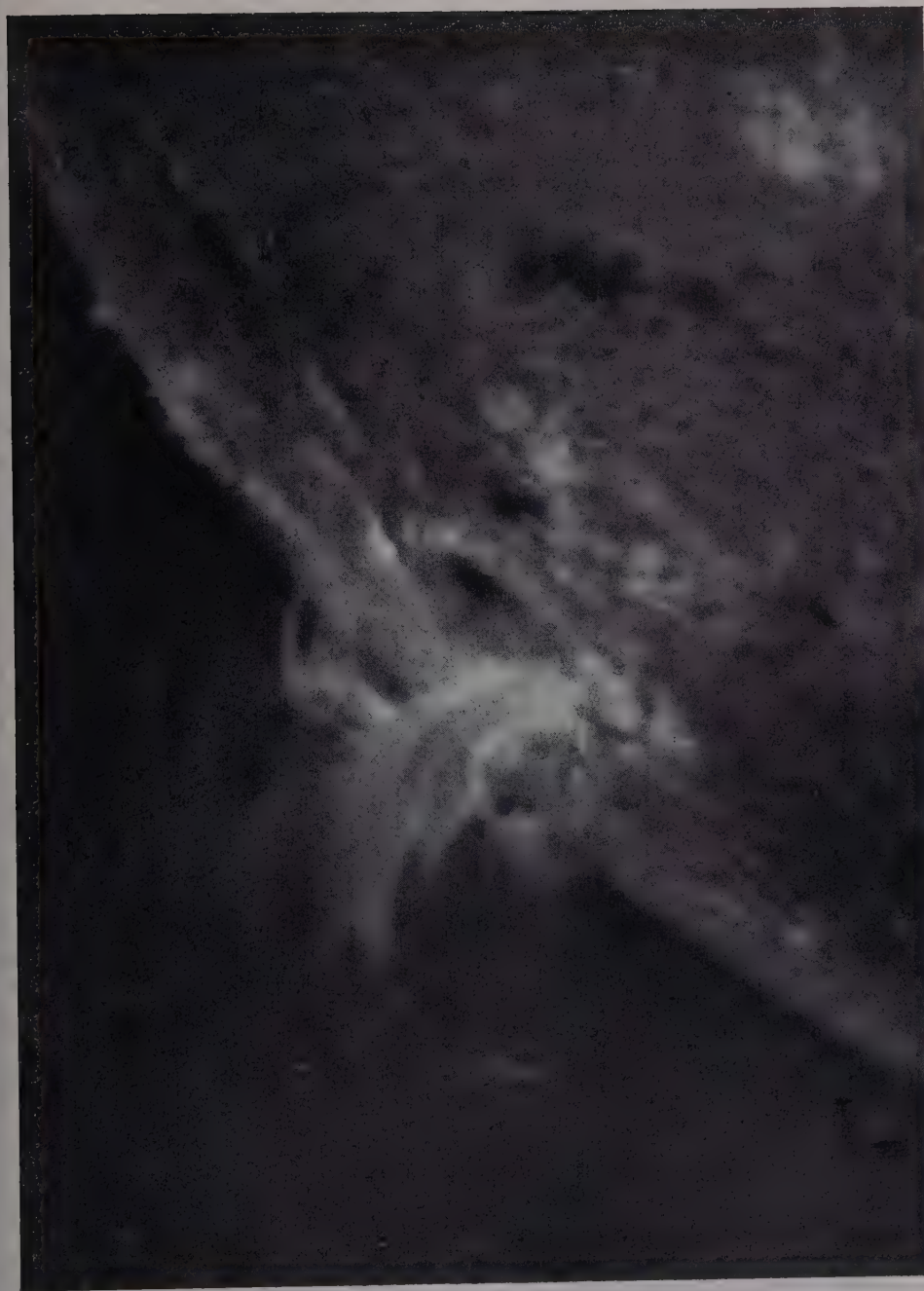


Fig. 4. — Ejection of chromospheric matter from the sun's limb. The flare which occurred simultaneously is well to be seen on the disk. Flare and flare surges form one complex phenomenon. $H\alpha$ -filtergram Fraunhofer Institut (Observatory Anacapri, May 15, 1957).

Coming closer to a sunspot group, in a «center of activity» the above cypresses become very much lengthened forming altogether a characteristic pattern around the sunspots, which sometime shows a pronounced vortical structure. In addition to this structure very long threads appear, connecting often the main spots of a bipolar group. All over the active region there are scattered like flowers in a lake little bright spots of faculae, which have a long life time. In the very vicinity of sunspots the faculae (also called plages) have more a surface structure forming bright areas of dimension of the order of $40\,000 \times 20\,000 \text{ km}^2$. Also the flares are part of this picture.

It is quite possible to obtain good single pictures and also high quality spectrograms of these phenomena. But it still needs a great effort to obtain complete series of such observations, which tell us something about their history. We still are especially far from being able to measure the magnetic field within these structures. And we are rather certain, that in the active areas of the sun's surface magnetic fields are determining forms and configurations. More effort should be devoted also to the study of the relations between the photospheric and the chromospheric phenomena. Interference filters with very narrow bands ($\Delta\lambda < 0.2 \text{ \AA}$) as being developed in Sydney will be of great help in this field of research.

Flares (Fig. 4). Flares are the most violent manifestations of solar activity. They are easy to observe, but they come unexpected in time and in location, develop often within the fraction of a minute. To get a complete record of a bigger flare as it might occur once a month, one has to record photographically continuously for a very long time, in order to get a significant record of the few important minutes. This is the main difficulty of the study of flares. Another problem is, that many things have to be observed simultaneously. The region of the sun, where a flare is to be expected has to be scanned therefore with the spectrograph. This means that a very large amount of recording has to be done. Almost nothing is known about the changes of magnetic field in or underneath a flare also the study of the relations between a flare and the underlying photosphere has not been done, mostly because for seeing difficulties. So in spite of the fact, that the routine observation and classification of flares and their association with sunspots is well developed, we have very little observational information about the physical properties of the central part of the flare and of the changes in or outside of it which produce it.

The ejection of chromospheric or photospheric matter, called surge, which often occurs close to a flare can be observed very well in H α and also sometime in integrated light. But the observations are not yet detailed enough as to show from where exactly and how the surge material is thrown out.

Prominences, filaments and corona. Prominences and filaments only occur in the corona and are even born mostly there. They should be observed there-

fore—at least at the sun's limb—together with the corona. The observation of the corona away from the sun's limb however is very difficult and is still the privilege of two large coronagraphs only (Sacramento Peak and Pic-du-Midi).

It would be very important also to obtain direct information about the magnetic field of prominences. At least in the vicinity of sunspots, the Zeeman effect of $H\alpha$ should be measurable in a prominence spectrum. And again, changes and accelerations in prominences and in the corona as documented so beautifully in recent films from Sacramento Peak should be traced simultaneously in the structures and magnetic fields in the underlying photosphere.

All together the interplay of corona, prominences and the sun's surface is not known at all. Only the *simultaneous* observation of all the three will help to come to a sound physical picture of the outer regions of our sun.

In general it must be said, that the observations of hydromagnetic phenomena on the sun available today are still quite insufficient for theoretical work. The simultaneous observation of the different aspects of one single solar phenomenon needs a new type of instrumentation as well as a great effort to get as continuous records as possible. The new kind of simultaneous observations can be carried out only by a few suitable observatories in good climates with very good seeing conditions. The interpretations of detailed observations made simultaneously at different stations have not proved to be very efficient. The measurement of weak magnetic fields on the sun within small areas as well as simultaneous observations of the corona, chromosphere and photosphere will be the most important and most difficult parts of this project.

REFERENCES

- [1] J. JANSSEN: *Journ. Ann. Obs.*, Paris Meudon 1 (1896).
- [2] J. B. ROGERSON: *Sky and Telescope*, 17, 112, (1958).
- [3] G. THIESSEN: *Zeits. Astrophys.*, 26, 16, (1949); K. O. KIEPENHEUER: *Astrophys. Journ.*, 117, 447 (1953); H. W. and H. D. BABCOCK in G. P. KUIPER: *The Sun* (Chicago, 1953), pag. 704 and V. SEVERN, A. B. BUMBA: *Observatory*, 78, 33 (1958).

The Scattering of Electromagnetic Waves by an Electron Beam.

H. WILHELMSSON

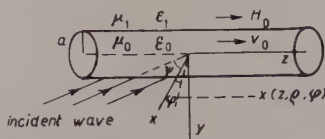
Nordic Institute for Theoretical Atomic Physics - Copenhagen. ()*

In recent years a considerably increased interest has been shown with regard to problems concerning the scattering of electromagnetic waves. There are several reasons for this renewed activity in a field which might be thought to have come to an end at the time when the early developments of quantum mechanics were made. Not only rapid technical developments, *e.g.* the invention of radar and its application to various fields, *e.g.* astronomy, have played an important role, but also, from a theoretical point of view, the analogy between the scattering theories in quantum mechanics and classical electromagnetic theory has stimulated the interest. The scattering of waves by regions containing ionized gas has attracted considerable attention *e.g.* in connection with the study of meteor trails. In several cases it is of interest to consider the interaction between electromagnetic waves and a stream of particles. Such streams appear *e.g.* in the solar corona and applications of the theory are found also in the fields of microwave electronics and thermonuclear reactions.

The following discussion will be devoted to the problem of scattering of an obliquely incident plane electromagnetic wave by an electron beam. The incident wave is assumed to be linearly polarized in an arbitrary direction. The frequency of the wave is assumed to be of such order that the ions can be regarded at rest. The small signal theory is used, *i.e.* all a.c. quantities are considered small compared to the corresponding static ones. We assume the beam to be of infinite extent and of cylindrical cross-section. We further assume that the d.c. density is constant over the beam cross-section and that the dielectric constants are different inside and outside the electron

(*) Now at Chalmers University of Technology, Gothenburg.

beam. A static magnetic field is considered in the direction of the beam axis. The electrons are treated relativistically and we use a macroscopic point of view in our procedure.



We assume the axial propagation to be represented by the factor $\exp[j(\omega t - k_1 z \sin \psi)]$, where $k_1 = \omega \sqrt{\mu_1 \epsilon_1}$ is the propagation constant of the incident plane wave. Let us further introduce $\alpha_1 = \omega/v_0$, «the phase constant» of the beam and k_{p_0} , the relative space charge wave propagation constant defined by $k_{p_0} = 2\pi/\lambda_{p_0} = \omega_c/v_0$, where λ_{p_0} is the plasmic wave length of an infinitely wide beam and $\omega_c = \sqrt{Ne^2/m\epsilon_0}$ the critical angular frequency of the beam with an electron density N .

The equation of motion for the electron

$$(1) \quad \frac{d}{dt}(m\mathbf{v}) = -e(\mathbf{E} + \mu_0 \mathbf{v} \times \mathbf{H}),$$

together with the equation of continuity enables us to calculate the small signal alternated current density components corresponding to the alternated components of the electric and magnetic fields

$$(2) \quad \left\{ \begin{aligned} J_z &= -j\omega\epsilon_0 \cdot \frac{k_{p_0}^2}{(\alpha_1 - k_1 \sin \psi)^2} \left\{ \eta^2 E_z + \frac{1}{\alpha_1} \frac{1}{\Delta_H^2} \eta \left[j \frac{1}{\rho} \frac{\partial}{\partial \rho} (\rho(E_\rho - \mu_0 v_0 H_\varphi)) - \right. \right. \\ &\quad \left. \left. - \frac{n}{\rho} (E_\varphi + \mu_0 v_0 H_\rho) - \frac{\omega_H}{\omega - v_0 k_1 \sin \psi} \eta \left(\frac{1}{\rho} \frac{\partial}{\partial \rho} (\rho(E_\varphi + \mu_0 v_0 H_\rho)) - \right. \right. \right. \\ &\quad \left. \left. \left. - j \frac{n}{\rho} (E_\rho - \mu_0 v_0 H_\varphi) \right) \right] \right\}, \\ J_\rho &= -j\omega\epsilon_0 \cdot \frac{k_{p_0}^2}{\alpha_1(\alpha_1 - k_1 \sin \psi)} \frac{1}{\Delta_H^2} \cdot \\ &\quad \cdot \eta \left\{ E_\rho - \mu_0 v_0 H_\varphi + j \frac{\omega_H}{\omega - v_0 k_1 \sin \psi} \eta (E_\varphi + \mu_0 v_0 H_\rho) \right\}, \\ J_\varphi &= -j\omega\epsilon_0 \cdot \frac{k_{p_0}^2}{\alpha_1(\alpha_1 - k_1 \sin \psi)} \frac{1}{\Delta_H^2} \cdot \\ &\quad \cdot \eta \left\{ E_\varphi + \mu_0 v_0 H_\rho - j \frac{\omega_H}{\omega - v_0 k_1 \sin \psi} \eta (E_\rho - \mu_0 v_0 H_\varphi) \right\}, \end{aligned} \right.$$

where $\omega_H = (e/m_0)\mu_0 H_0$ is the angular cyclotron frequency and H_0 the strength of the axial static magnetic field, $\eta = (1 - (v_0^2/c_0^2))^{\frac{1}{2}}$ and

$$(2a) \quad \Delta_H^2 = 1 - \frac{\omega_H^2 \eta^2}{(\omega - v_0 k_1 \sin \psi)^2}.$$

Introducing the above expressions for the components of the a.c. current density into Maxwell's equations we find that the equations satisfied by the axial components of the electric and magnetic field vectors will be coupled

$$(3) \quad \begin{cases} \frac{1}{\varrho} \frac{\partial}{\partial \varrho} \left(\varrho \frac{\partial H_z}{\partial \varrho} \right) + \left(q_H^2 - F_H G_H - \frac{n^2}{\varrho^2} \right) H_z = -j \frac{1}{Z_0} \Lambda_H \Lambda_0^2 F_H E_z, \\ \frac{1}{\varrho} \frac{\partial}{\partial \varrho} \left(\varrho \frac{\partial E_z}{\partial \varrho} \right) + \left(q_H^2 \Lambda_0^2 F_H - \frac{n^2}{\varrho^2} \right) E_z = j Z_0 \Lambda_H F_H H_z, \end{cases}$$

where

$$(3a) \quad \begin{cases} \Lambda_H = \frac{k_0(k_0^2 - \alpha_1 k_1 \sin \psi)}{\alpha_1^2(\alpha_1 - k_1 \sin \psi)} \cdot k_{a_0}^2 \cdot \frac{\omega_H}{\omega_H - v_0 k_1 \sin \psi} \cdot \frac{\eta^2}{\Lambda_H^2}, \\ F_H = \left[1 - \frac{k_{p_0}^2 \eta^3}{(\alpha_1 - k_1 \sin \psi)^2 \Lambda_H^2} \right]^{-1}, \\ \Lambda_0^2 = 1 - \frac{k_{p_0}^2 \eta^3}{(\alpha_1 - k_1 \sin \psi)^2}, \quad q_H^2 = k_0^2 \left(1 - \frac{k_{p_0}^2}{\alpha_1^2} \cdot \frac{\eta}{\Lambda_H^2} \right) - k_1^2 \sin^2 \psi, \\ s = 1 - \frac{k_0^4}{q_H^4} \cdot \frac{k_{p_0}^4}{\alpha_1^4} \cdot \frac{\omega_H^2}{(\omega - v_0 k_1 \sin \psi)^2} \cdot \frac{\eta^4}{\Lambda_H^4} \quad \text{and} \quad Z_0 = \sqrt{\frac{\mu_0}{\varepsilon_0}}. \end{cases}$$

Note that the coupling terms vanish when ω_H tends to zero or infinity, *i.e.* when there is no static magnetic field present or when there is an infinitely strong static magnetic field. Although it is possible to solve these coupled equations exactly we will confine our following discussion to the two cases where $\omega_H = \infty$ and $\omega_H = 0$.

1. - The case of a strong axial magnetic field.

When there is a strong static axial magnetic field present the transversal motions of the electrons can be neglected. In this case eq. (2) simply reduces to

$$J_z = -j\omega\varepsilon_0 \frac{k_{p_0}^2}{(\alpha_1 - k_1 \sin \psi)^2} E_z.$$

The solution of the problem for an arbitrarily polarized incident wave is obtained by superposition of two special cases; A) the magnetic, B) the electric field vector of the incident plane wave is perpendicular to the electron beam.

A) The magnetic field vector of the incident wave perpendicular to the electron beam.

The boundary conditions to be satisfied at the surface of the beam are that the components E_z , E_φ , H_z and H_φ vary continuously if we let the point of observation move through the beam surface. To be able to satisfy these boundary conditions it is necessary that the complete wave solution inside the electron beam contains solutions of both the transverse electric and the transverse magnetic types.

Inside the electron beam we then have (omitting the axial propagation factor $\exp[j(\omega t - k_1 z \sin \psi)]$ in the following):

TM-mode:

$$(4) \quad E_z^{\text{int}} = \sum_{M=0}^{\infty} A_{1n} J_n(\Delta_0 \sqrt{k_0^2 - k_1^2 \sin^2 \psi} \varrho) \cos n\varphi, \quad H_z^{\text{int}} = 0,$$

TE-mode:

$$(5) \quad H_z^{\text{int}} = \sum_{n=0}^{\infty} B_{1n} J_n(\sqrt{k_0^2 - k_1^2 \sin^2 \psi} \varrho) \sin n\varphi, \quad E_z^{\text{int}} = 0.$$

To describe an outgoing scattered wave at infinity we have to use Hankel functions outside the electron beam, where we find

TM-mode:

$$(6) \quad E_z^{\text{sc}} = \sum_{n=0}^{\infty} A_{2n} H_n^{(2)}(k_1 \varrho \cos \psi) \cos n\varphi, \quad H_z^{\text{sc}} = 0.$$

TE-mode:

$$(7) \quad H_z^{\text{sc}} = \sum_{n=0}^{\infty} B_{2n} H_n^{(2)}(k_1 \varrho \cos \psi) \sin n\varphi, \quad E_z^{\text{sc}} = 0.$$

The incident plane wave can be expanded in cylindrical co-ordinates so that for the assumed polarization:

$$(8) \quad E_z^{\text{inc}} = -A \cos \psi \sum_{n=0}^{\infty} \varepsilon_n j^n J_n(k_1 \varrho \cos \psi) \cos n\varphi \quad (\varepsilon_0 = 1, \varepsilon_{1,2,3,\dots} = 2).$$

The four coefficients A_{1n} , A_{2n} , B_{1n} and B_{2n} can now be determined from the condition that the sum of the TM and TE mode contributions inside the electron beam equals the sum of the TM and TE mode contributions outside the beam plus the contribution of the incident plane wave on the beam-surface for each of the components E_z , E_φ , H_z and H_φ .

In this way we find *e.g.* for the amplitude coefficients A_{1n} and A_{2n}

$$(9) \quad \begin{cases} A_{1n} = -A \cos \psi \varepsilon_n j^{n+1} \frac{2}{\pi} \frac{1}{y_1} \cdot \left(\kappa \frac{k_0 k_0 a}{k_1 y_0^2} n J_n(\Delta_0 y_0) H_n^{(2)}(y_1) \right)^{-1} F_n, \\ A_{2n} = -A \cos \psi \varepsilon_n j^n \left\{ j \frac{2}{\pi} \frac{1}{y_1} \left(\kappa \frac{k_0 k_0 a}{k_1 y_0^2} n (H_n^{(2)}(y_1))^2 \right)^{-1} F_n - \frac{J_n(y_1)}{H_n^{(2)}(y_1)} \right\}, \end{cases}$$

where

$$(10) \quad (F_n)^{-1} = \frac{\frac{Z_1}{Z_0} \frac{k_0}{k_1} \frac{y_1}{y_0} \Delta_0 J'_n(\Delta_0 y_0) H_n^{(2)}(y_1) - J_n(\Delta_0 y_0) H_n^{(2)'}(y_1)}{\kappa \frac{k_0}{k_1} \frac{k_0 a}{y_0^2} n J_n(\Delta_0 y_0) H_n^{(2)}(y_1) + \frac{\kappa \frac{k_0}{k_1} \frac{k_0 a}{y_0^2} n J_n(y_0) H_n^{(2)}(y_1)}{\frac{Z_0}{Z_1} \frac{k_0}{k_1} \frac{y_1}{y_0} J'_n(y_0) H_n^{(2)}(y_1) - J_n(y_0) H_n^{(2)'}(y_1)},$$

where

$$Z_0 = \sqrt{\frac{\mu_0}{\varepsilon_0}}, \quad Z_1 = \sqrt{\frac{\mu_1}{\varepsilon_1}},$$

$$(11) \quad y_0 = a \sqrt{k_0^2 - k_1^2 \sin^2 \psi},$$

$$(12) \quad y_1 = a k_1 \cos \psi$$

and the coupling coefficient

$$\kappa = \frac{k_1^2 - k_0^2}{k_0^2} \operatorname{tg} \psi.$$

We observe that in general the electric vector of the scattered wave has a different direction than that of the incident wave. When $k_0 = k_1$ or when $\psi = 0$ it follows that $\kappa = 0$, the current independent part of F_n vanishes and the expressions for A_{1n} and A_{2n} reduce considerably. In this case we also find $B_{1n} = B_{2n} = 0$ i.e. no TE modes are excited, and we have

$$(13) \quad A_{1n} = -A \cos \psi \varepsilon_n j^{n+1} \frac{2}{\pi} \frac{1}{y} [\Delta_0 J'_n(\Delta_0 y) H_n^{(2)}(y) - J_n(\Delta_0 y) H_n^{(2)'}(y)]^{-1},$$

$$(14) \quad A_{2n} = -A \cos \psi \varepsilon_n j^n \frac{J_n(\Delta_0 y) J'_n(y) - \Delta_0 y_n(J) J'_n(\Delta_0 y)}{\Delta_0 J'_n(\Delta_0 y) H_n^{(2)}(y) - J_n(\Delta_0 y) H_n^{(2)'}(y)},$$

where

$$y = k_0 a \cos \psi.$$

The case *B*) when the electric field vector of the incident plane wave is perpendicular to the electron beam can be calculated in the same way. It leads to the result that in general there is an alternated current density in the beam direction although we have no axial component of the electric vector of the incident plane wave. For this polarization, if $k_1 = k_0$ and $\psi = 0$ there is no interaction between the incident plane wave and the electron beam.

2. - The case of no static magnetic field.

We now want to compare the solution for the case when there is no static magnetic field present with the case of an infinitely strong magnetic field.

It is convenient to make use of the following notations:

$$(15) \quad \Delta_0^2 = 1 - \frac{k_{p_0}^2 \eta^3}{(\alpha_1 - k_1 \sin \psi)^2},$$

$$(16) \quad \Delta_t^2 = 1 - \frac{k_{p_0}^2 \eta}{\alpha_1 (\alpha_1 - k_1 \sin \psi)}.$$

The effective dielectric constants in Maxwell's equations can accordingly be written:

$$(17) \quad \varepsilon_z = \Delta_0^2 \varepsilon_0,$$

$$(17a) \quad \varepsilon_\varphi = \varepsilon_\psi = \Delta_t^2 \varepsilon_0.$$

Let us further introduce the notations

$$(18) \quad \xi = 1 - \frac{k_0^2}{\alpha_1^2} \frac{k_{p_0}^2 \eta}{k_1 \sin \psi (\alpha_1 - k_1 \sin \psi)},$$

$$(19) \quad q^2 = k_0^2 \left[1 - \left(\frac{\omega_c}{\omega} \right)^2 \eta \right] - k_1^2 \sin^2 \psi.$$

For the case A) when the magnetic field vector of the incident plane wave is perpendicular to the electron beam we find the wave solutions inside the electron beam ($\varrho < a$):

TM-mode:

$$(20) \quad E_z^{\text{int}} = \sum_{n=0}^{\infty} A_{1n} J_n(q\varrho) \cos n\varphi \quad H_z^{\text{int}} = 0.$$

TE-mode:

$$(21) \quad H_z^{\text{int}} = \sum_{n=0}^{\infty} B_{1n} J_n(q\varrho) \sin n\varphi \quad E_z^{\text{int}} = 0.$$

Outside the electron beam ($\varrho > a$):

TM-mode:

$$(22) \quad E_z^{\text{ext}} = \sum_{n=0}^{\infty} A_{2n} H_n^{(2)}(k_1 \cos \psi) \cos n\varphi \quad H_z^{\text{ext}} = 0.$$

TE-mode:

$$(23) \quad H_z^{(2)} = \sum_{n=0}^{\infty} B_{2n} H_n^{(2)}(k_1 \rho \cos \psi) \sin n\varphi \quad (E_z^{(2)} = 0).$$

We now find the following expressions for the A_{1n} and A_{2n} amplitude coefficients

$$(24) \quad A_{1n} = -A \cos \psi \varepsilon_n j^{n+1} \cdot \frac{2}{\pi} \frac{1}{y_1} \left[\operatorname{tg} \psi \frac{k_0^2 [1 - (\omega_c/\omega)^2] - k_1^2 (\sin^2 \psi + \xi \cos^2 \psi)}{q^2} \cdot \frac{1}{k_1 a} n J_n(qa) H(y_1) \right]^{-1} L_n,$$

$$(25) \quad A_{2n} = -A \cos \psi \varepsilon_n j^n \cdot \left\{ j \frac{2}{\pi} \frac{1}{y_1} \left[\operatorname{tg} \psi \frac{k_0^2 [1 - (\omega_c/\omega)^2] - k_1^2 (\sin^2 \psi + \xi \cos^2 \psi)}{q^2} \cdot \frac{1}{k_1 a} n (H_n^{(2)}(y_1))^2 \right]^{-1} L_n - \frac{J_n(y_1)}{H_n^{(2)}(y_1)} \right\},$$

where

$$(26) \quad (L_n)^{-1} = \frac{\frac{Z_1 k_0 y_1}{Z_0 k_1 qa} \Delta_i^2 J_n'(qa) H_n^{(2)}(y_1) - J_n(qa) H_n^{(2)}(y_1)}{\operatorname{tg} \psi \frac{k_0^2 [1 - (\omega_c/\omega)^2] - k_1^2 (\sin^2 \psi + \xi \cos^2 \psi)}{q^2} \cdot \frac{1}{k_1 a} n J_n(qa) H_n^{(2)}(y_1)} - \frac{\operatorname{tg} \psi \frac{k_0^2 [1 - (\omega_c/\omega)^2] - k_1^2}{q^2} \cdot \frac{1}{k_1 a} n J_n(qa) H_n^{(2)}(y_1)}{\frac{Z_0 k_0 y_1}{Z_1 k_1 qa} \Delta_i^2 J_n'(qa) H_n^{(2)}(y_1) - J_n(qa) H_n^{(2)}(y_1)}.$$

It is interesting to compare these results with the corresponding expressions in the case of a strong axial magnetic field. In that case we noticed that there were no TE-modes excited when $k_1 = k_0$. The above formulae show that this is not true when there is no magnetic field present. TE-modes will then always be excited in addition to the TM-modes for this polarization even if $k_1 = k_0$, with the exception of a perpendicular incidence. When there is no axial magnetic field the coupling factor corresponding to κ can (for non relativistic velocities) be written:

$$(27) \quad \delta = \frac{k_1^2 - k_0^2 [1 - (\omega_c/\omega)^2]}{k_0^2} \operatorname{tg} \psi.$$

BIBLIOGRAPHY

- H. WILHELMSSON: *The scattering of electromagnetic waves by an electron beam and a dielectric cylinder* (Dissertations at Chalmers University of Technology, Gothenburg, No. 18), 1958.

Magnetic Field in the Solar System.

T. GOLD

Harvard College Observatory - Cambridge, Mass.

The following types of observation give us information about the magnetic field near the sun and near the earth:

Coronal shapes,

Zeeman measurements of the photosphere,

Magnetic storm effects,

Cosmic rays increases and decreases.

The importance of magnetohydrodynamics for stellar phenomena arises from the large magnitude of the product (conductivity) \times (linear dimensions); it is impossible to approach the same magnitude in laboratory experiments.

The equation governing the behaviour of the magnetic field is

$$\frac{\delta B}{\delta t} = \text{curl } \mathbf{V} \wedge \mathbf{B} + \frac{1}{\mu\sigma} \nabla^2 \mathbf{B},$$

if we neglect space-charge convection, displacement currents, and (v/c^2) terms. If the dimensions of the system are of order L , and velocities of order v , the times characterizing change due to the first term (which describes convection of the field) T and due to the second term (which describes dissipation) τ , are given by

$$T = \frac{L}{v}, \quad \tau = L^2 \mu \sigma.$$

We may define a «magnetic Reynolds number» R_M by the equation

$$R_M = \frac{\tau}{T} = VL\mu\sigma.$$

The value of τ for sun's magnetic field is about 10^{10} years; that for a

sunspot about 10^5 years. Hence the effect of dissipation may be ignored in comparison with the convection of the field which occurs in much shorter times.

We now consider *the chromosphere*. The equation of motion is

$$\rho \frac{dV}{dt} = \rho g - \text{grad } P + \frac{1}{\mu} \text{curl } \mathbf{B} \wedge \mathbf{B}.$$

The processes that take place must be the consequences of the motions of the base points of the lines of force. These motions are dictated by the massive photosphere convection and no chromospheric effect can react back on that significantly.

The pressure appears to be small compared with the magnetic field so that the magnetic field must take up nearly force-free configurations. A large flare in the chromosphere releases about 10^{32} ergs; this can come only from the magnetic field since all other forms of energy amount to only 10^{28} ergs. It is proposed that this energy is released by instability of a horse-shoe shaped configuration of magnetic field lines induced by twisting of these lines at the base. This is a mechanism for transferring energy from the photosphere into the chromosphere. The magnetic fields are of order 100 gauss.

We now consider *the corona*. Although the temperature is high, the density is so low that the pressure is of the same order as or smaller than that of the magnetic field. One observes the long lived structure of the corona and the magnetohydrostatic interpretation of that has to be pursued first. The conducting gas is free to move only along the field lines. Hence we may imagine the gas as being contained in a large number of separate tubes, following the field lines in shape. In each of these tubes, the barometric equation will be satisfied, so that we may relate the density to radial height. However, we must expect the density to vary from tube to tube, due to patchiness of the chromosphere. We now see that such fluctuations at the chromosphere will give rise to a filamentary structure of the corona, as typified by the polar plumes.

We now have to justify the use of magnetohydrostatics, where

$$\rho g - \text{grad } P + \frac{1}{\mu} \text{curl } \mathbf{B} \times \mathbf{B} = 0.$$

The convective and dissipative terms in the equation determining the time variation of the magnetic field are equal if

$$R_M \equiv vL\mu\sigma = 1.$$

With values of L , μ and σ appropriate to the corona, this equality leads to

$v = 10^{-8}$ cm/s. Hence for velocities of interest, the dissipative term may be ignored. Now consider the ratio of the magnetic force

$$\frac{1}{\mu} \text{curl } B \wedge B \sim \frac{1}{\mu} \frac{B^2}{L},$$

and the inertial acceleration term

$$\varrho \frac{dV}{dt} \sim \varrho \frac{V^2}{L}.$$

These are equal in magnitude if $B = 10^{-17}$ Oe. Hence in our problem, since the field strength is much larger than this value, the inertial term may be ignored for a wide range of velocities; that is, the problem may be treated as one of statics rather than dynamics.

Let us now consider changes in configuration of the magnetic field lines which will arise if the gas pressure becomes significant. If one injects a mass of non-magnetized gas, this will be ejected by the pressure of the magnetic field, since the magnetic field is not linked with this mass. However, if the mass is originally magnetized, it cannot part company with its original lines of force. The thermal pressure of the gas will tend to lengthen the lines, but this in turn will increase the magnetic energy. The equilibrium configuration is that which minimizes $E_m + E_p$. This equilibrium will be stable only if the minimum is an absolute minimum.

We have already seen that one type of instability arises when the gas is completely non-magnetized. If the gas is weakly magnetized, it will be buoyant, rising through the region of strong magnetic field, but only to a certain height since it is elastically anchored by its field lines. The resulting configuration resembles the rupture of a muscular tissue. It is clear that magnetic pressure will vary widely over the corona, as does the gas pressure.

We shall now proceed to consider the configuration of the magnetic field in the space between the sun and the earth. We have obtained important information from the large increase in cosmic ray flux which was associated with the solar flare of 23 February 1956. Cosmic rays were received in the $(1 \div 10)$ GeV range at 200 times the normal flux. The anomalous flux exhibited a very sharp commencement, followed by a gradual decay over several hours. In the first few minutes it was sharply directional, coming from the Sun; the highest energies arrived first. After fifteen minutes, cosmic rays were arriving from other directions; after 30 minutes the directions were isotropic. It therefore appears that, in the solar system there was a magnetic field strong enough to deflect high-energy particles. The sharp onset of a cosmic ray flux indicates either that the space between the sun and the earth was field free, or

that the magnetic field lines were parallel to the radius vector from the sun to the earth. It is unreasonable to assume that the space was originally field free, since we are led to believe that, in the later phase, there was a strong field. We must therefore suppose that there is a magnetic field, of strength at least 10^{-5} gauss, which does not impede the early radial flow of particles, but which forms a closed system for the particles, filling up in about half an hour. Masses of gas thrown out by the sun will carry their original magnetic fields with them and the outburst will thus tend to take up an elongated shape like a tongue protruding ultimately out beyond the earth. The associated magnetic field would not be strong enough to impede the early radial flow, but would form a closed container which would later provide for the diffusion of the cosmic ray particles.

Since gas emitted from the sun seems to arrive at the earth every few days it is likely that the earth spends a large amount of time within solar gas, and hence within solar magnetic fields of such elongated shape. It is incompatible with observation to assume the existence of a co-rotating field at the earth's distance. However, if the tongues are thrown out rapidly they will have small angular momentum so that the field which they carry with them will not have the angular velocity of the sun.

It would appear, from the above outline, that particles from a solar flare will be emitted along only a small solid angle from the sun, since the surface magnetic intensity of 1 gauss is sufficient to localize particles of the GeV range to within 100 km. The chance of any reaching the earth would then appear to be much too small. This objection may be overcome by supposing that particles originally stored in the flare expand over a large region, forming an outburst. This part of the procedure may also account for the time delay which is observed between the flare and the time the particles may be computed to have set out.

We may note an important corollary of the above theory. If the magnetic field of the «tongue» can trap particles inside it, it can also keep particles outside. Hence if the earth finds itself in such a «magnetic» bottle, we should observe a decrease in the intensity of cosmic rays (other than those coming from the sun). In fact, such decreases are observed to be associated with flares, and call for field strengths of about 10^{-4} gauss for periods of about two days. Such a decrease preceded the sudden increase of solar-particle flux, and there is thus reason to suppose that the field configuration existed at the time.

We now pass to the discussion of magnetic storms.

A remarkable feature of magnetic storms is the very sudden commencement which is observed simultaneously all over the world, although the subsequent development of the storm varies greatly in detail from place to place. The initial pulse is only two minutes in length although the gas may have taken two days to stream from the sun to the earth. This strongly suggests that the

gas sets up a shock wave since this is the only way for a sharp front to be maintained. The two minute rise time of the signal would correspond to a front of only 100 000 km thickness. If the gas were non-magnetized, the width of the shock front would be much larger than that, since the shock-front width is normally a small multiple of the mean free path. However, if the interplanetary gas is permeated by a magnetic field, the shock-front will be magnetohydrodynamic in properties; we find that a field strength of about 10^{-6} gauss is sufficient to explain the observed shock width. This is therefore a further argument in favour of the existence of interplanetary fields.

The mean behaviour of magnetic storms has been explained by CHAPMAN and FERRARO in terms of a ring current encircling the earth at five earth's radii. However, there are very large differences between the observations of different stations, which indicate a scale of $(1000 \div 500)$ km to field fluctuations on the ground. This one may imagine to be produced by instabilities causing a break-up of the original stream, but it is clear that such variations cannot be attributed to a source five earth's radii out. If one is to ascribe storm characteristics to currents, there must be strong currents near the earth's surface: the hypothesis of a ring current far out is then redundant.

On the other hand, it is physically reasonable to assume currents to flow at a height of $(500 \div 1000)$ km, the height indicated by the scale of fluctuations, the currents may then easily be supported by atmospheric pressure since the current exerts a pressure of only $\sim 10^{-5}$ dynes/cm². We may suppose that the magnetic disturbances of the earth are similar to those of the solar corona, namely magnetohydrostatic extensions. It then follows that the « excited states » can correspond to a reduction of field strength at the surface of the earth only, but not to an increase. This in accord with the observations.

We may also mention van Allen's observations on aurorae, which indicate an incoming flux of $(10 \div 100)$ keV electrons of about 1 erg/cm² s for a light aurora. (The observed X-ray flux could not be ascribed to protons, since the required proton flux would be much higher than that existing at the sun.) Such low-energy electrons cannot have entered along individual « Störmer » orbits. They must therefore have entered the earth's atmosphere in association with a magnetic field, namely that part of the sun's magnetic field with which the particles were originally associated.

Tongues of this must have penetrated into the region of the earth's field. The solar stream must have broken up in some unstable fashion, and this is in accord with the patchy nature of the magnetic and auroral effects. This unstable flow may then account for the ability of the gas to penetrate much closer to the earth than was indicated by calculations that considered the field to be stable.

Recently VAN ALLEN has detected a phenomenon by means of the « Explorer » satellites, which requires a similar explanation as the auroral obser-

vations referred to. A flow of electrons of some tens of keV energy appears to penetrate frequently down to a height of 1000 km, and again this can occur only if in places the earth's field has been completely changed above this level. Such particles may of course enter along any tongues of solar material carrying fields sketched out from the solar surface. Any flux of such electrons that is generated on the solar surface would always populate all lines of force coming from there and therefore this observation may be taken to indicate the magnetic configurations that exist in the earth-sun space and near the earth.

INTERVENTIVE DISCUSSION

— V. FERRARO:

Professor GOLD has failed to mention an important characteristic of magnetic storms, namely, the fact that the horizontal force remains above the mean of the field after the sudden commencement for some hours before the main phase begins. This part of the storm is known as the first phase. Moreover, whilst I agree that an interplanetary shock wave could not exist in the absence of a magnetic field because of the extremely long free paths in interplanetary space, we have little detailed knowledge of the structure of a pure magnetic shock wave. It would be of interest to know, therefore, how GOLD arrives at the conclusion that a field of 10^{-6} G would be sufficient to set up an interplanetary shock wave.

The Origin of Cosmic Rays (*).

L. DAVIS, jr.

California Institute of Technology - Pasadena - Cal.

The cosmic rays of interest to nuclear physicists are mainly secondary cosmic rays—exotic mesons, etc.—produced in our atmosphere. The cosmic rays to be discussed in this lecture will be exclusively primary cosmic rays; *i.e.* those found outside our atmosphere, or better, outside the solar system. These primary cosmic rays are very energetic ions that almost surely are confined to our galaxy by magnetic fields and are accelerated either in the atmospheres of stars or in interstellar space by varying electromagnetic fields. Thus their production and storage touch on problems of interest in thermonuclear work. In addition, for reasons in part pointed out in earlier lectures by Professor VAN DE HULST, the study of primary cosmic rays provides a means of getting some interesting astronomical data. Finally, cosmic rays form an important—and occasionally neglected—element in astronomical problems. This lecture will present a brief summary of some of these topics.

As an introduction, we need a summary of some of the important observed properties of cosmic rays:

A) *Energy density.* The energy density just outside the atmosphere in particles with kinetic energies per nucleon greater than about 10^9 eV is very nearly $1 \text{ eV/cm}^3 = 1.6 \cdot 10^{-12} \text{ erg/cm}^3$. This is approximately the energy density in star light outside the solar system.

B) *Isotropy.* Except for effects due to the earth's atmosphere and magnetic field, or perhaps due to interplanetary magnetic fields, cosmic rays are observed to be isotropic to within limits that essentially do not exceed the statistical uncertainties. These limits are, roughly, a variation with direction of $10^{-3.5}$ at $4 \cdot 10^9$ eV, of $10^{-2.5}$ at 10^{15} eV, and of 10^{-1} at 10^{17} eV. Also the intensity does not seem to have varied much in time for at least 10^4 years, and there is some evidence for extending this to 10^6 years.

(*) This work was done while a Guest Professor at the Max-Planck-Institut für Physik, Göttingen.

C) *Distribution over the elements.* 1) Li, Be, and B are very much more abundant in cosmic radiation than in the sun or other stars. 2) Other elements appear to have about the same relative abundances in cosmic rays as in the galaxy as a whole except that there is a strong indication that there is some excess of heavy elements in cosmic radiation. A very rough review of the trend is given by the statement that the overabundance in cosmic radiation is by the factor A^n , where A is the atomic weight and n probably lies in or near the range $\frac{1}{2}$ to 1. 3) Very few if any primary electrons are found by cosmic ray techniques. The density of highly energetic electrons observed in radio astronomy is much less than the density of protons in cosmic radiation.

D) *Energy spectrum.* Particles with kinetic energies running from a bit below 10^9 eV per nucleon to 10^{18} or 10^{19} eV are observed in cosmic radiation. Large numbers of particles with lower energies are known to be present in the solar system, but they are not observed by cosmic ray techniques and usually are not classed as cosmic rays. If w is the total energy (rest energy plus kinetic energy), the distribution of cosmic rays over energy is given by the well known power law

$$N(>w) = N_0 w^{-\gamma}.$$

where the left-hand side is the number of particles per unit area, time, and solid angle arriving at the solar system with energies greater than w , N_0 and γ are constants, $\gamma \approx 1.6$ if $10^{10} < w < 10^{15}$ eV and $\gamma \approx 2$ at 10^{18} eV. The spectrum appears to be quite smooth and to have roughly the same γ for all elements if w is now interpreted as energy per nucleon.

Before considering the implications of these observations, a brief discussion of the most probable acceleration mechanisms is necessary. The problem is to accelerate particles from some 10^2 eV, which they have in the thermal motions of the solar corona and many other places, to 10^9 eV where they are observed as cosmic rays, and to carry a few particles on to 10^{18} or 10^{19} eV. It is convenient to treat the low and high energy parts of this separately, calling the former injection and the second acceleration. Both the shape of the energy spectrum at low energies and the theory of some acceleration mechanisms suggests that the dividing line between the two regimes be put at about 10^8 or 10^9 eV per nucleon; that is, at the point where the particles become relativistic. But it may turn out that the proper dividing line could be at, say, 10^{15} eV. It is of, course, quite possible that in fact the acceleration from 10^2 eV to 10^{19} eV is produced by a single mechanism operating in a single region. The division into two processes is suggested by the fact that it will be exceedingly difficult to devise any process that accelerates particles in the 10^2 to 10^6 eV range in interstellar space, and it seems very difficult to confine a 10^{18} eV proton to a region as small as a star during the last stages of

its acceleration. With this separation, injection takes place from stars and must have properties that account for the overabundance of heavy elements. The subsequent acceleration takes place in interstellar space and should have properties that account for the power-law energy-spectrum.

It seems certain that injection and acceleration are produced by electromagnetic forces on a macroscopic scale. All mechanisms that are seriously considered at present are variations of two main types. One, occasionally called the Cygnetron, and first proposed, I believe, by SWANN is a betatron process in which charged particles are carried steadily from thermal to relativistic energies by a continuously increasing magnetic field, as in a sun spot. Although circuits having very high electromotive forces are easy to find, ions will have big enough gyro-radii to gain significant amounts of energy only near the zeros in the magnetic field. Thus it seems difficult to deflect a large enough fraction of the magnetic energy into cosmic rays. Also, since this mechanism accelerates all ions in the region in question, the density must be very low or when the available energy is divided among the ions, none of them will be relativistic. The other accelerating mechanism is the Fermi statistical mechanism. Here, ions interact with varying magnetic fields, sometimes losing energy and sometimes gaining. In some variations one can think of the ions as colliding with clouds containing magnetic fields, but there are many other variations, some involving betatron processes. Often there is a steady average gain in energy and always there is a random walk in energy, since some particles will, by chance, gain more energy than the average and others will lose more. A more thorough discussion of these points will be found in the proceedings of the IUPAP Cosmic Ray Conference, Varenna, 1957 (*Supplemento* n. 2 al Vol. 8 (1958) del *Nuovo Cimento*).

In general, one gets a result of the form

$$(1) \quad F(\gamma) = t_1 / \beta_o^2 \tau,$$

where t_1 is the time for a single interaction of the cosmic ray particles with the changing magnetic field, $c\beta_o$ is the mean speed of the random motions of the gas clouds, and dt/τ is the probability that in a time dt the cosmic ray will escape from the region where it is being accelerated. $F(\gamma)$ is some simple function of γ that makes γ near 2, as required by observation, when the right hand side of (1) is near 1 or 2, or, in a few particularly efficient modifications of the Fermi mechanism, is about 30.

Consider now some of the implications of the observed properties of cosmic rays. A variety of arguments so convincing that it does not seem worth while to review them seem to exclude the possibility that cosmic rays are uniformly distributed through the universe or are confined to the solar system. This leaves us a galactic problem.

From points *A* and *B* (energy density and isotropy) we get the familiar arguments for storage. If cosmic rays move in straight lines, as does starlight, and have the same energy density as starlight, then the power supplies to each will have to be the same. There seems no conceivable way to find this much energy for cosmic radiation. Also some anisotropy related to the structure of the galaxy should be observable. But if cosmic ray trajectories are strongly curved on a galactic scale, each particle can stay in the disk for 10^4 times as long as starlight and the power supply need be only 10^{-4} as great. Thus if 10^{-4} of the thermal energy produced in the stars can be converted first to mechanical energy and then to cosmic ray energy, it will be enough. This seems a very high efficiency for the conversion of heat into particle energy in apparatus that is just thrown together and is not engineered for this specific purpose, but it is not an impossible efficiency. Still, the power required is so large that no uncommon processes can be involved.

To store the particles, we must deflect them without loss of energy. This requires magnetic fields and seems to me to be a very strong argument for the existence of galactic magnetic fields.

Any storage process of this kind reduces the anisotropy, but the observed nearly complete isotropy puts rather narrow limits on the possible storage mechanisms. Until recently storage in the disk or a spiral arm of the galaxy was favored; but now that cosmic ray physicists have learned of the existence of the galactic halo, it seems to be a much better place. Otherwise it is difficult to store 10^{17} eV protons (with radii of curvature of 35 light years in a 10^{-5} gauss field) for long enough times or to make them isotropic enough.

It is of interest to note that the pressure corresponding to a cosmic ray energy density of the order of 1 eV/cm³ is the same as that involved in a magnetic field of $0.7 \cdot 10^{-5}$ gauss or a gas with $nT = 10^4$ °K particles/cm³. Thus the cosmic ray and magnetic pressures are large compared with the ordinary gas pressure, for which Professor VAN DE HULST gave us the typical value $nT = 10^2$. The cosmic ray pressure can be safely ignored, as it so often is, as long as the cosmic ray density is uniform and there is no corresponding pressure gradient. But when one comes to the boundaries of the cosmic ray storage region, their pressure can no longer be ignored.

It has been argued that the Fermi mechanism is unlikely since even if astronomical conditions can be found for which the right hand side of (1) is not large, it would require an unlikely coincidence for three unrelated parameters to combine to give a value that is so near unity. This argument fails if the acceleration of cosmic rays is an important damping mechanism for the gas motions, as suggested by the large fraction of the energy of the gas motions converted into cosmic rays. Then only values of γ near unity give the right amount of damping. With larger values of γ , there is not much damping and β_v increases.

The kinds of gas motion that accelerate particles by the Fermi process also produce anisotropy since they tend to make the particle velocities parallel to the magnetic field. To allow acceleration to continue, it is necessary that some scattering process maintain the isotropy. Hence the importance to cosmic ray physics of yesterday's discussion of the microstructure of hydro-magnetic shock waves.

Now let us turn to *C 1*) (abundances of Li, Be, and B). The storage time is limited to the time in which nuclear encounters between cosmic rays heavier than boron and interstellar hydrogen will produce the observed amounts of Li, Be, and B. There is some dispute about the interpretation of the observations, but it seems most likely that storage in a spiral arm would have to be for $\tau \approx 5 \cdot 10^6$ years and that storage in the halo (provided the density is less than 10^{-3} particles/cm³) is for $5 \cdot 10^9$ years, or the life of the galaxy. The energy supply problem seems at first glance about the same in either case. With storage in the halo one has 10^3 times as long to pile up cosmic rays but must fill 10^3 times the volume. However, Professor BIERMANN, in our discussions of this problem in Göttingen, has pointed out that with storage for $5 \cdot 10^9$ years, it is entirely possible that most cosmic rays were accelerated early in the evolution of the galaxy, when there might have been more activity in the galaxy than at present. Consideration of several lines of argument, including the observed number of white dwarfs, suggests that this may indeed be the case and that, because of the increased energy supply thus available, it is necessary to divert perhaps only an order of magnitude less than 10^{-4} of the thermal energy to cosmic rays.

From *C 2*) (the abundances of the heavier elements) one concludes either that the injection processes favors heavier ions or that cosmic rays originate somewhere where heavy elements are more abundant than in the solar system. The larger gyro-radii and greater persistence of velocity of heavy ions, particularly when only partly ionized, seems likely to favor their injection since they will have a better chance of escaping from the crowd of ordinary gas ions and getting super-thermal velocities. If one looks for a region where heavy elements, in particular iron, are over-abundant, one thinks first of supernovae since one of the most acceptable modern theories of the origin of the elements holds that iron is produced in supernovae. Since we know that the supernova that made the Crab nebula produced many highly-relativistic electrons, the proposal that cosmic rays come from supernovae has recently seemed very attractive. But this does not explain the power-law energy spectrum and seems to require the conversion of an unreasonably large fraction of the total energy available into cosmic rays.

The conclusions drawn from *D* (power-law energy spectrum) fall into one of two groups. Perhaps the most popular school holds that the Fermi mechanism encounters too many difficulties when examined quantitatively. As in

all theories, it is difficult to get enough power, but in addition it is difficult to get enough power into hydromagnetic waves or turbulence with scales as short as 1 to 10 lt. yrs. Hence it is felt that the power law is probably only an approximate and largely accidental spectrum. The other school feels that the Fermi mechanism is too attractive to abandon and hence devotes its efforts to finding more efficient modifications and to looking for regions where conditions are particularly favorable. There is not enough time today to survey all the various possibilities, but some points can be made. First, to get the power law, we need storage for a time that is independent of energy and of atomic weight. This seems to me to require a relatively uniform magnetic field with diffusion only along the field lines. Thus if storage is in the disk, it should be in a spiral arm and the magnetic field should run along the spiral arm. Second, storage in the halo with no escape or loss due to nuclear collisions will not give the power law. Hence it is necessary to assume acceleration in a limited subregion out of which there is fairly rapid diffusion. In our discussions of this problem, Professor BIERMANN has suggested that this region might be the core, the central 3 kpc, of the galaxy during the early stages of its evolution. One would expect that at that time a great deal of gas would still remain and that there would be many hot young stars. It would be plausible to assume fairly large magnetic fields disturbed by vigorous hydromagnetic waves and shocks. The stars should be close together so that the wave lengths would be small. Thus conditions would be much more favorable for the Fermi mechanism than any that can be found at present.

It seems very attractive, then, to consider a model in which most of the cosmic rays were accelerated in the early stages of the evolution of the galaxy. Acceleration would take place in a limited region such as the core, out of which particles would diffuse with a time constant independent of energy and atomic number. The energy supply to cosmic rays would be an important drain on the hydromagnetic waves, and hence one would get the energy spectrum. The cosmic rays would then be stored in the halo, the cosmic ray pressure being important to the structure of the halo. All of these details, and many others, will have to be worked out quantitatively before this model can be accepted. It appears that many of these details will be of considerable interest in other fields of astronomy and in thermonuclear research, since the relatively efficient acceleration of particles to highly super-thermal energies is not an exclusively cosmic ray problem.

* * *

The author is greatly indebted to the National Science Foundation for a Fellowship and to the Fulbright Commission for a Travel Grant which made it possible to prepare this survey.

Some Theoretical Aspects of Magneto-Hydrodynamics and Thermonuclear Fusion.

R. LÜST

Max-Planck-Institut für Physik und Astrophysik - München

In this discussion we shall treat some theoretical aspects of plasma physics in connection with controlled fusion. The emphasis is on special problems which have been dealt with by the Göttingen group, such as the confinement of a plasma by magnetic fields; however, many aspects such as heating mechanisms are not discussed in this paper.

To confine a plasma by magnetic fields for a sufficient time one must consider three problems. Firstly, for stationary conditions there must be magneto-hydrostatic equilibrium which means an equilibrium configuration between the gas pressure and the pressure exerted by the magnetic fields. Secondly, this state of equilibrium must be stable against perturbations, otherwise the configuration will not be maintained for a finite time. Thirdly, it is essential that the configuration of the magnetic fields is of such a form that the individual charged particles do not escape from the volume enclosed by the magnetic fields. The first two problems can be treated by describing the plasma macroscopically as a fluid. For the third problem one must study the microscopic picture of the individual trajectories of the particles.

1. - Magnetohydrostatic equilibrium.

Here we are dealing with the magnetohydrostatic equation

$$(1) \quad \text{grad } p + \frac{1}{4\pi} \mathbf{B} \times \text{curl } \mathbf{B} = 0.$$

If this condition is not fulfilled it will become apparent in an approximate time taken by a pressure wave to traverse the plasma. This is usually of the

order of microseconds. On the other hand, the quasi-stationary condition must hold for a time of the order of seconds. From equation (1) it follows that the magnetic field \mathbf{B} and the current density \mathbf{j} (which is proportional to curl \mathbf{B}) lie in the surfaces $p = \text{constant}$, where p is the gas pressure.

Let us first assume for simplicity that we are dealing only with surface currents. This current is then given by a change in the magnetic field intensity, from the outside to the inside, of:

$$(2) \quad \mathbf{j} = \frac{c}{4\pi} \mathbf{n} \times (\mathbf{B}_e - \mathbf{B}_i),$$

and the pressure by

$$(3) \quad p = \frac{1}{8\pi} (B_e^2 - B_i^2),$$

where it is assumed that the pressure outside the plasma is zero. \mathbf{B}_e and \mathbf{B}_i are the external and internal field intensities, respectively, at the surface, and \mathbf{n} is the unit vector normal to this surface.

Let us further assume that the magnetic field \mathbf{B}_i inside the plasma is zero. From equation (3) it follows that B_e and \mathbf{j} must be constant over the whole surface of the plasma. We are mainly interested in toroidal plasmas, and in this case it can be shown that the magnetic fields produced by surface currents have only approximately these properties.

Let us discuss a simple example. If we start with cylindrical geometry which has only a surface current in the direction of the axis of symmetry, and an azimuthal magnetic field, the conditions for equilibrium are readily fulfilled. But if one now forms a torus from this cylinder, the magnetic lines of force on the inner side are more dense and the magnetic pressure is therefore greater than on the outer side, and there is now no real equilibrium. But by applying an external magnetic field it is possible to reduce the field on the inner side and increase it on the outer side. To a first order a homogeneous field parallel to the axis of symmetry fulfils this requirement.

The exact solution of this problem for azimuthal surface currents is given by BIERMANN, HAIN, JÖRGENS, and the author. The treatment is based upon the potential theory where the magnetic field is defined by a potential function φ , with $\mathbf{B} = \text{grad } \varphi$. There is a complication, however, in that there is not one boundary condition as for ordinary potential theory, but two due to the fact that the normal component of the magnetic field must vanish at the surface of the plasma and in addition there is the tangential component given by the pressure and by the value of \mathbf{B}_i .

More generally, KIPPENHAHN has investigated the question: for what kind of surfaces is it possible to fulfil the conditions of equilibrium? He showed

that the necessary and sufficient condition for an equilibrium configuration is that the surface is of a form that it can be covered with a network of curves which have equal distances and no singularities, provided B_e is zero (if B_e is not zero, the curves are not necessarily equidistant). For instance, it is not possible to cover a sphere with such curves without singularities, and therefore a sphere cannot be an equilibrium configuration. This holds for all surfaces of singly-connected regions. But for toroidal surfaces it is possible,; for instance, an azimuthal surface current of constant intensity forms a network of equidistant lines. A network of only meridional lines around a torus of circular cross-section does not meet this condition. A surface current having both an azimuthal and a meridional component can satisfy Kippenhahn's condition, provided the azimuthal component is sufficiently large that it is equal to or greater than zero on the inner side of the torus (*).

2. - Stability.

The next problem is to study whether such a configuration is stable against perturbations. To investigate the stability, one must use the complete plasma equations:

$$(4) \quad \rho \frac{d\mathbf{v}}{dt} = -\text{grad } p - \frac{1}{4\pi} \mathbf{B} \times \text{curl } \mathbf{B},$$

$$(5) \quad \frac{d\rho}{dt} = -\rho \text{div } \mathbf{v},$$

$$(6) \quad \frac{dp}{dt} = \gamma \frac{p}{\rho} \frac{d\rho}{dt},$$

$$(7) \quad \frac{\partial \mathbf{B}}{\partial t} = \text{curl } (\mathbf{v} \times \mathbf{B}),$$

$$(8) \quad \text{div } \mathbf{B} = 0.$$

where p is the mass density, \mathbf{v} the disturbance velocity, and γ the ratio of the specific heats. It is assumed that the electrical conductivity is infinitely large, and that the viscosity and thermal conductivity can be neglected.

For a number of equilibrium configurations KRUSKAL and SCHWARZSCHILD, and TAYLOR, have studied the various modes of small perturbations. But alternatively one can attempt to find some general criterion for stability

(*) Note added in proof. - F. MEYER and H. N. SCHMIDT could show that equilibrium configurations without a total azimuthal current exist. But in this case the cross-section of the torus depends on the azimuth.

without solving explicitly the differential equations. For this purpose an energy principle was derived by a group in Princeton and also in Göttingen. Briefly, this energy principle is derived in the following manner.

By assuming that the perturbations are small we can linearize equations (4) to (7). On differentiating equation (4) with respect to time and using equations (5) to (7) we finally obtain

$$(9) \quad \varrho_0 \frac{\partial^2 \mathbf{v}}{\partial t^2} = + \text{grad div } p_0 \mathbf{v} + (\gamma - 1) \text{grad } (p_0 \text{div } \mathbf{v}) - \\ - \frac{1}{4\pi} \text{curl } (\mathbf{v} \times \mathbf{B}_0) \times \text{curl } \mathbf{B}_0 - \frac{1}{4\pi} \mathbf{B}_0 \times \text{curl curl } (\mathbf{v} \times \mathbf{B}_0).$$

This differential equation determines the perturbation velocity \mathbf{v} ; the right hand side does not depend on the first derivative of \mathbf{v} with time, and all coefficients contain only the parameters \mathbf{B}_0 , p_0 , and ϱ_0 of the equilibrium configuration. Since the coefficients are independent of time, it is possible to write \mathbf{v} in the form

$$\mathbf{v} = \mathbf{v}_1(\mathbf{r}) \exp [i\omega t],$$

where \mathbf{v}_1 is a function only of the space variables. The left hand side of equation (9) is then equal to $-\omega^2 \varrho_0 \mathbf{v}_1$. One important property of this differential equation is that it is self-adjoint. Thus «over stability» cannot occur and the configuration is stable when the eigenvalue ω^2 is positive, and is unstable when ω^2 is negative.

If now one multiplies (9) by \mathbf{v} and integrates over the volume, then the integral on the left hand side is always of the same sign as $-\omega^2$. Therefore, the integral on the right-hand side determines the sign of ω^2 , and hence also the stability of the configuration. The problem of stability is reduced to the examination of an expression which in effect is equivalent to the potential energy, and this is roughly the same procedure as that adopted by the Princeton group.

Using this form it is possible, for instance, to obtain an estimation of the growth-rates of the perturbation in the case of instability, or alternatively in certain cases some sufficient conditions for stability. For example, with axial symmetry and only meridional fields all configurations are stable if at each point the lines of force are convex towards the region of greater pressure.

In the present investigation several serious assumptions have been made. These are as follows:

a) The perturbations are assumed to be small, and in most experiments this is certainly not true.

b) Obviously in low temperature plasmas, the conductivity cannot be assumed to be infinitely great.

c) The viscosity and the thermal conductivity have been neglected. But in most cases, the mean free path is very large and therefore these parameters have an appreciable value, particularly in the direction of the magnetic field. It would probably be a much better approximation to assume that they are infinitely great in this direction.

d) We have assumed that the pressure is isotropic, but if the charged particles spiral around the lines of force and the mean free path is large compared with the Larmor radius, a better approximation is to assume that the velocity distribution and therefore the pressure tensor is isotropic only in the plane perpendicular to the lines of force. Therefore, one should introduce the different pressures p_{\parallel} and p_{\perp} along and perpendicular to the magnetic field.

e) Finally, it should be mentioned that in some cases the problem of stability may require a closer examination of the microscopic picture.

3. - Particle losses.

For the purposes of studying the loss of individual particles the macroscopic equations cannot be used. It is now necessary to study the separate trajectories of the particles (losses due to charge exchange and other such mechanisms will not be discussed).

In this connection the adiabatic invariant theorem of the magnetic moment is often useful. The magnetic moment of a particle orbit is given by

$$(10) \quad \mu = \frac{\frac{1}{2} m v^2}{B},$$

and can be considered constant if the magnetic field varies slowly in space and time (v_{\perp} is the velocity component perpendicular to the magnetic field and m the mass of the particles). SCHLÜTER and HERTWECK and also KRUSKAL have studied to what degree of accuracy this theorem holds. SCHLÜTER and HERTWECK showed that the relative change in μ , between two different states where in each case the field is constant, decreases at least exponentially in ω_c/h . Here h represents the relative change in the magnetic field and ω_c is the gyration frequency.

For studying the trajectories of the particles any reaction on the magnetic field is neglected. One is therefore dealing with the equation of motion of a particle of charge Ze and mass m in a magnetic field:

$$(11) \quad m \frac{d\mathbf{v}}{dt} = \frac{Ze}{c} \mathbf{v} \times \mathbf{B}.$$

In the axially symmetric case a generalization of the law of conservation of angular momentum enables one to draw some conclusions about the motion of the particles without solving this equation explicitly. Only the meridional component of the magnetic field is important for confining the particles within a finite volume. However, it is necessary that the lines of force of the meridional field must be closed. If the particles have an energy which is not too great they will remain within a finite volume whose size can be calculated. In the limiting case when $v \rightarrow 0$ the particle will not depart by an amount greater than the Larmor radius from a closed surface generated by the rotation of a meridional line of flux around the axis of symmetry.

Therefore, the different components of the drift motion arising from the meridional and azimuthal magnetic fields do not just add together vectorially, and it is indeed possible to prevent the particles from leaving the surface, for example, of a toroidal plasma.

BIBLIOGRAPHY

- L. BIERMANN and A. SCHLÜTER: *Zeit. f. Naturf.*, **12 a**, 805 (1957).
L. BIERMANN, K. HAIN, K. JÖRGENS and R. LÜST: *Zeit. f. Naturf.*, **12 a**, 825 (1957).
R. KIPPENHAHN: *Zeit. f. Naturf.* **13 a**, 260 (1958).
M. D. KRUSKAL and M. SCHWARZSCHILD: *Proc. Roy. Soc.*, London A **223**, 348 (1954).
R. TAYLOR: *Proc. Roy. Soc.*, London B **70**, 31 (1957).
I. B. BERNSTEIN, E. A. FRIEMAN, M. D. KRUSKAL and R. M. KULSRUD: *Proc. Roy. Soc. A* **244**, 17 (1958).
K. HAIN, R. LÜST and A. SCHLÜTER: *Zeit. f. Naturf.*, **12 a**, 833 (1957).
O. F. CHOW, M. L. GOLDBERGER and F. E. LOW: *Proc. Roy. Soc.*, London A **236**, 112 (1956).
F. HERTWECK and A. SCHLÜTER: *Zeit. f. Naturf.*, **12 a**, 844 (1957).
R. LÜST and A. SCHLÜTER: *Zeit. f. Naturf.* **12 a**, 841 (1957).

PROPRIETÀ LETTERARIA RISERVATA

Direttore responsabile: G. POLVANI

Tipografia Compositori - Bologna

Questo Fascicolo del *Supplemento* è stato licenziato dai torchi il 7-XII-1959